University of Udine

Polytechnic Department of Engineering and Architecture

Doctoral Degree in

Environmental and Energy Engineering Science

XXIX Cycle

Energy benefit assessment of various refrigeration systems integrated with HVAC units in shopping malls

Author:

Alessio Polzot

Supervisors:

Prof. Giovanni Cortella

Prof. Paola D'Agaro

Declaration

The research leading to this work was partly funded by the European Community Seventh Framework Programme (FP7/2007-2013) under grant agreement n° 608678.

Abstract

Shopping malls are among the most energy intensive commercial buildings, mainly due to heating, air conditioning and refrigeration plants. In recent years new innovative solutions have been employed in both the building and the plants, in order to reduce as much as possible the energy requirement and to increase the energy conversion efficiency of the systems. This practice has been further motivated by the need for using low environmental impact refrigerants, thus giving place to a widespread renovation of plants. The growing awareness of the environmental protection and the strong push by the European Union towards the use of natural refrigerants has been promoting the spread of carbon dioxide as working fluid.

The CO_2 refrigeration units operating in cold climates perform better than solutions using synthetic and not environmentally friendly refrigerants, while in mild and warm climates, due to the low critical temperature of the carbon dioxide, transcritical operations in R744 systems can commonly take place, increasing substantially the energy consumption. On the other hand, the high temperatures reached by the CO_2 in the high pressure heat exchanger potentially allow recovering a large amount of heat at different temperature levels according to the supermarket needs. This leads to further opportunities for the spread of CO_2 as refrigerant in mild and warm climates. Heat recovery and the integration with the heating, ventilating and air conditioning (HVAC) units make the CO_2 competitive as refrigerant also in climates characterized by high outdoor temperatures.

In this perspective, dynamic simulations of complex systems and control strategies play a crucial role in the performance assessment and system management.

This work analyses the energy saving potential generated by the heat recovery from carbon dioxide refrigeration systems in favour of the heating system of the building and by the integration of the refrigeration systems with the supermarket HVAC units in shopping malls located in mild and warm climates.

A comprehensive model of the commercial building, the refrigerated food storage equipment, the HVAC units and the refrigeration systems is developed.

Sommario

I centri commerciali sono tra i servizi più energivori, principalmente a causa degli elevati consumi per il riscaldamento, per il condizionamento dell'aria e per la frigoconservazione. Negli ultimi anni sono state adottate molteplici soluzioni innovative sia negli edifici che negli impianti con lo scopo di ridurre il più possibile la domanda di energia e di aumentare l'efficienza energetica dei diversi sistemi. Ciò è stato inoltre motivato dalla necessità di utilizzare refrigeranti a basso impatto ambientale, dando luogo a un diffuso rinnovamento degli impianti. La crescente consapevolezza ambientale e la forte spinta dell'Unione Europea verso l'utilizzo di refrigeranti naturali hanno promosso la diffusione dell'anidride carbonica come fluido di lavoro.

I sistemi di refrigerazione a CO_2 in climi freddi forniscono prestazioni migliori rispetto alle tradizionali soluzioni che utilizzano refrigeranti sintetici e non eco-compatibili, mentre in climi miti e caldi, a causa della bassa temperatura critica dell'anidride carbonica, i sistemi a R744 lavorano frequentemente in condizioni transcritiche, aumentando considerevolmente i consumi. D'altra parte, le alte temperature raggiunte dalla CO_2 negli scambiatori di alta pressione permettono potenzialmente il recupero di grandi quantità di calore a differenti livelli di temperatura in accordo alle diverse esigenze dei supermercati. Questo genera ulteriori opportunità per la diffusione nei climi miti e caldi dell'anidride carbonica come refrigerante. Il recupero di calore e l'integrazione con le unità HVAC possono infatti rendere competitiva sia energeticamente che economicamente la CO_2 come refrigerante anche in climi caratterizzati da elevate temperature esterne.

In questa prospettiva, la simulazione dinamica di sistemi complessi e le strategie di controllo giocano un ruolo fondamentale nella valutazione delle performance e nella gestione dei diversi componenti.

Questo lavoro analizza i potenziali risparmi energetici ottenibili dal recupero di calore da sistemi di refrigerazione ad anidride carbonica in favore degli impianti di

riscaldamento e dall'integrazione di tali sistemi con le unità HVAC per supermercati e centri commerciali situati in climi miti e caldi.

A tale scopo sono stati sviluppati modelli di simulazione completi dell'edificio commerciale, degli apparecchi per lo stoccaggio e la conservazione degli alimenti, delle unità per il riscaldamento e la climatizzazione dell'aria e dei sistemi di refrigerazione.

Index

List of figures

List of tables

Nomenclature

A	area [m^2]
AHD	DXS with several heat pumps system
CAS	cascade refrigeration system
CHP	CAS with two heat pumps for DHW and heating system
CO_2	carbon dioxide
COP	coefficient of performance
c_p	specific heat capacity [$J \cdot kg^{-1} \cdot K^{-1}$]
DEC	Direct electric consumption
DHP	DXS with two heat pumps for DHW and heating system
DHW	domestic hot water
DXS	direct expansion refrigeration system
EER	energy efficiency ratio
FPT	fire prevention tank system
GWP	global warming potential [$kg_{CO_2} \cdot kg^{-1}$]
h	enthalpy [$kJ \cdot kg^{-1}$]
HFC	hydro-fluorocarbon
HFO	hydro-fluoroolefin
HP	high pressure
HS	high stage
HVAC	heating, ventilation and air conditioning
HX1	heat exchanger for domestic hot water production
HX2	heat exchanger for space heating purposes
k	thermal conductivity [$W \cdot m^{-1} \cdot K^{-1}$]
L	length [m]
LHR	latent heat ratio
LS	low stage
LT	low temperature
m	mass [kg]
$\dot{m}$	mass flow rate [$kg \cdot s^{-1}$]
MT	medium temperature
p	pressure [bar]
PCS	R744 transcritical booster system with auxiliary compression
$\dot{Q}$	thermal load [W]
R	resistance [$m^2 \cdot °C^{-1} \cdot W^{-1}$]
RH	relative humidity [%]
RTF	runtime fraction [-]
SCH	schedule [-]
t	temperature [°C]
TBS	R744 transcritical booster system
THR	PCS system with heat recovery and load evaporator

U	thermal conductance [$W \cdot m^{-2} \cdot K^{-1}$]
V	volume [m3]
$\dot{w}$	electric power per unit length [$W \cdot m^{-1}$]
$\dot{W}$	electric power [W]
WLB	WLHP system coupled with PCS with heat recovery from condensation system
WLC	WLHP system coupled with CAS with heat recovery system
WLD	WLHP system coupled with PCS with heat recovery from desuperheating system
WLHP	water loop heat pump
x	specific humidity [$kg \cdot kg^{-1}$]
z	depth [m]

Greek symbols

α	thermal diffusivity [$m^2 \cdot s^{-1}$]
β	pressure ratio [-]
Δ	difference
η	efficiency [-]
θ	time [s]
ρ	density [$kg \cdot m^{-3}$]

Subscripts

a	air
as	anti-sweat
AH	auxiliary heater
aux	auxiliary devices
cc	case credit
CC	cascade condenser
cond	condensing
CR	cold room
DC	dry cooler
dp	dew-point
env	envelope
evap	evaporating
fus	fusion
GC	gas cooler
HR	heat recovery
HS	high stage
inf	infiltration
INT	intermediate
lat	latent
LS	low stage
LT	low temperature
MT	medium temperature
o	operating
out	outlet
PC	parallel compressor
R	rated
RDC	refrigerated display cabinet
sen	sensible
sub	sublimation
w	water

Chapter I

Introduction

The reduction of the energy consumptions and the use of environmentally friendly working fluids are key elements of current European policies. Supermarkets are intensive energy consumers and approximately the 40% of their annual energy consumption is for refrigeration. Direct emissions of greenhouse gases associated with the use of high Global Warming Potential (GWP) refrigerants and the indirect impact on the environment related to the high electrical energy consumption, make shopping malls not sustainable buildings.

Furthermore, commercial refrigeration is being especially affected by the phase down schedule for the hydro-fluorocarbons (HFCs), recently forced in Europe through the EU F-gas Regulation 517/2014 (European Commission, 2014). In fact, as of 1st January 2022, placing on the market is prohibited for fluorinated greenhouse gases with a GWP of 150 or more used in multipack centralised refrigeration systems for commercial use with a rated capacity of 40 kW or more. Exception is made for the primary refrigerant circuit of cascade systems, where fluorinated greenhouse gases with a GWP lower than 1500 may be used. This directive represents a step towards a possible full ban of HFCs, as it has already happened in some countries (IIR, 2015), thus giving rise to the need for finding alternate solutions (Cavallini et al., 2014).

Despite its low critical temperature as well as high operating pressure levels, carbon dioxide (R744) is receiving growing attention, due to its favourable thermophysical properties, non-toxicity, non-flammability and to its very low GWP, which leads to a negligible direct contribution to the greenhouse effect. On the contrary, the indirect contribution could be negatively affected owing to the lower efficiency of CO_2 systems when compared with traditional HFCs refrigeration units. This is particularly true of applications in mild and warm climates, where the CO_2 systems operate for a long

period of time at transcritical conditions, with a significant decrease in their energy performance.

Research is ongoing to face design issues and improve the energy efficiency of CO_2 systems in such conditions (Kim et al., 2004) and various solutions have been identified and tested (Cavallini and Zilio, 2007; Cecchinato et al., 2009; Gullo et al., 2016b; Hafner et al., 2014; Sawalha, 2009, Sawalha et al., 2015, Sharma et al., 2014) also with more in-depth analyses involving system irreversibilities (Gullo et al., 2015).

The main concern at mild and warm climates is related to the high temperature of the refrigerant at the gas cooler exit, which is very effective on the performance of the system (Pettersen, 1997). For this reason, many efforts are devoted to investigate configurations where gas cooling can be promoted to the highest level, by means of internal heat exchangers (Cavallini et al., 2007; Ge and Tassou, 2011c; Sawalha, 2008; Yang and Zhang, 2011) with an average increase in the coefficient of performance (COP) of up to 10%, by means of by means of low temperature heat storages (Fidorra et al., 2015) or by means of the mechanical subcooling, i.e. performing subcooling thanks to another refrigerating unit (Hafner et al., 2014; Llopis et al., 2015; Qureshi and Zubair, 2012).

Further opportunities for energy saving emerge when the boundaries of the system into consideration are extended to the whole supermarket or shopping mall. In fact, heat recovery from the commercial refrigeration units in favour of HVAC systems and domestic hot water (DHW) production can be effectively performed (Colombo et al., 2014). Up to now the prevalent solution with conventional HFC refrigeration systems consists in using the waste heat rejected by the condensers directly for the whole space heating (Minea, 2010), in parallel to a heat pump to support space heating (Cecchinato et al., 2010), or for supplying the pre-heating coil of the air handling unit (Arias and Lundqvist, 2006; Ge and Tassou, 2011a; Ge and Tassou, 2011b). However, heat recovery affects negatively the performance of the refrigeration system: for an effective recovery, the condensing temperature must be raised (Ge and Tassou, 2014), thus preventing from taking advantage of a floating condensing control rule. In refrigeration systems in which the CO_2 is the only working fluid, the high temperature reached at the compressor discharge allows heat recovery at various temperature levels, i.e. for domestic hot water (70-50 °C) (Hafner et al., 2012; Sawalha, 2013), direct space heating (50-40 °C), space heating through a heat

pump, fresh air preheating or snow melting (40-30 °C). Bearing in mind that with CO_2 in transcritical mode heat is rejected through a gas cooler where carbon dioxide undergoes a single phase gas cooling, the three temperature levels mentioned above can be met through three heat exchangers: the first placed before the gas cooler (acting as a desuperheater in subcritical operations), the gas cooler itself (acting as a condenser in subcritical operations) and the third downstream of the gas cooler (acting as a subcooler in subcritical operations) (Sawalha, 2013). At all these conditions, when the R744 refrigeration system operates in transcritical mode, the gas cooler discharge pressure has to be optimized in order to achieve the maximum COP of the system (Liao et al., 2010).

Sawalha (2013) estimated that heat recovery from the desuperheater is able to cover the entire heating demand of an average size supermarket in relatively cold climate, leading to slightly lower annual energy consumption when compared to a conventional R404A refrigeration system with separate heat pump for heating needs. Furthermore, improvements in the energy efficiency can be achieved by means of parallel compression (Gullo et al., 2016a; Gullo et al., 2016b), i.e. an auxiliary compressor aimed at compressing directly to high pressure level the vapour exiting the receiver. The latter technology was proved to be beneficial to CO_2 refrigeration systems integrated with air conditioning (AC) system and operating in cold and mild climates (Karampour and Sawalha, 2015).

1.1 Aim of the study

In the last decade in Northern Europe, there has been a wide spread of commercial refrigeration systems using carbon dioxide as the only refrigerant. Thanks to its negligible direct greenhouse gas emissions and excellent thermophysical and heat transfer properties, the carbon dioxide is, by far, the best solution for the refrigeration systems located in cold climates. A further advantage of carbon dioxide as refrigerant in any climate is the implementation of heat recovery in favour of space heating and domestic hot water production. Considering the high compressor discharge temperature of the CO_2 refrigerating units, the potential heat recovery is much higher than that of a traditional HFC refrigeration system, creating additional and interesting

opportunities for energy savings. Heat recovery entail to a reduction in the total supermarket energy usage but it is not always able to cover the entire heating demand of the supermarket. Also, its control strategy plays an important role to increase as much energy saving as possible.

Owing to the low critical temperature and the high operating pressure of the carbon dioxide, at high ambient temperatures a basic CO_2 cycle operates in transcritical conditions and the high-side heat exchanger is not able to condense the refrigerant, decreasing substantially the efficiency of the system. Therefore, in mild and warm climates, where the CO_2 systems operate for a long period of time at transcritical conditions, the HFC refrigerating units achieve higher annual energy performance than the R744 systems.

Energy saving can be promoted by developing new technologies in order to enhance the performance of the commercial CO_2 refrigerating plants at high outdoor temperatures. Parallel compression has gaining a significant interest as it is considered the simplest technology to increase the efficiency of R744 systems. The use of thermal storages to raise the gas cooling at the highest level during high ambient temperatures is an interesting solution to reduce energy demand peaks. Despite this, a few studies on these technologies are available in these climate conditions. This is due to the poor knowledge in transcritical CO_2 refrigeration systems in mild and warm regions because these countries (e.g. Italy) have been fond of synthetic refrigerants owing to the poor performance of basic CO_2 system in these climate conditions. Due to the EU F-gas Regulation, which will force the replacement of high GWP refrigerants, carbon dioxide is expected to be used all over Europe, even in Italy.

Therefore, this study aims to bridge this scientific gap by evaluating the energy savings achievable by CO_2 refrigeration systems equipped with parallel compression working in various Italian climatic contexts.

Another relevant aspect of the present work is the assessment of the energy benefits related to the implementation of heat recovery in such climate conditions. In fact, as mentioned above, relevant benefits can be obtained by using this solution in any climate. On the other hand, few studies are available in mild and warm climates. The quality of the present work is additionally enhanced by the fact that a suitable control strategy has been extensively investigated in order to achieve great reduction in

energy saving and by the evaluation of the benefits related to an additional evaporator. This technology is extremely interesting as it can significantly increase of the amount of recoverable heat and further promote the use of carbon dioxide in any climatic context.

Furthermore, additional benefits are expected to be achieved by using thermal storages to cool down the CO_2 gas cooler exit temperature during high ambient temperature periods.

Therefore, in this study a R744 system with parallel compression integrated with a fire prevention tank as thermal storage has been exhaustively investigated. The availability of the fire prevention tank allows to take advantage of a free great capacity heat storage as cold sink. The assessment of different control strategies, which play a crucial role in the minimization of energy consumption of the refrigeration system, is an additional relevant aspect of this work.

Finally, the benefits related to the integration of CO_2 system equipped with parallel compression with several HVAC units through a water loop have also been studied. The optimization of the water loop temperature to reduce the heat pumps defrost operations and maximize the heat recovery from refrigeration during the winter season and to decrease the heat pumps condensation temperature during summer season has been carried out.

1.2 Publications

1.2.1 International journals

- Polzot, A., D'Agaro, P., Gullo, P., Cortella, G., 2016. Modelling commercial refrigeration systems coupled with water storage to improve energy efficiency and perform heat recovery. International Journal of Refrigeration 69, 313-323.
- Polzot, A., D'Agaro, P., Cortella, G., 2016. Energy analysis of a transcritical CO_2 supermarket refrigeration system with heat recovery. (Being printed in Energy Procedia).

1.2.2 National journals

- Polzot, A., Gullo, P., 2017. Analisi delle prestazioni di un sistema integrato a CO_2 per la refrigerazione, il riscaldamento e l'ACS nei supermercati. ZeroSottoZero (accepted manuscript).
- Gullo, P., Polzot, A., 2017. La valutazione delle prestazioni di macchine frigorifere a CO_2 per applicazioni commerciali in climi caldi. ZeroSottoZero 2 - 2017, 54-61

1.2.3 International conferences

- Polzot, A., Gullo, P., D'Agaro, P., Cortella, G., 2016. Performance evaluation of a R744 booster system for supermarket refrigeration, heating and DHW. Proceedings of the 12th IIR Gustav Lorentzen Natural Working Fluids Conference, Edinburgh, United Kingdom.
- Gullo, P., Cortella, G., Minetto, S., Polzot, A., 2016. Overfed evaporators and parallel compression in commercial R744 booster refrigeration systems – An assessment of energy benefits. Proceedings of the 12th IIR Gustav Lorentzen Natural Working Fluids Conference, Edinburgh, United Kingdom.
- Polzot, A., D'Agaro, P., Cortella, G., Gullo, P., 2016. Supermarket refrigeration and air conditioning systems integration via a water storage. Proceedings of the 4th IIR Conference on Sustainability and the Cold Chain, Auckland, New Zealand.
- Gullo, P., Cortella, G., Polzot, A., 2016. Energy and environmental comparison of commercial R744 refrigeration systems operating in warm climates. Proceedings of the 4th IIR Conference on Sustainability and the Cold Chain, Auckland, New Zealand.
- Polzot, A., D'Agaro, P., Gullo, P., Cortella, G., 2015. Water storage to improve the efficiency of CO_2 commercial refrigeration systems. Proceedings of the 24th International Congress of Refrigeration, Yokohama, Japan.
- Cortella, G., D'Agaro, P., Saro, O., Polzot A., 2014. Modelling integrated HVAC and refrigeration systems in a supermarket. Proceedings of the 3rd IIR International Conference on Sustainability and the Cold Chain, London, United Kingdom.

1.3 Reference

- Arias, J., Lundqvist, P., 2006. Heat recovery and floating condensing in supermarkets. Energy and Buildings 38 (2), 73-81.
- Cavallini, A., Zilio, C., 2007. Carbon dioxide as a natural refrigerant. International Journal of Low-Carbon Technologies 2–3, 225–249.
- Cavallini, A., Corradi, M., Fornasieri, E., 2007. Experimental investigation on the effect of the internal heat exchanger and intercooler effectiveness of the energy performance of a two stage transcritical carbon dioxide cycle. Proceedings of the 22nd International Congress of Refrigeration, Beijing, China.
- Cavallini, A., Zilio, C., Brown, J.S., 2014. Sustainability with prospective refrigerants. International Journal of Energy Research 38, 285–298.
- Cecchinato, L., Chiarello, M., Corradi, M., Fornasieri, E., Minetto, S., Stringari, P., Zillio, C., 2009. Thermodynamic analysis of different two-stage transcritical carbon dioxide cycles. International Journal of Refrigeration 32, 1058–1067.
- Cecchinato, L., Corradi, M., Minetto, S., 2010. Energy performance of supermarket refrigeration and air conditioning integrated systems. Applied Thermal Engineering 30, 1946–1958.
- Colombo, I., Maidment, G. G., Chaer, I., Missenden, J. M., 2014. Carbon dioxide refrigeration with heat recovery for supermarkets. International Journal of Low-Carbon Technologies 9, 38–44.
- European Commission, 2014. Regulation (EU) n° 517/2014 of the European Parliament and of the Council of 16 April 2014 on fluorinated greenhouse gases and repealing Regulation (EC) n° 842/2006.
- Fidorra, N., Hafner, A., Minetto, S., Köhler, J., 2015. Low temperature heat storages in CO_2 supermarket refrigeration systems. Proceedings of the 24th International Congress of Refrigeration, Yokohama, Japan.
- Ge, Y. T., Tassou, S. A., 2011a. Performance evaluation and optimal design of supermarket refrigeration systems with supermarket model “SuperSim”. Part I:

Model description and validation. International Journal of Refrigeration 34, 527-539.

- Ge, Y. T., Tassou, S. A., 2011b. Performance evaluation and optimal design of supermarket refrigeration systems with supermarket model “SuperSim”. Part II: Model applications. International Journal of Refrigeration 34, 540-549.
- Ge, Y.T., Tassou, S.A., 2011c. Thermodynamic analysis of transcritical CO_2 booster refrigeration systems in supermarket. Energy Conversion and Management 52, 1868–1875.
- Ge, Y.T., Tassou, S.A., 2014. Control optimizations for heat recovery from CO_2 refrigeration systems in supermarket. Energy Conversion and Management 78, 245–252.
- Gullo, P., Elmegaard, B., Cortella, G., 2015. Energetic, exergetic and exergoeconomic analysis of R744 refrigeration systems operating in warm climates. Proceedings of the 28th International Conference on Efficincy, Cost, Optimization, Simulation and Environmental Impact of Energy Systemises, Pau, France.
- Gullo P., Cortella G., Polzot A., 2016a. Energy and Environmental Comparison of Commercial R744 Refrigeration Systems operating in Warm Climates. Proceedings of the 4th IIR Conference on Sustainability and the Cold Chain, Auckland, New Zealand.
- Gullo, P., Elmegaard, B., Cortella, G., 2016a. Energy and environmental performance assessment of R744 booster supermarket refrigeration systems operating in warm climates. International Journal of Refrigeration 64, 61–79.
- Hafner, A., Poppi, S., Nekså, P., Minetto, S., Eikevik, T.M., 2012. Development of commercial refrigeration systems with heat recovery for supermarket buildings. Proceedings of the 10th IIR Gustav Lorentzen Conference on Natural Working Fluids, Delft, Nederland.
- Hafner, A., Hemmingsen, A.K., Van de Ven, A., 2014. R744 refrigeration system configurations for supermarkets in warm climates. Proceddings of the 3rd IIR

International Conference on Sustainability and the Cold Chain, London, United Kingdom.

- IIR, 2015. Overview of regulations restricting HFC Use: focus on the EU F-Gas regulation. 26th Informatory Note on Refrigeration Technologies, International Institute of Refrigeration, Paris.
- Karampour M., Sawalha S., 2015. Theoretical analysis of CO_2 trans-critical system with parallel compression for heat recovery and air conditioning system in supermarkets. Proceedings of the 24th International Congress of Refrigeration, Yokohama, Japan.
- Kim, M.H., Pettersen, J., Bullard, C.W., 2004. Fundamental process and system design issues in CO_2 vapor compression systems. Progress in Energy and Combustion Science 30 (2), 119–174.
- Liao, S. M., Zhao, T. S., Jakobsen, A., 2000. A correlation of optimal heat rejection pressures in transcritical carbon dioxide cycles. Applied Thermal Engineering 20, 831-841.
- Llopis, R., Cabello, R., Sanchez, D., Torrella, E., 2015. Energy improvement of CO_2 transcritical refrigeration cycles using dedicated mechanical subcooling. International Journal of Refrigeration 55, 129–141.
- Minea, V., 2010. Using heat pumps for energy recovery in supermarket refrigeration systems. IEA Heat Pump Centre Newsletter, 28 (4), 24- 30.
- Pettersen, J. 1997. Experimental results of carbon dioxide in compression systems. Proceedings of the ASHRAE/NIST Conference: Refrigerants for the 21st Century, Gaithersburg, Maryland.
- Qureshi, B.A., Zubair, S.M., 2012. The impact of fouling on performance of a vapor compression refrigeration system with integrated mechanical sub-cooling system. Applied Energy 92, 750–762.
- Sawalha, S., 2008. Theoretical evaluation of trans-critical CO_2 systems in supermarket refrigeration. Part II: system modifications and comparisons of different solutions. International Journal of Refrigeration 31, 525–534.

- Sawalha, S., 2009. Reulens, W. (Ed.), Module 3: Commercial Refrigeration, Natural Refrigerant CO_2. Katholieke Hogeschool Limburg, Diepenbeek, 100-176.
- Sawalha S., 2013. Investigation of heat recovery in CO_2 trans-critical solution in supermarket refrigeration. International Journal of Refrigeration 36, 145- 156.
- Sawalha, S., Karampour, M., Rogstam, J., 2015. Field measurements of supermarket refrigeration systems. Part I: Analysis of CO_2 trans-critical refrigeration systems. Applied Thermal Engineering 87, 633-647.
- Sharma, V., Fricke, B., Bansal, P., 2014. Comparative analysis of various CO_2 configurations in supermarket refrigeration systems. International Journal of Refrigeration 46, 86-99.
- Yang, L., Zhang, C.L., 2011. On subcooler design for integrated two-temperature supermarket refrigeration system. Energy and Buildings 43, 224–231.

Chapter II

Modelling environment

The use of building energy simulations is already widespread within other building categories, whereas in shopping malls it is still rather new due to the complexity of such systems concerning thermal zones with different uses, interaction of several components and technologies and implementation of different scenarios and control strategies. For these reasons, the development of energy models for this kind of buildings can be time consuming due to the need of developing numerical models for those technologies specific for shopping malls and the definition of the inputs and schedules for the different types of thermal zones.

Shopping malls become complex systems in the time of the co-existing of different systems on the same building. It is common practice to install and operate each system, i.e. lighting, refrigeration, HVAC, ventilation, electric and/or thermal storages, independently although they are directly or indirectly interconnected.

The management of several different systems which play a role in different final use zones is not an easy task neither the assessment of the building performance is guaranteed.

For these reasons, a numerical model of the whole shopping mall can help to:

- assess the building behaviour;
- assess the systems performances;
- develop and test a comprehensive control which is able to manage the whole system.

The building numerical model aims at reproducing the energetic behaviour of the shopping mall.

The modelling environment consists of a simulation ambient where the different aspects of a whole building system are implemented together. To this aim, the TRNSYS environment (TRNSYS, 2016) is chosen as the simulation environment.

TRNSYS software has a quite flexible structure that allows defining a modular and parametric modelling environment.

The whole building system is divided in base blocks. Technologies can be considered as building blocks which will make up the building model: base elements are joined at system level, which, again, are joined at building level. Trnsys has a modular structure which is a key factor in the shopping malls modelling. Every component or technology can be developed independently from the other parts of the building model and then gathered together into sub-systems.

The HVAC and refrigeration systems is implemented in the Trnsys environment in terms of numerical model of the components and control system. Base elements as the TRNSYS-types is used mainly for HVAC systems, while special components specific of shopping mall, as the refrigerated display cabinets, the cold rooms and the refrigeration units is developed within this work (Klein et al., 2010).

As regarding the refrigeration system, the refrigerated display cabinets and the cold rooms models are modelled by developing in-house Types based on mathematical equations. The different refrigeration units and the heat pumps for space heating, air conditioning and domestic hot water production are developed basing on thermodynamic relations. BITZER Software (BITZER, 2016) and Frascold Software (Frascold, 2016) are used to define the global efficiencies of the compressors whereas the thermodynamic properties are obtained by using CoolProp libraries (Bell et al., 2014).

The models of the cycles are implemented also in Engineering Equation Solver (EES) (F-Chart Software, 2015) which are based on the fundamental thermodynamic equations at steady state. These models are used for the simulation and the optimization of the refrigeration cycles.

Finally, for all the thermodynamic cycles evaluated, the following assumptions have been made:

- pressure drop in pipes and heat exchangers as well as heat losses are considered to be negligible;
- the expansion in all valves is considered isenthalpic;
- only saturated liquid and saturated vapor exit the receiver.

2.1 Reference

- Bell, I.H., Wronski, J., Quoilin, S., Lemort, V., 2014. Pure and Pseudo-pure Fluid Thermophysical Property Evaluation and the Open-Source Thermophysical Property Library CoolProp. Industrial & Engineering Chemistry Research 53 (6), 2498–2508.
- BITZER, 2016. BITZER Software version 6.4.4.1464. Available at: https://www.bitzer.de/websoftware/ [accessed 15/12/2016].
- F-Chart Software, 2016. Enginnering Equation Solver (EES), Academic Professional version 10.093. Available at: http://www.fchart.com/ees/ [accessed 15/12/2015].
- Frascold, 2016. FSS.3 (Frascold selection software) Software. Available at: http://www.frascold.it/it/download/software/ [accessed 15/12/2016].
- Klein, S.A., Beckman, W.A., Duffie, J.A. et al., 2010. TRNSYS version 17: a transient system simulation program manual. Solar Energy Laboratory, University of Wisconsin, Madison.
- TRNSYS, 2016. TRNSYS Software, Transient system simulation tool. Available at: http://sel.me.wisc.edu/trnsys/ [accessed 15/12/2016]

Chapter III

Building

The building is a modern shopping mall with a grocery, medium and small shops and parking lots below and above ground. The underground floor is assigned to the parking lots and warehouses, while the commercial floor involves two common areas running on the main axes of the building, surrounded by shops and two media stores on the wings of the building. A big food store is located next to the glazed hallway.
The shopping mall has a gross floor area of 21245 m^2 and a gross leasable area of 24349 m^2.
The number of opening hours per day and the number of opening days per week are assumed to be 12 and 7, respectively, and the shopping mall is closed for 4.5 days per year.

3.1 Thermal zones

The building model is divided into 37 thermal zones grouped into 7 different typologies:

- food store;
- hallways and common areas;
- media stores;
- parking lots;
- restaurants;
- services;
- shops;
- warehouses.

The food store vending area is equal to 6352 m^2 while the total vending area of the shops and the media stores is 10708 m^2. The hallways, the galleries and the common areas occupy an area of 3667 m^2.

Next to the shopping mall there is a hotel and a fitness centre which are neglected from the model. Every surface adjacent with these zones has an adiabatic boundary condition, assuming that temperature set-points of these zone are the same as those ones set for the analysed zones. The underground parking area are considered as unconditioned thermal zones with an high ventilation rate to simulate their connection to the outside.

The shading effect of overhangs and surrounding buildings are considered in the model.

Table 3.1.a, Table 3.1.b and Table 3.1.c report the area, the volume and the air-node capacitance of the 37 thermal zones considered.

Zone number	**Typology**	**Area**	**Height**	**Volume**	**Air-node capacitance**
		[m^2]	[m]	[m^3]	[$kJ \cdot K^{-1}$]
1	Service	140	4.0	560	8400
2	Service	71	4.0	284	4260
5	Warehouse	156	4.0	624	9360
6	Warehouse	461	4.0	1844	27660
7	Warehouse	571	4.0	2284	34260
28	Restaurant	155	4.0	620	9300
29	Restaurant	830	4.0	3320	49800
31	Parking	222	4.0	888	13320
32	Parking	191	4.0	764	11460
33	Parking	8846	3.0	26538	530760
34	Parking	9742	3.0	29226	584520

Table 3.1.a - Underground floor zones data summary.

Zone number	Typology	Area [m^2]	Height [m]	Volume [m^3]	Air-node capacitance [$kJ \cdot K^{-1}$]
3	Service	88	6.4	563	7814
4	Service	187	6.4	1197	16588
8	Warehouse	338	6.4	2163	30014
9	Warehouse	1091	6.4	6982	96881
10	Shop	292	6.4	1869	25930
11	Shop	134	6.4	858	11899
12	Shop	126	6.4	806	11189
13	Shop	596	6.4	3814	52925
14	Shop	439	6.4	2810	38983
15	Shop	733	6.4	4691	65090
16	Shop	1325	4.5	5963	79500
17	Shop	721	4.5	3245	43260
18	Hallways	208	6.4	1331	18470
19	Hallways	884	6.4	5658	74947
20	Hallways	128	6.4	819	11366
21	Hallways	871	6.4	5574	77345
22	Hallways	510	6.4	3264	45288
23	Hallways	561	6.4	3590	49817
24	Hallways	545	4.5	2453	32700
25	Media store	217	6.4	1389	19270
26	Media store	2855	6.4	18272	253524
27	Media store	3562	4.5	16029	213720

Table 3.1.b - Ground floor zones data summary (part I).

Zone number	Typology	Area [m^2]	Height [m]	Volume [m^3]	Air-node capacitance [$kJ \cdot K^{-1}$]
30	Food store	6352	6.4	40653	564058
35	Parking	292	6.4	1869	25930
36	Parking	131	6.4	838	11633
37	Parking	518	6.4	3315	45998

Table 3.1.c - Ground floor zones data summary (part II).

Figure 3.1.a and Figure 3.1.b show how the thermal zones are distributed over the building underground and ground plans, respectively.

Figure 3.1.a - Thermal zones for the underground floor of the shopping mall.

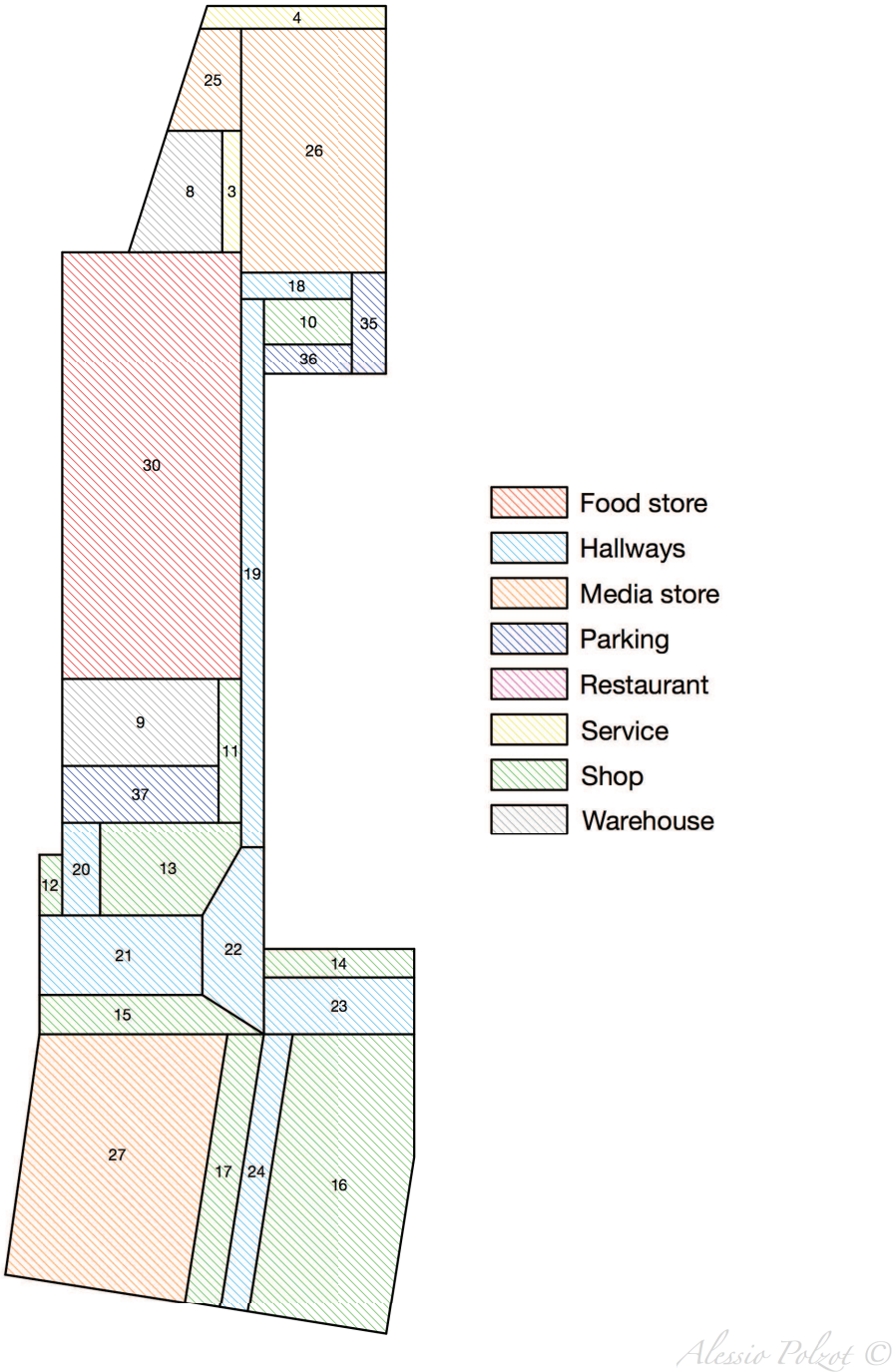

Figure 3.1.b - Thermal zones for the ground floor of the shopping mall.

3.2 Envelope

The building envelope characteristics are based on the technical report required by the Italian law Legge 9 gennaio 1991 n. 10 (1991). The thermal transmittance of the opaque envelope elements as well as the thermal transmittance and the solar energy transmittance of the transparent envelope elements are reported in Table 3.2.a and in Table 3.2.b, respectively.

Element	**Description**	**Floor**	**Thermal transmittance** $[W \cdot m^{-2} \cdot K^{-1}]$
W1	Exterior wall	Underground	0.261
W2	Exterior wall	Ground	0.340
W3	Interior wall	Underground	0.668
W4	Interior wall	Ground	0.668
F1	Ground floor	Underground	0.366
F2	Interior ceiling	Underground	0.302
F3	Exterior roof	Ground	0.262

Table 3.2.a - Thermal transmittance of the opaque envelope elements.

Element	**Description**	**Thermal transmittance of the glazing** $[W \cdot m^{-2} \cdot K^{-1}]$	**Thermal transmittance of the frame** $[W \cdot m^{-2} \cdot K^{-1}]$	**Solar energy transmittance of glass** [-]
G1	Window	1.400	3.030	0.600
S1	Skylight	0.354	3.030	0.300

Table 3.2.b - Thermal and solar energy transmittances of the transparent envelope elements.

3.3 Infiltration

The infiltration rates are assumed to be constant. The air changes per hour are set to 0.5 in the whole building.

3.4 Ventilation

The ventilation rates are set to 0.5 air changes per hour in the warehouses, 2 air changes per hour in the shops, in the media stores, in the food store and in the hallways and common areas, 3 air changes per hour in the services and 4 air changes per hour in the restaurants. The ventilation rates are reduced by 80 % during the shopping mall closing time and the heat recovery is activated when the moving average of the outside temperature over the previous 24 hours is lower than 12 °C. The ventilation rate of the parking zones is set to 10 air changes per hour to simulate their connection to the outside environment.

3.5 Occupancy

The internal gain due to the presence of persons is calculated as the product of the specific density of occupants in the zone, the total heat flux per person and the daily occupancy schedule. For retail stores, where people are standing and performing light work, the ISO 7730:2005 (2005) recommends to consider a total heat flux of 185 W per person which takes into account both sensible and latent gains. The specific density of persons considered for each thermal zone is reported in Table 3.5.a.

Thermal zone	Specific density [person · m^{-2}]
Food store	0.25
Hallways	0.20
Media store	0.25
Restaurant	0.25
Shop	0.20
Warehouse	0.10

Table 3.5.a - Density of occupants in the thermal zones.

The occupancy loads are considered from 8 am to 9 pm during the whole week for the food store, the hallways and common areas, the shops and the media stores, from 6 am to 7 pm during the whole week for the warehouses and from 8 am to 11 pm during the whole week for the restaurants. The daily occupancy schedule for each thermal zone is reported in Figure 3.5.a.

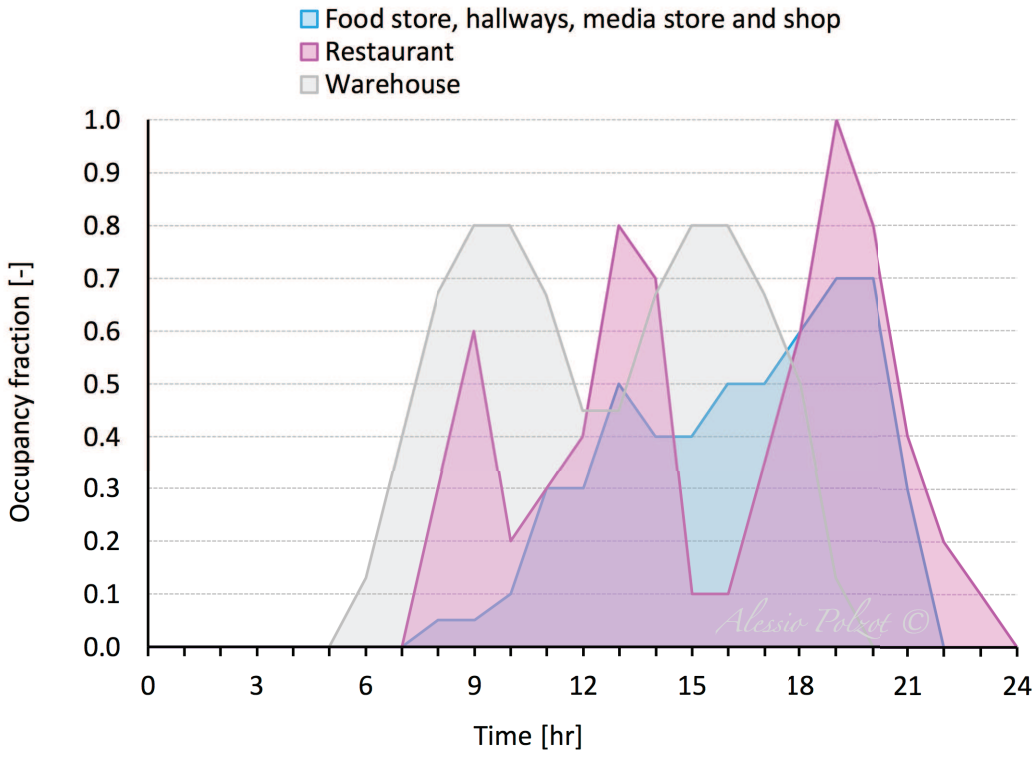

Figure 3.5.a - Occupancy fraction schedule for thermal zones.

3.6 Lighting

The internal gain due to the lighting systems is calculated as the product of the lighting specific heat load, which is divided between convective and radiative fractions, and the daily lighting schedule. The convective and the radiative fractions are set to 0.60 and 0.40, respectively, for each thermal zone. The specific heat load considered for each thermal zone is reported in Table 3.6.a.

Thermal zone	**Specific lighting load** [W · m^{-2}]
Food store	30.0
Hallways	8.0
Media store	27.0
Parking	2.2
Restaurant	28.2
Service	15.0
Shop	30.0
Warehouse	15.0

Table 3.6.a - Specific heat load for lighting in the thermal zones.

The daily lighting schedules are reported in Figure 3.6.a.

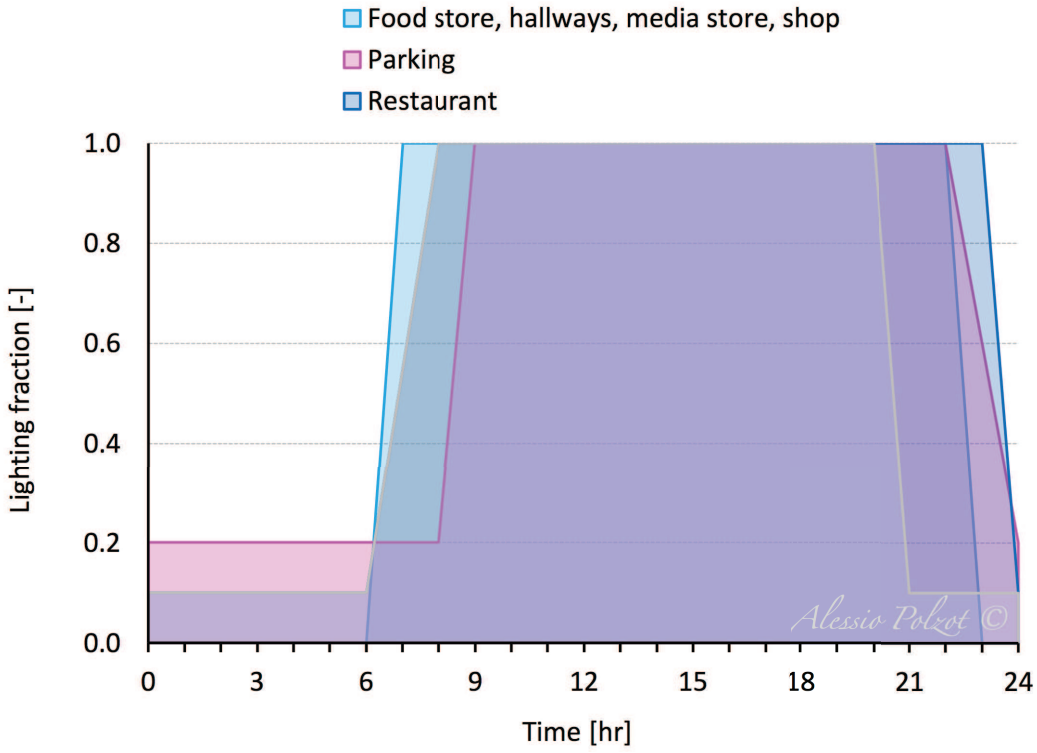

Figure 3.6.a - Lighting fraction schedule for thermal zones.

3.7 Appliance

The internal gain due to the electric equipment is calculated as the product of the specific heat load, which is divided between convective and radiative fractions, and the daily appliance schedule. The convective and the radiative fractions are set to 0.73 and 0.27, respectively. The specific heat load considered for each thermal zone is reported in Table 3.7.a.

Thermal zone	Specific appliance load [W · m^{-2}]
Food store	5.0
Hallways	5.0
Media store	10.0
Restaurant	10.0
Service	5.0
Shop	10.0
Warehouse	10.0

Table 3.7.a - Specific heat load for appliance in the thermal zones.

The daily appliance schedules are reported in Figure 3.7.a.

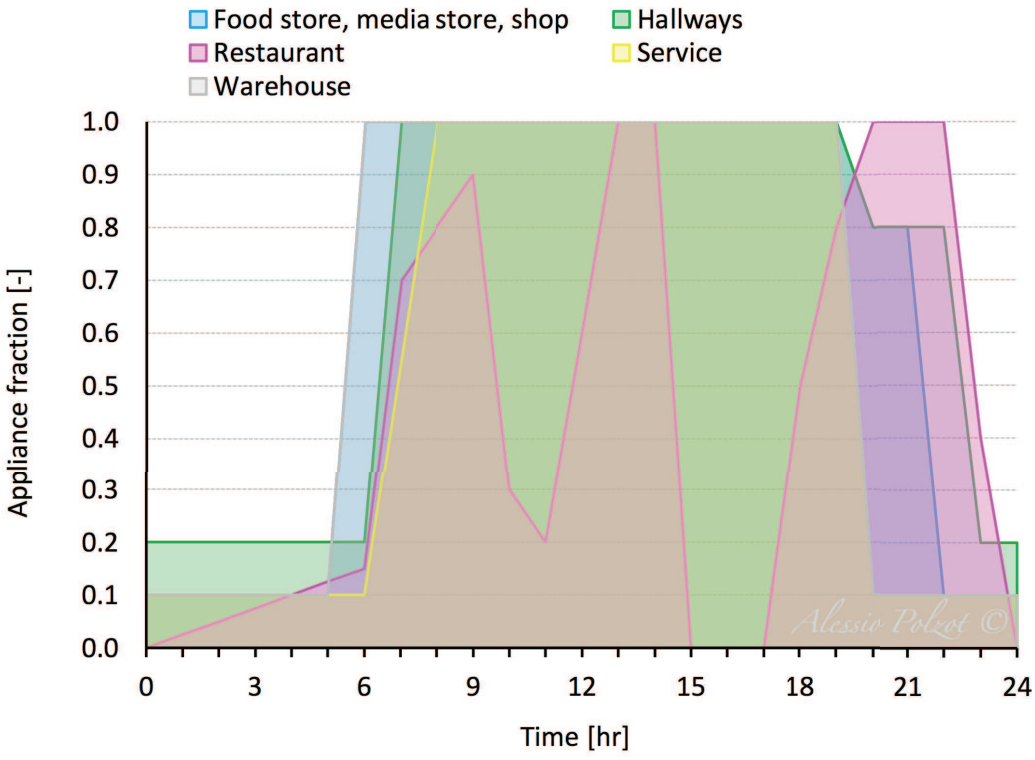

Figure 3.7.a - Appliance fraction schedule for thermal zones.

3.8 Temperature set-points

The heating demand of the shopping mall is calculated assuming a heating set-point temperature of 20 °C and a heating set-back temperature of 15°C for the food store, the media stores, the hallways and the common areas, the shops and the restaurant. The set-point temperature and the set-back temperature for the warehouses and the services are assumed to be 18 °C and 13 °C, respectively. Figure 3.8.a reports the heating set-points for each thermal zone.

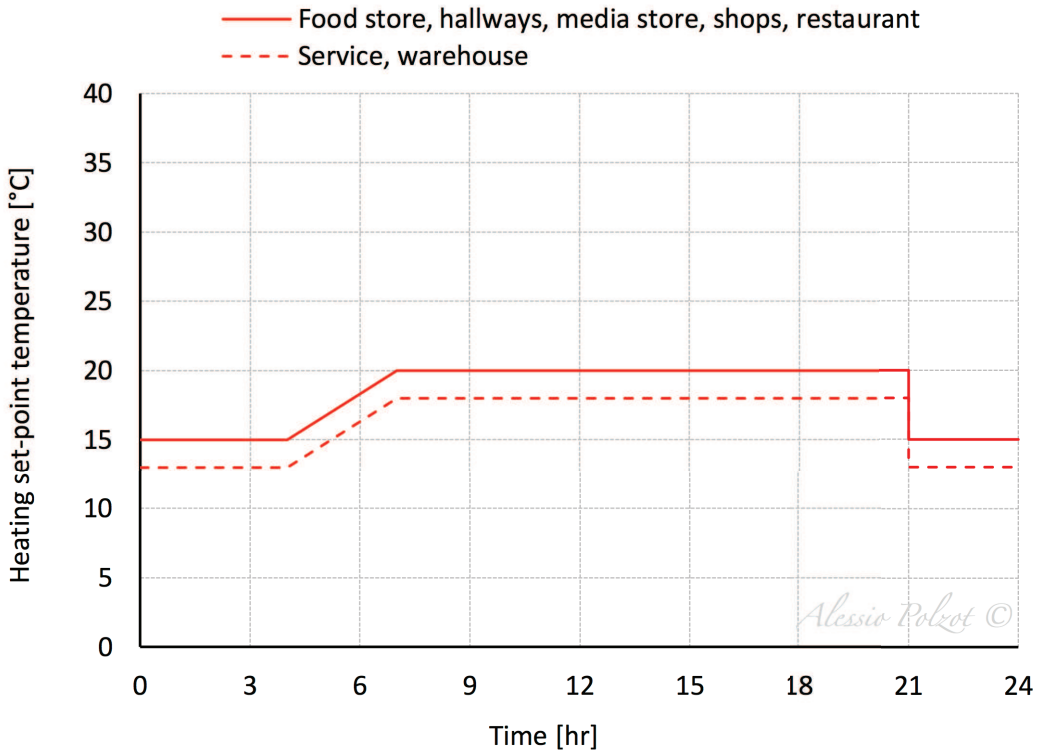

Figure 3.8.a - Heating set-points schedule for thermal zones.

The cooling demand of the shopping mall is calculated assuming a cooling set-point temperature of 26 °C and a cooling set-back temperature of 30°C for the food store, the media stores, the hallways and common areas, the shops and the restaurant. The set-point temperature and the set-back temperature for the warehouses and the services is assumed to be 30 °C and 35 °C, respectively. Figure 3.8.b reports the cooling set-points for each thermal zone.

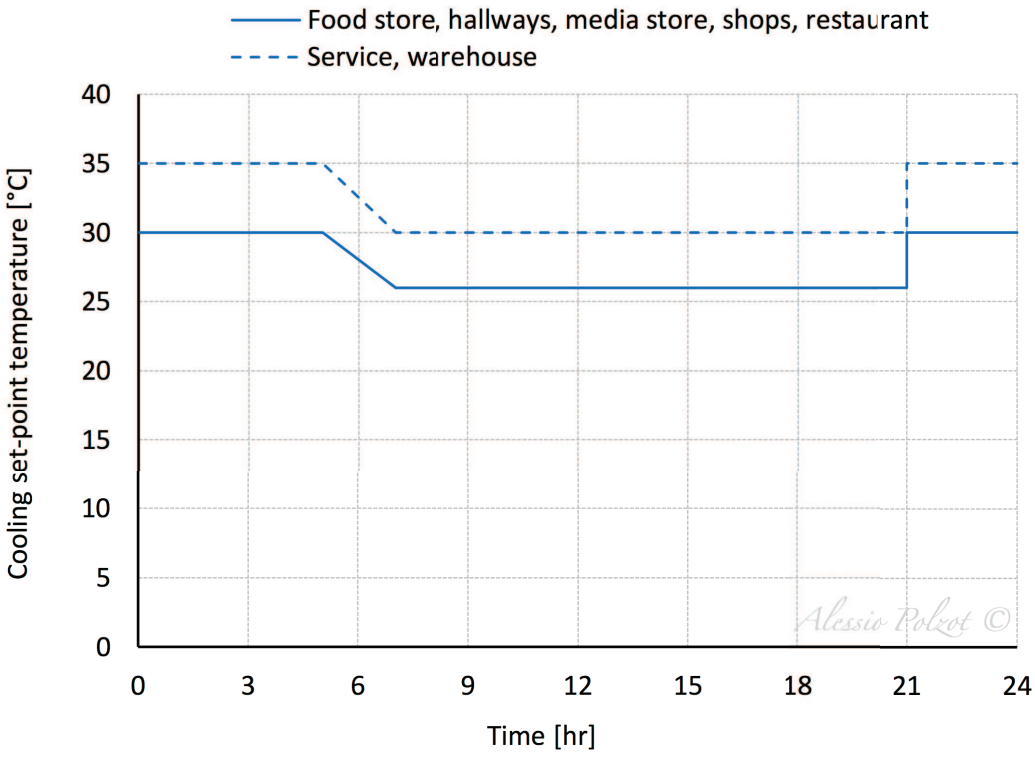

Figure 3.8.b - Cooling set-points schedule for thermal zones.

3.9 Reference

- ISO 7730:2005, 2005. Ergonomics of the thermal environment - Analytical determination and interpretation of thermal comfort using calculation of the PMV and PPD indices and local thermal comfort criteria.
- Legge 9 gennaio 1991 n. 10, 1991. Norme per l'attuazione del Piano energetico nazionale in materia di uso nazionale dell'energia, di risparmio energetico e di sviluppo delle fonti rinnovabili di energia.

Chapter IV

Mild and warm climates

In this study the same building model is simulated in five different Italian locations characterized by mild and warm climate conditions:

- Genoa;
- Milan;
- Palermo;
- Rome;
- Venice.

The weather files, which describe the weather trends in the above mentioned locations, are extrapolated by Meteonorm (Remund et al., 2014). The data for the external temperature, the humidity, the wind speed and the precipitations are collected from 2000 to 2009, while the solar radiation data are collected from 1991 to 2010.

4.1 Dry-bulb temperature

The chosen climate conditions have different annual average temperature, which ranges from 11.6 °C in Milan to 18.6 °C in Palermo, and different annual temperature fluctuations, which ranges from 13.4 K in Palermo and 22.2 K in Milan. The daily temperature fluctuation ranges from 10.6 K in Palermo, which is the warmest climate investigated, to 23.7 K in Milan.

Table 4.1.a reports the above mentioned parameters and the heating degree days of the investigated climate conditions.

		Genoa	Milan	Palermo	Rome	Venice
Annual average temperature	[°C]	16.4	11.6	18.6	15.5	13.0
Average annual temperature fluctuation	[K]	15.8	22.2	13.4	16.0	20.2
Maximum daily temperature fluctuation	[K]	10.4	23.7	10.6	14.8	14.9
Heating degree days	[-]	1435	2404	751	1415	2345

Table 4.1.a - Climate conditions considered.

A frequency analysis of the dry-bulb ambient temperature of the five different Italian locations is conducted and the outdoor air temperature distribution is reported in Figure 4.1.a, Figure 4.1.b, Figure 4.1.c, Figure 4.1.d and Figure 4.1.e.

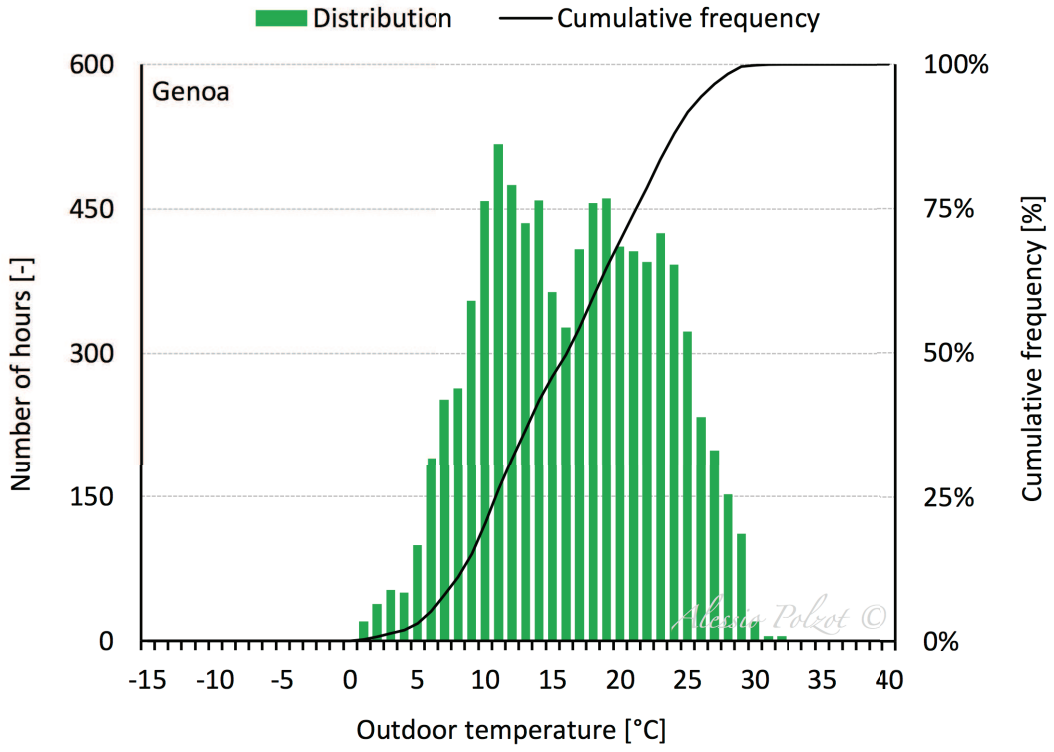

Figure 4.1.a - Ambient temperature distribution for Genoa.

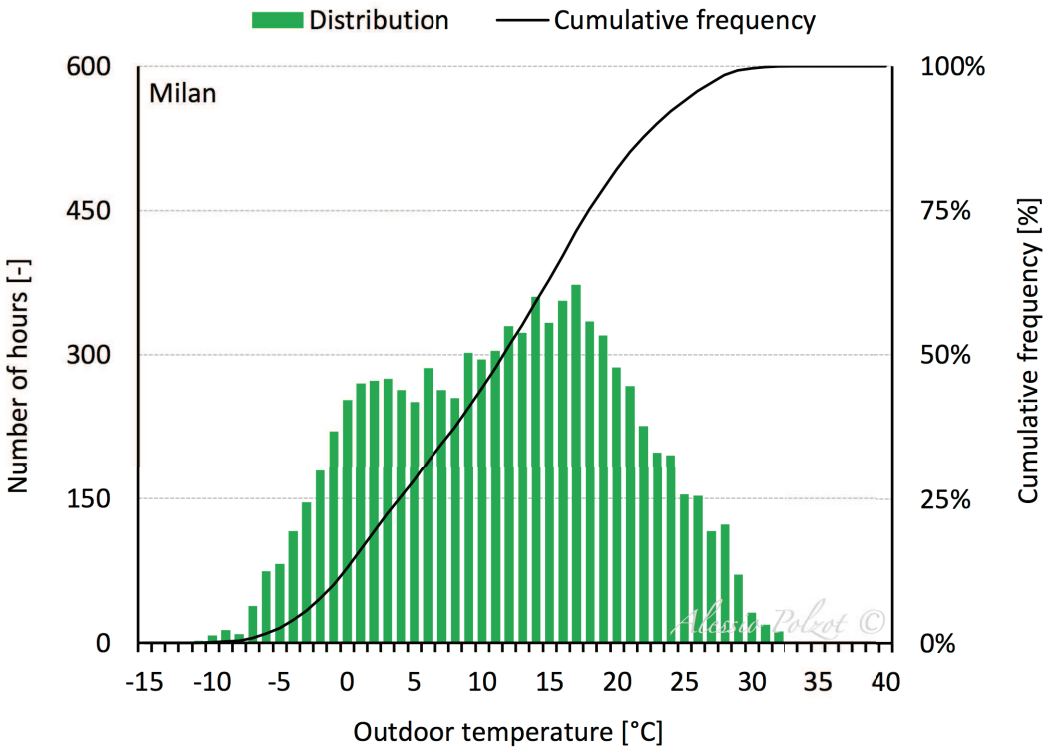

Figure 4.1.b - Ambient temperature distribution for Milan.

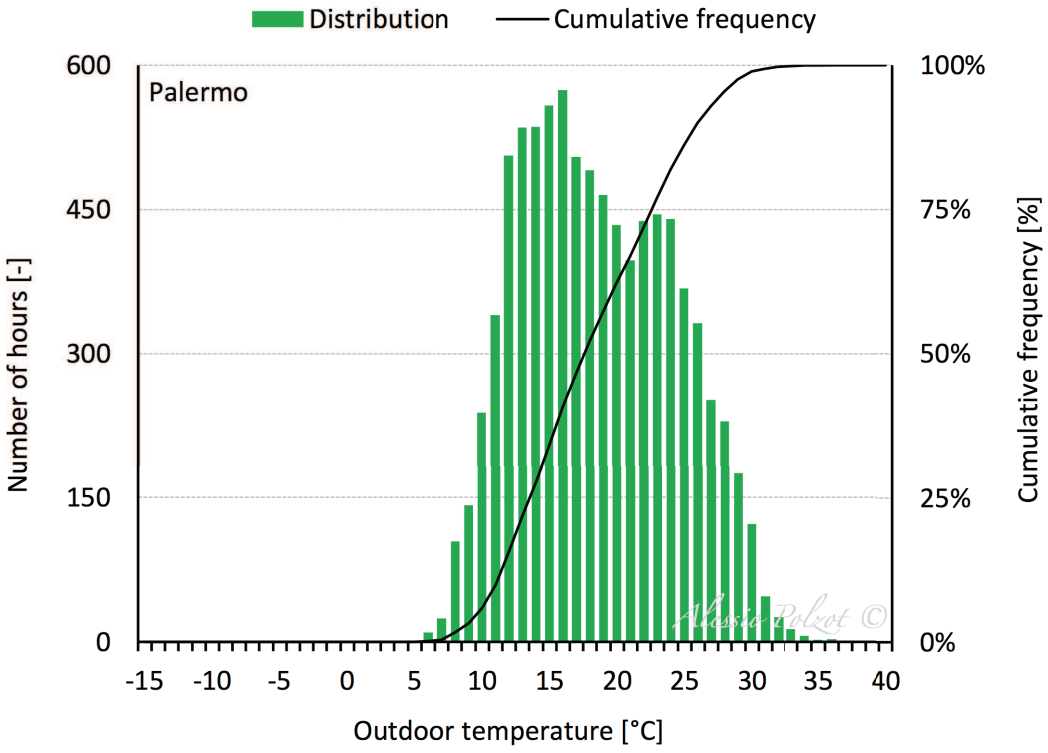

Figure 4.1.c - Ambient temperature distribution for Palermo.

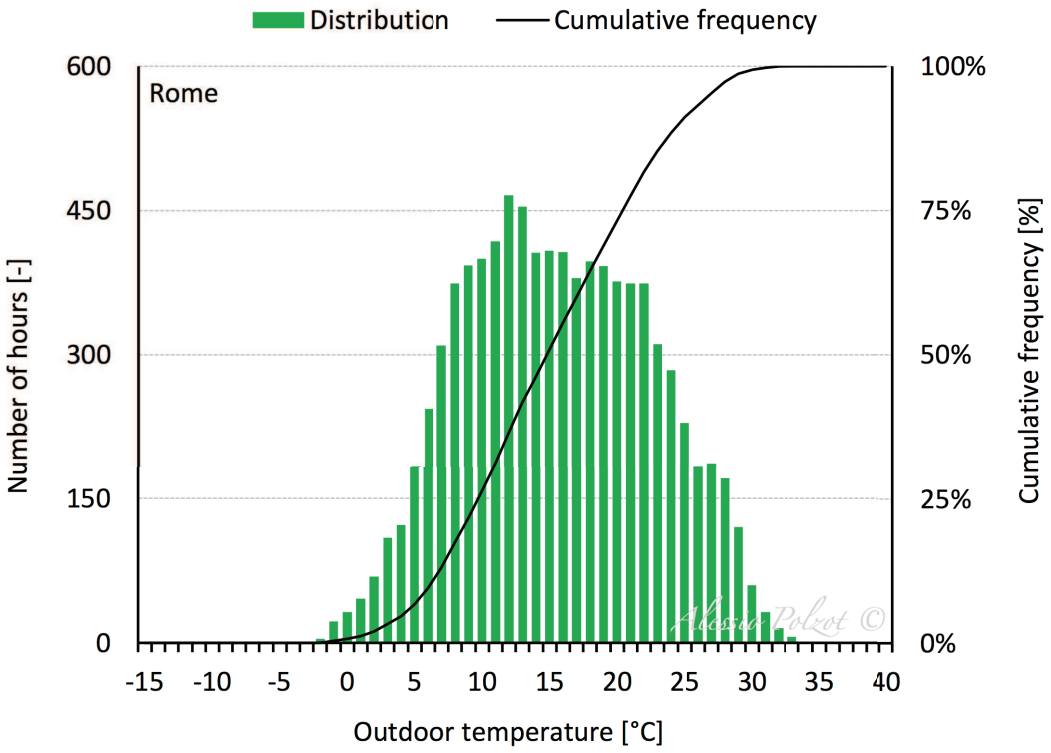

Figure 4.1.d - Ambient temperature distribution for Rome.

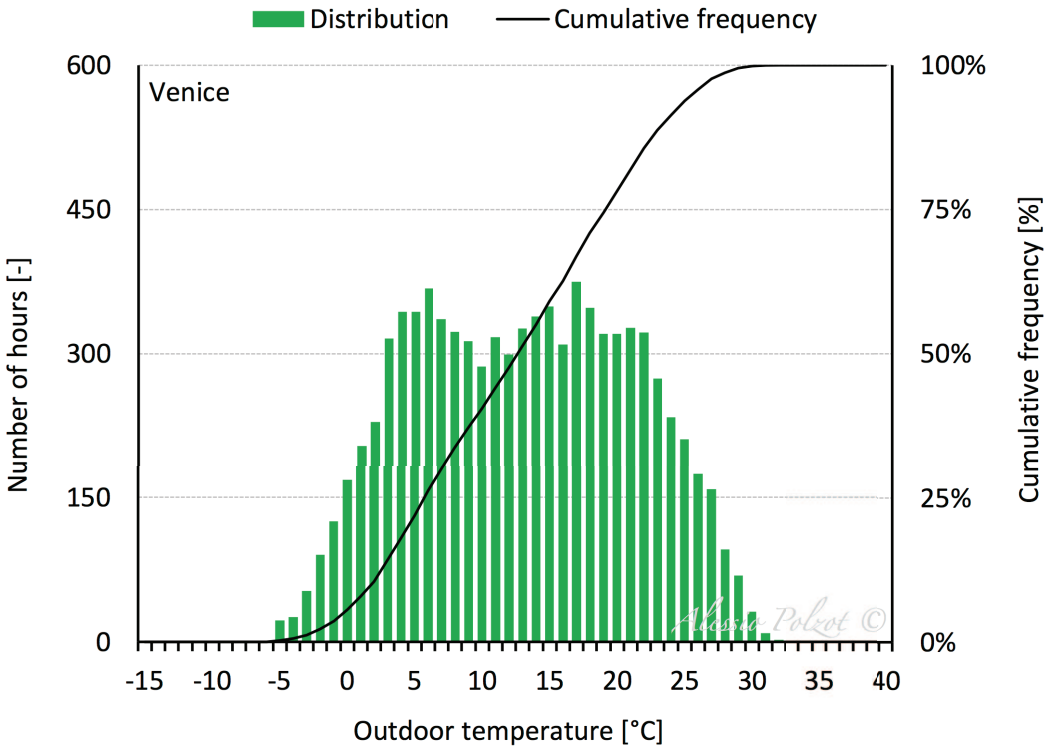

Figure 4.1.e - Ambient temperature distribution for Venice.

4.2 Relative humidity

A frequency analysis of the ambient relative humidity of the five different Italian locations is conducted and its distribution is reported in Figure 4.2.a, Figure 4.2.b, Figure 4.2.c, Figure 4.2.d and Figure 4.2.e.

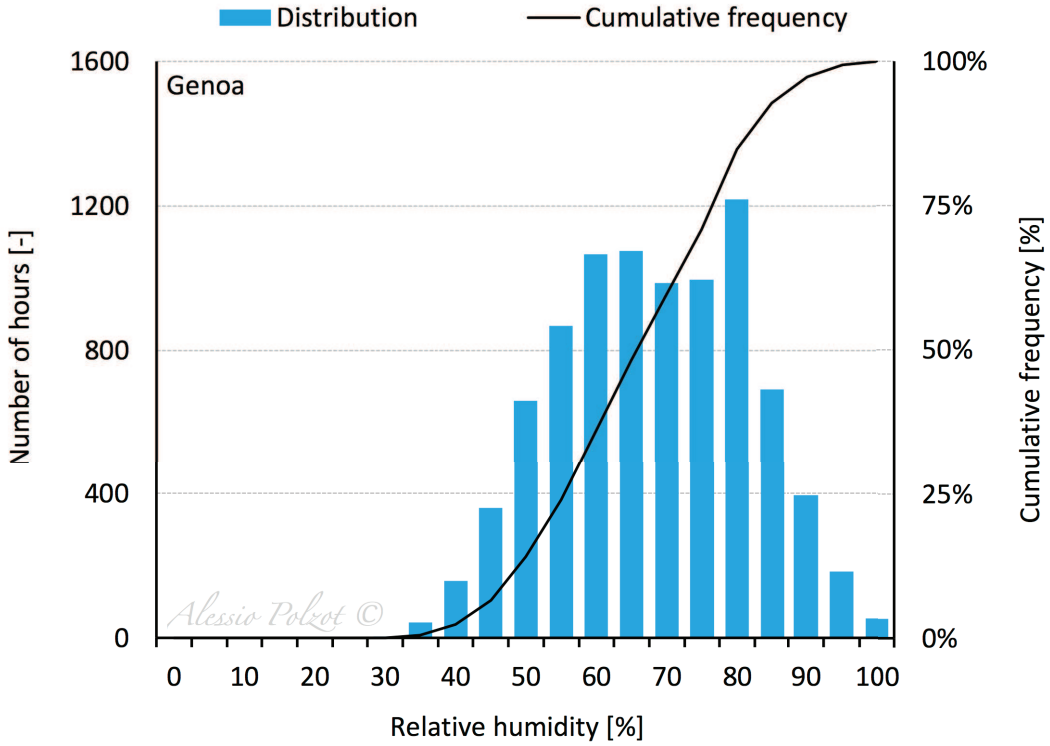

Figure 4.2.a - Ambient relative humidity distribution for Genoa.

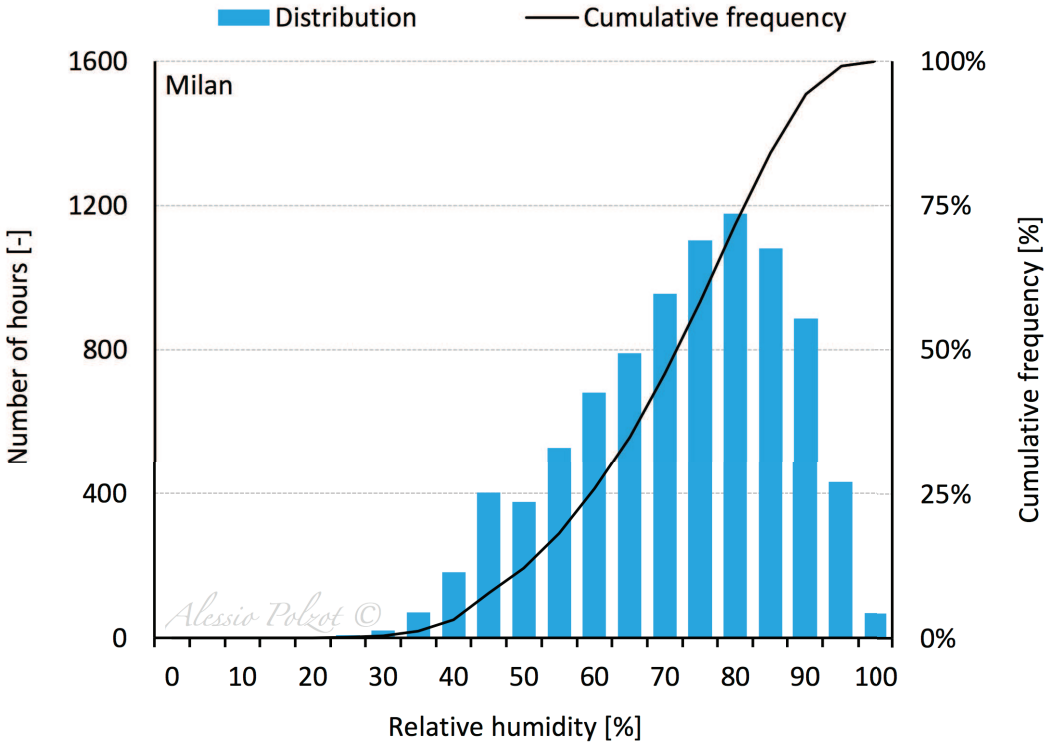

Figure 4.2.b - Ambient relative humidity distribution for Milan.

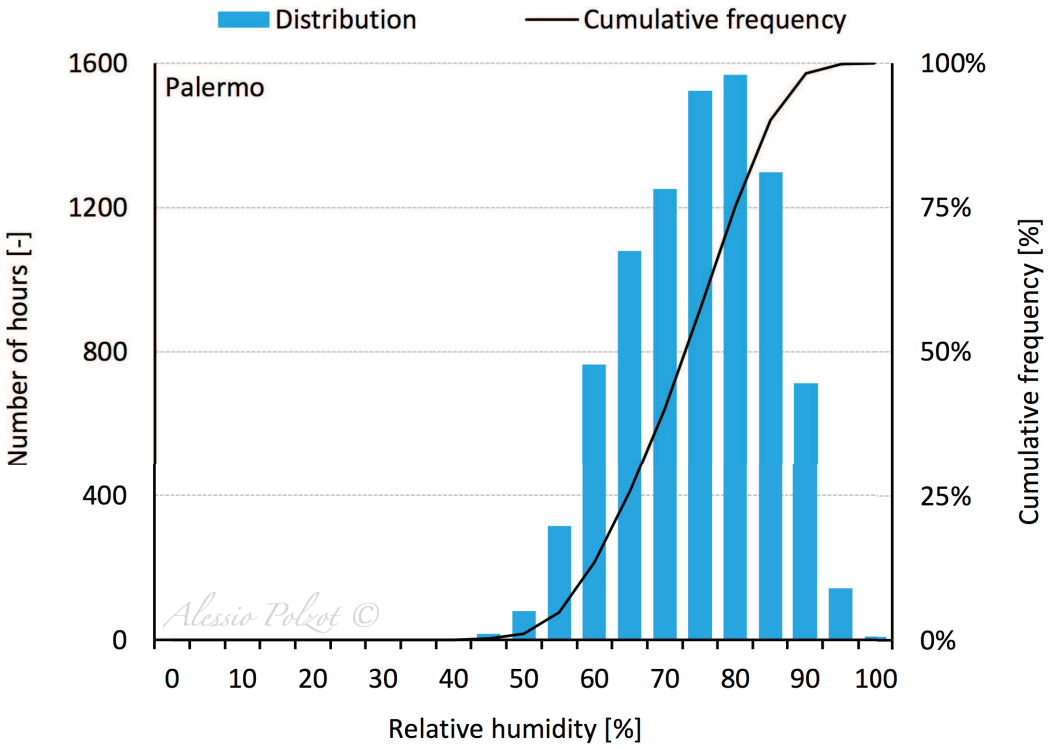

Figure 4.2.c - Ambient relative humidity distribution for Palermo.

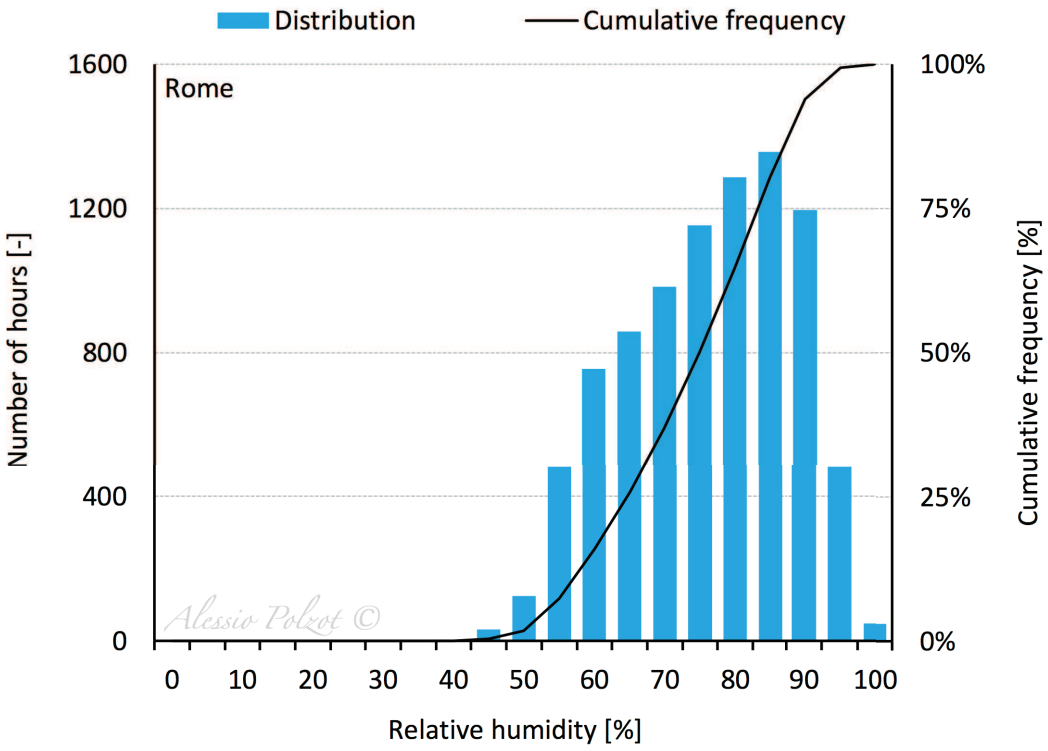

Figure 4.2.d - Ambient relative humidity distribution for Rome.

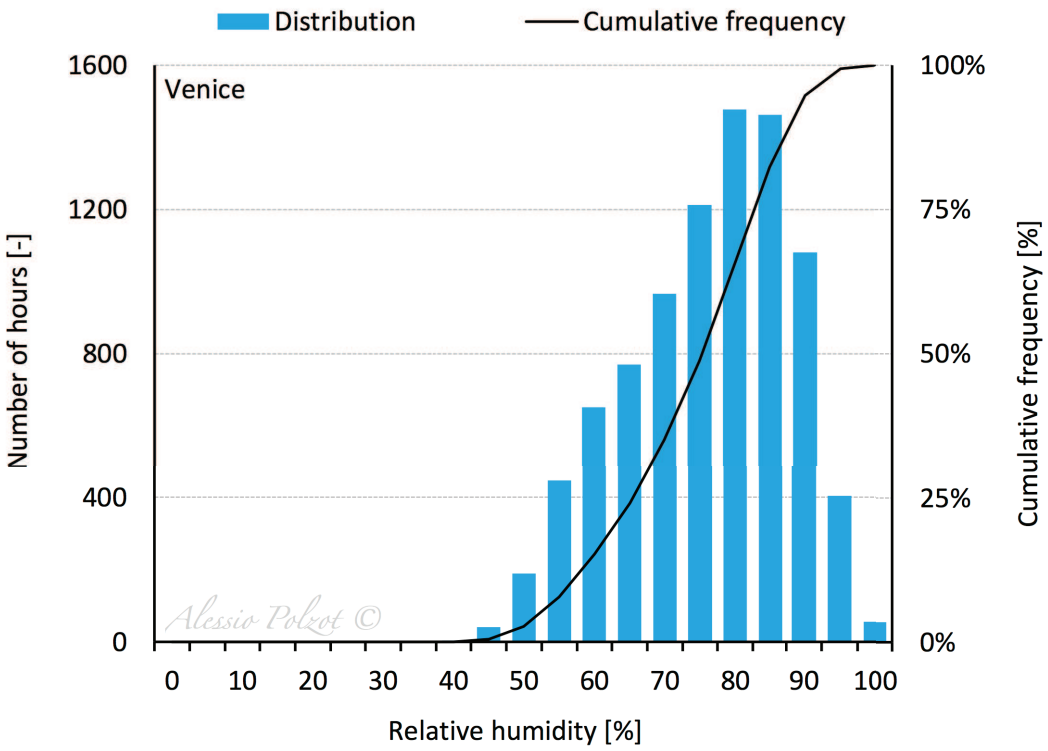

Figure 4.2.e - Ambient relative humidity distribution for Venice.

4.3 Global horizontal radiation

A frequency analysis of the global horizontal radiation of the five different Italian locations is conducted and its distribution is reported in Figure 4.3.a, Figure 4.3.b, Figure 4.3.c, Figure 4.3.d and Figure 4.3.e.

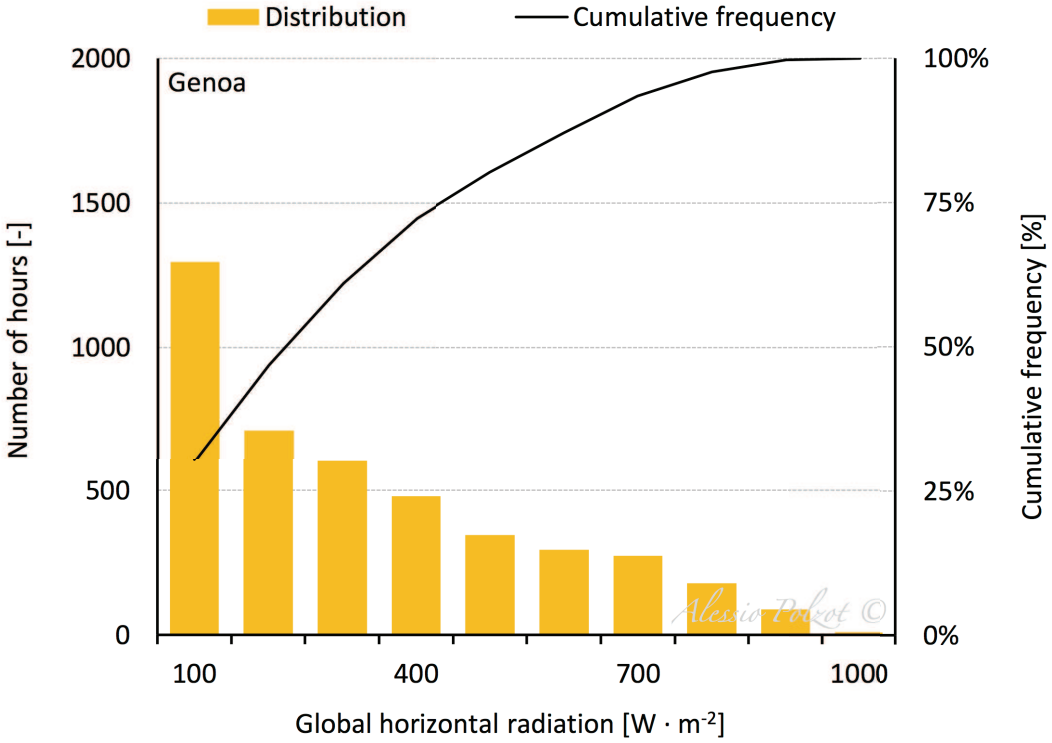

Figure 4.3.a - Global horizontal radiation distribution for Genoa.

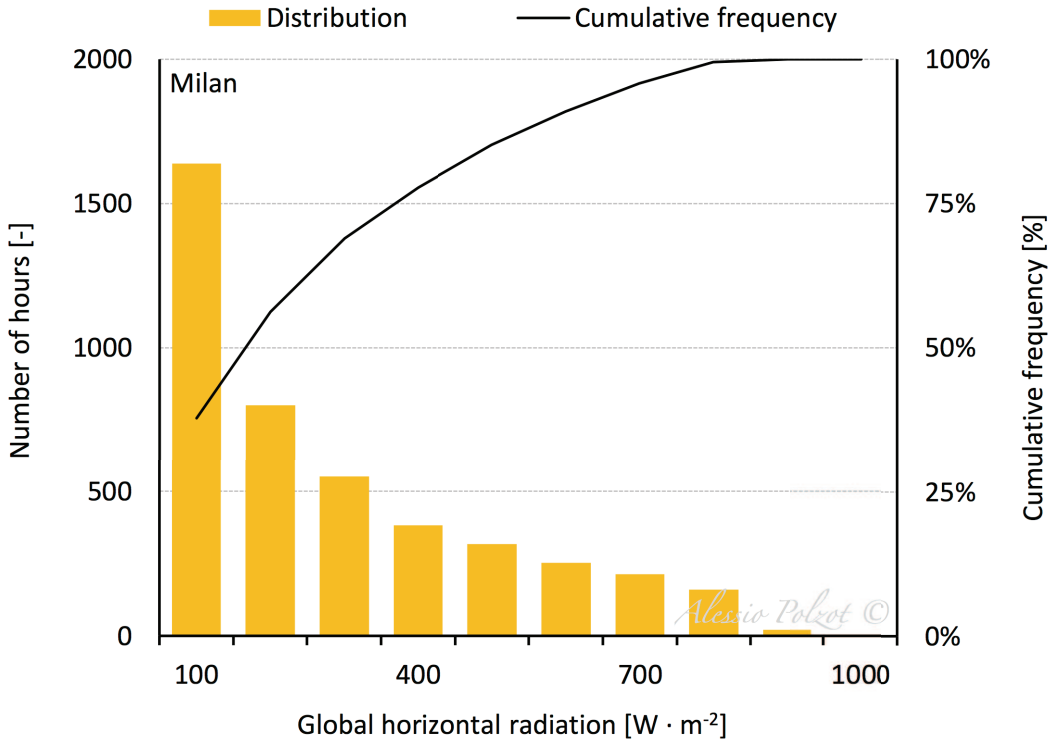

Figure 4.3.b - Global horizontal radiation distribution for Milan.

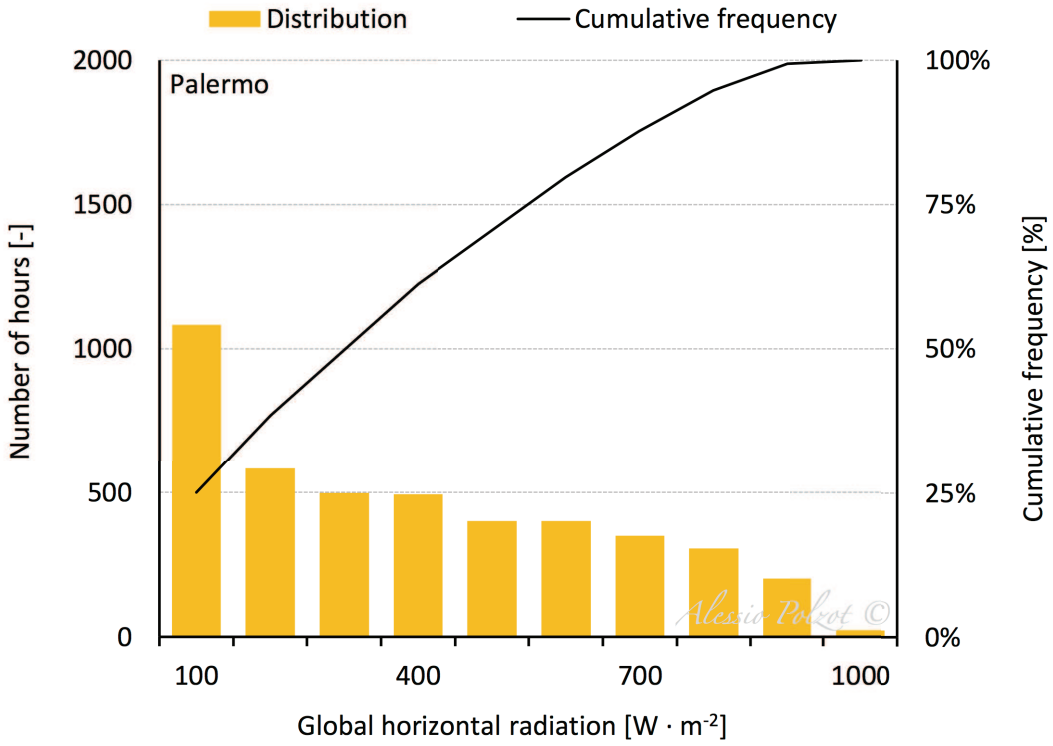

Figure 4.3.c - Global horizontal radiation distribution for Palermo.

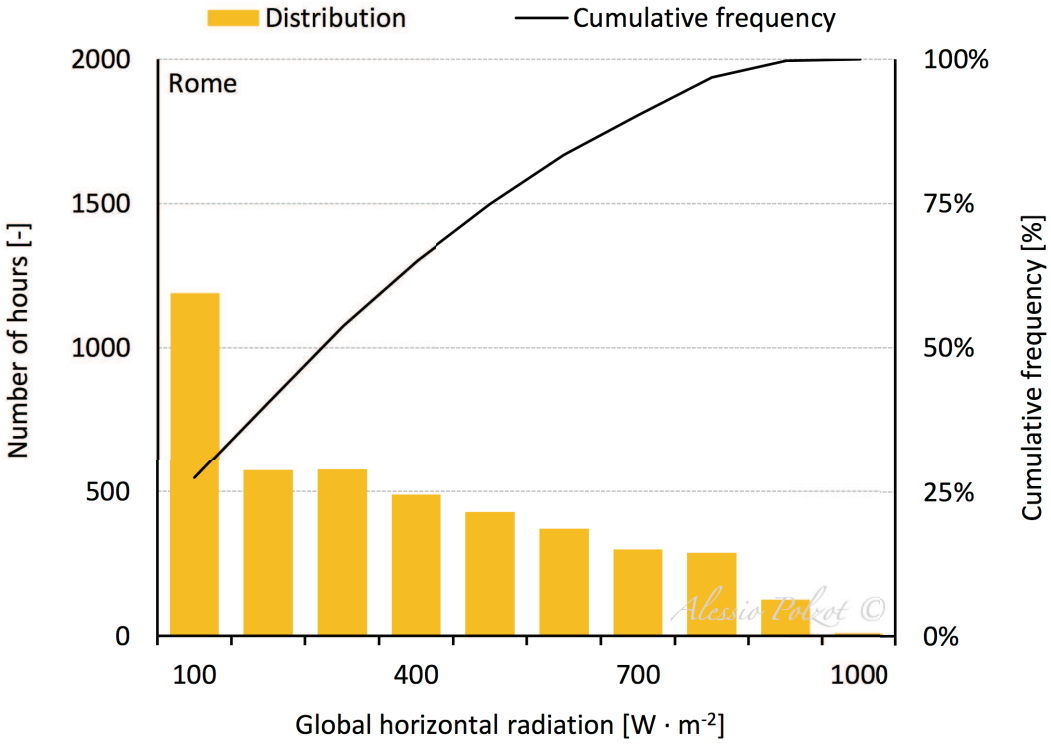

Figure 4.3.d - Global horizontal radiation distribution for Rome.

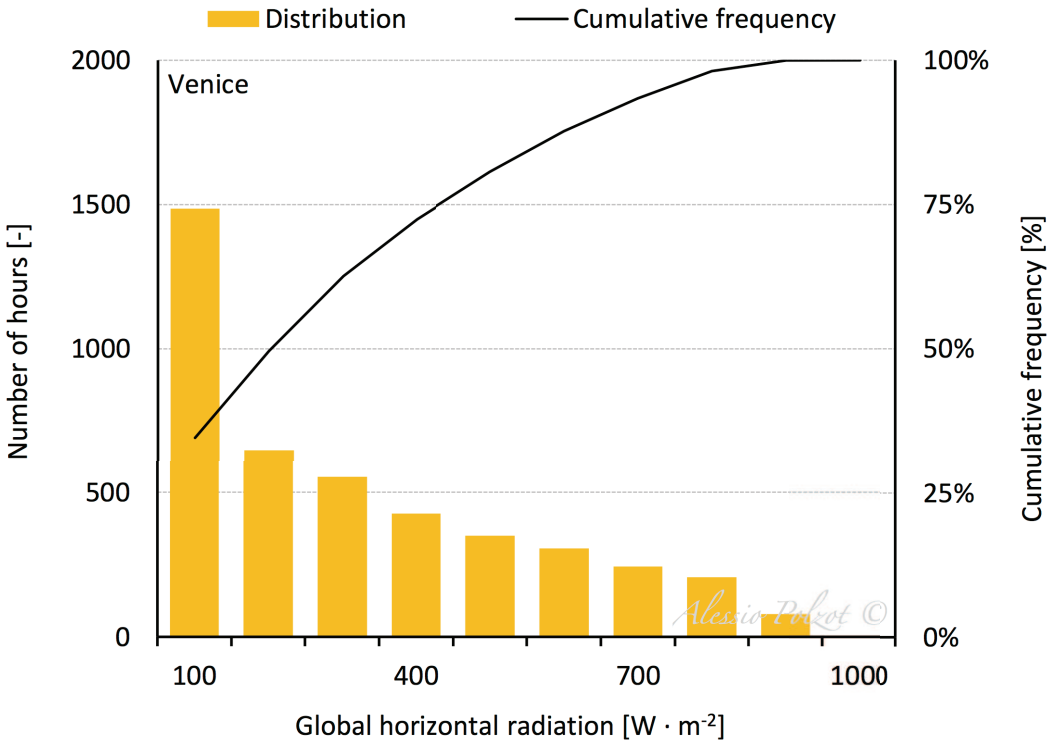

Figure 4.3.e - Global horizontal radiation distribution for Venice.

4.4 Ground temperature

The vertical temperature distribution of the ground is calculated using the Kasuda equation (Kasuda and Archenbach, 1965) given the mean ground surface temperature for the year, the amplitude of the ground surface temperature for the year, the time difference between the begging of the year and the occurrence of the minimum surface temperature and the thermal diffusivity of the soil.

In the Kasuda equation the temperature of the undisturbed ground is a function of the time of year and the depth below surface and it is described by the following correlation:

$$t = t_s - \Delta t_s \, e^{-z\sqrt{\frac{\pi}{\tau\,\alpha}}} \cos\left(\frac{2\pi}{\tau}\left[\theta - \theta_s - \frac{z}{2}\sqrt{\frac{\tau}{\pi\,\alpha}}\right]\right) \quad (1)$$

where:

t_s is the mean surface temperature [°C];

Δt_s is the amplitude of surface temperature [K];

z is the depth below surface [m];

τ is a time constant and it is equal to 31536000 [s];

α is the thermal diffusivity of the ground [$m^2 \cdot s^{-1}$];

θ is the current time [s];

θ_s is the phase shift or the time of the minimum surface temperature [s].

The thermal diffusivity of the ground is given by:

$$\alpha = \frac{k}{c_p\,\rho} \quad (2)$$

where:

k is the thermal conductivity of the ground [$W \cdot m^{-1} \cdot K^{-1}$];

c_p is the specific heat capacity of the ground [$J \cdot kg^{-1} \cdot K^{-1}$];

ρ is the density of the ground [$kg \cdot m^{-3}$].

The annual profile of the ground surface temperature and the annual profiles of the ground temperature at two different depth below the surface are reported in Figure 4.4.a, Figure 4.4.b, Figure 4.4.c, Figure 4.4.d and Figure 4.4.e.

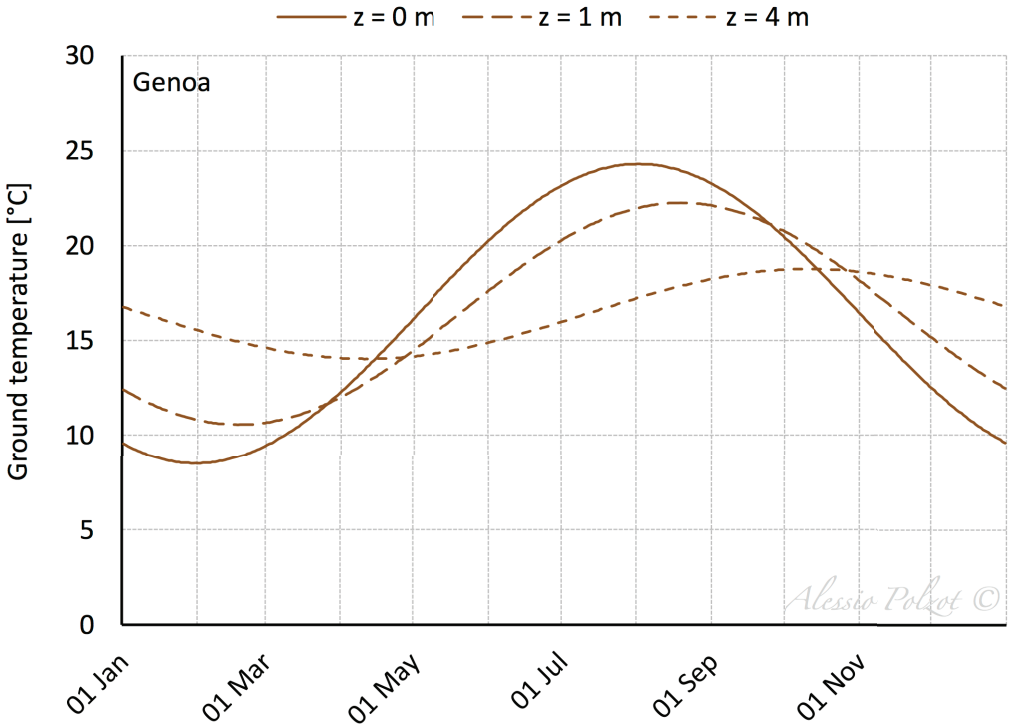

Figure 4.4.a - Annual profiles of the ground temperature for Genoa.

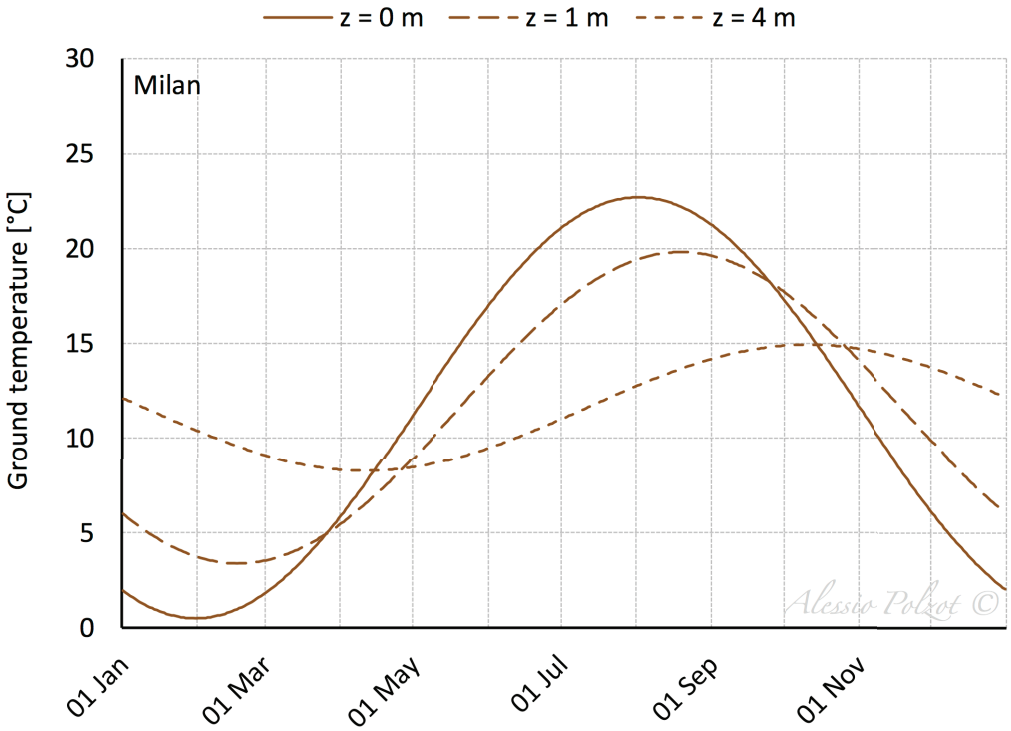

Figure 4.4.b - Annual profiles of the ground temperature for Milan.

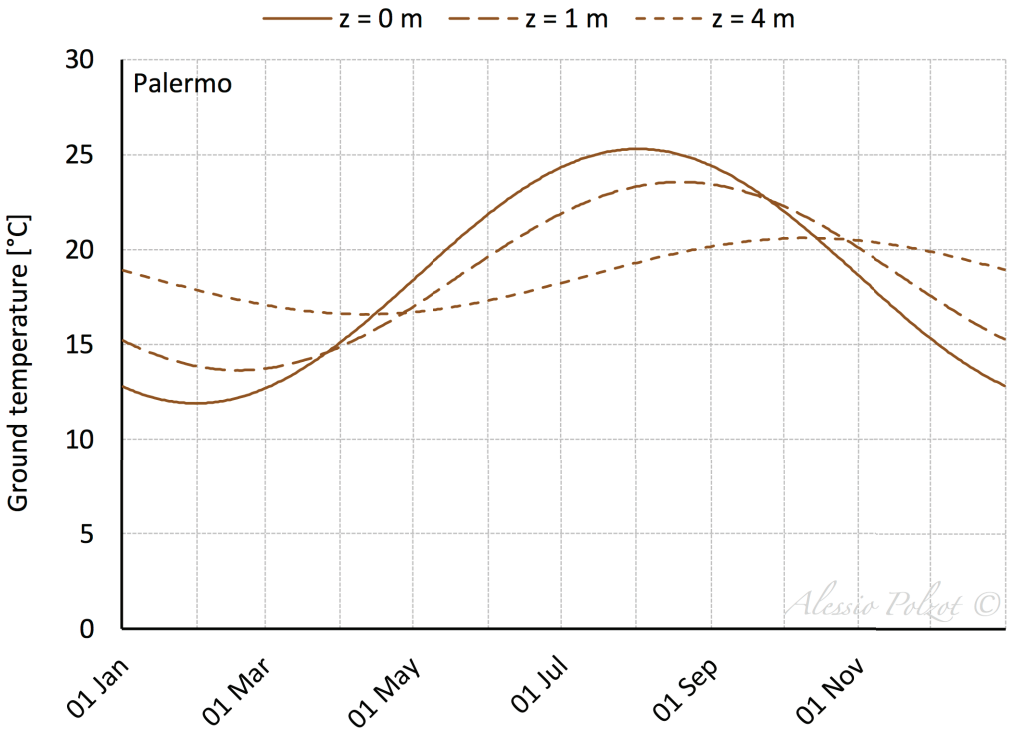

Figure 4.4.c - Annual profiles of the ground temperature for Palermo.

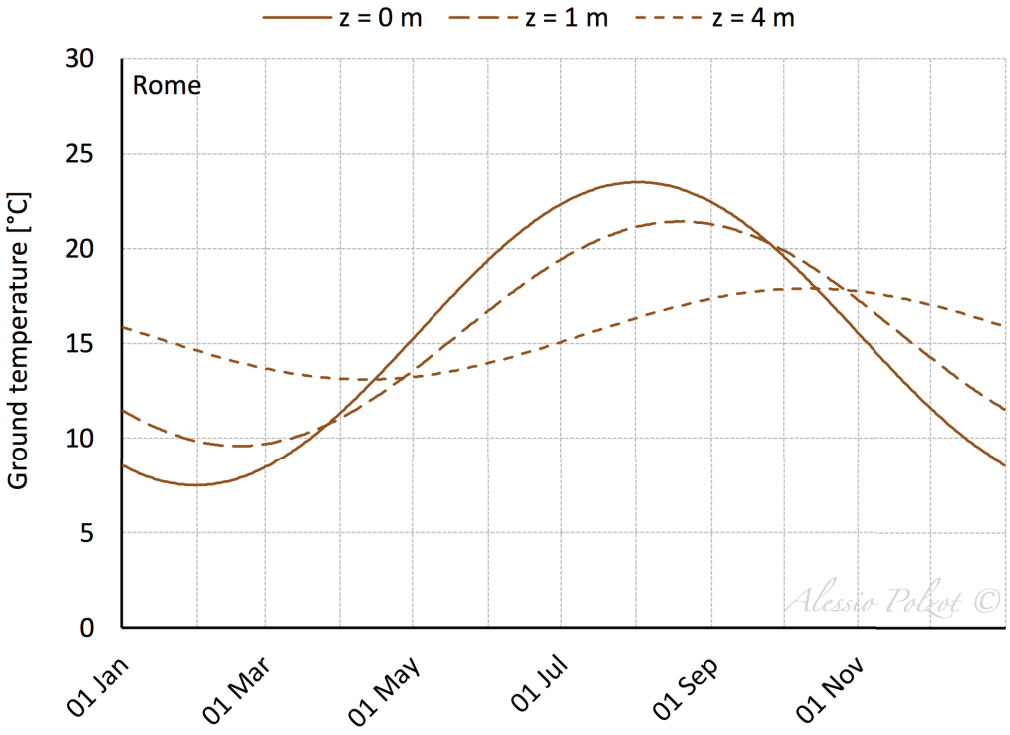

Figure 4.4.d - Annual profiles of the ground temperature for Rome.

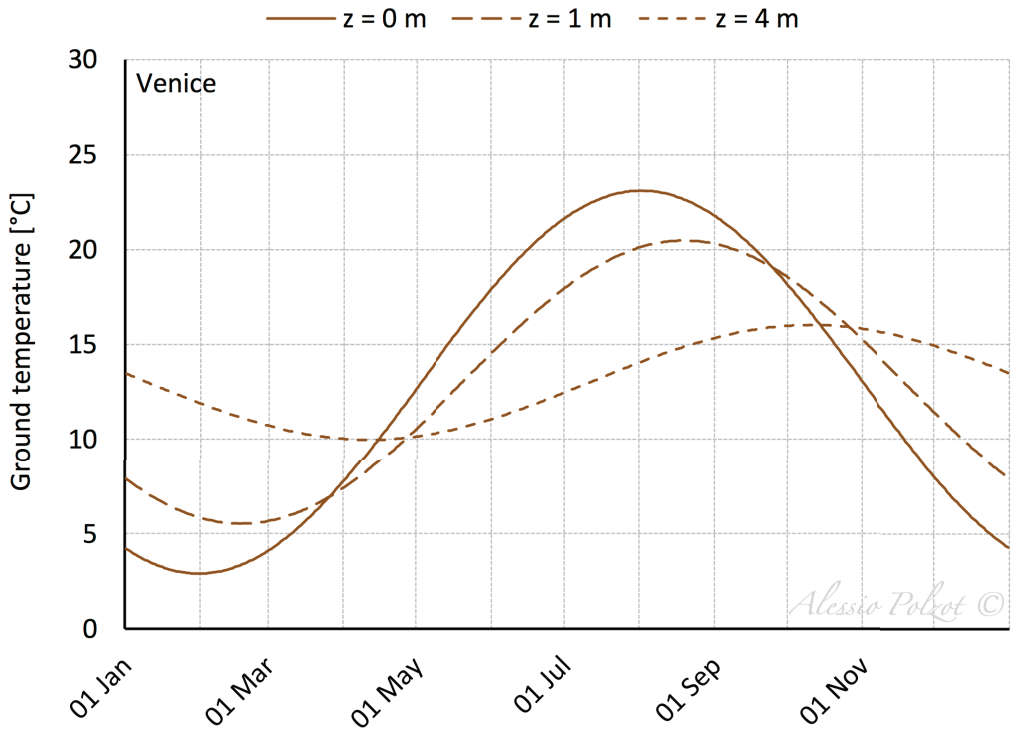

Figure 4.4.e - Annual profiles of the ground temperature for Venice.

4.5 Reference

- Kasuda, T., Archenbach, P.R., 1965. Earth temperature and thermal diffusivity at selected stations in the United States. ASHRAE Transactions 71(1), 61-74.
- Remund, J., Lang, R., Kunz, S., 2014. Meteonorm. Metotest, Bern (CH).

Chapter V

Refrigerated display cabinets and cold rooms

5.1 Refrigerated display cabinets

The refrigerated display cabinet model developed calculates the performance at off-rated conditions using the performance information at rated conditions, the performance curves for the latent heat exchange with the surrounding environment and the defrost heat load. The energy use for the auxiliary devices is based on the nominal power of the devices, the control type and the time schedules (EnergyPlus, 2013).

The sensible and latent heat exchange with the environment, which impacts the temperature and humidity in the zone where the refrigerated display cabinet is located, is taken into account along with the sensible load from the auxiliary devices. The heat extraction rate at the cabinet evaporator, Q_{RDC}, is made up of three parts:

$$\dot{Q}_{RDC} = \dot{Q}_{sen} + \dot{Q}_{lat} + \dot{Q}_{aux} \quad (3)$$

where:

$\dot{Q}_{sen}$ is the sensible load, which includes the sensible heat transfer by ambient air infiltration in the refrigerated display cabinet volume through the air curtains in open fronted cabinets or via door openings, the conductive heat transfer through the cabinet walls due to the difference between the operating dry-bulb temperature and the zone air dry-bulb temperature and the radiative heat transfer to the cabinet [W];

$\dot{Q}_{lat}$ is the latent heat transfer by ambient air infiltration in the refrigerated volume [W];

$\dot{Q}_{aux}$ is the sensible load from auxiliary devices as a fraction of their electric power which has to be removed from the refrigerated volume [W]:

$$\dot{Q}_{aux} = \dot{Q}_{lights} + \dot{Q}_{as} + \dot{Q}_{defrost} + \dot{Q}_{fan} \quad (4)$$

where:

$\dot{Q}_{lights}$ is the lighting heat load [W];

$\dot{Q}_{as}$ is the anti-sweat heater heat load [W];

$\dot{Q}_{defrost}$ is the defrost heat load [W];

$\dot{Q}_{fan}$ is the evaporator fan heat load [W];

The total cooling capacity at rated conditions, typically 25 °C and 60 % relative humidity according to ISO 23953-1:2015 (2015) and ISO 23953-2:2015 (2015), is provided by the refrigerated display cabinet manufacturer and is adjusted taking into account the actual and time-dependent working conditions in a supermarket (off-rated conditions). The influence of indoor air temperature and humidity on the sensible and latent fractions of the cooling load are considered as well as the time schedule for auxiliary devices. The estimation of the cooling load is based on the model proposed by Faramarzi (Faramarzi, 1999, Cortella et al., 2011). The latent air infiltration load is calculated through the latent heat ratio (LHR), which typically ranges from 0.1 to 0.3 (ASHRAE, 2002; Howell, 1993a; Howell, 1993b) depending on the refrigerated display cabinet configuration and operating temperature.

The sensible load is calculated by subtracting the auxiliary devices sensible loads at rated conditions from the rated total cooling capacity of the cabinet. Whenever the total heat load on the cabinet is greater than the available evaporator capacity, such as during defrost operations, the load is accumulated to be met during subsequent time steps.

5.1.1 Fan

The fan is turned off during the entire scheduled defrost drip-down time period for refrigerated display cabinets with hot-gas or electric defrost while it operates continuously for off-cycle defrost or for cabinets without defrost.

The electric power of the fan is given by:

$$\dot{W}_{fan} = \dot{w}_{fan,R}\, L_{RDC}\, (1 - SCH_{dripdown}) \quad (5)$$

where:

$\dot{w}_{fan,R}$ is the operating cabinet fan power per unit length [W · m^{-1}];

L_{RDC} is the refrigerated display cabinet length [m];

$SCH_{dripdown}$ is the defrost drip-down schedule. It is 0 when the cabinets with hot-gas or electric defrost is being defrosting, otherwise it is 1 [-].
All fan power results in a direct heat load on the evaporator:

$$\dot{Q}_{fan} = \dot{W}_{fan} \tag{6}$$

5.1.2 Lighting

The electric power of the refrigerated display cabinet lights is given by:

$$\dot{W}_{lights} = \dot{w}_{lights,R}\, L_{RDC}\, SCH_{lights} \tag{7}$$

where:
$\dot{w}_{lights,R}$ is the installed lighting power per unit length of the cabinet [W · m^{-1}];
L_{RDC} is the refrigerated display cabinet length [m];
SCH_{lights} is the lighting schedule and it ranges from 0, when the lights are turned off, to 1, when the lights are fully on at the installed lighting power level [-].
The fraction of the lighting energy that directly contributes to the evaporator heat load is:

$$\dot{Q}_{lights} = \dot{W}_{lights}\, y_{lights} \tag{8}$$

where:
$\dot{W}_{lights}$ is the electric power of the cabinet lights [W];
y_{lights} is the fraction of lighting energy to the cabinet [-].

5.1.3 Anti-sweat heater

The anti-sweat heaters warm the refrigerated display cabinet doors to provide protection from the moisture condensation. Different control strategies are used to control this devices depending on the operating temperature of the cabinet and the type of the device installed.
The electric power and the heat load for the refrigerated display cabinets without anti-sweat heater are:

$$\dot{W}_{as} = 0 \tag{9}$$

$$\dot{Q}_{as} = 0 \tag{10}$$

When cycling of the heaters is not recommended the electric power and the heat load are:

$$\dot{W}_{as} = \dot{w}_{as,R}\, L_{RDC} \tag{11}$$

$$\dot{Q}_{as} = \dot{W}_{as}\, y_{as} \tag{12}$$

where:

$\dot{w}_{as,R}$ is the anti-sweat heater power per unit length of the cabinet [W · m^{-1}];

L_{RDC} is the refrigerated display cabinet length [m];

y_{as} is the fraction of anti-sweat heater energy to the cabinet [-].

A better control strategy to save energy is to reduce the anti-sweat power at lower ambient relative humidity levels:

$$\dot{W}_{as} = \dot{w}_{as,R}\, L_{RDC} \left(1 - \frac{RH_R - RH}{RH_R - RH_{min}}\right) \tag{13}$$

$$\dot{Q}_{as} = \dot{W}_{as}\, y_{as} \tag{14}$$

where:

$\dot{w}_{as,R}$ is the anti-sweat heater power per unit length of the cabinet [W · m^{-1}];

L_{RDC} is the refrigerated display cabinet length [m];

RH_R is the rated ambient relative humidity (typically 55 %) [%];

RH is the relative humidity of the zone air [%];

RH_{min} is the relative humidity at zero anti-sweat heater energy [%];

y_{as} is the fraction of anti-sweat heater energy to the cabinet [-].

A similar control strategy is to vary the anti-sweat heater power linearly based on the ambient air dew-point temperature and the operating temperature of the cabinet:

$$\dot{W}_{as} = \dot{w}_{as,R}\, L_{RDC} \left(\frac{t_{dp} - t_o}{t_{dp,R} - t_o}\right) \tag{15}$$

$$\dot{Q}_{as} = \dot{W}_{as}\, y_{as} \tag{16}$$

where:

$\dot{w}_{as,R}$ is the anti-sweat heater power per unit length of the cabinet [W · m^{-1}];

L_{RDC} is the refrigerated display cabinet length [m];

t_{dp} is the dew-point temperature of the zone air [°C];

t_o is the operating temperature of the cabinet [°C];

$t_{dp,R}$ is the rated ambient dew-point temperature [°C];

y_{as} is the fraction of anti-sweat heater energy to the cabinet [-].

Henderson and Khattar (1999) presented a theoretical model to simulate the performance of anti-sweat heater operation based on a heat balance equation. The model calculates the amount of heat required to hold the surface at the dew-point temperature of the ambient air:

$$\dot{W}_{as} = L_{RDC} \left(\frac{\left(t_{dp} - t\right) H}{R_{air}} + \frac{\left(t_{dp} - t_o\right) H}{R_{cabinet}} \right) \quad (17)$$

$$\dot{Q}_{as} = \dot{W}_{as}\, y_{as} \quad (18)$$

where:

L_{RDC} is the refrigerated display cabinet length [m];

t_{dp} is the dew-point temperature of the zone air [°C];

t is the dry-bulb temperature of the zone air [°C];

H is the height of the cabinet [m];

R_{air} is the air film resistance [$m^2 \cdot °C \cdot W^{-1}$];

t_o is the operating temperature of the cabinet [°C];

$R_{cabinet}$ is the heat transfer resistance of the cabinet [$m^2 \cdot °C \cdot W^{-1}$];

y_{as} is the fraction of anti-sweat heater energy to the cabinet [-].

The heat transfer resistance of the cabinet can be determined by rearranging the above equation at rated conditions assuming that the rated anti-sweat heater power is required to avoid moisture condensation at rated ambient air conditions, while the air film resistance can be assumed constant:

$$R_{air} = 0.3169 \quad (19)$$

$$R_{cabinet} = \frac{t_{dp,R} - t_o}{\frac{\dot{w}_{as,R}}{H} - \frac{t_{dp,R} - t_R}{R_{air}}} \quad (20)$$

where:

$t_{dp,R}$ is the rated ambient dew-point temperature [°C];

t_o is the operating temperature of the cabinet [°C];

$\dot{w}_{as,R}$ is the anti-sweat heater power per unit length of the cabinet [W · m^{-1}];
H is the height of the cabinet [m];
t_R is the rated ambient dry-bulb temperature [°C];
R_{air} is the air film resistance [m^2 · °C · W^{-1}].

5.1.4 Defrost

The refrigerated display cabinets require a specific number of defrost cycles per day for a pre-determined length of time. In this periods the evaporator of the cabinet is turned off to melt the frost accumulated and an additional drip-down time can be scheduled to allow the water to drip from the evaporator and drain from the case.
The electric power of the defrost is given by:

$$\dot{W}_{defrost} = \dot{w}_{defrost,R}\, L_{RDC}\, SCH_{defrost}\, x_{defrost} \tag{21}$$

where:
$\dot{w}_{defrost,R}$ is the defrost power per unit length and it is different from 0 only for cabinets with electric defrost [W · m^{-1}];
L_{RDC} is the refrigerated display cabinet length [m];
$SCH_{defrost}$ is the defrost schedule and it is 1 when defrost is running, otherwise it is 0 [-];
$x_{defrost}$ is the fraction of maximum defrost time [-].
The frost accumulation is a function of the humidity level in the zone air and the defrost operations can be reduced when zone air humidity level is low. A correction curve based on the operating temperature of the cabinet can be used. For cabinets without defrost control:

$$x_{defrost} = 1 \tag{22}$$

while the correction curve is:

$$x_{defrost} = 1 - (RH_R - RH)\,(a_1 + a_2\, t_o + a_3\, t_o^2 + a_4\, t_o^3) \tag{23}$$

where:
RH_R is the rated ambient relative humidity (typically 55 %) [%];
RH is the relative humidity of the zone air [%];

t_o is the operating temperature of the cabinet [°C];

a_i are the curve coefficients [-].

The correction curves of four different refrigerated display cabinets is represented in Figure 5.1.a.

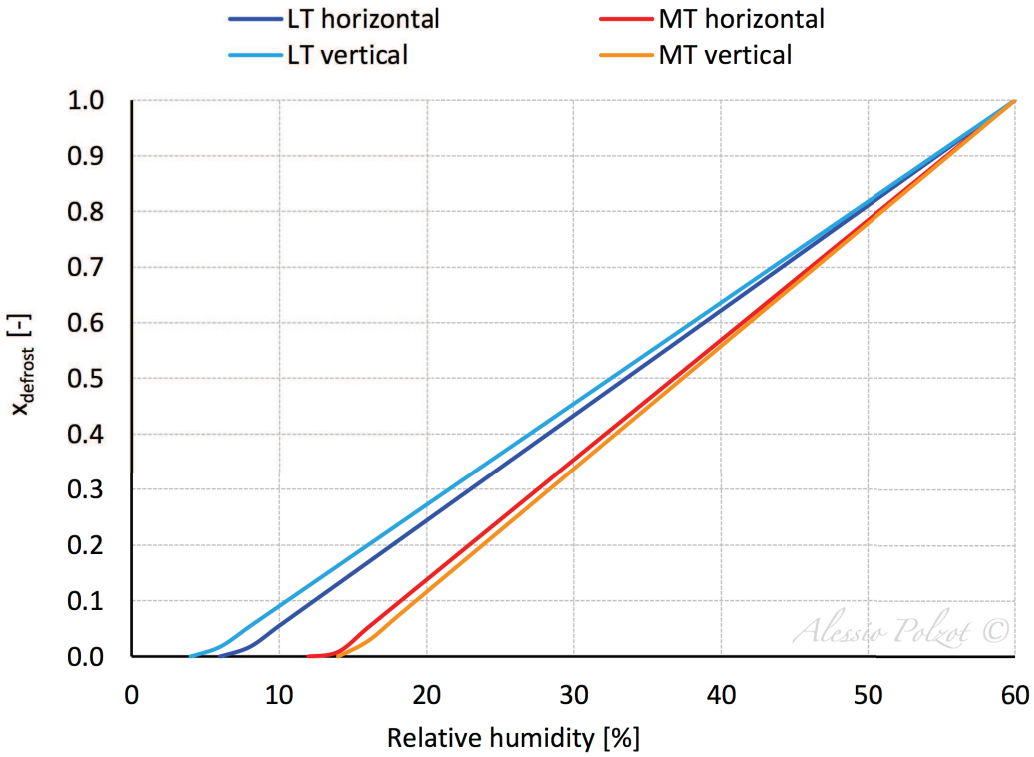

Figure 5.1.a - Defrost correction curves for different refrigerated display cabinets.

The defrost energy which does not contributes directly to melting the frost results as a heat load on the evaporator:

$$\dot{Q}_{defrost} = \max\left(0;\ \dot{W}_{defrost}\, SCH_{defrost} - \frac{m_{frost}\,\lambda_f}{\Delta\theta}\right) \qquad (24)$$

where:

$\dot{W}_{defrost}$ is the electric power of the defrost [W];

$SCH_{defrost}$ is the defrost schedule;

m_{frost} is the amount of accumulated frost on the evaporator [kg];

λ_f is the specific latent heat of fusion of water [J · kg^{-1}];

$\Delta\theta$ is the simulation time step [s].

5.1.5 Sensible load

The refrigerated display cabinets remove sensible energy from the environment. At rated conditions this energy is the difference between the rated total cooling capacity of the cabinet and the auxiliary devices sensible loads:

$$\dot{Q}_{sen,R} = \dot{q}_{RDC,R}\, L_{RDC}\, RTF\, (1 - LHR) - \left(\dot{Q}_{fan} + \dot{Q}_{lights} + \dot{Q}_{as}\right) \quad (25)$$

where:

$\dot{q}_{RDC,R}$ is the rated total cooling capacity per unit length of the cabinet [W · m^{-1}];

L_{RDC} is the refrigerated display cabinet length [m];

RTF is the runtime fraction of the cabinet and it ranges typically from 0.8 to 0.9. Even at rated conditions, the refrigerated display cabinets include additional cooling capacity to account for product stocking and recovery from defrost [-];

LHR is the latent heat ratio [-];

$\dot{Q}_{fan}$ is the evaporator fan heat load [W];

$\dot{Q}_{lights}$ is the lighting heat load [W];

$\dot{Q}_{as}$ is the anti-sweat heater heat load [W].

The sensible load at rated conditions is adjusted to account the time-dependent working conditions of the cabinet and the sensible load at off-rated conditions is given by:

$$\dot{Q}_{sen} = \dot{Q}_{sen,R}\, \frac{t - t_o}{t_R - t_o}\, SCH_{cc} \quad (26)$$

where:

$\dot{Q}_{sen,R}$ is the sensible load at rated conditions [W];

t is the dry-bulb temperature of the zone air [°C];

t_o is the operating temperature of the cabinet [°C];

t_R is the rated ambient temperature (typically 25 °C) [°C];

SCH_{cc} is the case credit fraction schedule. This value, which ranges from 0 to 1, takes into account the different working conditions of the cabinet during unoccupied hours. For example, in this time period a covering can be applied on the refrigerated display cabinets reducing the air infiltration and the sensible load [-].

The impact of the cabinet on the surrounding environment include the fractions of the lighting energy and of anti-sweat heater energy that contribute to the zone heat load and the sensible energy removed from the zone by the cabinet:

$$\dot{Q}_{sen,zone} = \dot{W}_{lights}\left(1 - y_{lights}\right) + \dot{W}_{as}\left(1 - y_{as}\right) - \dot{Q}_{sen} \quad (27)$$

where:

$\dot{W}_{lights}$ is the electric power of the cabinet lights [W];

y_{lights} is the fraction of lighting energy to the cabinet [-];

$\dot{W}_{as}$ is the electric power of the cabinet anti-sweat heater [W];

y_{as} is the fraction of anti-sweat heater energy to the cabinet [-];

$\dot{Q}_{sen}$ is the sensible load [W].

5.1.6 Latent load

The latent load is the product of the latent heat transfer by ambient air infiltration in the refrigerated volume and a factor which takes into account the different humidity levels of the zone:

$$\dot{Q}_{lat} = \dot{q}_{RDC,R}\, L_{RDC}\, RTF\, LHR\, SCH_{cc}\, x_{lat} \quad (28)$$

where:

$\dot{q}_{RDC,R}$ is the rated total cooling capacity per unit length of the cabinet [W · m^{-1}];

L_{RDC} is the refrigerated display cabinet length [m];

RTF is the runtime fraction of the cabinet [-];

LHR is the latent heat ratio [-];

SCH_{cc} is the case credit fraction schedule [-];

x_{lat} is ratio of the off-rated conditions latent load to rated conditions latent load [-].

The latent load on the cabinet evaporator is a function of the relative humidity of the zone and the ratio of the off-rated latent load to rated latent load can be calculate through two different curves, depending on the type of the cabinet. The first curve is based on the operating temperature of the cabinet:

$$x_{lat} = 1 - \left(RH_R - RH\right)\left(b_1 + b_2\, t_o + b_3\, t_o^2 + b_4\, t_o^3\right) \quad (29)$$

where:

RH_R is the rated ambient relative humidity (typically 55 %) [%];

RH is the relative humidity of the zone air [%];

t_o is the operating temperature of the cabinet [°C];

b_i are the curve coefficients [-].

The first curve of four different refrigerated display cabinets is represented in Figure 5.1.b.

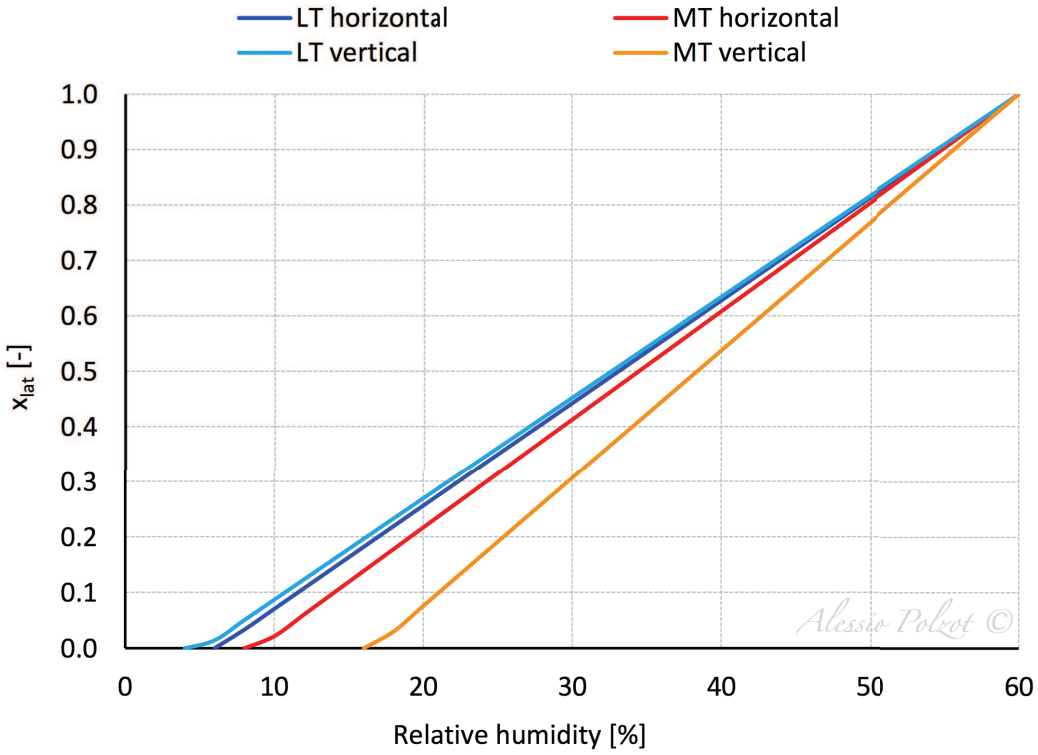

Figure 5.1.b - Latent curve based on the operating temperature for different refrigerated display cabinets.

The second curve is based on the relative humidity of the zone:

$$x_{lat} = c_1 + c_2\, RH + c_3\, RH^2 + c_4\, RH^2 \qquad (30)$$

where:

RH is the relative humidity of the zone air [%];

c_i are the curve coefficients [-].

The second curve of two different open refrigerated display cabinets is represented in Figure 5.1.c.

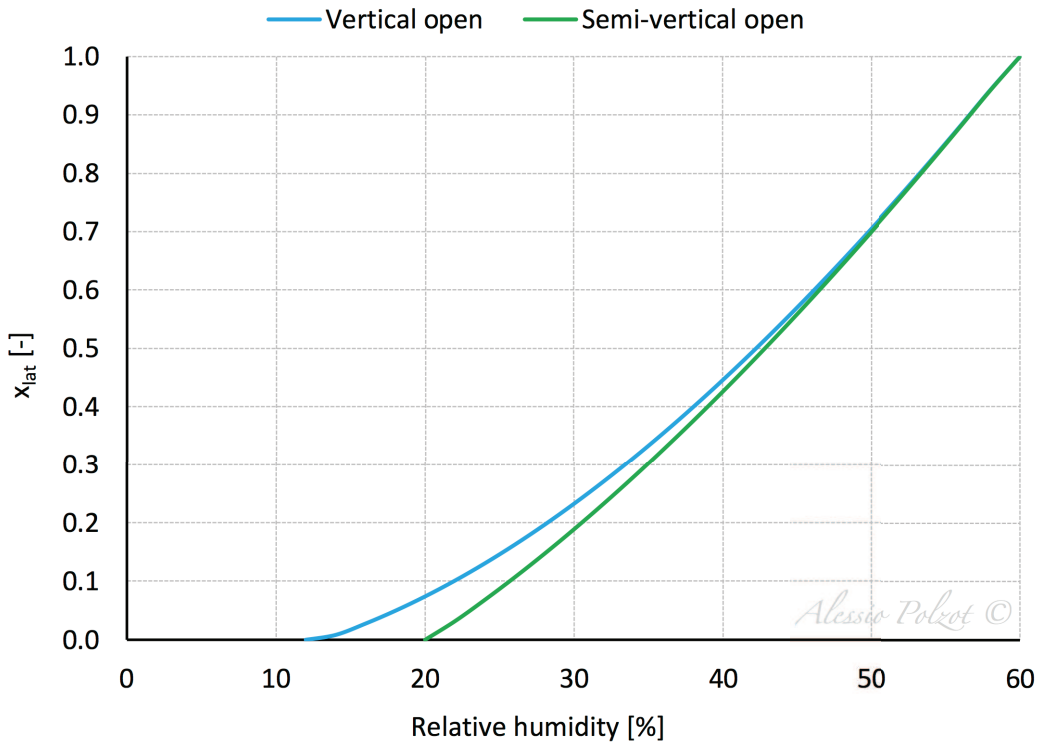

Figure 5.1.c - Latent curve based on the relative humidity of the zone for different refrigerated display cabinets.

5.2 Cold rooms

The cold room model developed is based on the ASHRAE load model (ASHRAE, 2006; ASHRAE, 2009) and it calculates the performance at off-rated conditions using the performance information at rated conditions (EnergyPlus, 2013).

The cold rooms differ from the refrigerated display cabinets in that they are always equipped with doors or door protections. The mass flow rate infiltrating into the cold room through the door is calculated according to the analytical model by Gosney and Olama (1975), which has proven to fit the experimental data better than other models in the comparison carried out in Foster et al. (2003).

The energy use for the auxiliary devices is based on the nominal power of the devices, the control type and the time schedules.

The heat extraction rate at the cold room evaporator, Q_{CR}, is made up of four parts:

$$\dot{Q}_{CR} = \dot{Q}_{env} + \dot{Q}_{inf} + \dot{Q}_{defrost} + \dot{Q}_{aux} \quad (31)$$

where:

$\dot{Q}_{env}$ is the conductive heat transfer through the cold room envelope [W];

$\dot{Q}_{inf}$ is the heat load due to sensible and latent heat transfer by air infiltration through doorway in the refrigerated volume [W];

$\dot{Q}_{defrost}$ is the defrost heat load [W];

$\dot{Q}_{aux}$ is the sensible load from auxiliary devices as a fraction of their electric power which has to be removed from the refrigerated volume [W]:

$$\dot{Q}_{aux} = \dot{Q}_{lights} + \dot{Q}_{heaters} + \dot{Q}_{fan} \quad (32)$$

where:

$\dot{Q}_{lights}$ is the lighting heat load [W];

$\dot{Q}_{heaters}$ is the heaters heat load [W];

$\dot{Q}_{fan}$ is the fan heat load [W].

5.2.1 Lighting

The electric power of the cold room lights is given by:

$$\dot{W}_{lights} = \dot{W}_{lights,R}\, SCH_{lights}\, F_d \quad (33)$$

where:

$\dot{W}_{lights,R}$ is the installed lighting power [W];

SCH_{lights} is the lighting schedule and it ranges from 0, when the lights are turned off, to 1, when the lights are fully on at the installed lighting power level [-].

F_d is the fraction of time the door is open and it ranges from 0 to 1 if the cold room has a control strategy which turn on the lights when the door is open, otherwise it is equal to 1 [-];

The sensible energy of the lighting that contributes to the evaporator heat load is:

$$\dot{Q}_{lights} = \dot{W}_{lights} \quad (34)$$

where:

$\dot{W}_{lights}$ is the electric power of the cold room lights [W].

5.2.2 Heaters

The electric power of the cold room heaters is given by:

$$\dot{W}_{heaters} = \dot{W}_{heaters,R}\, SCH_{heaters} \quad (35)$$

where:

$\dot{W}_{heaters,R}$ is the installed heaters power, including the anti-sweat heaters, the floor heaters and the door heaters [W];

$SCH_{heaters}$ is the heaters schedule [-].

The sensible energy of the heaters that contributes to the evaporator heat load is:

$$\dot{Q}_{heaters} = \dot{W}_{heaters} \quad (36)$$

where:

$\dot{W}_{heaters}$ is the electric power of the cold room heaters [W].

5.2.3 Fan

The fan is turned off during the entire scheduled defrost drip-down time period for cold rooms with hot-fluid or electric defrost while it operates continuously for off-cycle defrost.

The electric power of the fan is given by:

$$\dot{W}_{fan} = \dot{W}_{fan,R}\, (1 - SCH_{dripdown}) \quad (37)$$

where:

$\dot{W}_{fan,R}$ is the installed fan power [W];

$SCH_{dripdown}$ is the defrost drip-down schedule. It is 0 when the cabinets with hot-fluid or electric defrost is being defrosting, otherwise it is 1 [-].

The sensible energy of the fan that contributes to the evaporator heat load is:

$$\dot{Q}_{fan} = \dot{W}_{fan} \quad (38)$$

5.2.4 Conductive heat transfer

The conductive heat transfer describes the sensible energy exchange which takes place between the surfaces of the cold room and the surrounding zone, and it is split into three parts:

$$\dot{Q}_{env} = \dot{Q}_{walls} + \dot{Q}_{door} + \dot{Q}_{floor} \tag{39}$$

where:

$\dot{Q}_{walls}$ is the sensible heat transfer through the walls and the ceiling of the cold room [W];

$\dot{Q}_{door}$ is the sensible heat transfer through the closed door of the cold room [W];

$\dot{Q}_{floor}$ is the sensible heat transfer through the floor of the cold room [W].

The above mentioned sensible heat transfers are given by:

$$\dot{Q}_{walls} = U_{walls}\, A_{walls}(t - t_o) \tag{40}$$

$$\dot{Q}_{door} = U_{door}\, A_{door}(t - t_o) \tag{41}$$

$$\dot{Q}_{floor} = U_{floor}\, A_{floor}(t_{ground} - t_o) \tag{42}$$

where:

U_{walls} is the thermal conductance of the walls and the ceiling of the cold room [W · m^{-2} · K^{-1}];

A_{walls} is the area of the walls and the ceiling of the cold room [m^2];

t is the dry-bulb temperature of the zone air [°C];

t_o is the operating temperature of the cold room [°C];

U_{door} is the thermal conductance of the cold room door [W · m^{-2} · K^{-1}];

A_{door} is the area of the cold room door [m^2];

U_{floor} is the thermal conductance of the cold room floor [W · m^{-2} · K^{-1}];

A_{floor} is the area of the cold room floor [m^2];

t_{ground} is the ground temperature [°C].

5.2.5 Infiltration load

The heat load due to the air infiltration through the doorway is both a sensible and a latent load as well as the corresponding loads upon the surrounding zone. The mass of dry air infiltrating into the cold room is assumed to be equal to the mass of dry air infiltrating out of the cold room into the zone and the air within the cold room is assumed to be at 90 % relative humidity.

The sensible and latent infiltration load for fully established flow is:

$$\dot{Q}_{inf,ff} = 0.221 A_{door}(h - h_{CR})\rho_{CR}\sqrt{1 - \frac{\rho}{\rho_{CR}}}\sqrt{gH_{door}}\,F_m \qquad (43)$$

where:

A_{door} is the area of the cold room door [m^2];

h is the enthalpy of the zone air [$J \cdot kg^{-1}$];

h_{CR} is the enthalpy of the cold room air [$J \cdot kg^{-1}$];

ρ_{CR} is the density of the cold room air [$kg \cdot m^{-3}$];

ρ is the density of the zone air [$kg \cdot m^{-3}$];

g is the gravitational acceleration (9.78 $m \cdot s^{-2}$) [$m \cdot s^{-2}$];

H_{door} is the height of the door [m];

F_m is the density factor (ASHRAE, 2001) [-]:

$$F_m = \sqrt{\left(\frac{2}{1 + \sqrt[3]{\frac{\rho_{CR}}{\rho}}}\right)^3} \qquad (44)$$

where:

ρ_{CR} is the density of the cold room air [$kg \cdot m^{-3}$];

ρ is the density of the zone air [$kg \cdot m^{-3}$].

The infiltration load for fully established flow is adjusted taking into account the difference between the dry-bulb temperature of the zone air and the operating temperature of the cold room, the fraction of time the door is open and the doorway protection type:

$$\dot{Q}_{inf} = \dot{Q}_{inf,ff} F_d F_f \left(1 - F_p\right) \qquad (45)$$

where:

F_d is the fraction of time the door is open [-];

F_f is the flow factor and it is equal to 0.8 if the difference between the dry-bulb temperature of the zone air and the operating temperature of the cold room is greater than 11°C, otherwise it is equal to 1.1 [-];

F_p is the doorway protection factor and it is equal to 0.9 if there is a strip curtain, it is equal to 0.5 if there is an air curtain and it is equal to 0 if there is no protection [-].

The sensible fraction of the load on the cold room evaporator continue throughout the defrost and drip-down periods, however the latent fraction is assumed to be null during the drip-down periods:

$$\dot{Q}_{inf,lat} = \dot{m}_w \, \Delta H_{sub} \left(1 - SCH_{dripdown}\right) \tag{46}$$

where:

$\dot{m}_w$ is the mass flow rate of water removed from the infiltrating air [kg · s^{-1}];

ΔH_{sub} is the latent heat of sublimation [J · kg^{-1}];

$SCH_{dripdown}$ is the defrost drip-down schedule [-].

The sensible load due to air infiltration is given by:

$$\dot{Q}_{inf,sen} = \dot{Q}_{inf} - \dot{m}_w \, \Delta H_{sub} \tag{47}$$

where:

$\dot{Q}_{inf}$ is the heat load due to sensible and latent heat transfer by air infiltration through doorway in the refrigerated volume [W];

$\dot{m}_w$ is the mass flow rate of water removed from the infiltrating air [kg · s^{-1}];

ΔH_{sub} is the specific latent heat of sublimation [J · kg^{-1}].

The mass flow rates of dry air infiltrating into the cold room and of water removed from the infiltrating air can be calculated with:

$$\dot{m}_a = \frac{\dot{Q}_{inf}}{h - h_{CR}} \tag{48}$$

$$\dot{m}_w = \dot{m}_a (x - x_{CR}) \tag{49}$$

where:

$\dot{Q}_{inf}$ is the heat load due to sensible and latent heat transfer by air infiltration through doorway in the refrigerated volume [W];

h is the enthalpy of the zone air [J · kg^{-1}];

h_{CR} is the enthalpy of the cold room air [J · kg^{-1}];

x is the specific humidity of the zone air [kg · kg^{-1}];

x_{CR} is the specific humidity of the cold room air [kg · kg^{-1}].

5.2.6 Defrost

The amount of frost added to the evaporator coils is calculated when the defrost operations does not take place and it is used to determine the load upon the cold room during the defrost operations:

$$m_{ice} = \dot{m}_w \, \Delta\theta \, (1 - SCH_{dripdown}) \tag{50}$$

$\dot{m}_w$ is the mass flow rate of water removed from the infiltrating air [kg · s^{-1}];

$\Delta\theta$ is the simulation time step [s].

$SCH_{dripdown}$ is the defrost drip-down schedule [-].

The defrost load placed upon the cold room is calculated as product of the defrost capacity and the defrost schedule and it is reduced according to the amount of accumulated ice melted:

$$\dot{Q}_{defrost} = \dot{Q}_{def,R} \, SCH_{defrost} - \frac{m_{ice,melted} \, \Delta H_{fus}}{\Delta\theta} \tag{51}$$

where:

$\dot{Q}_{def,R}$ is the installed defrost power [W];

$SCH_{defrost}$ is the defrost schedule [-];

$m_{ice,melted}$ is the amount of ice melted during time step [kg];

ΔH_{fus} is the specific latent heat of fusion [J · kg^{-1}];

$\Delta\theta$ is the simulation time step [s].

If the cold room has a defrost temperature termination controller, the defrost cycle is assumed to end when all the frost added to the evaporators coils is melted. If the defrost schedule ends before all the frost is melted, the ice continues to accumulate until the next defrost cycle. A fraction of the defrost heat goes to raising the temperature of the coils and another fraction is transferred to the cold room environment. Baxter and Mei (2002) estimated that the fraction of defrost energy that goes directly to melt the ice is 0.7 for electric defrost and 0.3 for hot-fluid defrost.

The electric power of the defrost for cold rooms with electric defrost is given by:

$$\dot{W}_{defrost} = \dot{Q}_{def,R} \; SCH_{defrost} \tag{52}$$

where:

$\dot{Q}_{def,R}$ is the installed defrost electric power [W];

$SCH_{defrost}$ is the defrost schedule [-].

5.2.7 Sensible load

The sensible fraction of the cold room impact on the surrounding environment include the heat transfer through the door, the walls and the ceiling and the sensible fraction of the infiltration load:

$$\dot{Q}_{sen,zone} = -\left(\dot{Q}_{inf,sen} + \dot{Q}_{door} + \dot{Q}_{walls}\right) \tag{53}$$

where:

$\dot{Q}_{inf,sen}$ is the sensible load due to air infiltration [W]:

$\dot{Q}_{door}$ is the sensible heat transfer through the closed door of the cold room [W];

$\dot{Q}_{walls}$ is the sensible heat transfer through the walls and the ceiling of the cold room [W].

5.2.8 Latent load

The latent load on the surrounding zone is due to the latent heat transfer by ambient air infiltration in the refrigerated volume:

$$\dot{Q}_{lat,zone} = -\dot{Q}_{inf,lat} \tag{54}$$

where:

$\dot{Q}_{inf,lat}$ is the latent fraction of the infiltration load [W].

5.3 Database

The refrigerated display cabinet model developed uses a database file where the parameters necessary to define a cabinet are described. The model has as input the temperature class, the typology and the climate class of the cabinet and it reads from

the database the operating and the evaporator temperatures, the rated total cooling capacity per unit length, the latent heat ratio (LHR), the runtime fraction (RTF) and the parameters of the auxiliary devices.

The temperature classes describe the performance ranges of the cabinets and they are defined in Table 1 of the ISO 23953-2 (ISO 23953-2:2015, 2015):

- L1;
- L2;
- L3;
- M1;
- M2;
- H1;
- H2;
- S.

The climate classes, defined in Table 3 of the ISO 23953-2 (ISO 23953-2:2015, 2015), describe the room climate conditions where the cabinet is tested and where the rated conditions are calculated.

The different typology of refrigerated display cabinets are shown in Figure 5.3.a, Figure 5.3.b, Figure 5.3.c, Figure 5.3.d, Figure 5.3.e and Figure 5.3.f.

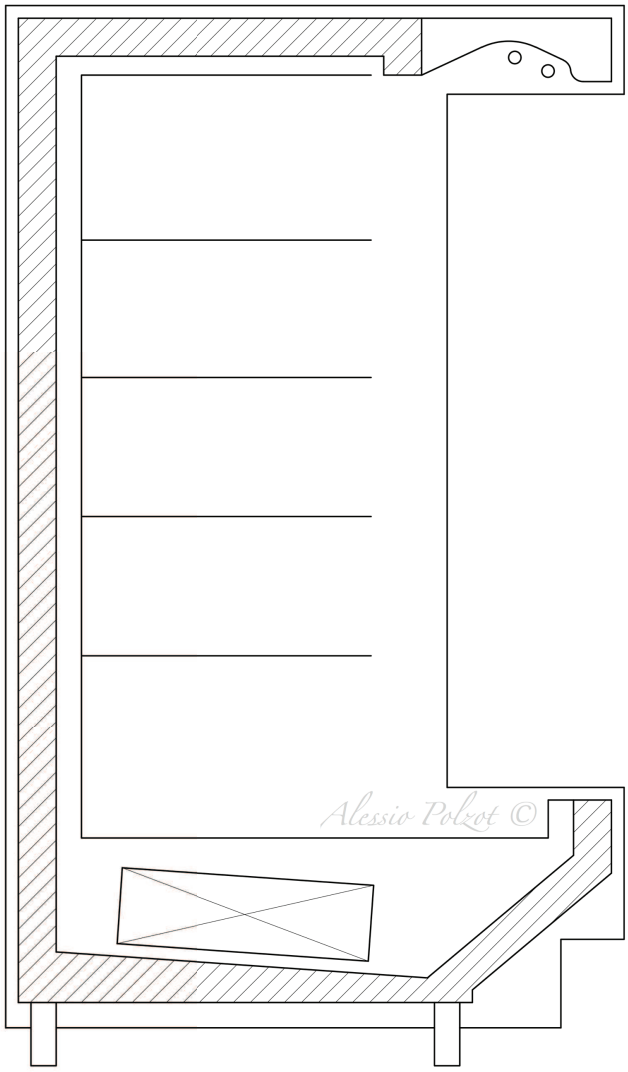

Figure 5.3.a - Vertical open refrigerated display cabinet.

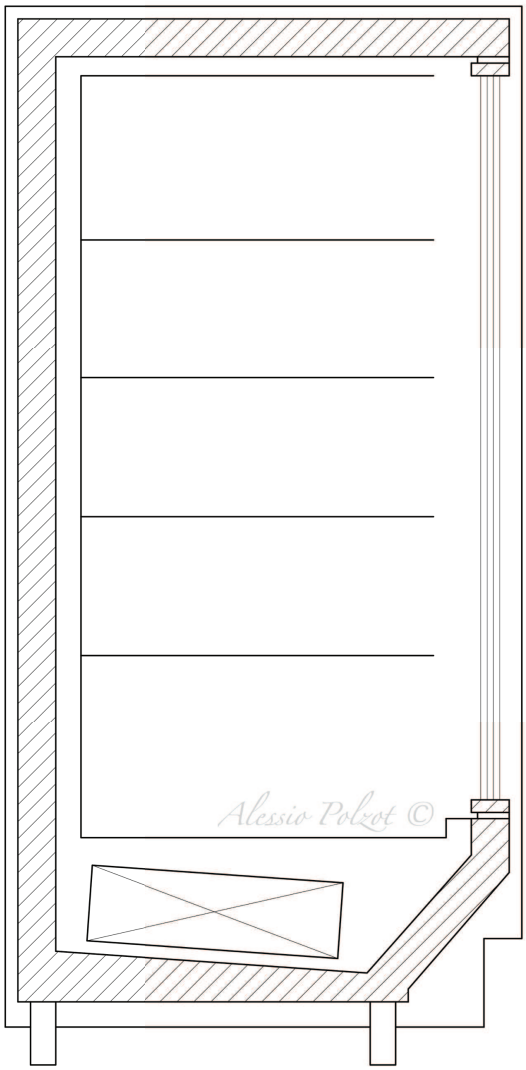

Figure 5.3.b - Vertical closed refrigerated display cabinet.

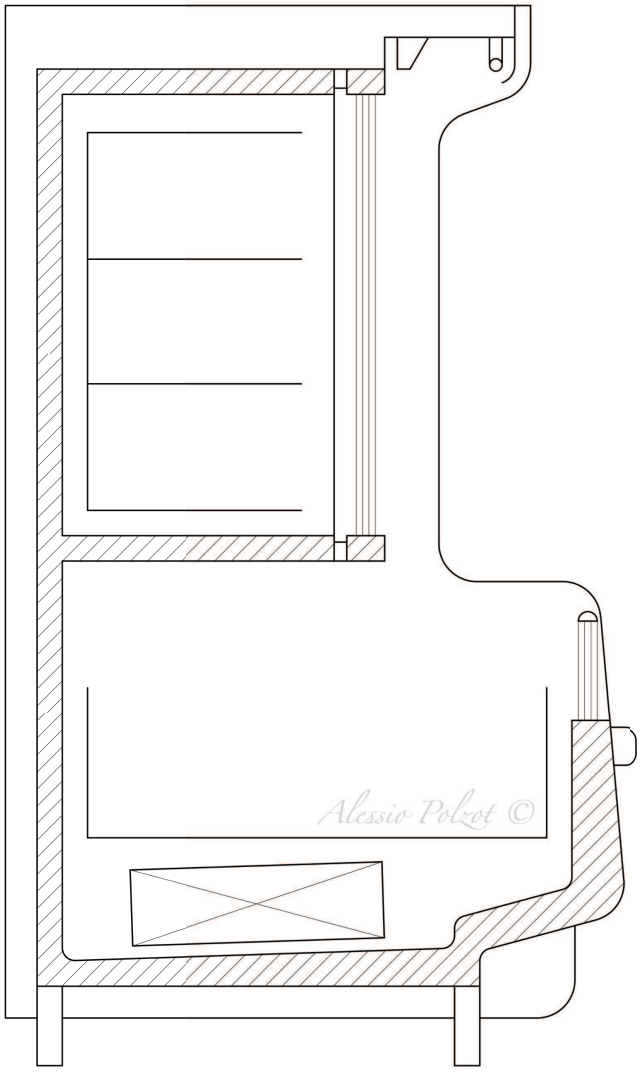

Figure 5.3.c - Combined refrigerated display cabinet.

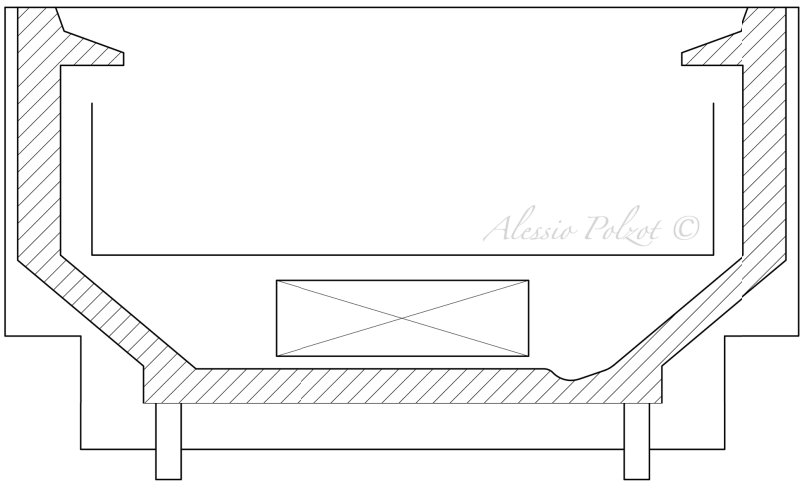

Figure 5.3.d - Horizontal refrigerated display cabinet.

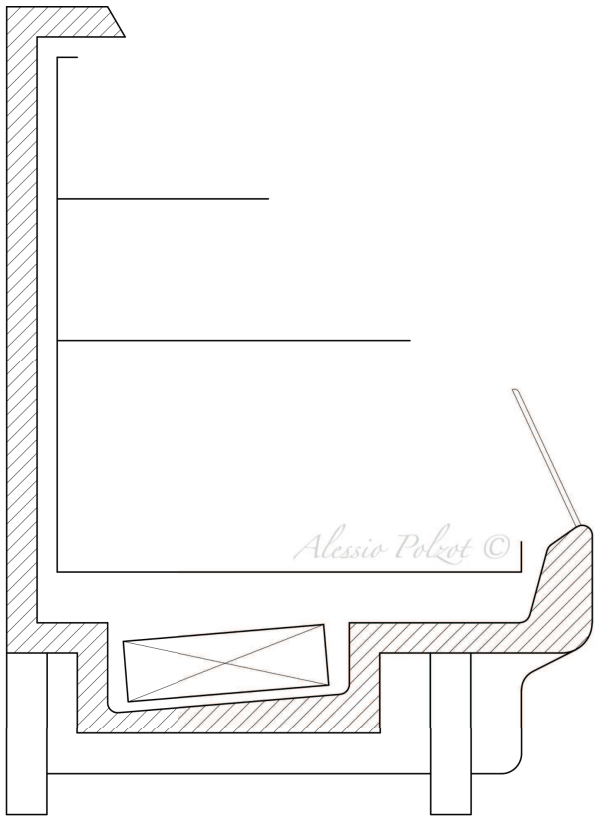

Figure 5.3.e - Semi-vertical refrigerated display cabinet.

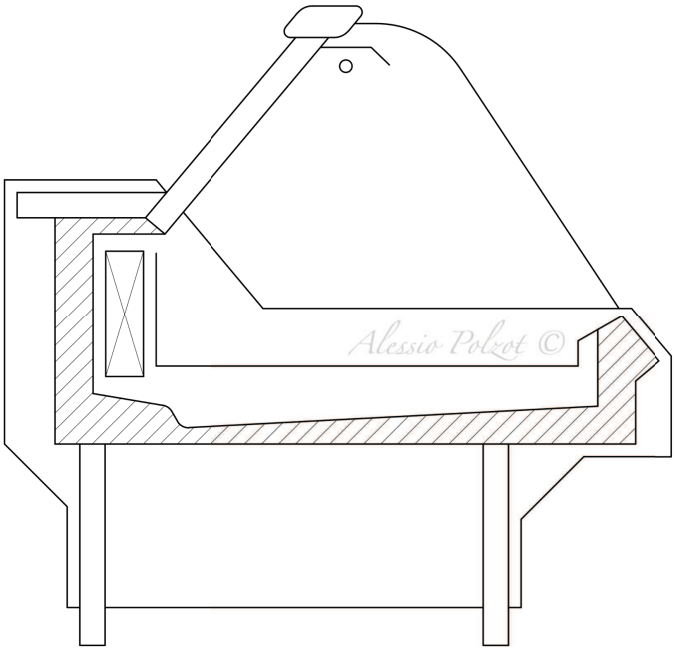

Figure 5.3.f - Serve-over refrigerated display cabinet.

Table 5.3.a shows an example of the database where a medium temperature cabinet (RDC01) and a low temperature cabinet (RDC02) are reported.

Parameter	Unit	RDC01	RDC02
Temperature class	[-]	M2	L2
Typology	[-]	Horizontal	Combined
Open or closed	[-]	Open	Closed
Climate class	[-]	3	3
Operating temperature	[°C]	-5.0	-27.5
Evaporator temperature	[°C]	-7.0	-35.0
Rated total capacity per unit length	[$W \cdot m^{-1}$]	620.0	553.0
Latent heat ratio	[-]	0.200	0.266
Runtime fraction	[-]	0.85	0.85
Latent ratio curve	[-]	1^{st}	1^{st}
Lighting power per unit length	[$W \cdot m^{-1}$]	44.8	28.2
Lighting fraction to case	[-]	0.85	0.85
Defrost type	[-]	Off-cycle	Electric
Defrost power per unit length	[$W \cdot m^{-1}$]	0.0	1280.8
Defrost cycles per day	[-]	4	1
Defrost time	[min]	70.0	40.0
Drip-down time	[min]	0.0	10.0
Fan power per unit length	[$W \cdot m^{-1}$]	31.2	7.4
Anti-sweat control	[-]	Dew-point	Dew-point
Anti-sweat power	[$W \cdot m^{-1}$]	60.0	281.4
Anti-sweat heater fraction to case	[-]	0.2	0.2
Case credit fraction	[-]	0.7	0.95

Table 5.3.a - Example of the refrigerated display cabinets databases.

5.4 Food storage equipment layout

The supermarket layout foresees 11 refrigerated display cabinets and 10 cold rooms from the medium temperature and 3 frozen food display cases and 2 cold rooms from the low temperature. Three different databases for the refrigerated display cabinets and two different typologies of cold rooms are used.

5.4.1 Old generation cabinets

The refrigerated display cabinets layout using a database of old generation cases is reported in Table 5.4.a.

ID	L_{RDC} [m]	N° [-]	Class	Typology	$\dot{q}_{RDC,R}$ [W · m^{-1}]	$\dot{Q}_{RDC,R}$ [kW]	t_{evap} [°C]
LT1	3.5	10	L1	Horizontal open	510	17.85	-40.0
LT2	2.5	12	L1	Horizontal open	510	15.30	-40.0
LT3	3.5	6	L2	Combined closed	680	14.28	-36.0
MT1	2.5	4	H2	Vertical open	1120	11.20	-5.0
MT2	3.5	12	H1	Vertical open	1765	74.13	-7.0
MT3	2.5	6	H1	Vertical open	1765	26.48	-7.0
MT4	2.5	6	M1	Vertical open	1662	24.93	-10.0
MT5	3.5	6	H1	Vertical open	1765	37.07	-7.0
MT6	3.5	4	M1	Vertical open	1662	23.27	-10.0
MT7	2.5	2	M2	Horizontal open	325	1.63	-10.0
MT8	2.5	8	M2	Horizontal open	325	6.50	-10.0
MT9	3.5	11	H1	Horizontal open	325	12.51	-7.5
MT10	2.5	8	H1	Horizontal open	325	6.50	-7.5
MT11	2.5	3	H1	Horizontal open	325	2.44	-7.5

Table 5.4.a - Old generation refrigerated display cabinets layout.

The cabinets design cooling capacities for the low temperature cycle and for the medium temperature cycle are 47.43 kW and 226.66 kW, respectively.
The low evaporation temperature is fixed at -40 °C, while the medium evaporation temperature is fixed at -13 °C.

5.4.2 New generation cabinets

The refrigerated display cabinets layout using a database of new generation cases is reported in Table 5.4.b.

ID	L_{RDC} [m]	N° [-]	Class	Typology	$\dot{q}_{RDC,R}$ [W · m^{-1}]	$\dot{Q}_{RDC,R}$ [kW]	t_{evap} [°C]
LT1	3.5	10	L1	Horizontal closed	208	7.28	-30.0
LT2	2.5	12	L1	Horizontal closed	208	6.24	-30.0
LT3	3.5	6	L2	Combined closed	553	11.61	-35.0
MT1	2.5	4	H1	Vertical open	1068	10.68	-3.0
MT2	3.5	12	M2	Vertical open	1278	53.68	-4.0
MT3	2.5	6	M2	Vertical open	1278	19.17	-4.0
MT4	2.5	6	M1	Vertical open	1548	23.22	-9.0
MT5	3.5	6	H1	Semi-vertical open	1016	21.34	-2.0
MT6	3.5	4	M2	Serve-over open	1260	17.64	-6.0
MT7	2.5	2	M2	Horizontal open	620	3.10	-7.0
MT8	2.5	8	M2	Horizontal open	620	12.40	-7.0
MT9	3.5	11	H1	Horizontal open	556	21.41	-4.0
MT10	2.5	8	H1	Horizontal open	556	11.12	-4.0
MT11	2.5	3	H1	Horizontal open	556	4.17	-4.0

Table 5.4.b - New generation refrigerated display cabinets layout.

The cabinets design cooling capacities for the low temperature cycle and for the medium temperature cycle are 25.13 kW and 197.92 kW, respectively.

The low evaporation temperature is fixed at -35 °C, while the medium evaporation temperature is fixed at -10 °C.

5.4.3 New generation cabinets with doors

The refrigerated display cabinets layout using a database of new generation cases with doors is reported in Table 5.4.c.

ID	L_{RDC}	N°	Class	Typology	$\dot{q}_{RDC,R}$	$\dot{Q}_{RDC,R}$	t_{evap}
	[m]	[-]			[W · m^{-1}]	[kW]	[°C]
LT1	3.5	10	L1	Horizontal closed	208	7.28	-30.0
LT2	2.5	12	L1	Horizontal closed	208	6.24	-30.0
LT3	3.5	6	L2	Combined closed	553	11.61	-35.0
MT1	2.5	4	M2	Vertical closed	558	5.58	-3.0
MT2	3.5	12	M2	Vertical closed	558	23.44	-3.0
MT3	2.5	6	M2	Vertical closed	558	8.37	-3.0
MT4	2.5	6	M1	Vertical closed	650	9.75	-6.0
MT5	3.5	6	M2	Vertical closed	558	11.72	-2.0
MT6	3.5	4	M1	Vertical closed	650	9.10	-6.0
MT7	2.5	2	M2	Horizontal open	620	3.10	-7.0
MT8	2.5	8	M2	Horizontal open	620	12.40	-7.0
MT9	3.5	11	H1	Horizontal open	556	21.41	-4.0
MT10	2.5	8	H1	Horizontal open	556	11.12	-4.0
MT11	2.5	3	H1	Horizontal open	556	4.17	-4.0

Table 5.4.c - New generation refrigerated display cabinets with doors layout.

The cabinets design cooling capacities for the low temperature cycle and for the medium temperature cycle are 25.13 kW and 120.15 kW, respectively.
The low evaporation temperature is fixed at -35 °C, while the medium evaporation temperature is fixed at -8 °C.

5.4.4 Old generation cold rooms

The cold rooms layout using an old generation typologies of cold rooms is reported in Table 5.4.d.

ID	V_{CR} [m^3]	A_{floor} [m^2]	U_{walls} [$W \cdot m^{-2} \cdot K^{-1}$]	U_{floor} [$W \cdot m^{-2} \cdot K^{-1}$]	$\dot{Q}_{CR}$ [kW]	t_{evap} [°C]
CR1	30.0	10.0	0.28	0.44	2.37	-30.0
CR2	16.8	7.0	0.28	0.44	1.66	-30.0
CR3	75.0	25.0	0.28	1.13	4.27	-8.0
CR4	45.0	15.0	0.28	1.13	2.56	-8.0
CR5	10.5	5.0	0.28	1.13	0.85	-8.0
CR6	48.0	16.0	0.28	1.13	2.73	-8.0
CR7	39.0	13.0	0.28	0.84	2.91	-2.0
CR8	51.0	17.0	0.28	1.13	2.90	-5.0
CR9	24.0	8.0	0.28	1.13	1.37	-5.0
CR10	7.4	3.5	0.28	1.13	0.60	-5.0
CR11	7.4	3.5	0.28	1.13	0.60	-8.0
CR12	57.0	19.0	0.28	0.84	4.25	0.0

Table 5.4.d - Old generation cold rooms layout.

The cold rooms design cooling capacities for the low temperature cycle and for the medium temperature cycle are 4.03 kW and 23.04 kW, respectively.

The low evaporation temperature and the medium evaporation temperature is fixed at -40 °C and at -13 °C, respectively, in accordance with the old generation refrigerated display cabinets evaporation temperatures, which are reported in paragraph 5.4.1.

5.4.5 New generation cold rooms

The cold rooms layout using a new generation typologies of cold rooms is reported in Table 5.4.e.

ID	V_{CR}	A_{floor}	U_{walls}	U_{floor}	$\dot{Q}_{CR}$	t_{evap}
	[m^3]	[m^2]	[$W \cdot m^{-2} \cdot K^{-1}$]	[$W \cdot m^{-2} \cdot K^{-1}$]	[kW]	[°C]
CR1	30.0	10.0	0.28	0.44	1.70	-30.0
CR2	16.8	7.0	0.28	0.44	1.19	-30.0
CR3	75.0	25.0	0.28	1.13	3.81	-8.0
CR4	45.0	15.0	0.28	1.13	2.28	-8.0
CR5	10.5	5.0	0.28	1.13	0.76	-8.0
CR6	48.0	16.0	0.28	1.13	2.43	-8.0
CR7	39.0	13.0	0.28	0.84	2.47	-2.0
CR8	51.0	17.0	0.28	1.13	2.59	-5.0
CR9	24.0	8.0	0.28	1.13	1.22	-5.0
CR10	7.4	3.5	0.28	1.13	0.53	-5.0
CR11	7.4	3.5	0.28	1.13	0.53	-8.0
CR12	57.0	19.0	0.28	0.84	3.61	0.0

Table 5.4.e - New generation cold rooms layout.

The cold rooms design cooling capacities for the low temperature cycle and for the medium temperature cycle are 2.89 kW and 20.23 kW, respectively.

The low evaporation temperature and the medium evaporation temperature is fixed at -35 °C and at -10 °C or -8 °C, respectively, in accordance with the new generation and new generation with doors refrigerated display cabinets evaporation temperatures, which are reported in paragraphs 5.4.2 and 5.4.3.

5.5 Results

In this paragraph, three different supermarket layouts are considered and analysed in terms of direct electric consumption, cooling capacities, influence on air conditioning and electric consumption of a direct expansion refrigeration system.
The first layout (old generation) is made up of the old generation cabinets layout reported in paragraph 5.4.1 and the old generation cold rooms layout reported in paragraph 5.4.4. The second one (new generation) is composed of the new generation cabinets layout reported in paragraph 5.4.2 and the new generation cold rooms layout reported in paragraph 5.4.5. The last one (new generation with doors) is the union of the new generation cabinets with doors layout reported in paragraph 5.4.3 and the new generation cold rooms layout reported in paragraph 5.4.5.

5.5.1 Direct electric consumption

The direct electric consumption (DEC) is the electric consumption of the auxiliary devices of the refrigerated display cabinets as well as the cold rooms, i.e. the lighting system, the fans, the heaters and the electric defrost system.
Figure 5.5.a and Figure 5.5.b show the daily profile of the direct electric consumption in a typical winter day and in a typical summer day in the supermarket located in Milan. During the defrost operations the direct electric consumption has a peak and in the old generation cabinets and cold rooms the number of defrost operations per day is greater than the new generation ones. This leads to a substantial increment in the annual direct electric consumption of the refrigeration system.
During the closing time of the supermarket the DEC is reduced by a percentage which ranges from about 35 % to 57 %. This is due to the lighting switching off and to the covering applied to the open refrigerated display cabinets during unoccupied hours.
In a typical winter day in a supermarket located in Milan the new generation layout and the new generation with doors layout show a direct electric consumption daily profile which is on average 42 % and 44% less than the old generation layout one.
In a typical summer day in a supermarket located in Milan, the percentages above mentioned decrease and they are equal to 29 % and 31 %.

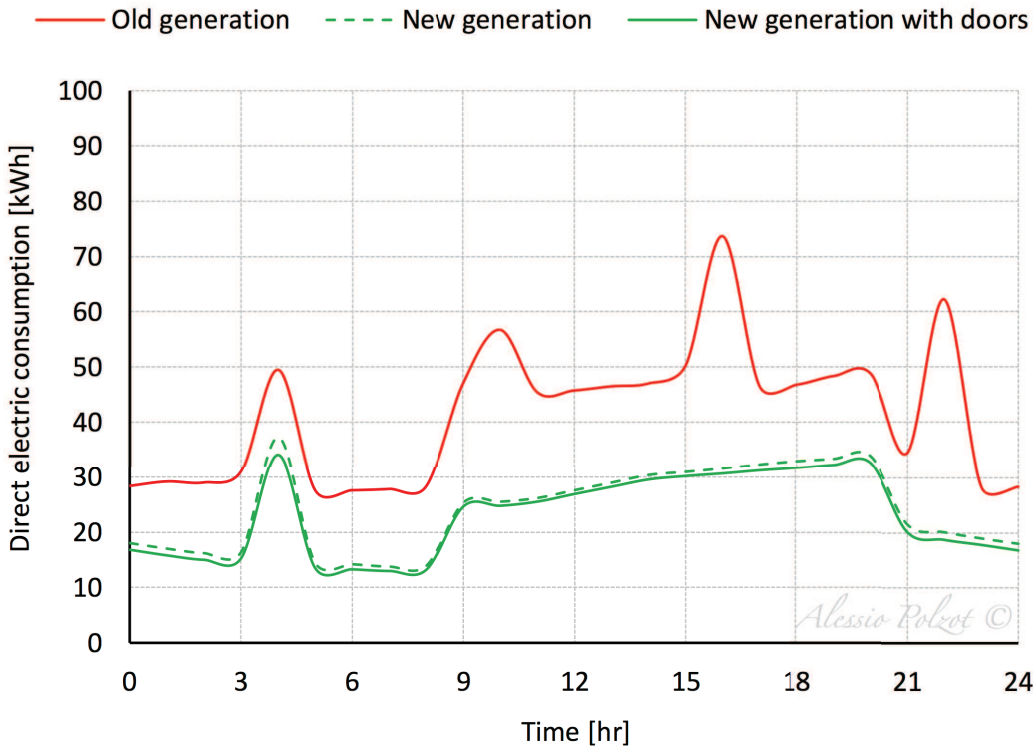

Figure 5.5.a - Direct electric consumption in a typical winter day in Milan.

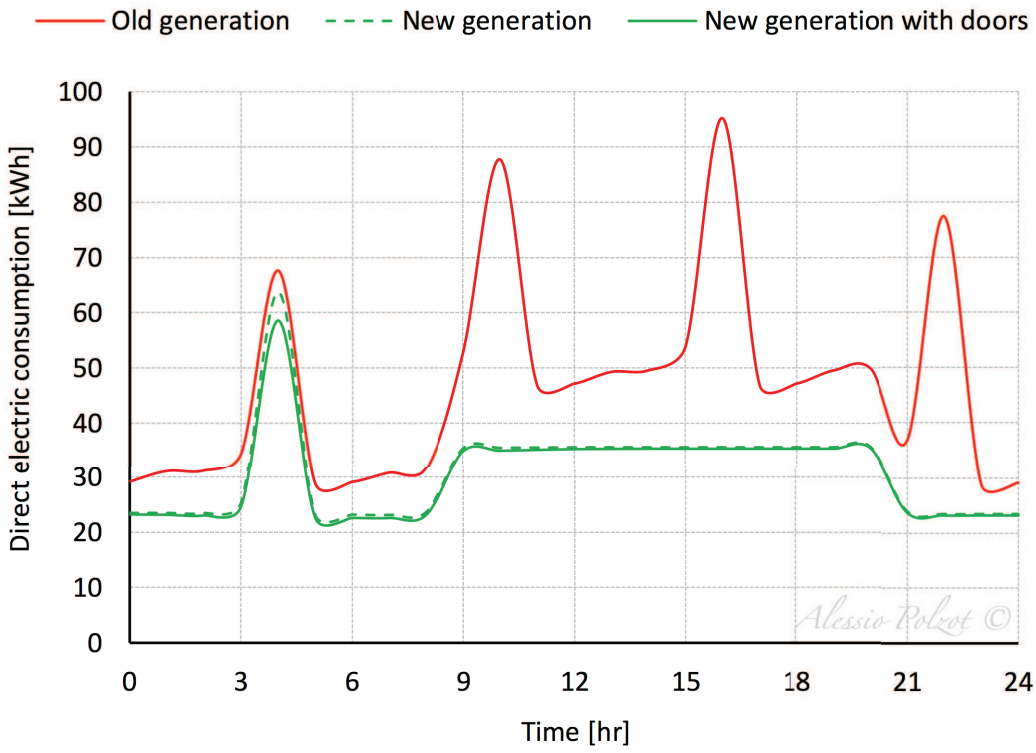

Figure 5.5.b - Direct electric consumption in a typical summer day in Milan.

Figure 5.5.c reports the monthly direct energy consumption of the three supermarket layouts for the supermarket located in Milan. The annual energy usage of the old generation layout is 398 MWh while the new generation layout and the new generation with doors layout consume about 37 % and 40 % less energy, respectively. Table 5.5.a reports the values above mentioned for the supermarkets located in the other cities.

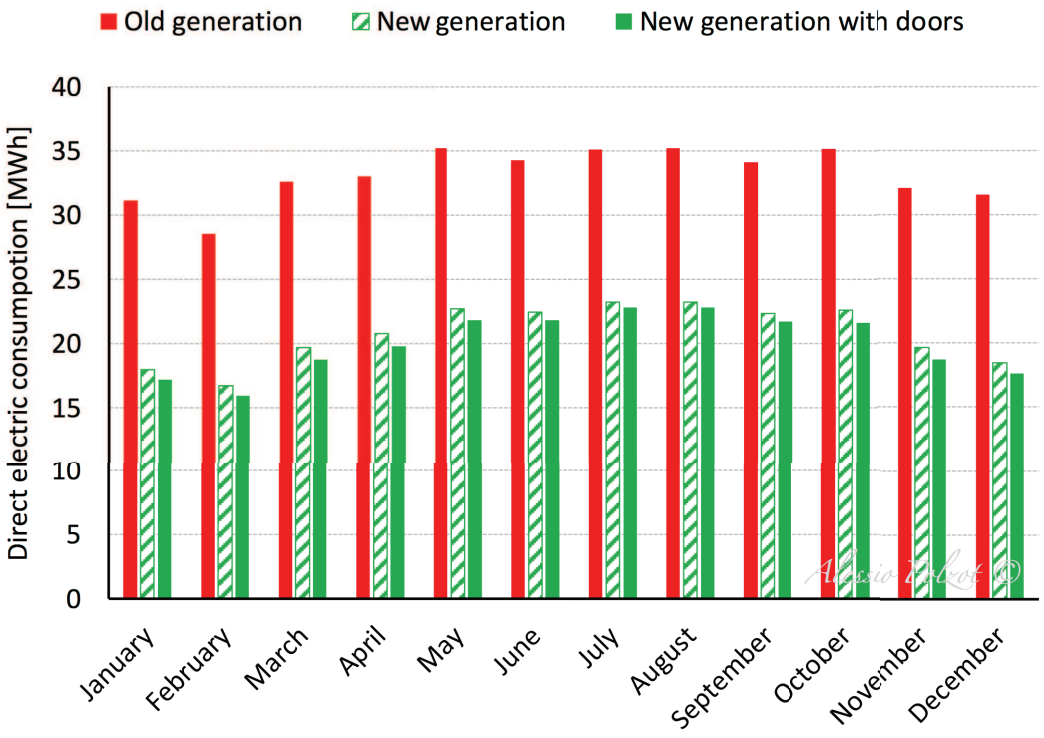

Figure 5.5.c - Monthly direct energy consumption in Milan.

Location	Old generation DEC	New generation relative energy usage	New generation with doors relative energy usage
	[MWh]	[%]	[%]
Genoa	411	-36	-38
Palermo	421	-35	-37
Rome	415	-36	-38
Venice	407	-26	-29

Table 5.5.a - Annual direct energy consumption and relative annual energy usage in comparison with the old generation supermarket layout.

5.5.2 Cooling capacities

Figure 5.5.d and Figure 5.5.e show the daily profile of the low temperature (LT) cooling capacities of the different supermarket layouts considered in a typical winter day and in a typical summer day in the supermarket located in Milan. During the defrost operations the evaporator of the refrigerated display cabinet or the cold room one is turned off and the cooling load relating to that cabinet or cold room is zero. When more than one refrigerated display cabinet or cold room start defrost operations simultaneously the total cooling capacity has a negative peak. During the defrost operations the operating temperature increases and it needs to be decreased to the standard value when the defrost operation is ended. This leads to have a positive peak immediately after the negative peak.

Figure 5.5.f and Figure 5.5.g show the daily profile of the medium temperature (MT) cooling capacities of the different supermarket layouts considered in a typical winter day and in a typical summer day in the supermarket located in Milan.

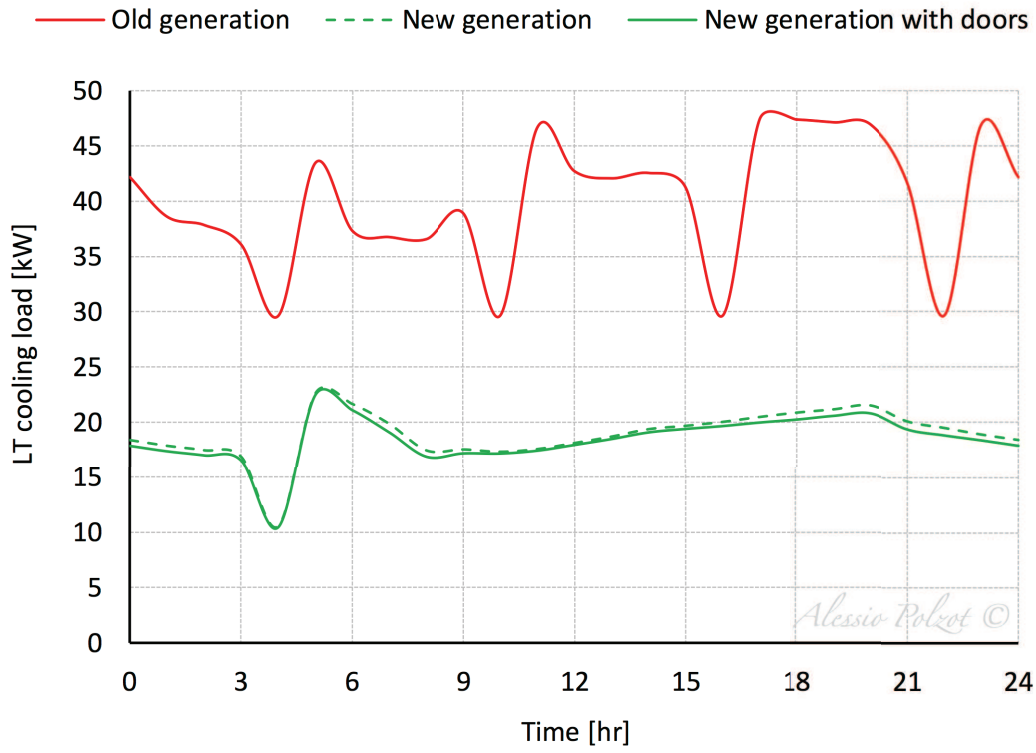

Figure 5.5.d - Low temperature cooling capacities in a typical winter day in Milan.

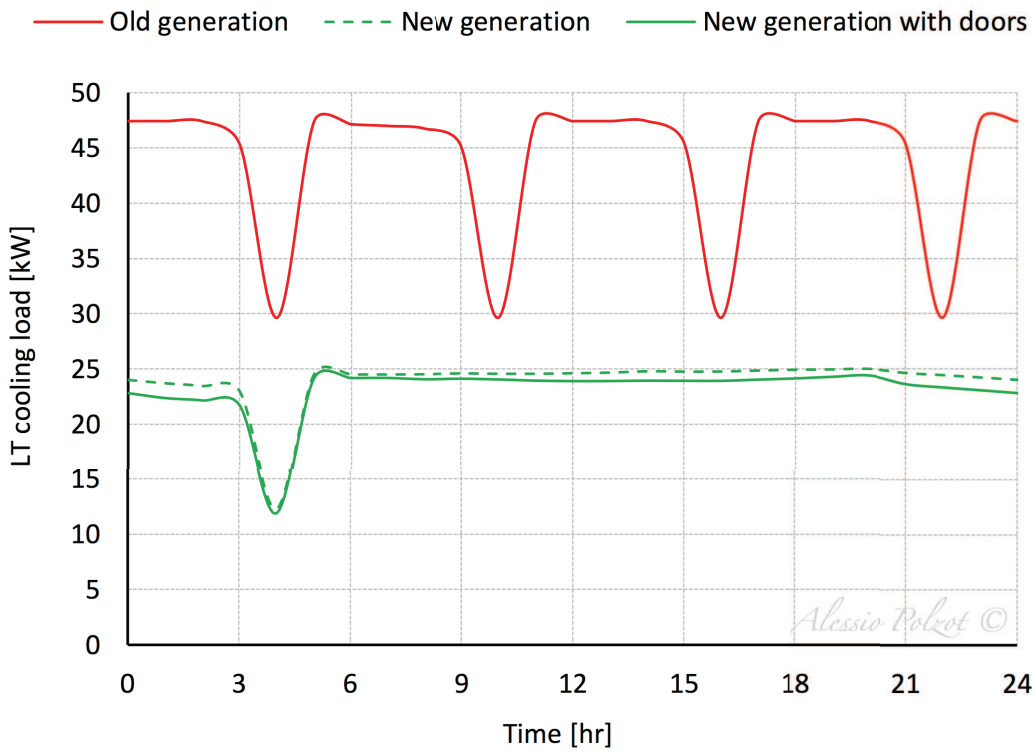

Figure 5.5.e - Low temperature cooling capacities in a typical summer day in Milan.

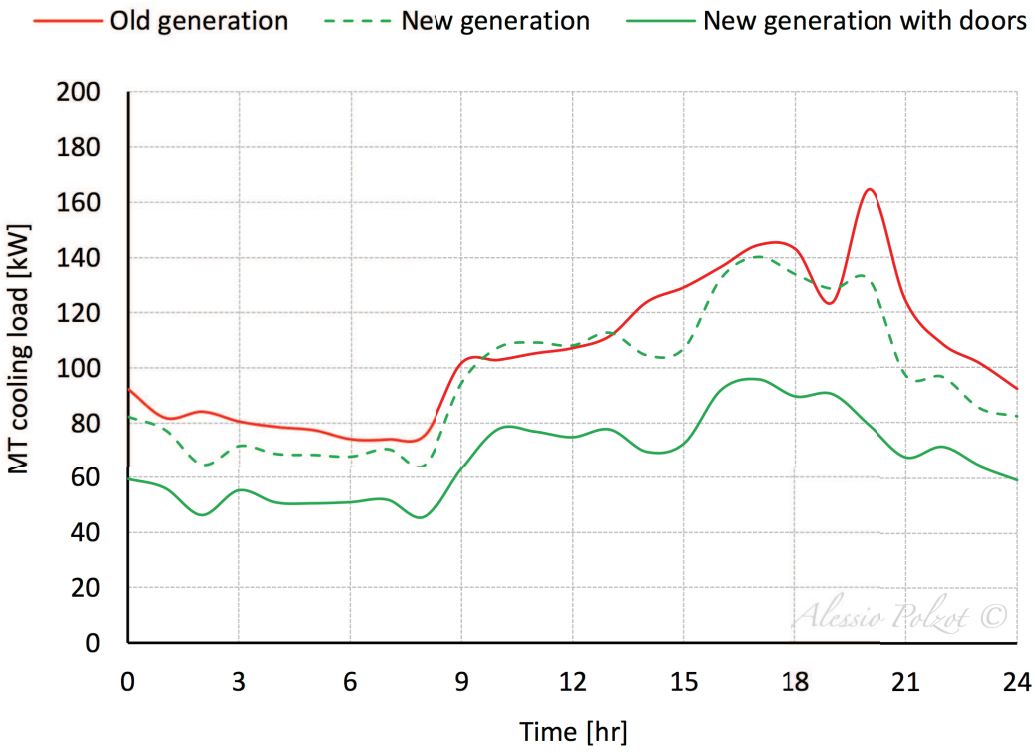

Figure 5.5.f - Medium temperature cooling capacities in a typical winter day in Milan.

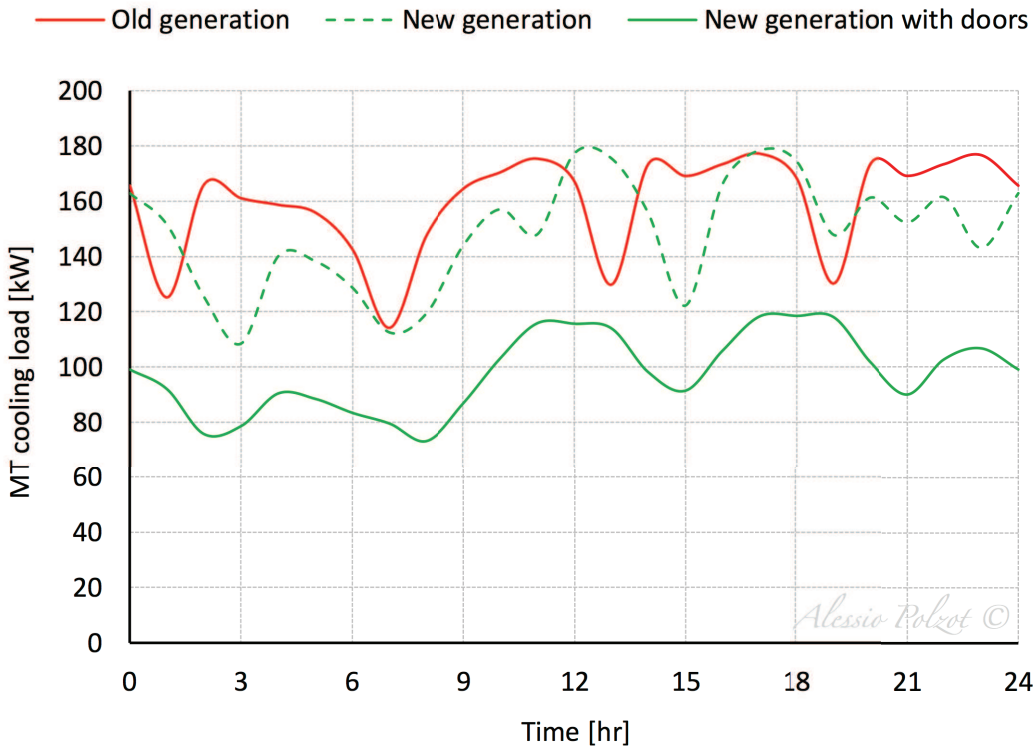

Figure 5.5.g - Medium temperature cooling capacities in a typical summer day in Milan.

5.5.3 Influence on air conditioning

The refrigerated display cabinets and the cold rooms remove energy from the surrounding environment. The impact of the cabinets on the surrounding environment include the fractions of the lighting and the anti-sweat heater energies that contribute to the zone heat load and the sensible and latent energy removed from the zone by the cabinet. The sensible fraction of the cold room impact on the zone include the heat transfer through the door, the walls and the ceiling and the sensible and latent loads due to the heat transfer by ambient air infiltration in the refrigerated volume.

Figure 5.5.h shows the total annual heating and cooling demands of the supermarket warehouse (zone 9 in Figure 3.1.b), where the cold rooms are located, and the food store (zone 30 in Figure 3.1.b), where the refrigerated display cabinets are located.

The installation of the doors in the vertical open refrigerated display cabinets leads to decrease the heating demand of the zone. This is due to the reduction of the air mass flow rate infiltrating into the refrigerated volume. On the contrary, for the same reason the cooling demand of the food store increases.

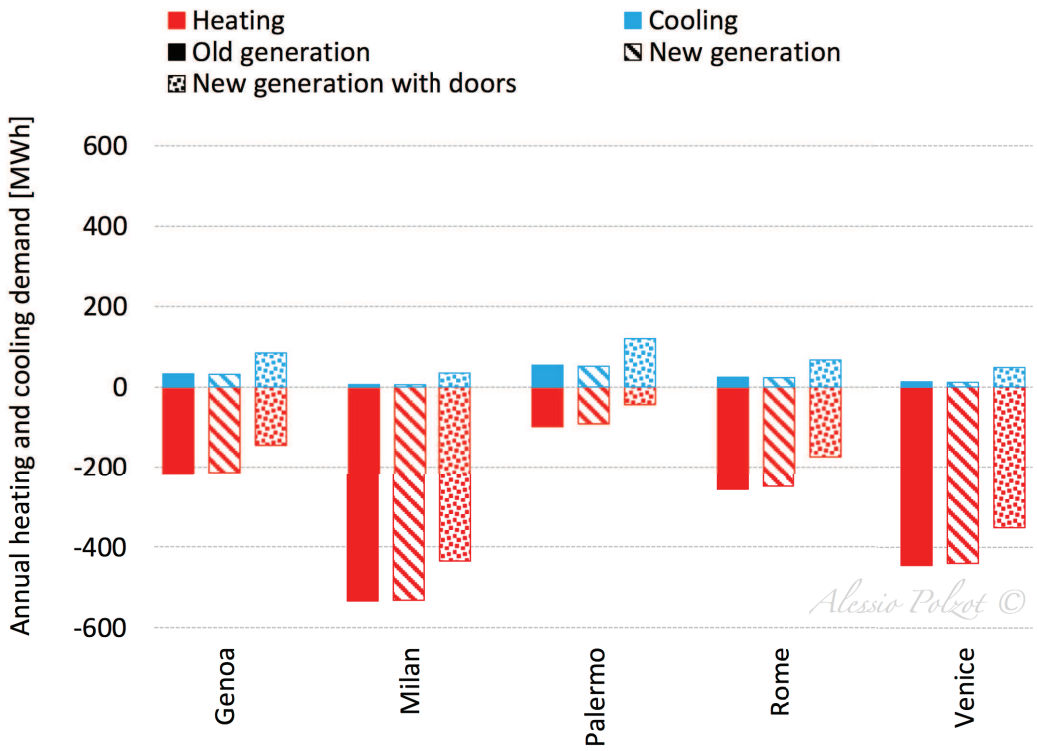

Figure 5.5.h - Annual heating and cooling demand of the supermarket with different refrigerated display cabinets and cold rooms layouts.

5.5.4 Direct expansion refrigeration system electric consumption

The direct expansion refrigeration system is a solution where two completely separate systems using hydro-fluorocarbon (HFC) refrigerants supplies both the medium temperature and the low temperature loads.

The electric consumption associated with the compressors power input and with the condenser fans energy usage is calculated for the three different supermarket layouts.

Figure 5.5.i show the daily profiles of the energy usage of the refrigeration system relating to the different supermarket layouts. The installation of the doors on the refrigerated display cabinets leads to a reduction of the cooling capacities and consequently to a reduction of the power input associated with the compressors power input.

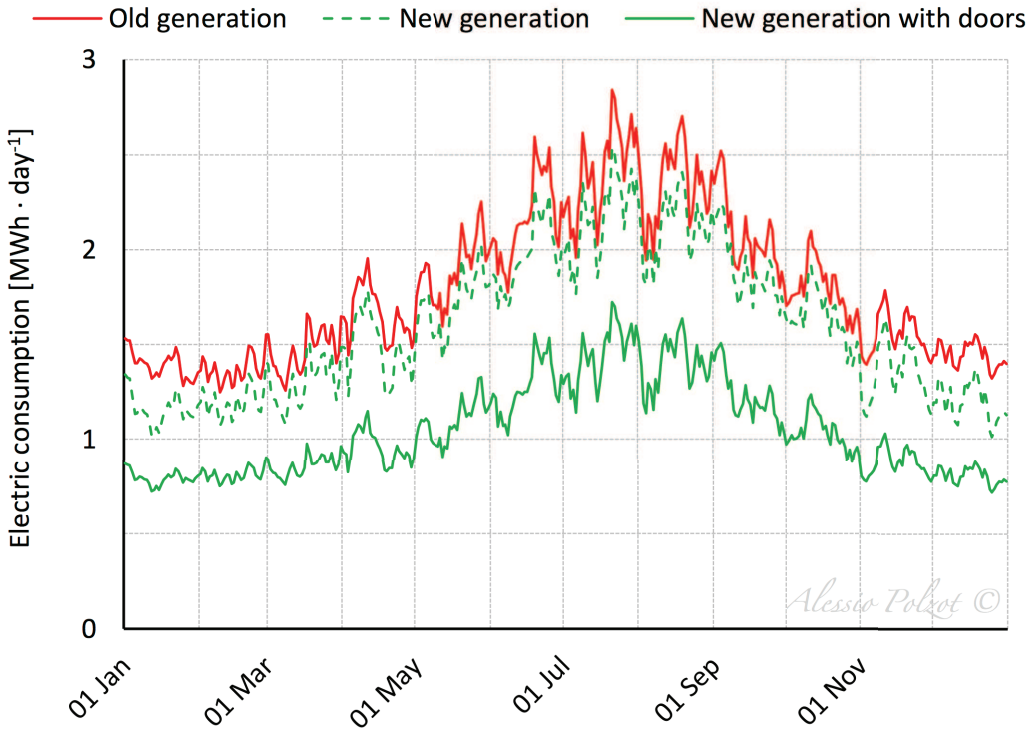

Figure 5.5.i - Daily electric consumption profiles of a direct expansion refrigeration system for different refrigerated display cabinets and cold rooms layouts.

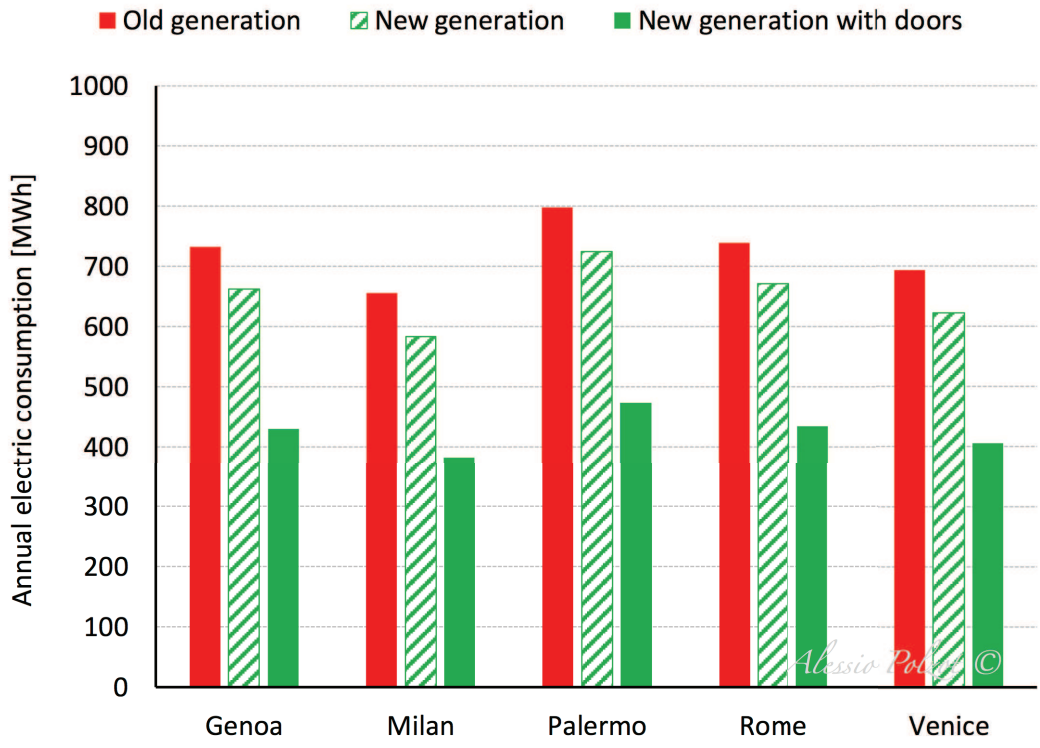

Figure 5.5.j - Annual electric consumption of a direct expansion refrigeration system for different refrigerated display cabinets and cold rooms layouts.

Looking at the annual electrical energy consumption of the direct expansion refrigeration systems relating to the different supermarket layouts, Figure 5.5.j shows a drastic reduction of the refrigeration system energy usage relating to the new generation layouts in all the investigated locations.
In comparison with the refrigeration system energy usage associated with the old generation layout, in the new generation layout and in the new generation with doors layout the direct expansion system consumes respectively about 10 % and 41 % less energy in all the locations considered.

5.6 Reference

- ASHRAE, 2001. Fundamentals Handbook, Chapter 6. Atlanta: American Society of Heating, Refrigerating and Air-Conditioning Engineers.
- ASHRAE, 2002. Refrigeration Handbook, Chapter 47. Atlanta: American Society of Heating, Refrigerating and Air-Conditioning Engineers.
- ASHRAE, 2006. Refrigeration Handbook, Chapter 13. Atlanta: American Society of Heating, Refrigerating and Air-Conditioning Engineers.
- ASHRAE, 2009. Fundamentals Handbook, Chapter 1. Atlanta: American Society of Heating, Refrigerating and Air-Conditioning Engineers.
- Baxter, V. D., Mei, V.C, 2002. Warm liquid defrosting technology for supermarket display cases. Proceedings of the IIF-IIR Commission D1, B1 Meeting: New Technologies in Commercial Refrigeration, Paris (FR).
- Cortella G., D'Agaro P., Franceschi M., Saro O., 2011. Prediction of the energy consumption of a supermarket refrigeration system. Proceedings of the 23rd International Congress of Refrigeration, Prague (CZ).
- EnergyPlus, 2013. EnergyPlus Engineering Reference: The Reference to EnergyPlus Calculations. US Department of Energy.
- Faramarzi R., 1999. Efficient display case refrigeration. ASHRAE Journal, Volume 41, Issue 11, Pages 46-54.

- Foster, A.M., Swain, M.J., Barrett, R., James, S.J., 2003. Experimental verification of analytical and CFD predictions of infiltration through cold store entrances. International Journal of Refrigeration 26, 918–925.
- Gosney, W.B., Olama, H.A.L., 1975. Heat and enthalpy gains through cold room doorways. Proceedings of the Institute of Refrigeration 72, 31-41.
- Henderson H.I., Khattar M., 1999. Measured Impacts of Supermarket Humidity Level on Defrost Performance and Refrigerating System Energy Use. ASHRAE Transactions 105(1), 508-520. Atlanta: American Society of Heating, Refrigerating and Air-Conditioning Engineers.
- Howell R.H., Rosario L., Bula A., 1993. Effects of Store Relative Humidity on Refrigerated Display Case Performance. ASHRAE Transactions 99(1), 667-678. Atlanta: American Society of Heating, Refrigerating and Air-Conditioning Engineers.
- ISO 23953-1:2015, 2015. Refrigerated display cabinets - Part 1: Vocabulary.
- ISO 23953-2:2015, 2015. Refrigerated display cabinets - Part 2: Classification, requirements and test conditions.

Chapter VI

Refrigeration systems

This chapter deals with a comparison in terms of energy consumption of different refrigeration systems without integration with the heating or the air conditioning system of the supermarket. The first two solutions, i.e. the direct expansion system and the cascade system, involve the use of hydro-fluorocarbon (HFC) refrigerants and they are used as baseline for the performance evaluation of a CO_2 transcritical booster system and a CO_2 transcritical booster system with auxiliary compression.

6.1 Direct expansion system

The direct expansion system (DXS) is a refrigeration system which uses an HFC refrigerant, the R404A, to satisfy both the frozen and the chilled refrigerated display cabinets and cold rooms loads.

This solution, as shown in Figure 6.1.a, comprise two completely separate systems, one satisfy the low temperature (LT) load and one to supply the medium temperature (MT) cabinets and cold rooms. Each system uses a multi-compressor rack consisting of between three to eight semi-hermetic reciprocating compressors and it is connected to an external air-cooled condenser. High pressure refrigerant liquid is fed to the evaporators and the refrigerant vapour exiting the evaporators then returns to the compressors rack via the suction line. The condenser pressure is typically controlled by varying the air flow. This ensures that the condensing pressure is kept as low as possible, consistent with satisfactory expansion valve control when outdoor air temperatures are low.

Table 6.1.a reports the operating conditions considered for the DXS solution, while the thermodynamic cycles of the direct expansion system is described in log(p)-h diagram in Figure 6.1.b.

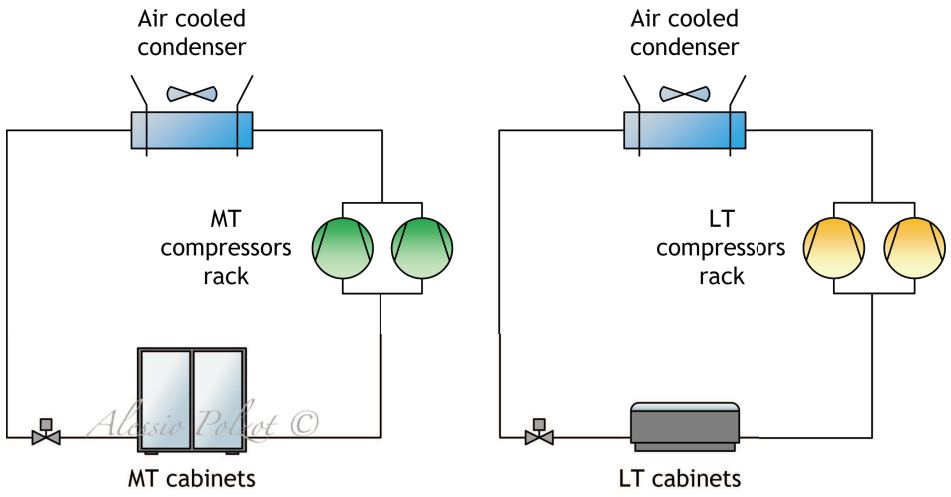

Figure 6.1.a - Schematic of a R404A direct expansion system (DXS).

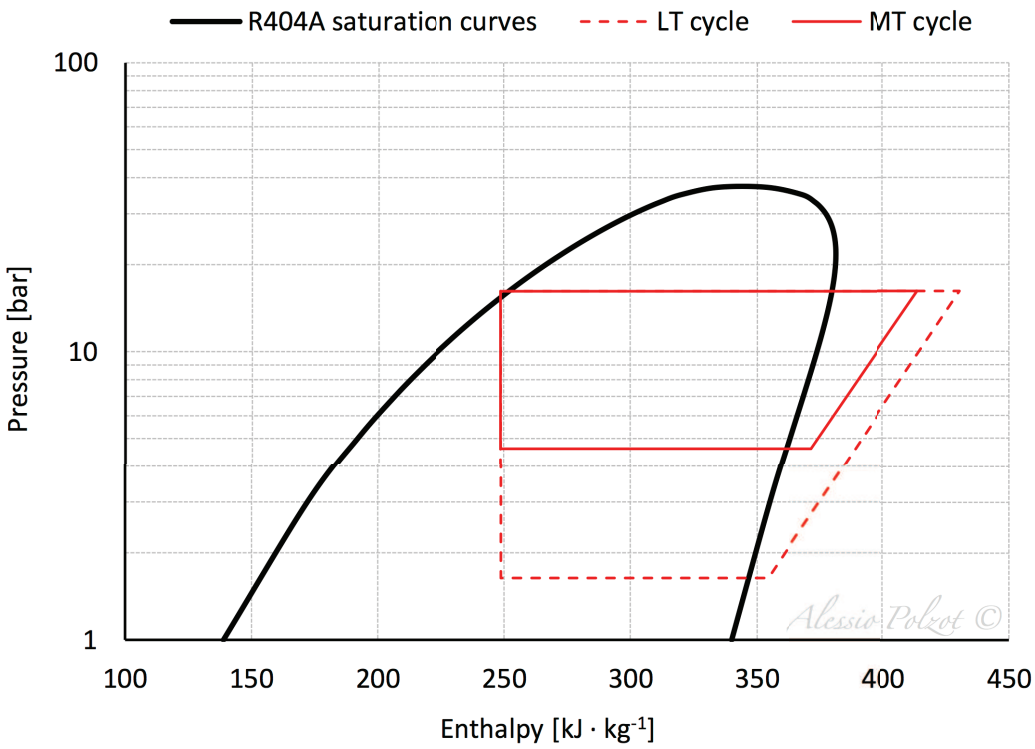

Figure 6.1.b - Log(p)-h diagram of DXS system.

DXS operating conditions	Unit	Value
Useful superheating	K	5.0
Superheating in the suction lines	K	5.0
Subcooling	K	2.0
Approach temperature of the condenser	K	10.0
Minimum condensing temperature	°C	25.0

Table 6.1.a - R404A direct expansion system (DXS) operating conditions.

6.2 Cascade system

The cascade system (CAS), which schematic is shown in Figure 6.2.a, is a refrigeration technology where an HFC direct expansion system is used for the MT loads while the LT system has a separate circuit that discharges its heat into the suction stage of the MT system.

The LT cycle has a low condensation temperature, so a natural refrigerant as the carbon dioxide (R744) can be applied in subcritical mode without excessive pressures. The discharge pressure of the low temperature cycle is around 30 to 35 bar and the temperature difference required to drive the heat transfer across the cascade condenser heat exchanger represents a slight loss in energy efficiency.

The HFC refrigerant considered in this work is the R134a. The operating conditions evaluated are reported in Table 6.2.a and the thermodynamic cycles of the direct expansion system is described in log(p)-h diagram in Figure 6.2.b.

CAS operating conditions	Unit	Value
Useful superheating	K	5.0
Superheating in the suction lines	K	5.0
Pinch point temperature of the cascade condenser	K	5.0
Approach temperature of the condenser	K	10.0
Minimum condensing temperature	°C	25.0

Table 6.2.a - R134a cascade system (CAS) operating conditions.

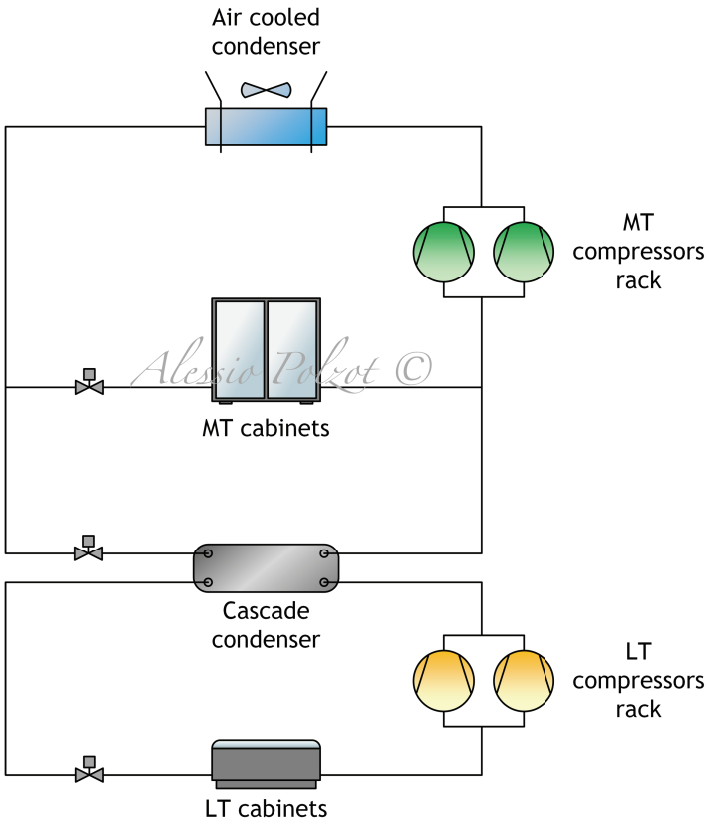

Figure 6.2.a - Schematic of a R134a cascade system (CAS).

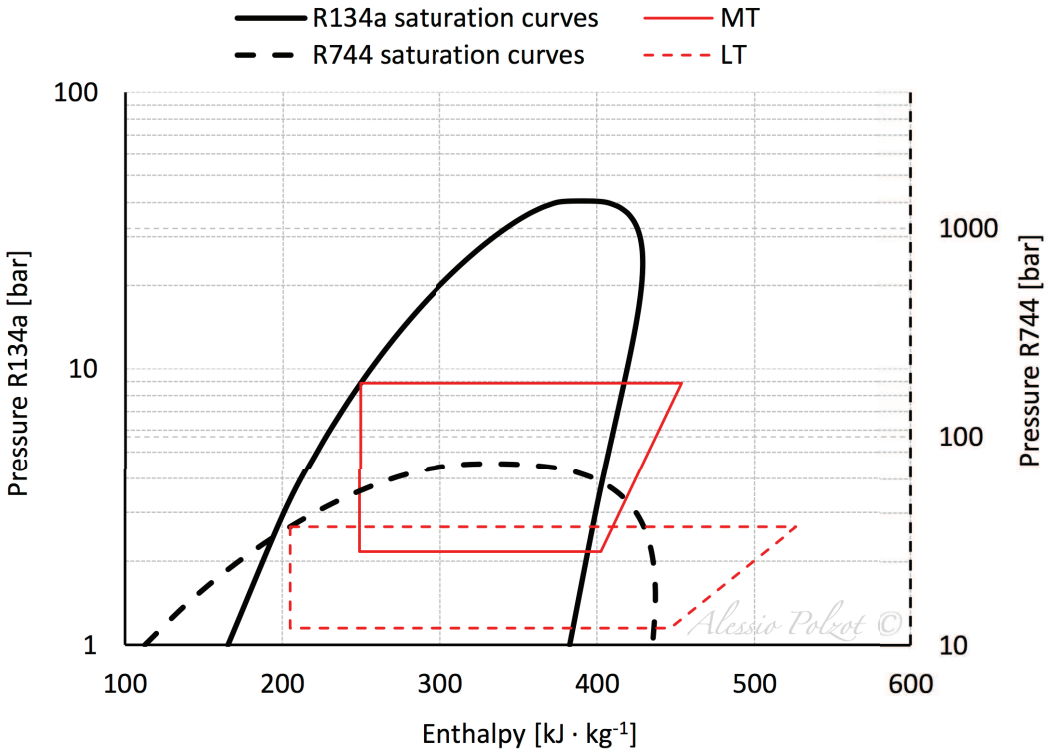

Figure 6.2.b - Log(p)-h diagram of CAS system.

6.3 R744 transcritical booster system

This R744 transcritical booster system (TBS) uses carbon dioxide (CO_2) in both the MT and LT cycles. The low stage (LS) compressors rack, which compress the vapour exiting from the LT evaporators, act as a booster to raise the vapour pressure from the LT level to the level of the MT evaporators. The schematic of the system is depicted in Figure 6.3.a.

At ambient temperatures above approximately 26 °C the high stage (HS) compressor rack discharges the gas above the critical pressure of the carbon dioxide (74 bar). The condenser then acts as a gas cooler and reduces the temperature of the discharge gas without condensing it into liquid. Cooled fluid passes through a high pressure (HP) expansion valve, at which point a portion condenses into liquid and the rest remains as gas. Liquid and gas are separated in a liquid receiver controlled by the pressure relief valve at an intermediate pressure of around 35 to 40 bar. The liquid is then distributed to the MT and LT cabinets and cold rooms via the liquid line at this intermediate pressure. The flash gas is taken via an additional expansion device, the vapour by-pass valve, to the suction of the MT compressors.

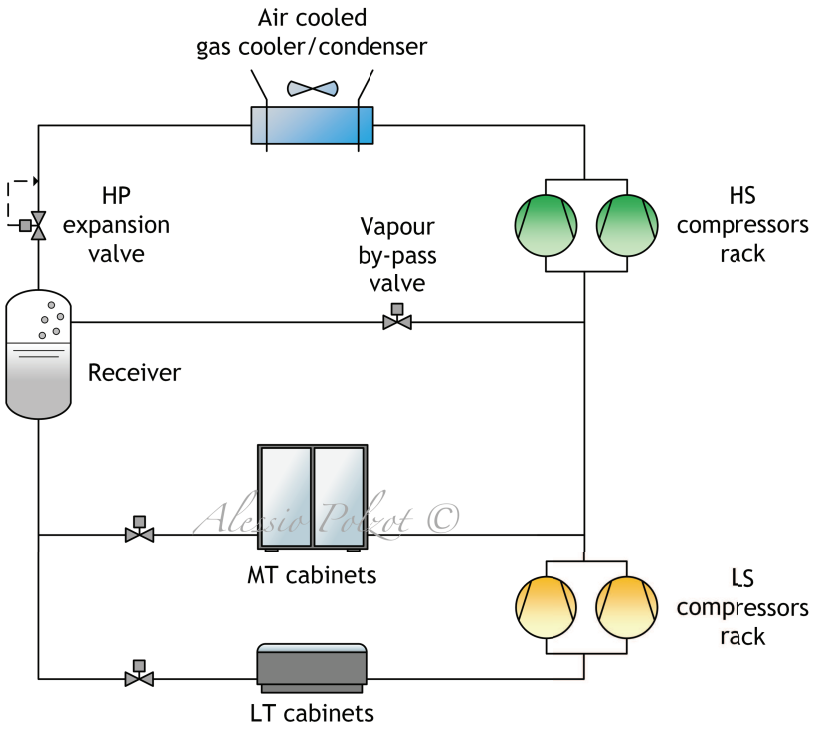

Figure 6.3.a - Schematic of a R744 transcritical booster system (TBS).

The TBS system operates in subcritical conditions (dashed line in Figure 6.3.b) at low ambient temperatures, whereas transcritical operations (solid line in Figure 6.3.b) occurs at high external temperatures, as previously explained. In order to improve the performance of the system at intermediate outdoor temperature, it is necessary to define a transition zone. A procedure similar to the one adopted by Cecchinato et al. (2007) is used to define the conditions in which transition operations take place.

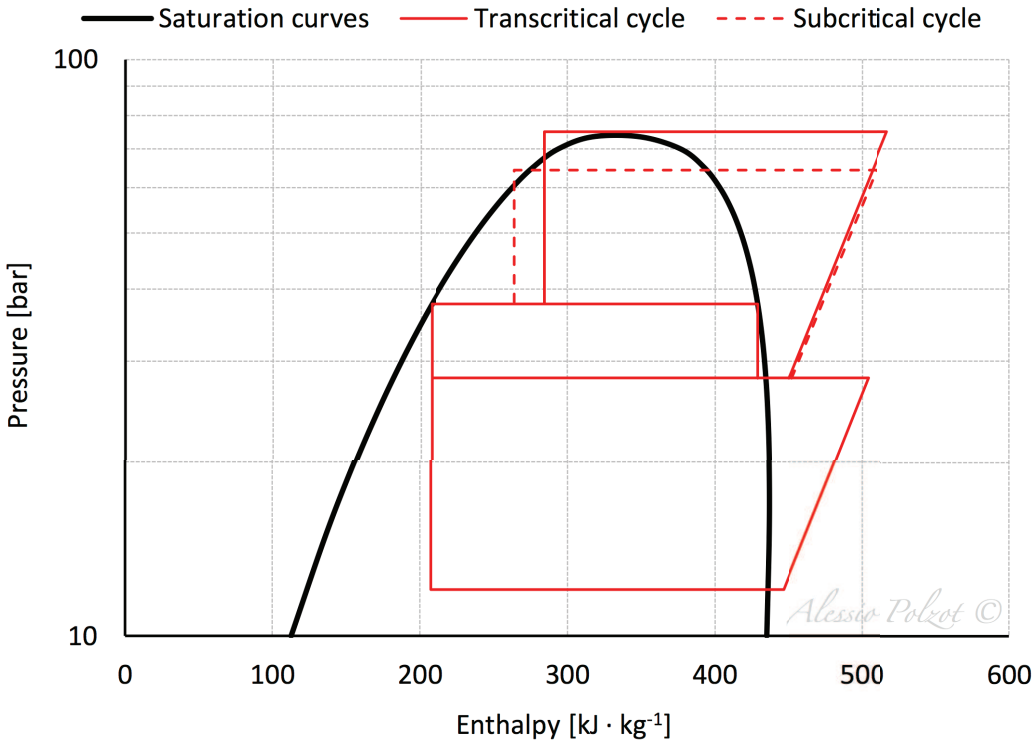

Figure 6.3.b - Log(p)-h diagram of TBS system.

As sketched in Figure 6.3.c, four operational points and three operational modes are defined. The first operational point is referred to the subcritical condition in which, the condensing temperature is equal to its minimum value, in accordance with Table 6.3.a.

At outdoor temperatures which is such that the CO_2 outlet condenser/gas cooler temperature is lower than 6 °C, the condensing temperature is fixed to its minimum value. In the subcritical zone a degree of subcooling of 2 K is selected and the condensing temperature is ranged according to the outdoor temperature.

The second point marks the transition between the subcritical zone to the transition operating conditions. The transition zone is the one where the system moved

gradually from the subcritical conditions to the transcritical ones. These conditions, in accordance to the selected operating conditions of the system, arose at CO_2 outlet condenser/gas cooler temperatures higher than 20 °C. According to Cecchinato et al. (2007), this zone is defined by the second and the third operational points, which identify an upper and a lower limit in terms of high pressure and gas cooler/condenser outlet temperature. In accordance with the external temperature, the high pressure heat exchanger varied its working conditions linearly from the second operational point to the third one. The condenser outlet temperature and the condensing one at the second point is set to 23 °C and 25 °C, respectively. The gas cooler outlet temperature and the high pressure at the third operational point is equal to 29 °C and 75 bar, respectively. The temperature of the CO_2 exiting from the condenser/gas cooler follows the ambient temperature in accordance with the approach temperature of the high pressure heat exchanger, while the high pressure is given by:

$$p_{GC} = 1.788\, t_{out,GC} + 23.146 \tag{55}$$

where:

p_{GC} is the gas cooler pressure [bar];

$t_{out,GC}$ is the temperature of the CO_2 exiting from the condenser/gas cooler [°C].

The transcritical conditions take place at outdoor temperatures over 29 °C. In this operating conditions the gas cooler discharge pressure has to be optimized in order to maximize the COP (Liao et al., 2000; Kim et al., 2004; Ge and Tassou, 2011) and an optimal gas cooler pressure has to be evaluated as a function of the outlet condenser/gas cooler temperature, as shown in Figure 6.3.d:

$$p_{GC} = 2.140\, t_{out,GC} + 12.940 \tag{56}$$

where:

p_{GC} is the gas cooler pressure [bar];

$t_{out,GC}$ is the temperature of the CO_2 exiting from the condenser/gas cooler [°C].

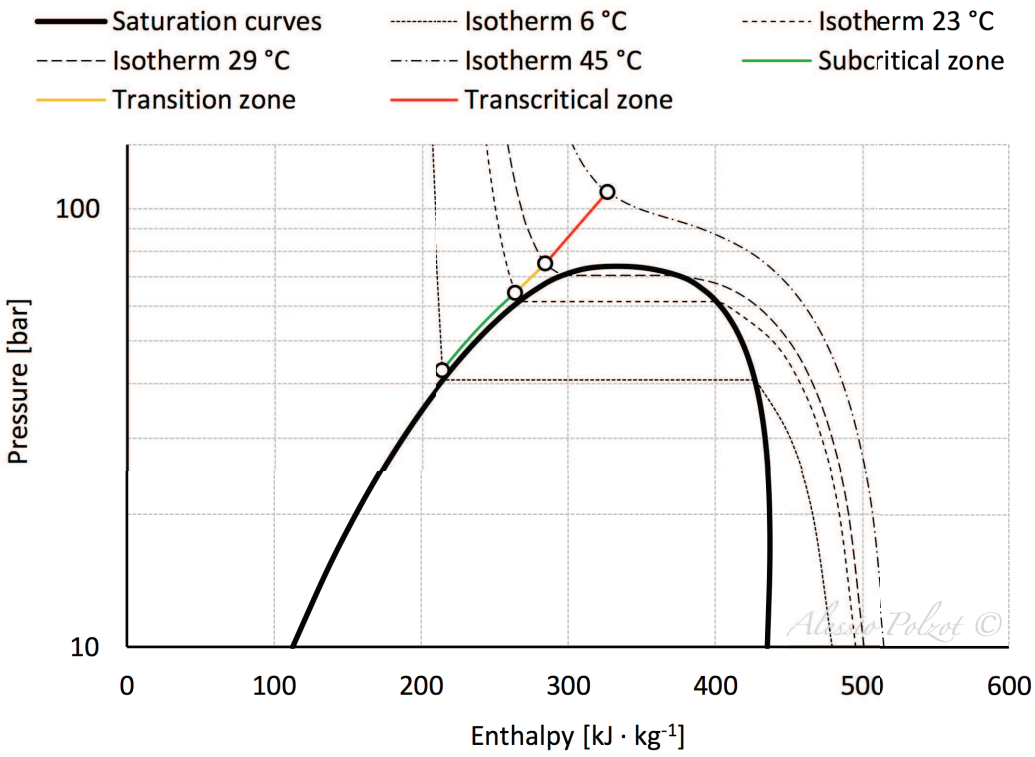

Figure 6.3.c - Operating zones of the TBS system.

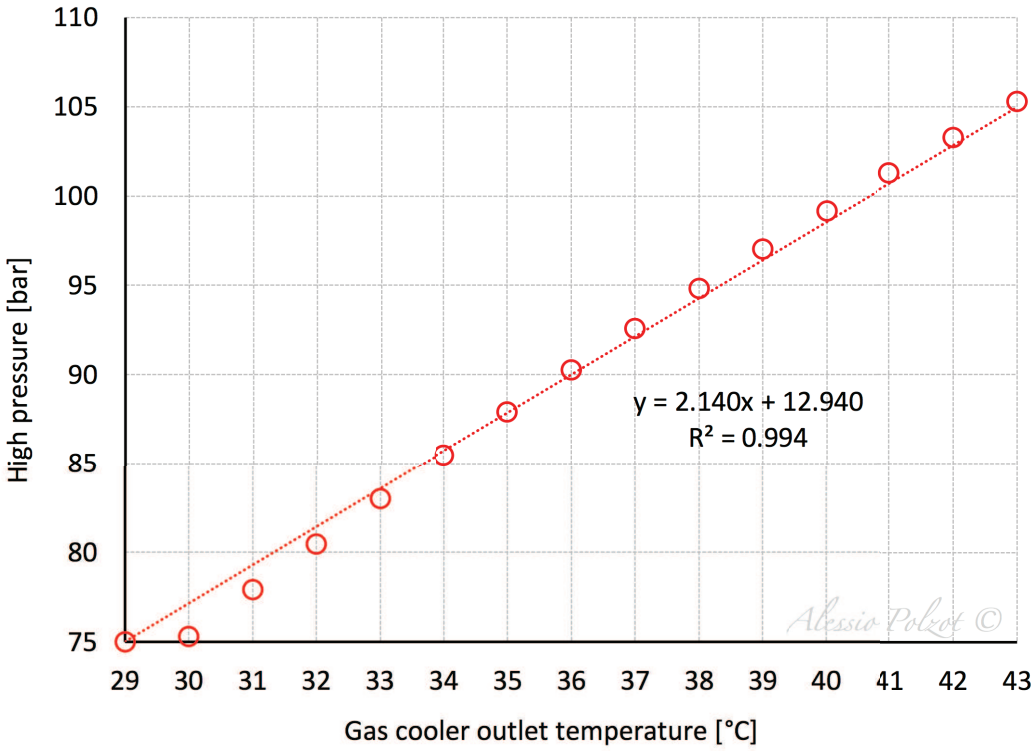

Figure 6.3.d - Optimal gas cooler discharge pressure in transcritical conditions for TBS system.

TBS operating conditions	Unit	Value
Useful superheating	K	5.0
Superheating in the suction lines	K	5.0
Approach temperature of the condenser/gas cooler	K	3.0
Minimum condensing temperature	°C	8.0
Subcooling in subcritical operations	K	2.0
Liquid receiver pressure	bar	37.7

Table 6.3.a - R744 transcritical booster system (TBS) operating conditions.

6.4 R744 transcritical booster system with auxiliary compression

The R744 transcritical booster system with auxiliary compression or parallel compression (PCS), which schematic is shown in Figure 6.4.a, differs from the TBS system defined in paragraph 6.3 in an additional compressor.

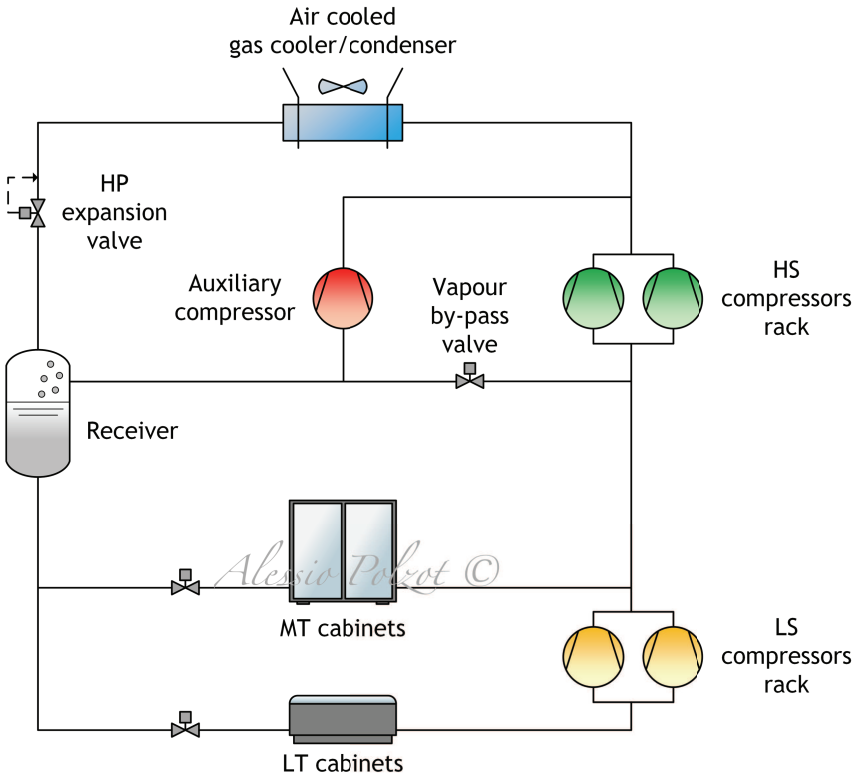

Figure 6.4.a - Schematic of a R744 transcritical booster system with auxiliary compression (PCS).

In a CO_2 booster system, in transcritical operations, the mass flow rate of the flash gas is on average the 45 % of the total mass flow rate (Gullo et al., 2016). As previously mentioned, in a TBS system the flash gas is expanded from intermediate pressure to the MT pressure and then it is drawn from the MT compressors rack and it is compressed to the high pressure.

The adoption of the auxiliary compressor allows compressing the flash gas directly from the intermediate pressure to the high one, as shown in the thermodynamic cycle of the PCS system described in a log(p)-h diagram in Figure 6.4.b.

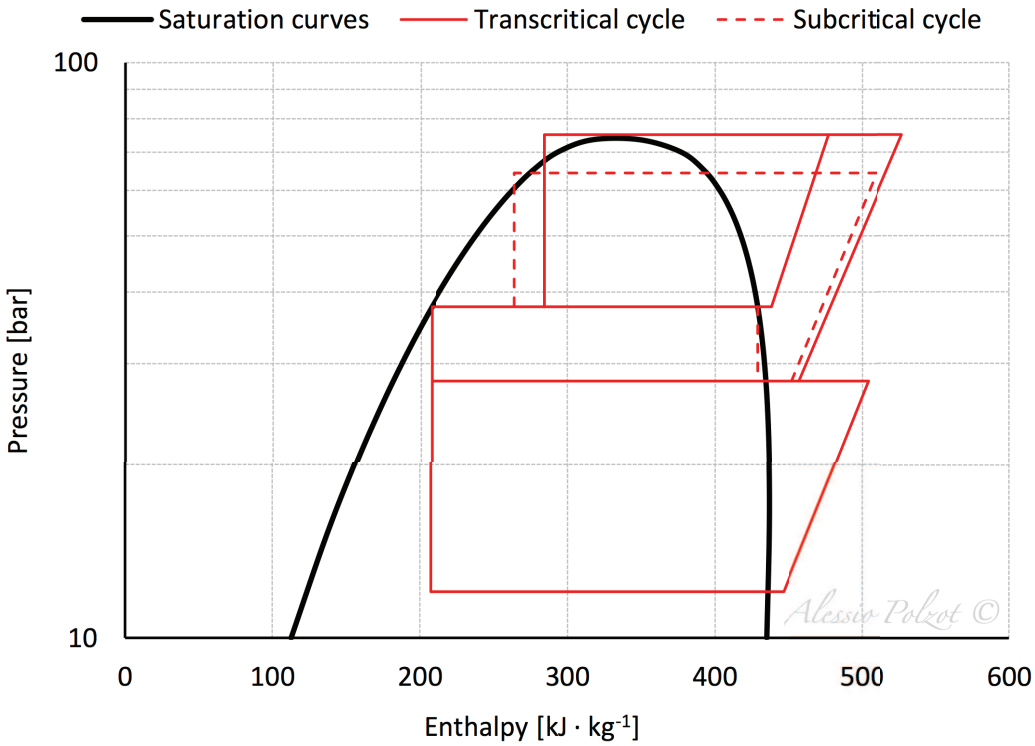

Figure 6.4.b - Log(p)-h diagram of TBS system.

As suggested by Chiariello et al. (2010), Minetto et al. (2005) and Sarkar and Agrawal (2010), in the R744 transcritical booster system with auxiliary compression the overall system has to be optimized in terms of both the high pressure and the intermediate one. In transcritical running mode, the high pressure is an additional independent variable and the system is optimized as a function of the gas cooler exit temperature The lower and upper limits is set to 35 bar and 55 bar for the intermediate pressure and to 75 bar and 110 bar for the discharge pressure. The maximisation of the COP is chosen as the objective function (Gullo et al., 2016).

In order to guarantee a suitable minimum mass flow rate for the auxiliary compressor, the latter is activated as soon as the transition conditions are reached. Consequently, in subcritical mode the system runs as the TBS system, the high pressure is ranged according to the outdoor temperature and the intermediate pressure is fixed:

$$p_{INT} = 37.7 \tag{57}$$

where:

p_{INT} is the intermediate pressure [bar].

In transition zone, the high pressure is varied linearly from the same second operational points point of the TBS system (yellow solid line in Figure 6.4.e), while the intermediate pressure is optimized and has to be evaluated as a function of the outlet condenser/gas cooler temperature, as shown in Figure 6.4.c:

$$p_{INT} = -0.010\, t_{out,GC}^2 + 1.244\, t_{out,GC} + 17.058 \tag{58}$$

where:

p_{INT} is the intermediate pressure [bar];

$t_{out,GC}$ is the temperature of the CO_2 exiting from the condenser/gas cooler [°C].

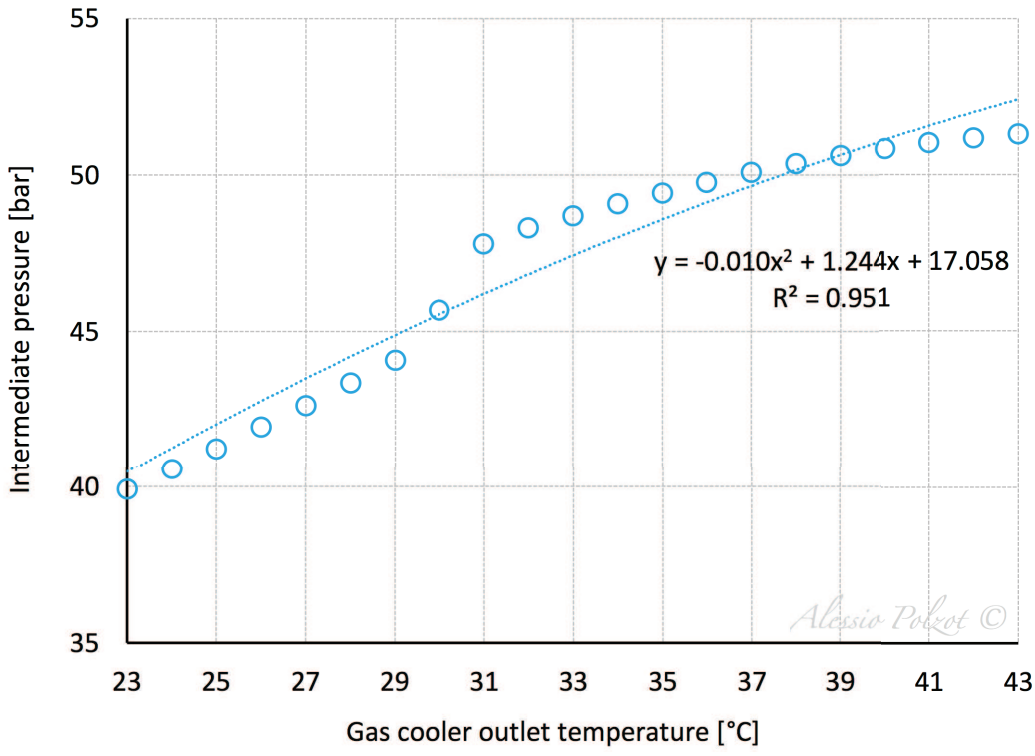

Figure 6.4.c - Optimal intermediate pressure in transition and transcritical conditions for PCS system.

In transcritical operating conditions, the optimal intermediate pressure and the optimal high one (Figure 6.4.d) are evaluated as a function of the outlet condenser/gas cooler temperature with the correlation (58) and (59), respectively.

$$p_{GC} = 1.998\, t_{out,GC} + 17.058 \qquad (59)$$

where:

p_{GC} is the gas cooler pressure [bar];

$t_{out,GC}$ is the temperature of the CO_2 exiting from the condenser/gas cooler [°C].

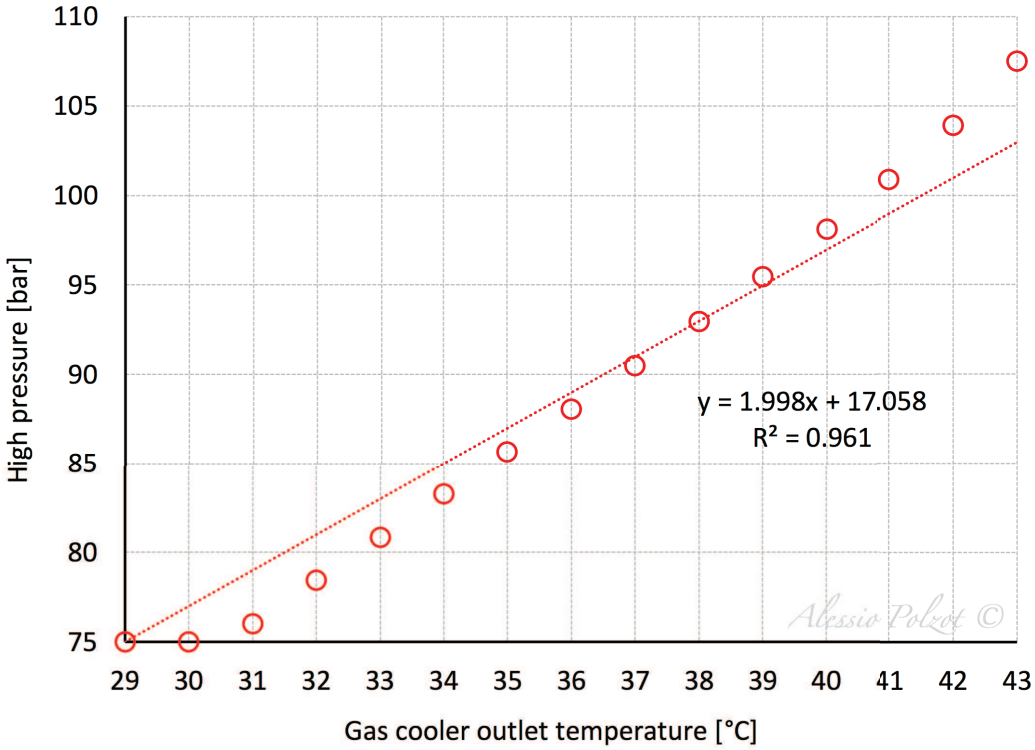

Figure 6.4.d - Optimal gas cooler discharge pressure in transcritical conditions for TBS system.

The optimal gas cooler discharge pressure of the PCS system (red solid line in Figure 6.4.e) is slightly lower than the one of TBS system (red dotted line in Figure 6.4.e). The operating conditions evaluated are reported in Table 6.4.a.

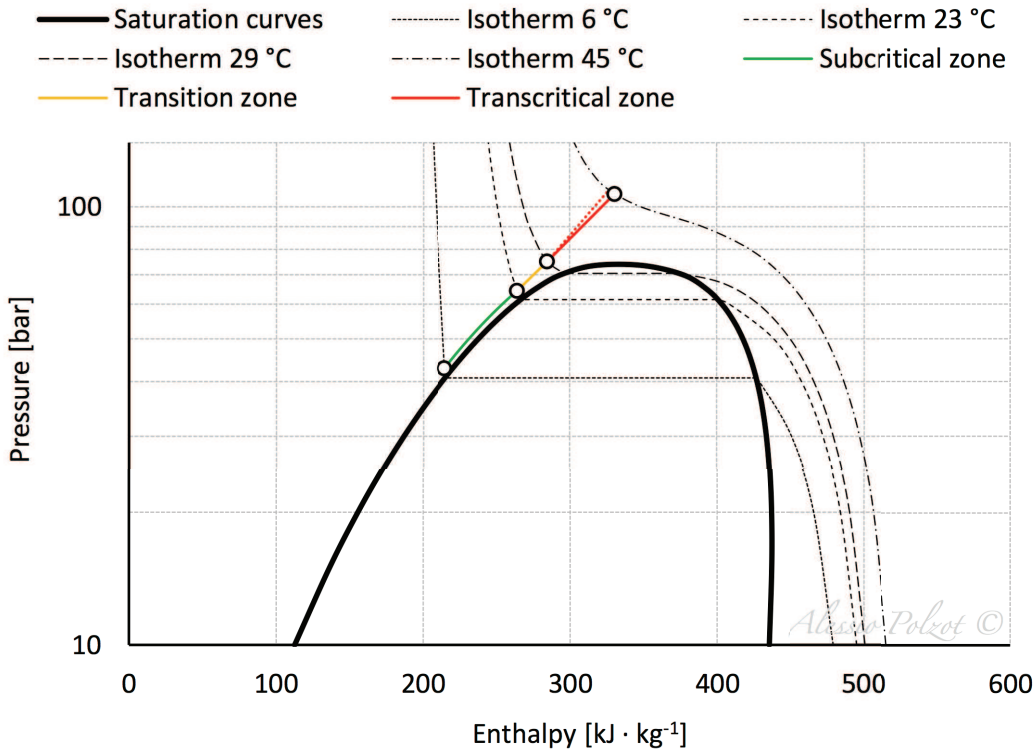

Figure 6.4.e - Operating zones of the PCS system.

PCS operating conditions	Unit	Value
Useful superheating	K	5.0
Superheating in the suction lines	K	5.0
Approach temperature of the condenser/gas cooler	K	3.0
Minimum condensing temperature	°C	8.0
Subcooling in subcritical operations	K	2.0

Table 6.4.a - R744 transcritical booster system with auxiliary compression (PCS) operating conditions.

6.5 Compressors global efficiency

The compressors are all semi-hermetic reciprocating compressors and all their suggested technological constraints are respected.

Their global efficiencies are obtained as a function of the pressure ratio by using BITZER Software (BITZER, 2016). The global efficiency is defined as the ratio of the

power input calculated at isentropic conditions to the power input declared by the manufacturers.

6.5.1 DXS system

The global efficiencies of the compressors in DXS system, which are depicted in Figure 6.5.a, are given by:

$$\eta_{LT} = -0.0025\,\beta_{LT}^2 + 0.0457\,\beta_{LT} + 0.4252 \quad (60)$$

$$\eta_{MT} = -0.0108\,\beta_{MT}^2 + 0.0969\,\beta_{MT} + 0.4007 \quad (61)$$

where:

β_{LT} is the pressure ratio of the LT cycle (62) [-];

β_{MT} is the pressure ratio of the MT cycle (63) [-].

$$\beta_{LT} = \frac{p_{cond,LT}}{p_{evap,LT}} \quad (62)$$

$$\beta_{MT} = \frac{p_{cond,MT}}{p_{evap,MT}} \quad (63)$$

where:

$p_{cond,LT}$ is the condensing pressure of the LT cycle [bar];

$p_{evap,LT}$ is the evaporating pressure of the LT cycle [bar];

$p_{cond,MT}$ is the condensing pressure of the MT cycle [bar];

$p_{evap,LT}$ is the evaporating pressure of the MT cycle [bar].

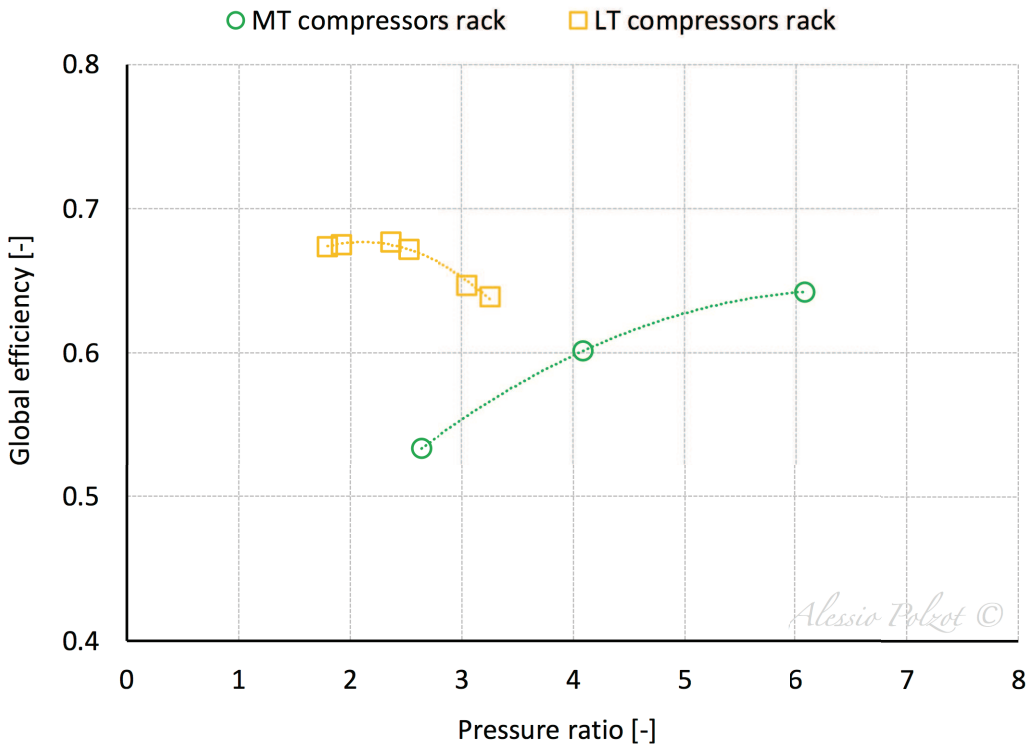

Figure 6.5.a - Compressors global efficiency for DXS system.

6.5.2 CAS system

The global efficiencies of the compressors in CAS system, which are depicted in Figure 6.5.b, are given by:

$$\eta_{LT} = -0.0302\,\beta_{LT}^2 + 0.1274\,\beta_{LT} + 0.5426 \tag{64}$$

$$\eta_{MT} = -0.0075\,\beta_{MT}^2 + 0.0970\,\beta_{MT} + 0.3303 \tag{65}$$

where:

β_{LT} is the pressure ratio of the LT cycle (66) [-];

β_{MT} is the pressure ratio of the MT cycle (67) [-].

$$\beta_{LT} = \frac{p_{cond,CC}}{p_{evap,LT}} \tag{66}$$

$$\beta_{MT} = \frac{p_{cond,MT}}{p_{evap,MT}} \tag{67}$$

where:

$p_{cond,CC}$ is the CO_2 condensing pressure in the cascade condenser [bar];

$p_{evap,LT}$ is the evaporating pressure of the LT cycle [bar];

$p_{cond,MT}$ is the condensing pressure of the MT cycle [bar];

$p_{evap,LT}$ is the evaporating pressure of the MT cycle [bar].

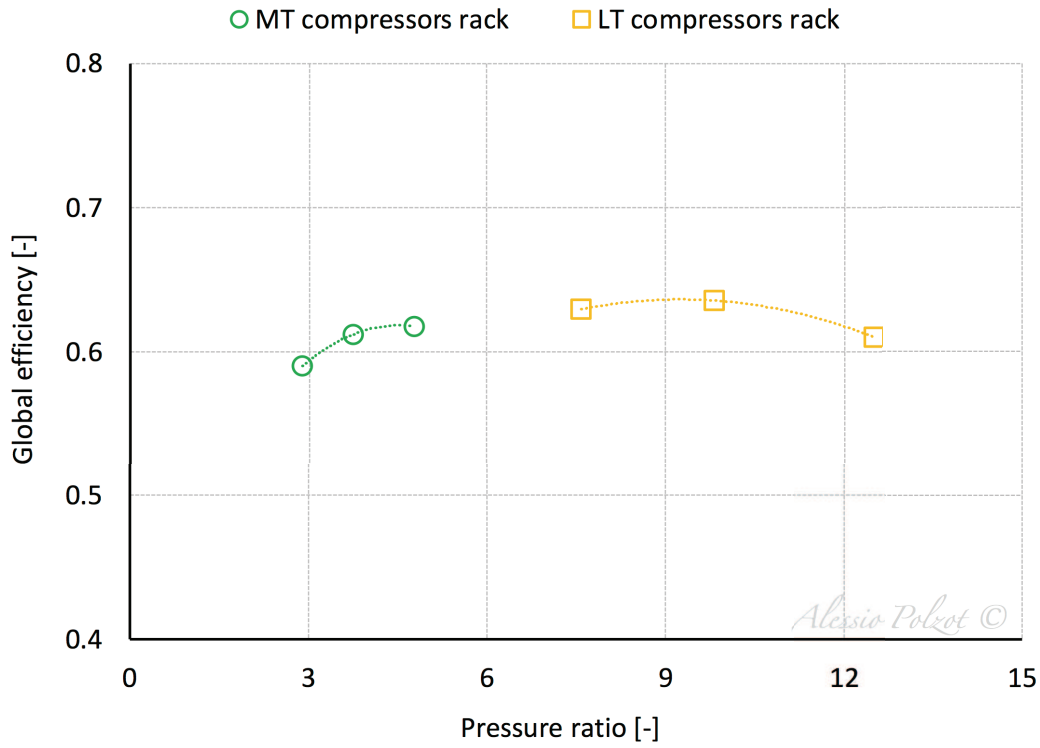

Figure 6.5.b - Compressors global efficiency for CAS system.

6.5.3 TBS system

The global efficiencies of the compressors in TBS system, which are depicted inFigure 6.5.c, are given by:

$$\eta_{LS} = -0.0378\,\beta_{LS}^2 + 0.1796\,\beta_{LS} + 0.4553 \tag{68}$$

$$\eta_{HS} = -0.0509\,\beta_{HS}^2 + 0.2883\,\beta_{HS} + 0.2550 \tag{69}$$

where:

β_{LS} is the pressure ratio of the low stage cycle (70) [-];

β_{HS} is the pressure ratio of the high stage cycle (71) [-].

$$\beta_{LS} = \frac{p_{evap,MT}}{p_{evap,LT}} \tag{70}$$

$$\beta_{MT} = \frac{p_{GC}}{p_{evap,MT}} \tag{71}$$

where:

$p_{evap,MT}$ is the medium temperature evaporating pressure [bar];

$p_{evap,LT}$ is the low temperature evaporating pressure [bar];

p_{GC} is the condenser/gas cooler discharge pressure [bar];

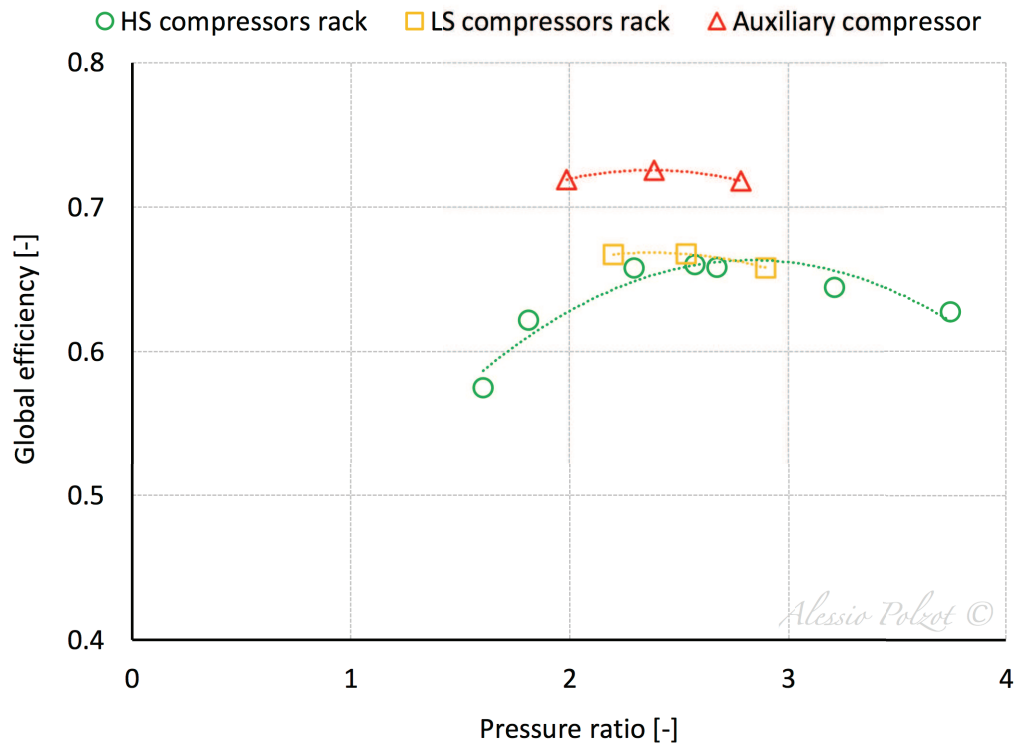

Figure 6.5.c - Compressors global efficiency for TBS and PCS systems.

6.5.4 PCS system

In PCS system, the global efficiencies of the LS and HS compressors racks are given by the same correlations uses for TBS system, (68) and (69), respectively.

The global efficiency of the auxiliary compressor, which is depicted in red dotted line inFigure 6.5.c, is given by:

$$\eta_{PC} = -0.0434\,\beta_{PC}^2 + 0.2058\,\beta_{PC} + 0.4815 \tag{72}$$

where:

β_{PC} is the pressure ratio of the auxiliary compression (73) [-].

$$\beta_{PC} = \frac{p_{GC}}{p_{INT}} \tag{73}$$

where:

p_{GC} is the condenser/gas cooler discharge pressure [bar];

p_{INT} is the intermediate pressure [bar].

6.6 Results

The results are reported in terms of performance of the system at different outdoor temperatures and in terms of annual energy consumption of the refrigeration system.

6.6.1 COP

Figure 6.6.a makes a comparison in terms of coefficient of performance (COP) among the evaluated solutions. At low outdoor temperatures, the DXS system performs better than the CAS system, while the latter has a better COP at external temperatures above 22 °C.

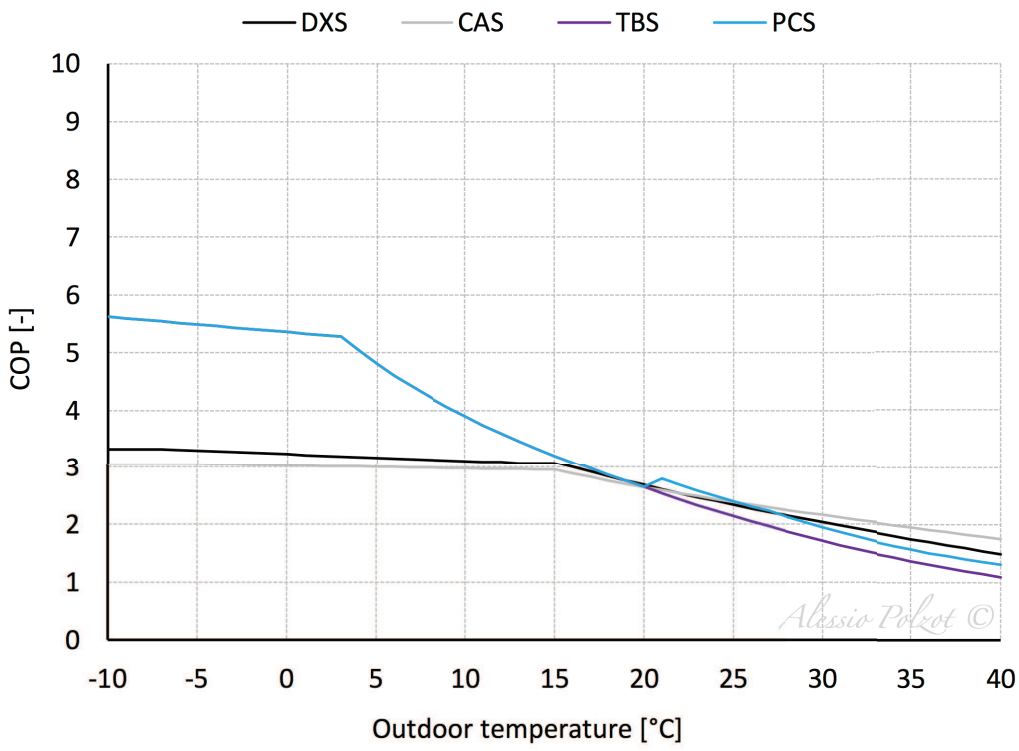

Figure 6.6.a - COP of the investigated solutions at outdoor temperatures from -10 °C to 40 °C.

In subcritical operation, when the auxiliary compressor is not activated, the PCS system works as a TBS system. Below the outdoor temperature of 19 °C, the CO_2 refrigeration systems offer better efficiencies than the conventional systems.
At high outdoor temperatures, when the transition and transcritical modes take place, the performance of the R744 refrigeration system degrade and for outdoor temperatures from 20 °C to 40 °C, the TBS system has a COP on average 15 % lower than the DXS system.
The auxiliary compressor allows achieving better values of COP than DXS until the ambient temperature of 28 °C. In transitional and transcritical conditions, the activation of the auxiliary compressor allows to the PCS system achieving values of COP which are on average 14 % higher than the ones presented by TBS system.

6.6.2 Operational modes

The annual performance of the CO_2 refrigeration system depends strongly on the climates conditions where the system is running. Location plays an important role and the warmer is the climate, the more the system operates in transcritical mode, the more the R744 systems perform worse than the traditional systems.
Figure 6.6.b shows the annual percentages of hours in which the carbon dioxide refrigeration systems work in the different operational conditions for the five mild and warm climates considered.
In a year, the TBS and the PCS systems works for about 5 % of the time in transcritical mode in Milan and Venice, the coldest climates considered, and for about 12 % of time, about 1020 hours, in Palermo. The transition operating condition takes place for about 1250 hours in a year in Milan, about 1600 in Venice, about 1850 in Rome, about 2260 in Genoa and about 2470 in Palermo.

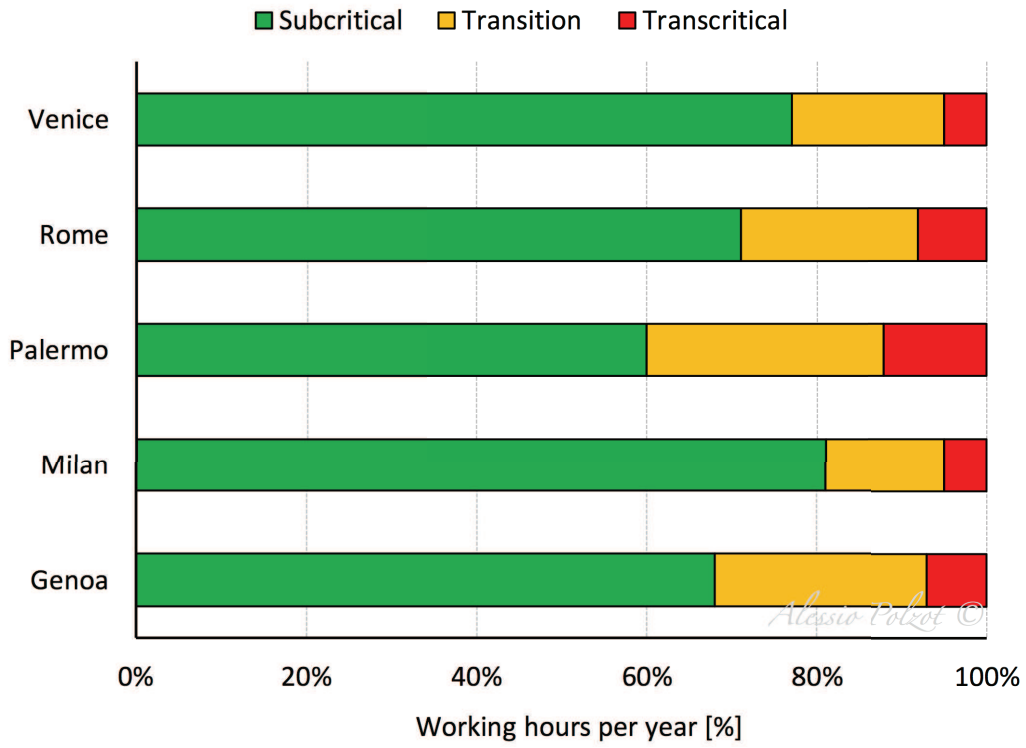

Figure 6.6.b - Operational modes working hours per year for the R744 refrigeration systems in the climate conditions considered.

6.6.3 Annual energy consumption

In this paragraph, the annual energy consumption of the refrigeration systems investigated performing in the climates conditions considered are compared.

Figure 6.6.c, Figure 6.6.e, Figure 6.6.g, Figure 6.6.i and Figure 6.6.k show the daily profile of the electrical energy consumption of the refrigeration system for all the investigated solutions in Genoa, Milan, Palermo, Rome and Venice, respectively. In the winter season in all the evaluated locations the TBS (violet solid line) and the PCS (blue solid line) systems perform better than the traditional systems. In the summer season the auxiliary compressor allows shaving the energy consumption peaks.

Figure 6.6.d, Figure 6.6.f, Figure 6.6.h, Figure 6.6.j and Figure 6.6.l report the monthly electrical energy consumption of the refrigeration system for all the investigated solutions. In January the PCS system consumes 37.6 % less energy than DXS in Milan, 36.1 % in Venice, 23.5 % in Rome, 21.5 % in Genoa and 10.6 % in Palermo. In August in Palermo while the PCS system perform slightly better than the DXS system, the TBS consume 11.9 % more energy than the R404A traditional system.

6.6.3.1 Genoa

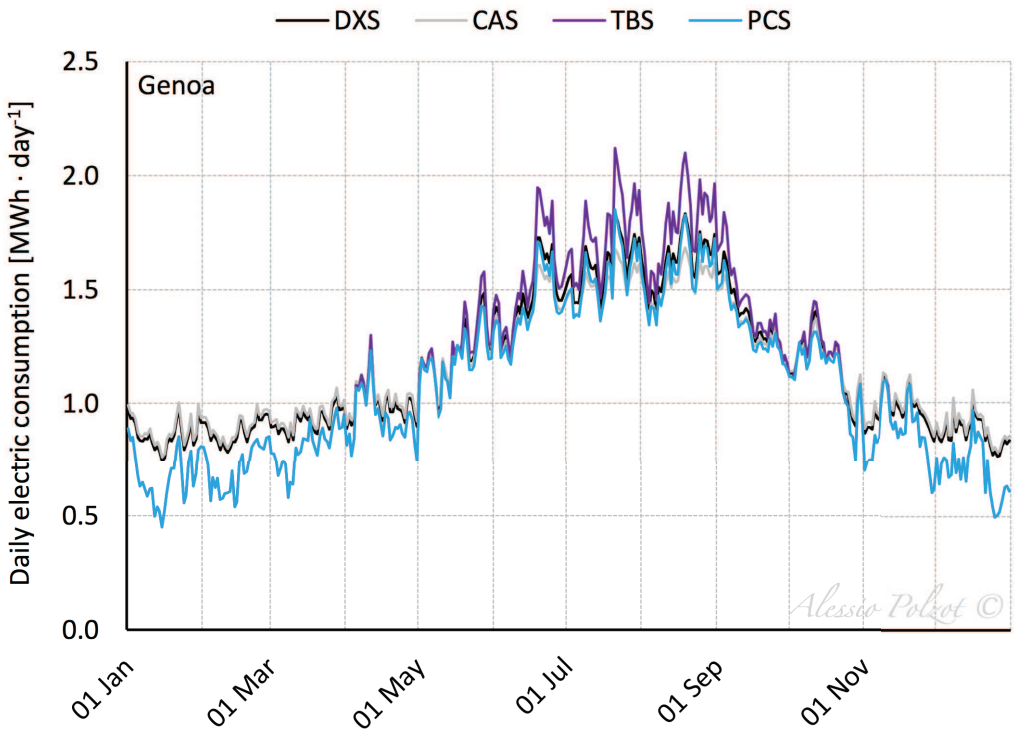

Figure 6.6.c –Energy consumption daily profiles of the investigated refrigeration systems in Genoa.

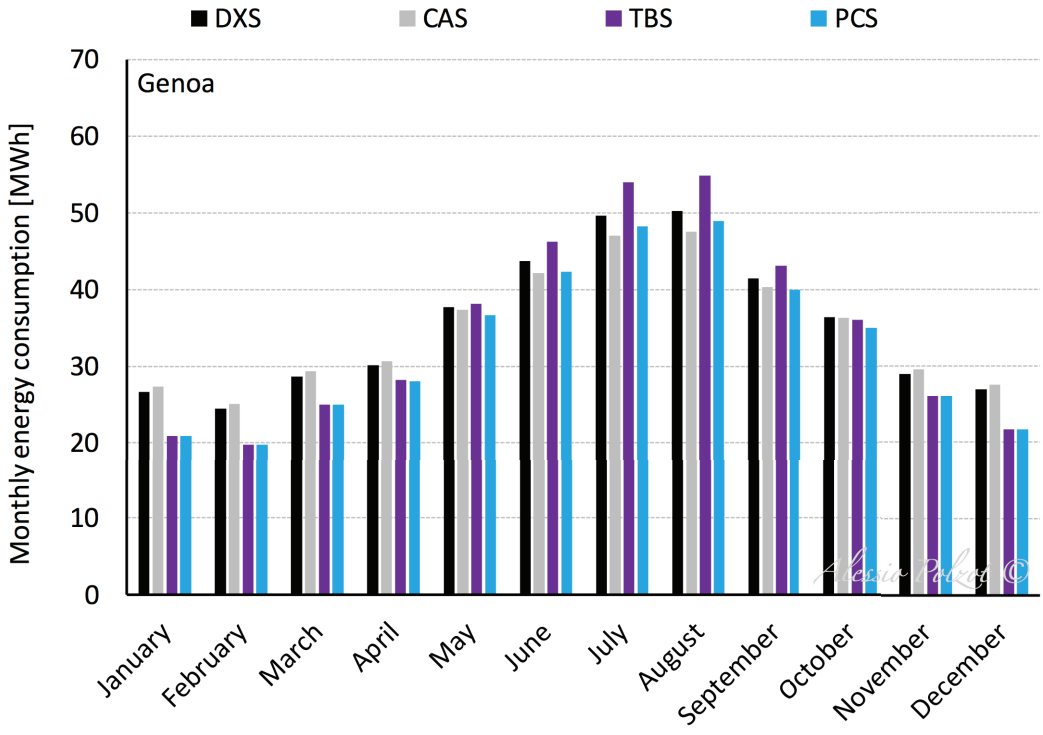

Figure 6.6.d - Monthly energy consumption of the investigated refrigeration systems in Genoa.

6.6.3.2 Milan

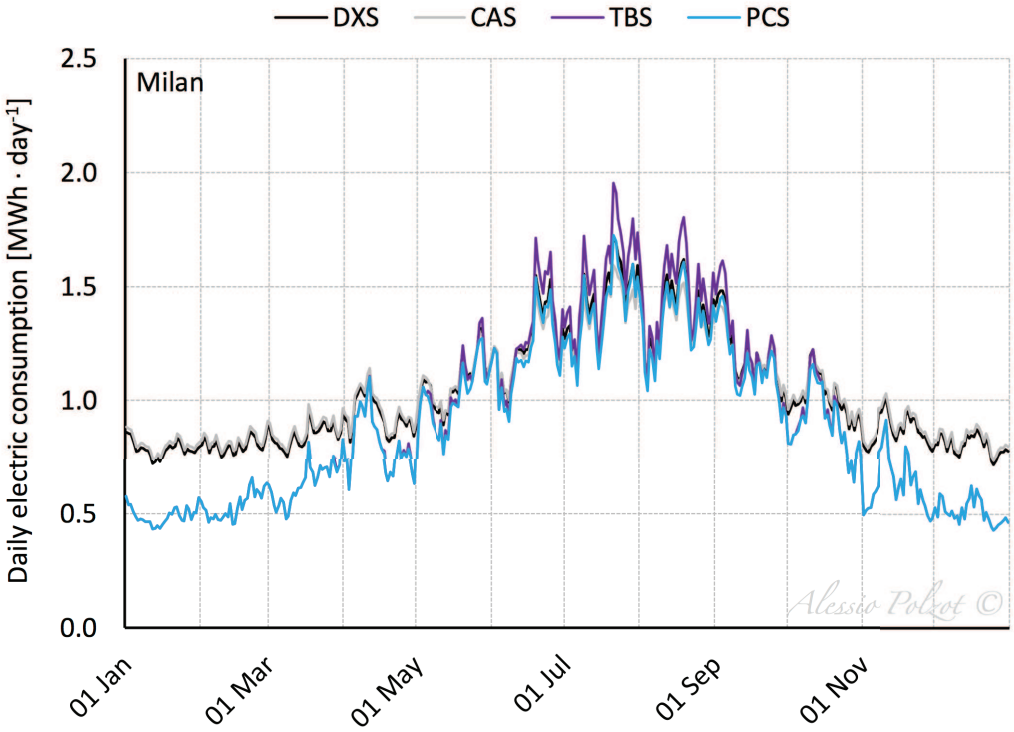

Figure 6.6.e - Energy consumption daily profiles of the investigated refrigeration systems in Milan.

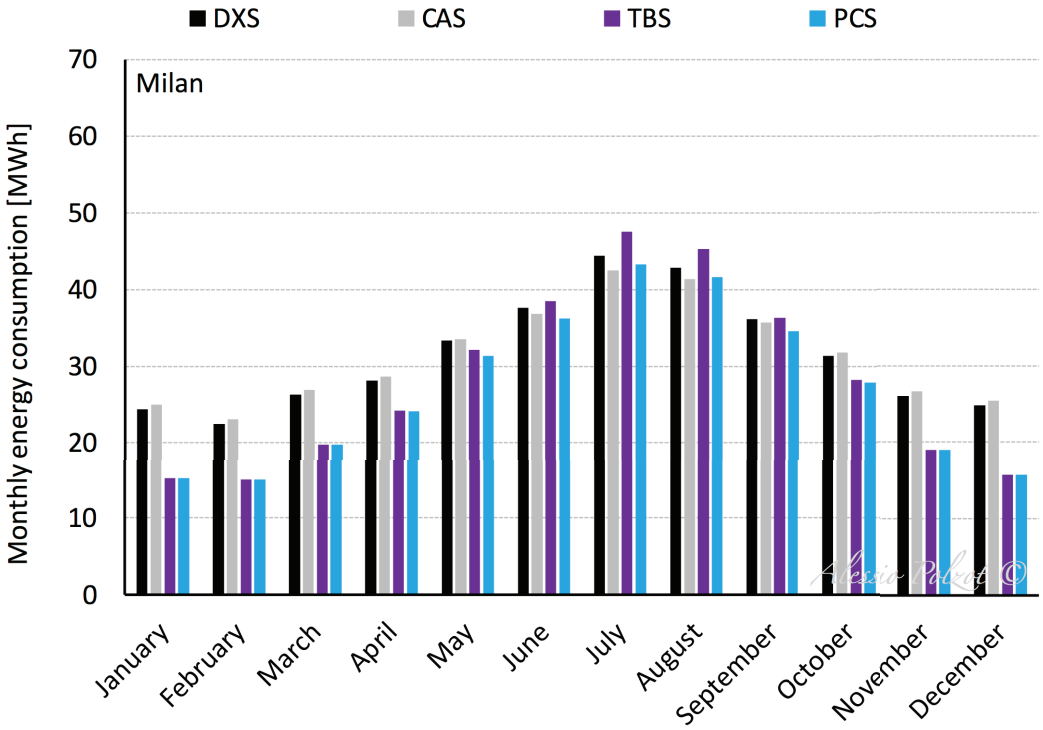

Figure 6.6.f - Monthly energy consumption of the investigated refrigeration systems in Milan.

6.6.3.3 Palermo

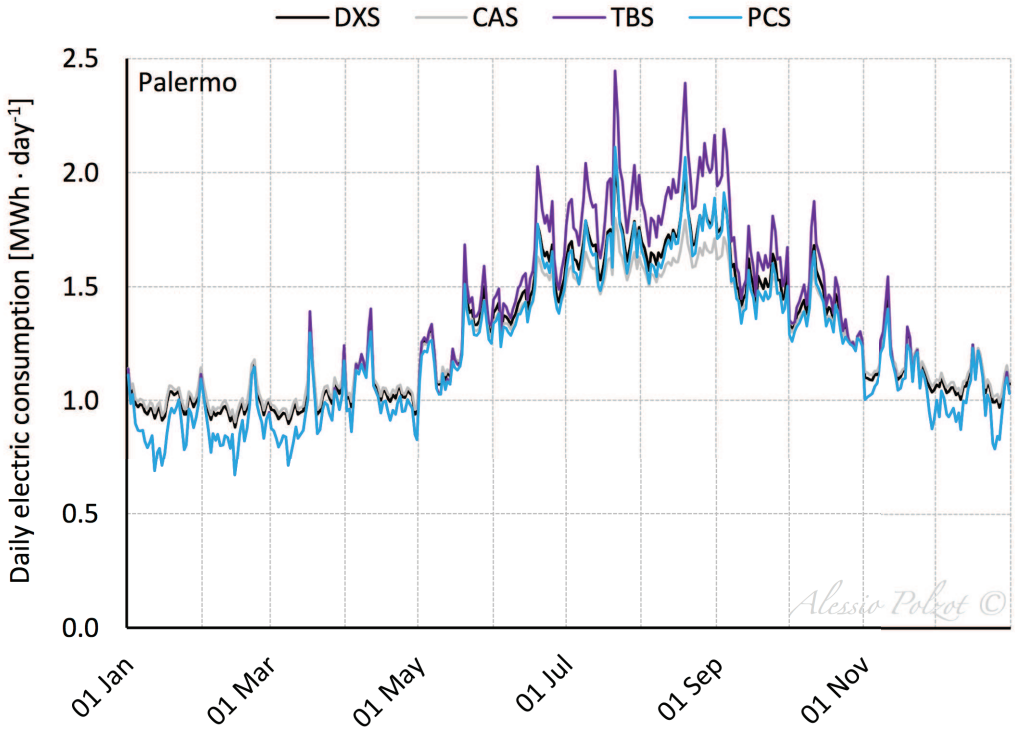

Figure 6.6.g - Energy consumption daily profiles of the investigated refrigeration systems in Palermo.

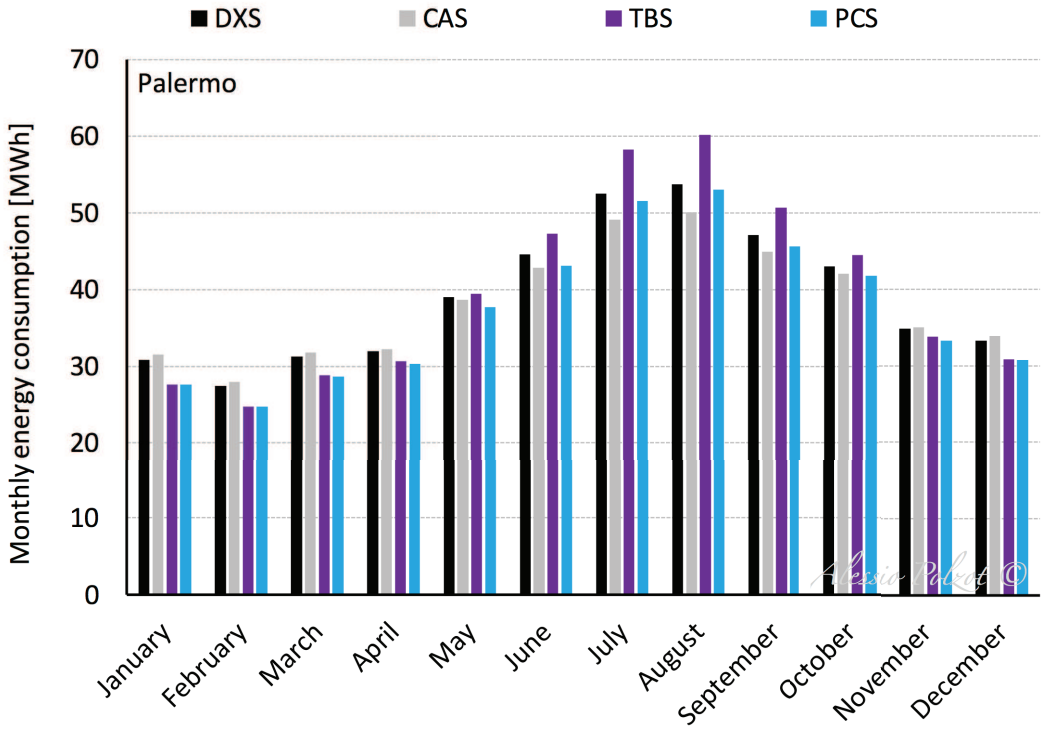

Figure 6.6.h - Monthly energy consumption of the investigated refrigeration systems in Palermo.

6.6.3.4 Rome

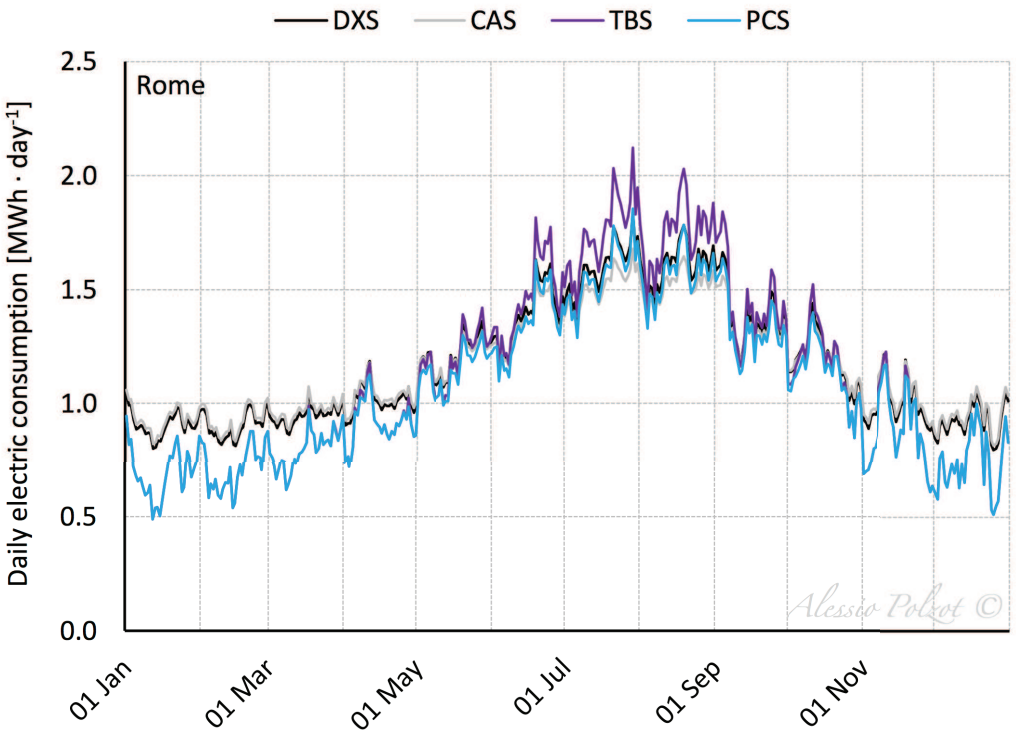

Figure 6.6.i - Energy consumption daily profiles of the investigated refrigeration systems in Rome.

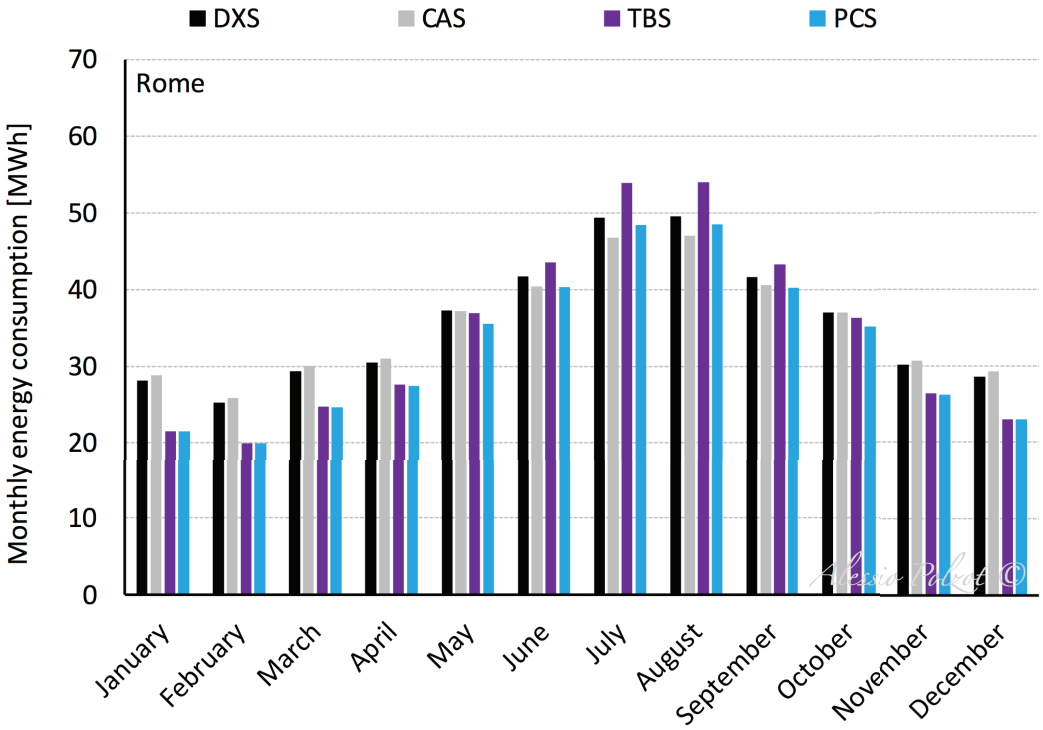

Figure 6.6.j - Monthly energy consumption of the investigated refrigeration systems in Rome.

6.6.3.5 Venice

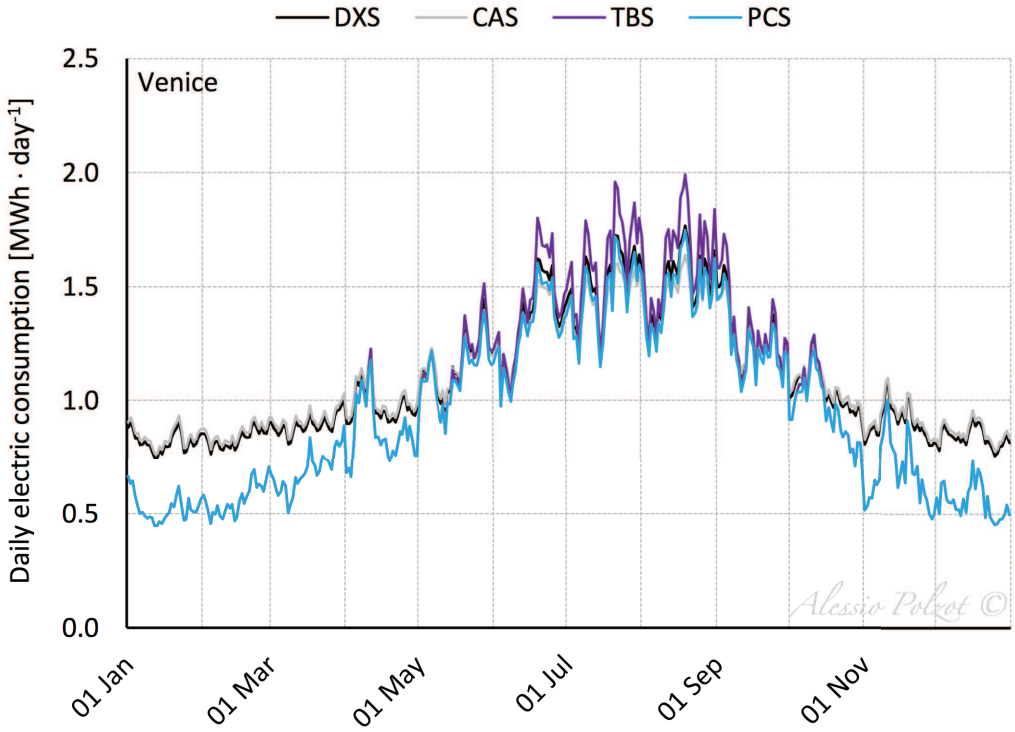

Figure 6.6.k - Energy consumption daily profiles of the investigated refrigeration systems in Venice.

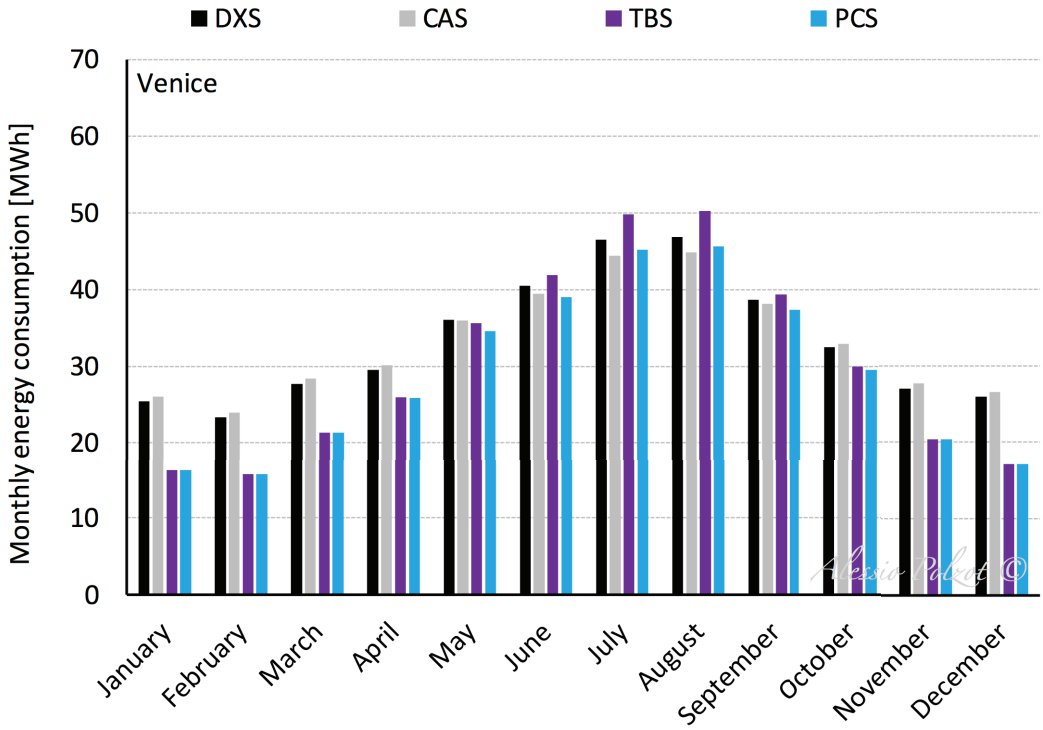

Figure 6.6.l - Monthly energy consumption of the investigated refrigeration systems in Venice.

The annual energy consumption of the DXS system and the relative energy consumption of the other solutions in comparison with the DXS one are reported in Table 6.6.a. Only in Palermo, the TBS system consume more energy over the year than the traditional solution, while the energy saving, which can be achieve with the PCS solution, ranges from 4.5 % to 13.0 %.

	Annual energy consumption	**Relative energy consumption**		
	[MWh]	[%]		
	DXS	**CAS**	**TBS**	**PCS**
Genoa	425	-1.2%	-2.6%	-7.6%
Milan	378	-0.1%	-10.8%	-14.3%
Palermo	470	-2.0%	1.6%	-4.5%
Rome	429	-1.0%	-4.1%	-8.8%
Venice	400	-0.4%	-9.1%	-13.0%

Table 6.6.a - Annual energy consumption of DXS system and relative energy consumption of the investigated solutions in comparison with DXS.

6.6.4 Auxiliary compressor

Figure 6.6.m shows for the PCS solution the percentage of time over the year in which the auxiliary compressor is working in all the climates condition evaluated. The additional compressor is activated 2859 hours per year in Genoa, 1705 in Milan, 3493 in Palermo, 2520 in Rome and 2052 in Venice.

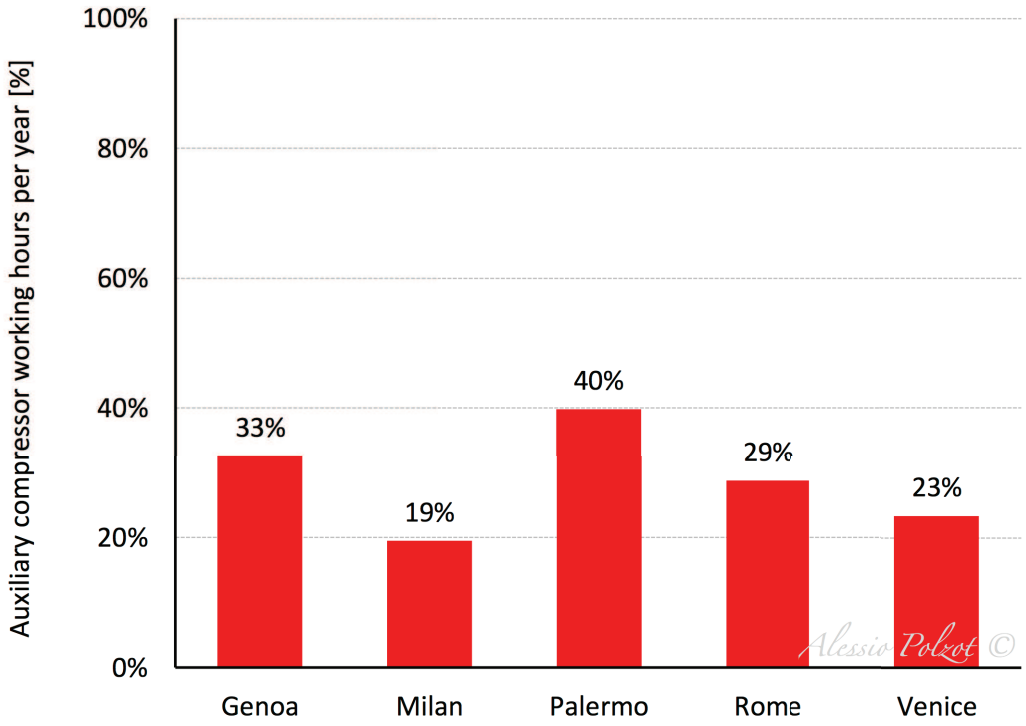

Figure 6.6.m - Auxiliary compressor working hours per year in the evaluated climates conditions.

6.7 Reference

- BITZER, 2016. BITZER Software 6.4.4.1464. Available at: https://www.bitzer.de/websoftware/ [accessed 15/12/2016].
- Cecchinato, L., Corradi, M., Minetto, S., Chiesaro, P., 2007. An experimental analysis of a supermarket plant working with carbon dioxide as refrigerant. Proceedings of the 22nd IIR International Congress of Refrigeration, Beijing, China.
- Chiarello, M., Girotto, S., Minetto, S., 2010. CO_2 supermarket refrigeration system for hot climates. Proceedings of the 9th IIR Gustav Lorentzen Conference on Natural Refrigerants, Sydney, Australia.
- Ge, Y.T., Tassou, S.A., 2011. Thermodynamic analysis of transcritical CO_2 booster refrigeration systems in supermarket. Energy Conversion and Management 52 (4), 1868–1875.

- Gullo, P., Elmegaard, B., Cortella, G., 2016. Energy and environmental performance assessment of R744 booster supermarket refrigeration systems operating in warm climates. International Journal of Refrigeration 64, 61–79.
- Kim, M.-H., Pettersen, J., Bullard, C.W., 2004. Fundamental process and system design issues in CO_2 vapor compression systems. Progress in Energy and Combustion Science 30 (2), 119–174.
- Liao, S.M., Zhao, T.S., Jakobsen, A., 2000. A correlation of optimal heat rejection pressures in transcritical carbon dioxide cycles. Applied Thermal Engineering 20, 831–841.
- Minetto, S., Cecchinato, L., Corradi, M., Fornasieri, E., Zilio, C., 2005. Theoretical and experimental analysis of a CO_2 refrigerating cycle with two-stage throttling and suction of the flash vapour by an auxiliary compressor. Proceedings of IIR International Conferences - Thermophysical Properties and Transfer Processes of Refrigerants, Vicenza Italy.
- Sarkar, J., Agrawal, N., 2010. Performance optimization of transcritical CO_2 cycle with parallel compression economization. International Journal of Thermal Sciences 49 (5), 838–843.

Chapter VII

Water loop heat pump

This chapter analyses the energy saving potential of integrated supermarket air conditioning and refrigeration systems using a water loop. In the Water Loop Heat Pump system (WLHP), a water loop is used as a heat source/sink for a number of electric reversible heat pumps which provide climate control on the different thermal zones (Buonomano et al., 2012). A basic CO_2 booster commercial refrigeration system with auxiliary compression and heat recovery is considered as the refrigeration system.

As baseline a traditional R404A direct expansion refrigeration system (DXS) and several electric reversible heat pumps are considered. Additional solution where the R744 booster system with heat recovery is replaced with a cascade refrigeration system (CAS) is evaluated.

7.1 System description

The WLB and WLD systems, which are sketched in Figure 7.1.a, are made up of a traditional WLHP system (blue solid line in Figure 7.1.a), where a number of electric reversible heat pumps provide climate control on the various thermal zones of the building, and a PCS refrigeration system, i.e. R744 transcritical booster system with auxiliary compression, with an additional high pressure heat exchanger (water cooled gas cooler/condenser in Figure 7.1.a) for heat recovery. This systems allow for simultaneous cooling and heating of spaces in the shopping mall with independent control of temperature and operation, with an easy accounting of energy consumption. Heat recovery from the refrigeration circuit is performed in the heating

season by heating up the water loop through the high pressure side heat exchanger of the refrigeration system.

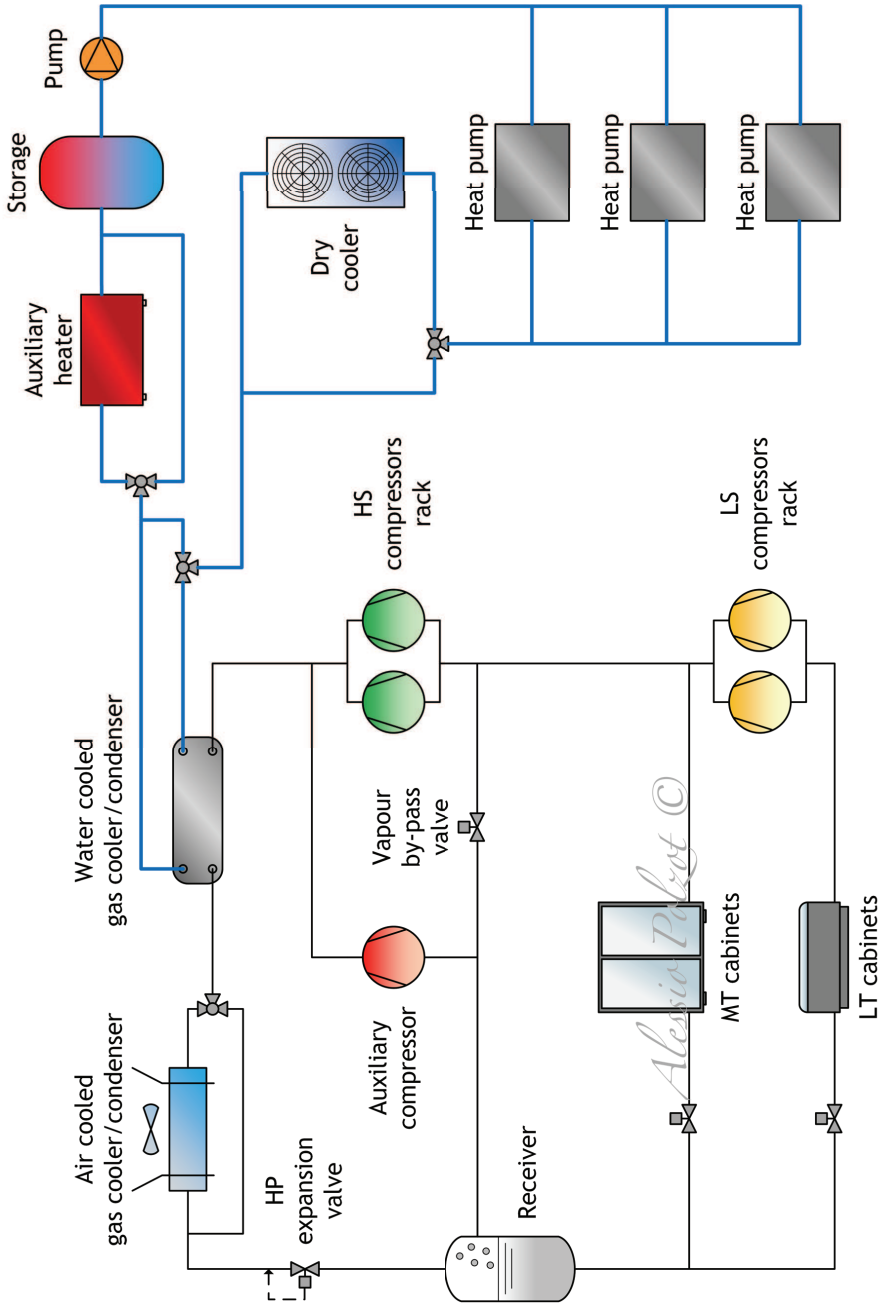

Figure 7.1.a - Schematic of a WLHP system with PCS system as refrigeration system (WLB and WLD).

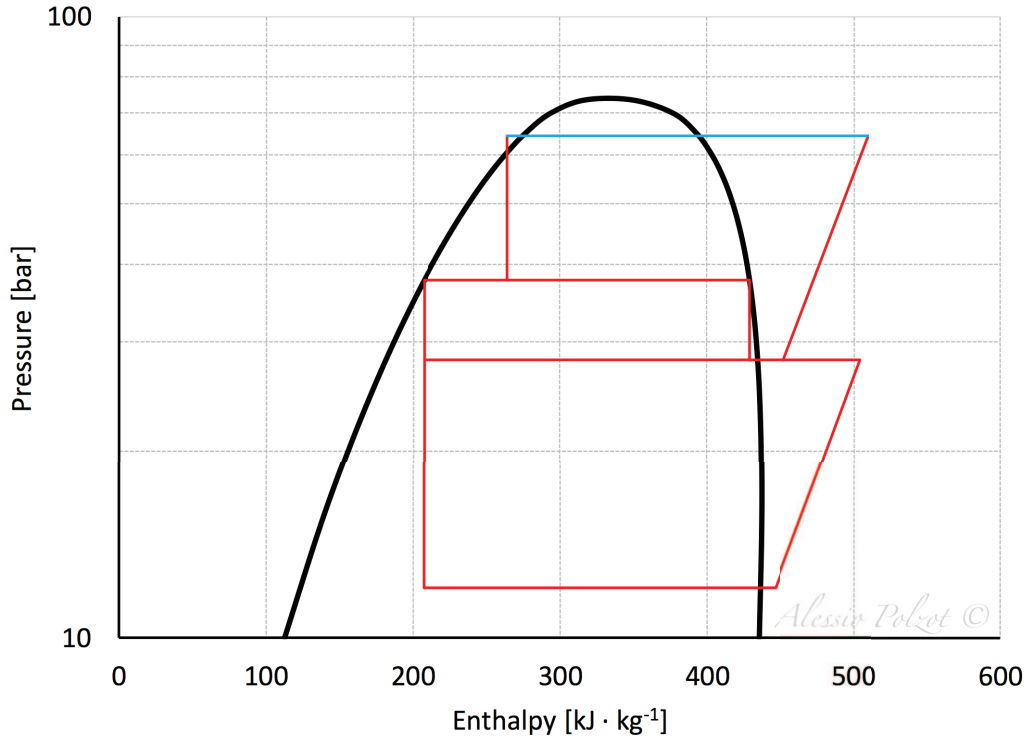

Figure 7.1.b - Log(p)-h diagram of the refrigeration system in WLB system.

The air cooled gas cooler/condenser can be by-passed (WLB system) and all the condensing process take place in the water cooled condenser (blue solid line in the log(p)-h diagram in Figure 7.1.b). Otherwise, in the water cooled heat exchanger takes place only the desuperheating process (WLD system). When the amount of heat available from the refrigeration system is low, the water loop temperature can be increased through an auxiliary heater. An additional air to water heat pump is considered as auxiliary system.

In the cooling season, when heat pumps are operating for air conditioning, a dry cooler on the water loop allows heat rejection to outdoors.

The water loop acts as source for the water to water or water to air heat pumps, and its temperature is a crucial factor in the operation of the whole system. In fact, in winter time the temperature should be as high as possible to favour the heat pumps, but this is a drawback for the refrigeration system which could take advantage of the low external temperature. Thus it is essential to balance the needs and adequately control the loop temperature. On the contrary, in summer time the water loop temperature should be as low as possible to favour the heat pump.

Both large roof top heat pumps and medium/small units are employed and the mass flow rate in the loop is kept constant throughout the year, and its value is the sum of the mass flow rate values required by the various heat pumps at rated conditions. Finally, a water reservoir is provided for the sake of thermal storage.

As a reference for comparison, a traditional DXS system is chosen as the refrigeration system and several electric air to air or air to water reversible heat pumps provide the climate control of the zones (AHD system).

An additional solution (WLC) is investigated (Cortella et al., 2014). A WLHP system for the climate control of the building and a CAS system with heat recovery for refrigeration are considered. The latter is sketched in Figure 7.1.c, where the HX2 heat exchanger as the same function of the water cooled heat exchanger in the WLD system.

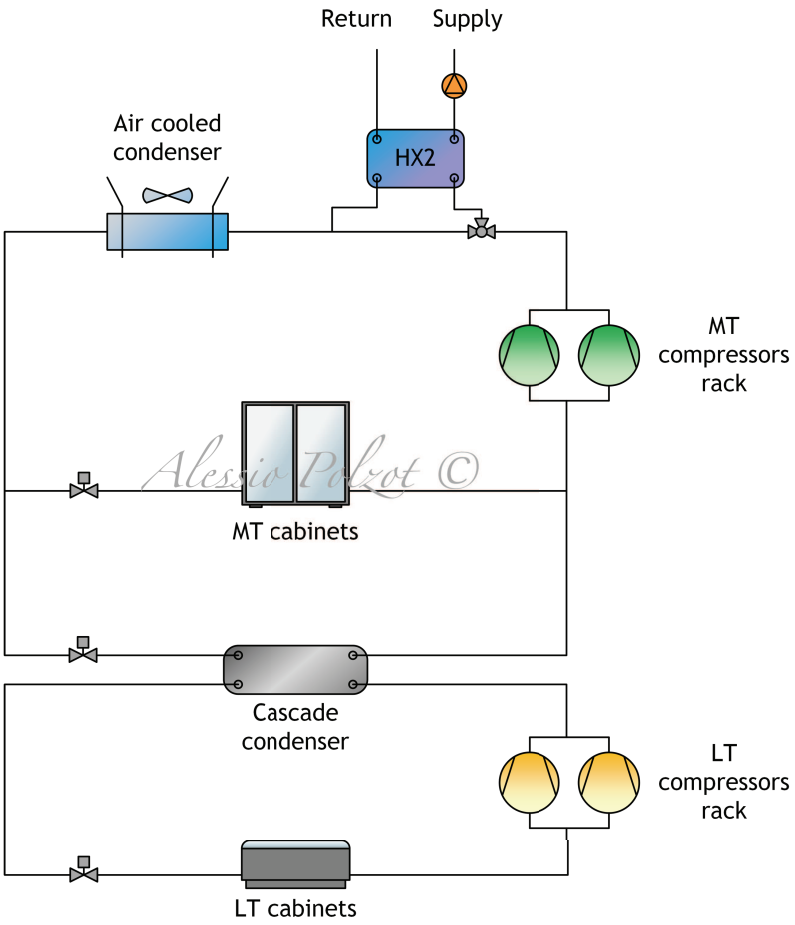

Figure 7.1.c - - Schematic of a CAS system with heat recovery.

The operating conditions proposed in Chapter VI are used to simulate the refrigeration systems, while the approach temperature of all the water cooled heat exchangers is set to 5 K.

7.2 Heat pumps

Two different reversible heat pumps are evaluated, one uses a HFC as working fluid and it is considered in AHD and WLC systems, the second one uses a hydro-fluoroolefin (HFO) as refrigerant and it is considered in WLB system. In AHD and WLC a specific HFC heat pump is used for domestic hot water (DHW) production while in WLB system the refrigeration system through another high pressure heat exchanger satisfy the DHW demand of the supermarket. The refrigerants considered are:

- R410A for HFC reversible heat pumps which provide the climate control of the thermal zones (operating conditions in Table 6.1.a and Table 7.2.b);
- R1234ze(E) for HFO reversible heat pumps which provide the climate control of the thermal zones (operating conditions in Table 7.2.c);
- R134a for the HFC heat pump which provide domestic hot water (operating conditions in Table 7.2.d and Table 7.2.e).

R410A heat pump operating conditions	Unit	Value
Useful superheating	K	4.0
Superheating in the suction lines	K	4.0
Subcooling in heating mode	K	3.5
Subcooling in cooling mode	K	2.0
Approach temperature of the source heat exchanger	K	10.0
Approach temperature of the load heat exchanger	K	5.0
Minimum condensing temperature in cooling mode	°C	25.0
Defrost capacity reduction	%	11.0
Defrost power reduction	%	1.0

Table 7.2.a - Operating conditions of the R410 heat pumps with outdoor air as heat source/sink in AHD.

R410A heat pump operating conditions	Unit	Value
Useful superheating	K	4.0
Superheating in the suction lines	K	4.0
Subcooling in heating mode	K	3.5
Subcooling in cooling mode	K	2.0
Approach temperature of the source heat exchanger	K	5.0
Approach temperature of the load heat exchanger	K	5.0
Minimum condensing temperature in cooling mode	°C	25.0
Defrost capacity reduction	%	0.0
Defrost power reduction	%	0.0

Table 7.2.b - Operating conditions of the R410 heat pumps with water loop as heat source/sink in WLC.

R1234ze(E) heat pump operating conditions	Unit	Value
Useful superheating	K	4.0
Superheating in the suction lines	K	4.0
Subcooling in heating mode	K	3.5
Subcooling in cooling mode	K	2.0
Approach temperature of the source heat exchanger	K	5.0
Approach temperature of the load heat exchanger	K	5.0
Minimum condensing temperature in cooling mode	°C	25.0
Defrost capacity reduction	%	0.0
Defrost power reduction	%	0.0

Table 7.2.c - Operating conditions of the R1234ze(E) heat pumps with water loop as heat source/sink in WLB.

The defrost capacity and power reductions of the heat pumps, which has the water loop as the heat source/sink, are set to zero since the temperature of the water loop never falls below 4 °C.

R134a heat pump operating conditions	Unit	Value
Useful superheating	K	4.0
Superheating in the suction lines	K	4.0
Subcooling	K	3.5
Approach temperature of the source heat exchanger	K	10.0
Approach temperature of the load heat exchanger	K	5.0
Defrost capacity reduction	%	11.0
Defrost power reduction	%	1.0

Table 7.2.d - Operating conditions of the R134a heat pump with outdoor air as heat source/sink in AHD.

R134a heat pump operating conditions	Unit	Value
Useful superheating	K	4.0
Superheating in the suction lines	K	4.0
Subcooling	K	3.5
Approach temperature of the source heat exchanger	K	5.0
Approach temperature of the load heat exchanger	K	5.0
Defrost capacity reduction	%	0.0
Defrost power reduction	%	0.0

Table 7.2.e - Operating conditions of the R134a heat pump with water loop as heat source/sink in WLC.

Figure 7.2.a, Figure 7.2.b and Figure 7.2.c make a comparison in terms of coefficient of performance (COP) and energy efficiency ratio (EER) among the different heat pumps considered. The heat pumps for thermal zones climate control provide in the heating season hot water at 40 °C with a return water temperature of 30 °C and in the cooling season cold water at 7 °C with a return water temperature of 12 °C. The heat pumps for the DHW production provide hot water at 60 °C to avoid growth of legionella. The COP and EER values are related to the above mentioned set-point values.

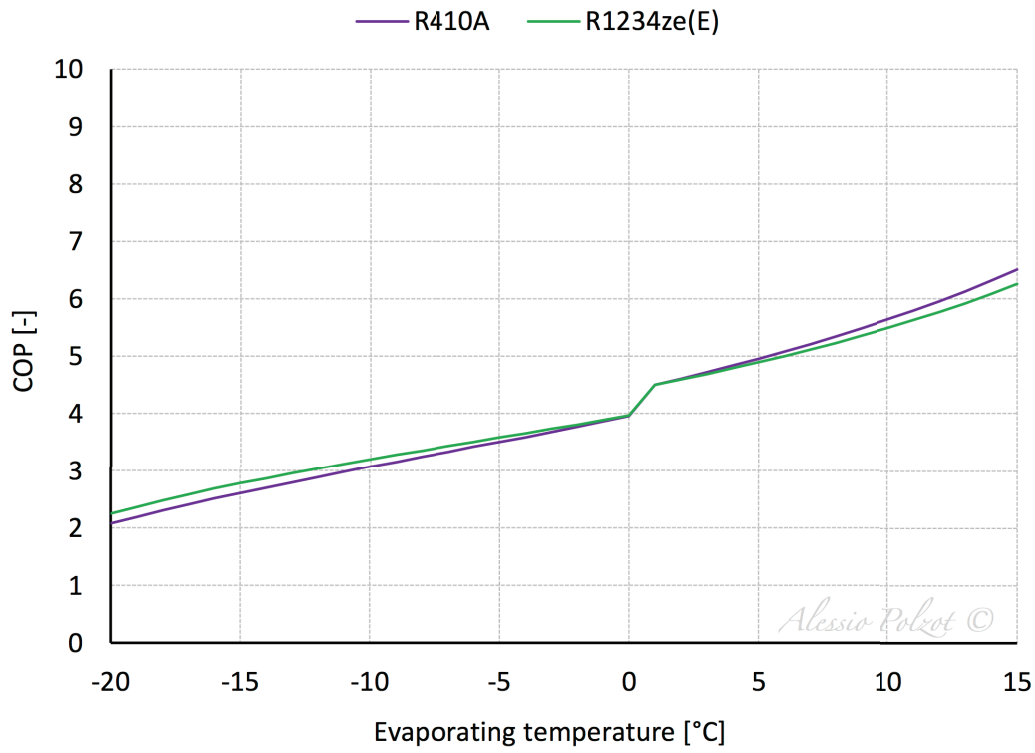

Figure 7.2.a - COP of the investigated reversible heat pumps.

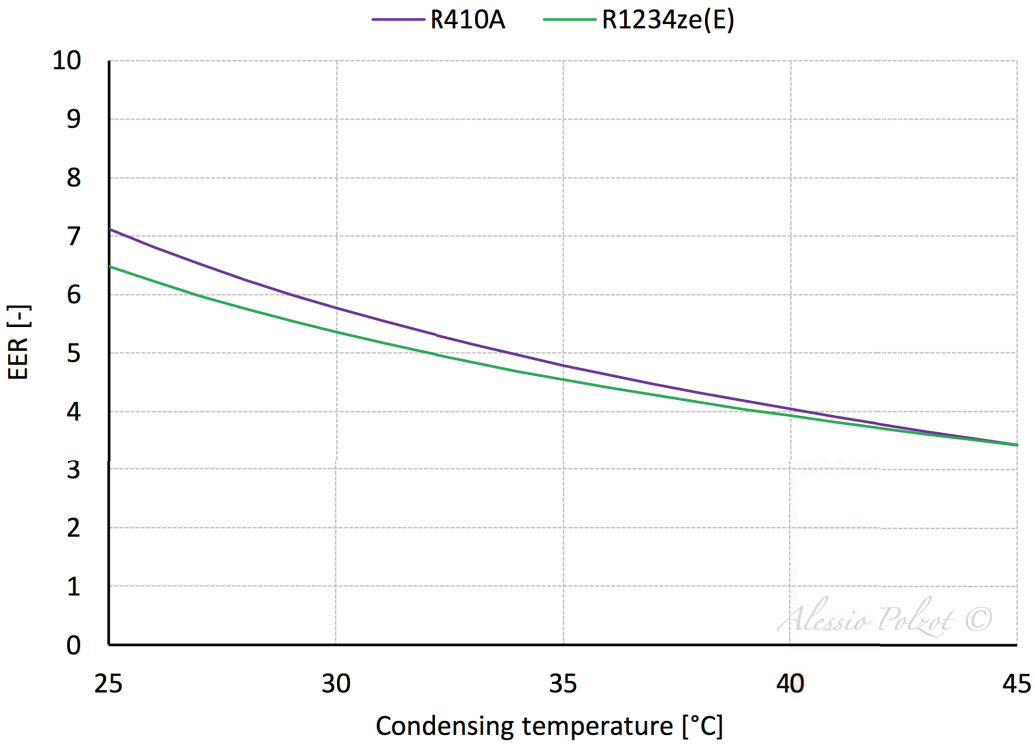

Figure 7.2.b - EER of the investigated reversible heat pumps.

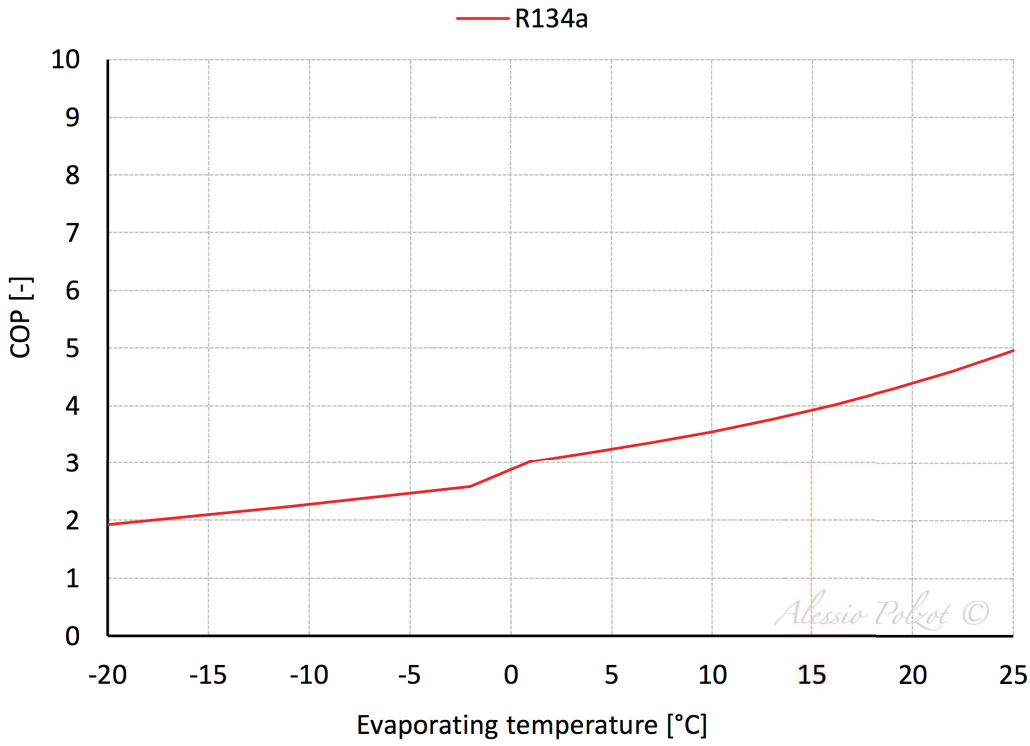

Figure 7.2.c - COP of the investigated heat pump for DHW production.

7.3 Heat pumps compressors global efficiency

The compressors, which are selected for the heat pumps used in all the investigated solutions, are:

- scroll compressors for the R410A reversible heat pumps;
- semi-hermetic reciprocating compressors for the R134a heat pumps;
- semi-hermetic screw compressors for the R1234ze(E) reversible heat pumps.

All their suggested technological constraints are respected.

Their global efficiencies are obtained as a function of the pressure ratio by using BITZER Software (BITZER, 2016) for the HFC heat pumps and Frascold Software (Frascold, 2016) for the HFO heat pumps.

The global efficiency is defined as the ratio of the power input calculated at isentropic conditions to the power input declared by the manufacturers.

7.3.1 R410a heat pumps

The compressors global efficiency of the R410a heat pumps is depicted in Figure 6.5.a and it is given by:

$$\eta_{R410A} = -0.0207\,\beta^2 + 0.1370\,\beta + 0.5229 \tag{74}$$

where:

β is the pressure ratio (62) [-];

$$\beta = \frac{p_{cond}}{p_{evap}} \tag{75}$$

where:

p_{cond} is the condensing pressure [bar];

p_{evap} is the evaporating pressure [bar].

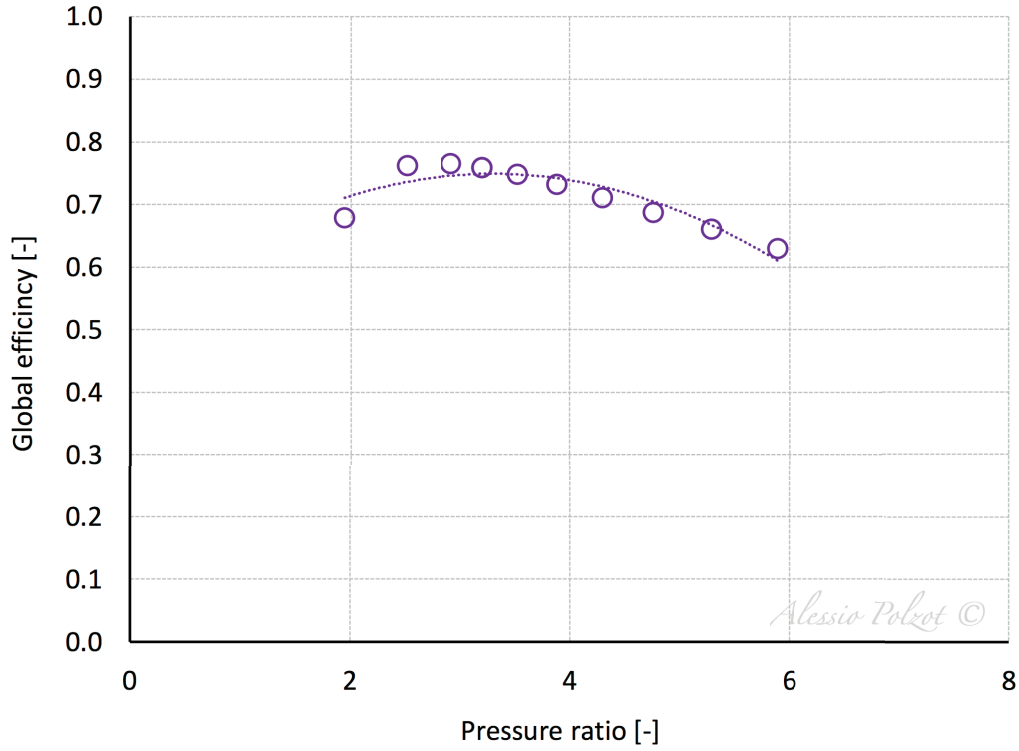

Figure 7.3.a - Compressor global efficiency of R410A reversible heat pump.

7.3.2 R1234ze(E) heat pumps

The compressors global efficiency of the R1234ze(E) heat pumps is shown in Figure 6.5.b and it is given by:

$$\eta_{R1234ze(E)} = -0.0112\,\beta^2 + 0.1125\,\beta + 0.4175 \quad (76)$$

where:

β is the pressure ratio (62) [-].

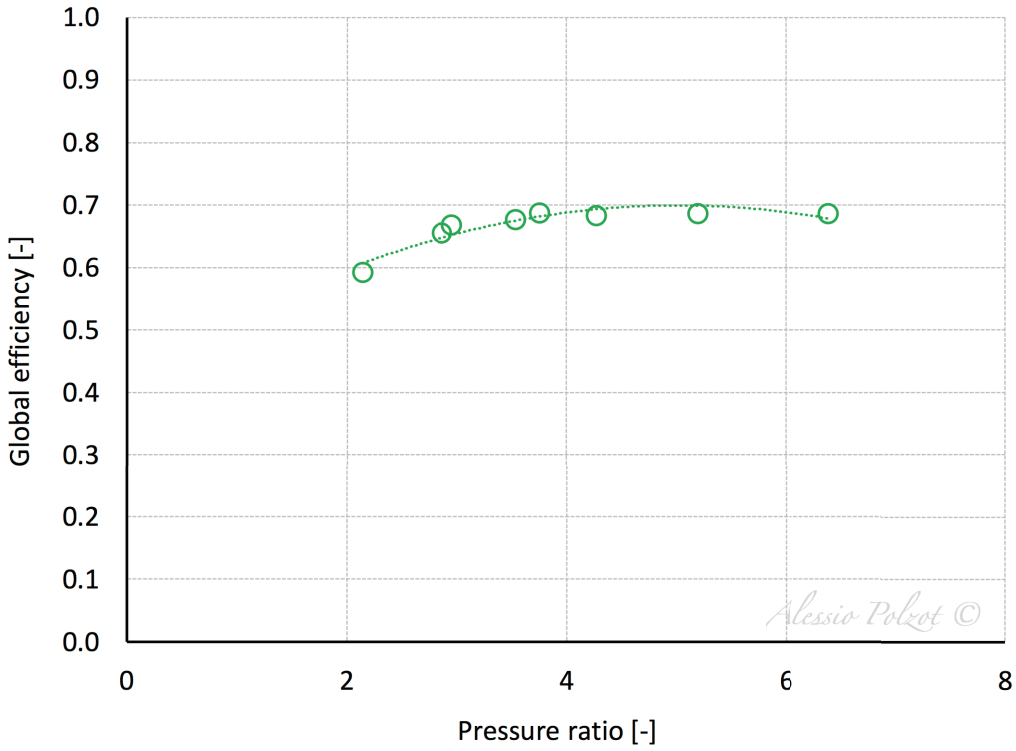

Figure 7.3.b - Compressor global efficiency of R1234ze(E) reversible heat pump.

7.3.3 R134a heat pumps

The compressors global efficiency of the R134a heat pumps is portrayed in Figure 6.5.c and it is given by:

$$\eta_{R134a} = -0.0008\,\beta^2 + 0.0103\,\beta + 0.6527 \quad (77)$$

where:

β is the pressure ratio (62) [-].

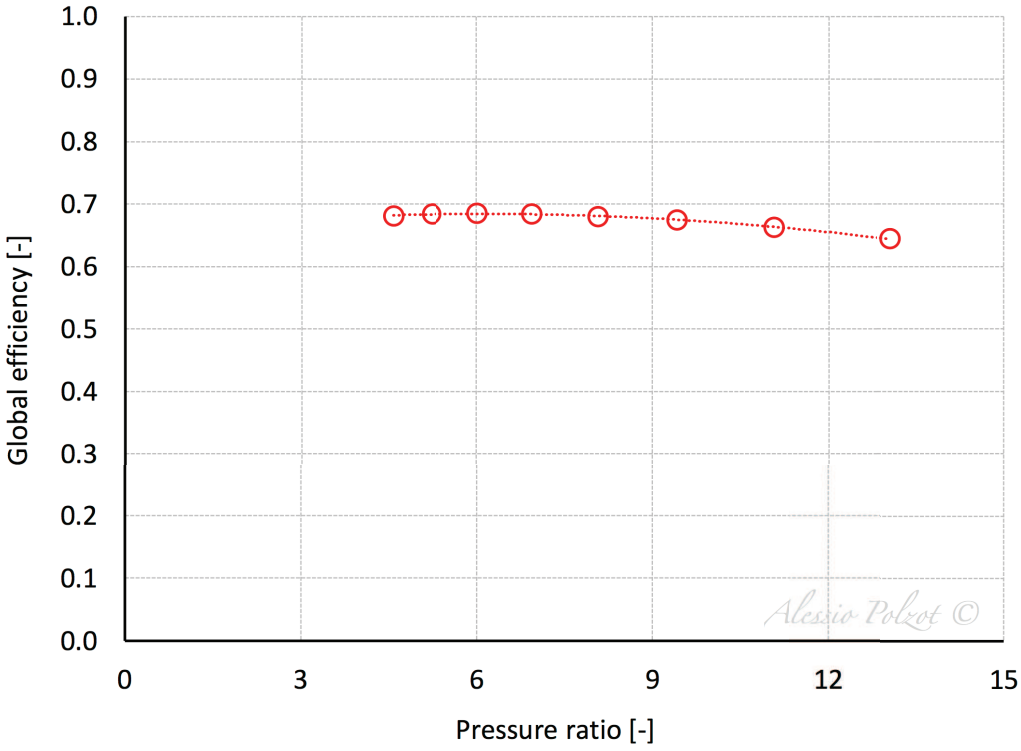

Figure 7.3.c - Compressor global efficiency of R134a heat pump.

7.4 Heating, cooling and DHW demands

The water loop heat pump system provide climate control of 12 thermal zones of the shopping mall considered (Paragraph 3.1). The heat pumps supply heat and cool to all the hallways and common areas of the ground floor, to the warehouses, the food store and the services. The thermal zones are:

- 3 - service
- 4 - service
- 8 -warehouse
- 9 - warehouse
- 18 - hallways
- 19 - hallways
- 20 - hallways
- 21 - hallways
- 22 - hallways
- 23 - hallways

- 24 - hallways
- 30 - food store

In Figure 7.4.a, Figure 7.4.b, Figure 7.4.c, Figure 7.4.d and Figure 7.4.e are shown the monthly heating and cooling demands of the thermal zones. The heating demand is reported as a negative value, while cooling demand is depicted as a positive value. The domestic hot water usage is estimated at a maximum value of 250 dm^3 per hour during the opening hours. In Figure 7.4.f the monthly domestic hot water demand is depicted.

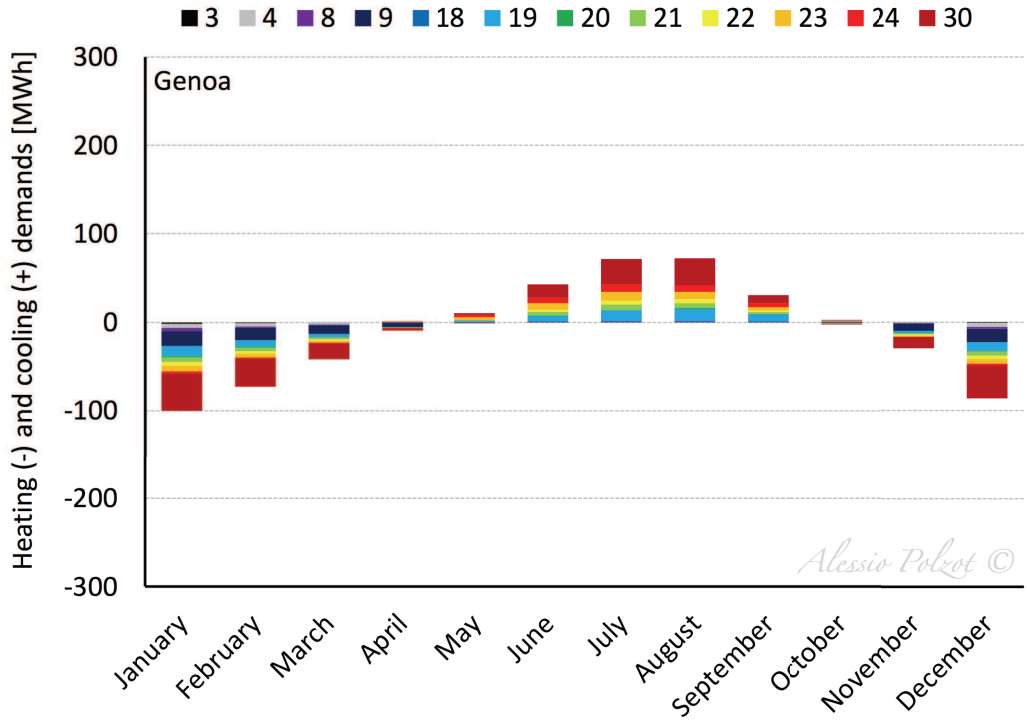

Figure 7.4.a - Heating and cooling demands of the WLHP thermal zones in Genoa.

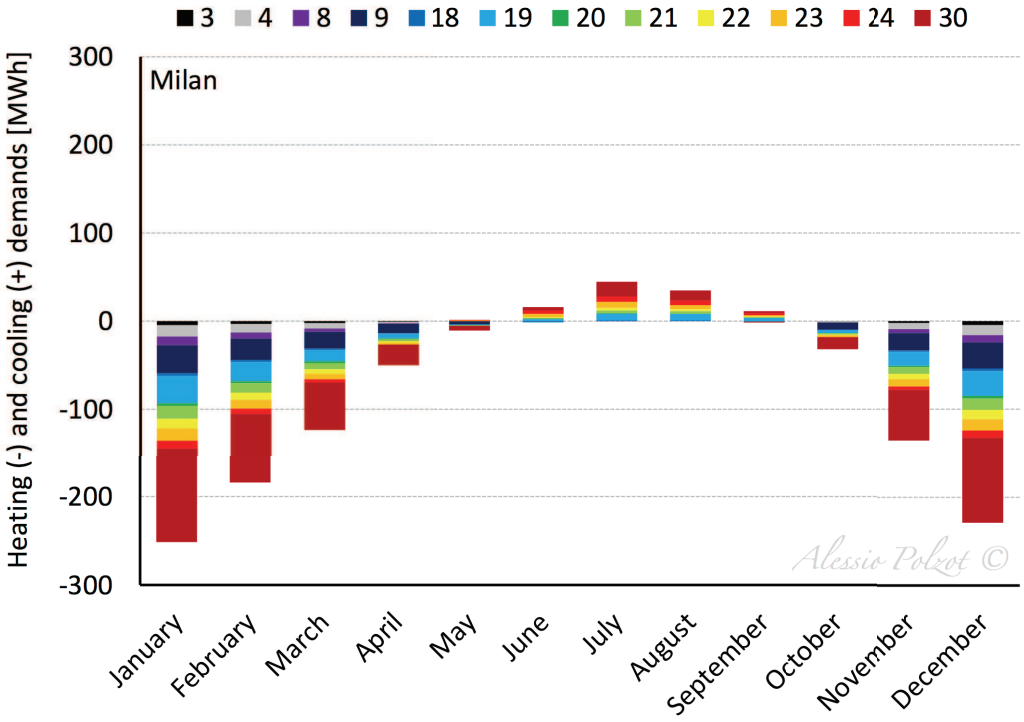

Figure 7.4.b - Heating and cooling demands of the WLHP thermal zones in Milan.

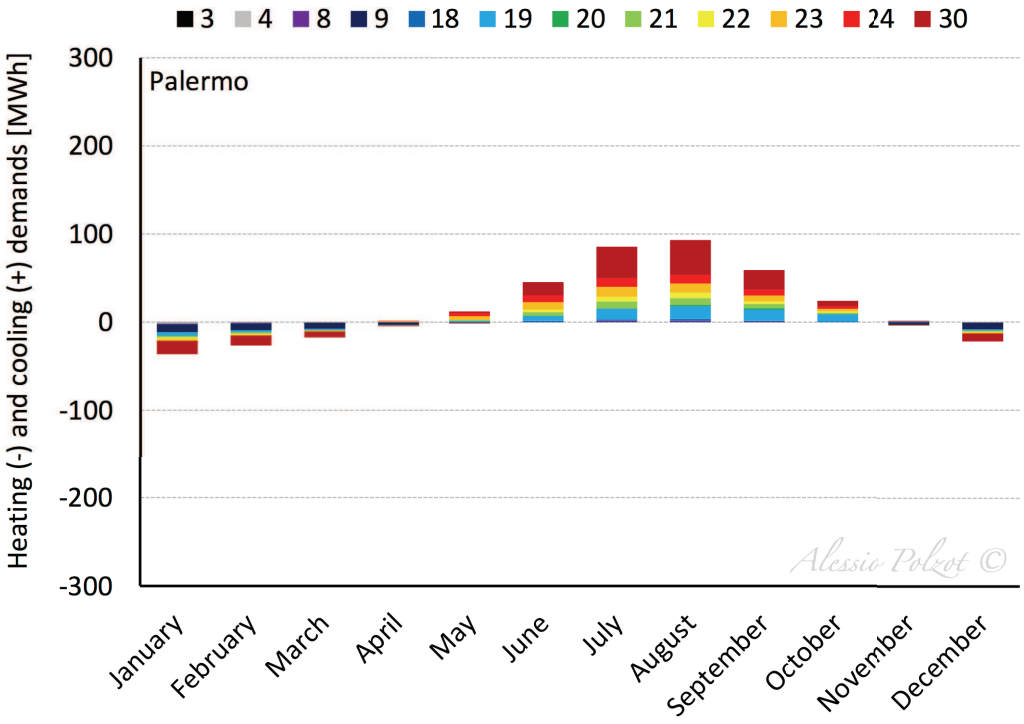

Figure 7.4.c - Heating and cooling demands of the WLHP thermal zones in Palermo.

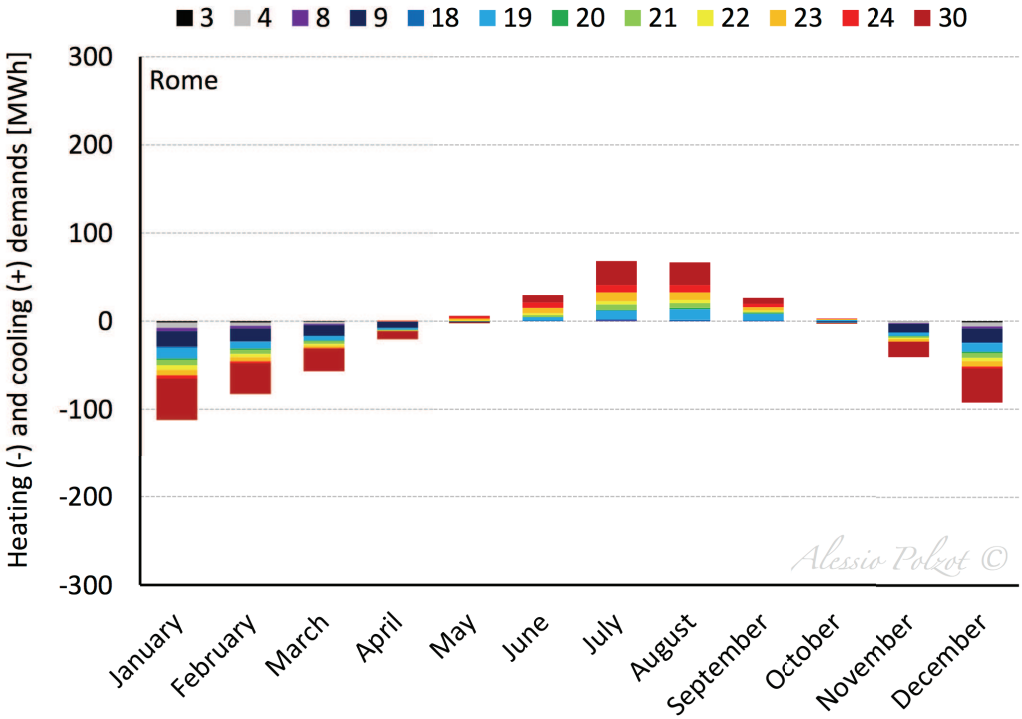

Figure 7.4.d - Heating and cooling demands of the WLHP thermal zones in Rome.

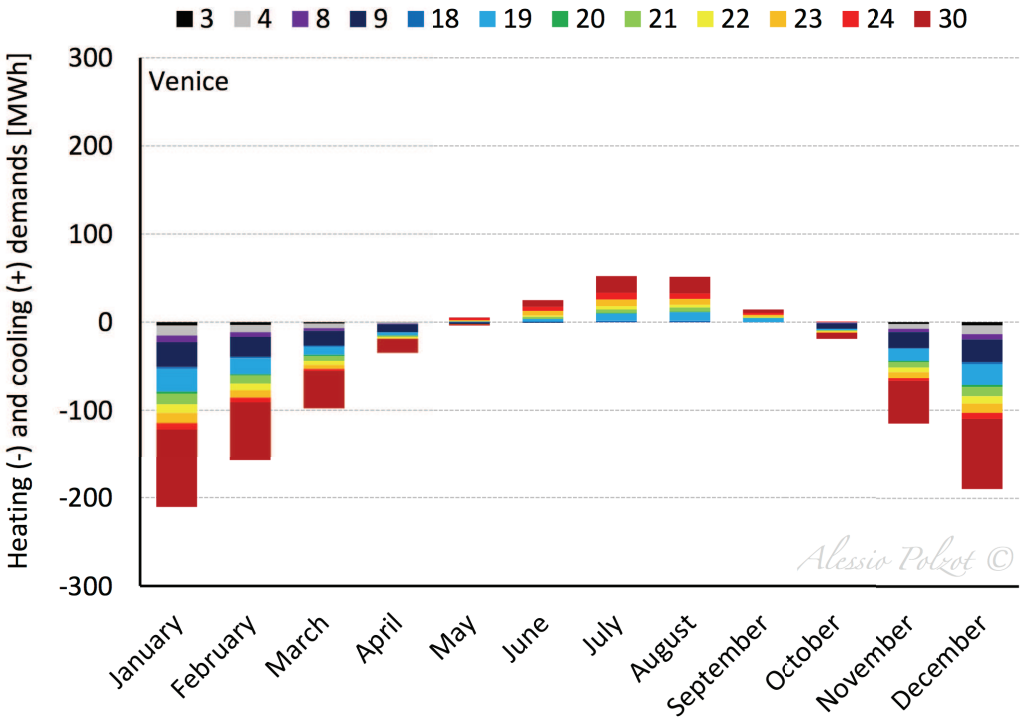

Figure 7.4.e - Heating and cooling demands of the WLHP thermal zones in Venice.

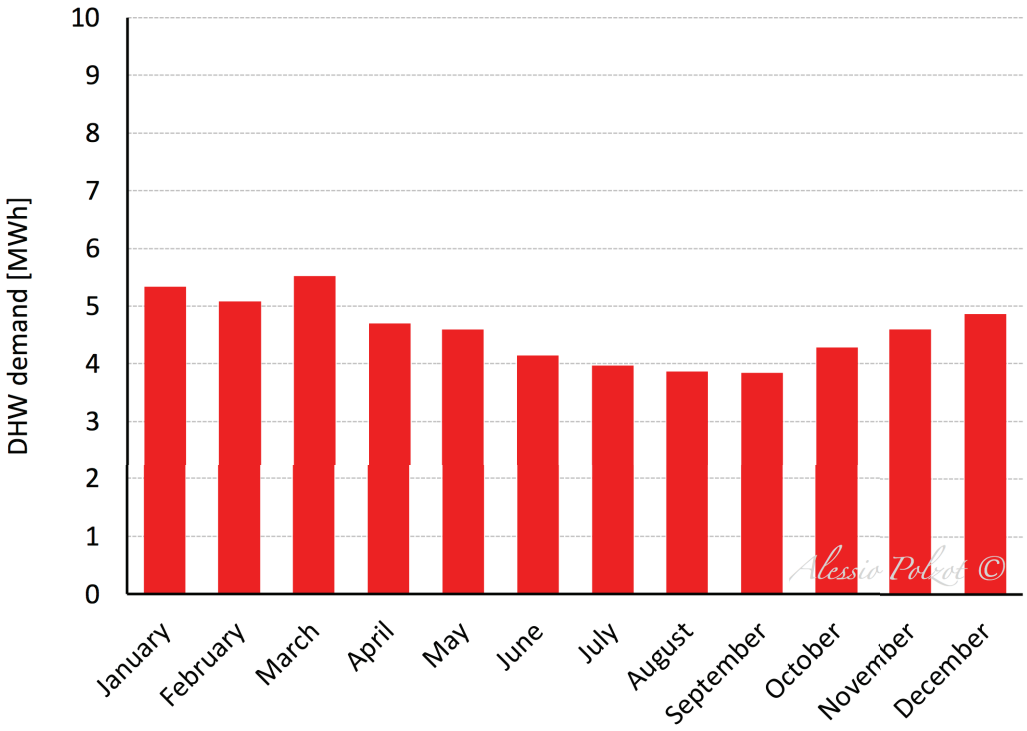

Figure 7.4.f - Domestic hot water demand of the building.

7.5 Results

The results are reported in terms of temperature profiles of the water loop over the year, and in terms of annual energy consumption of the air conditioning system, of the refrigeration system and of the overall system.

The auxiliary devices of the water loop and the heat recovery is controlled by the following control strategy:

- when the water loop temperature drops below a heating set-point temperature (t_{HR}), the heat recovery from refrigeration is activated to heat the water loop;
- when the water loop temperature drops below a second heating set-point temperature (t_{AH}), which is lower than the first one, the auxiliary heater is activated;
- when the water loop temperature rises to a cooling set-point temperature (t_{DC}) the dry-cooler is activated to cool the water loop in accordance with the outdoor temperature and the dry-cooler approach temperature.

The above mentioned set point values and the volume of the storage (V_S) for the WLC system are reported in Table 7.5.a.

		Unit	Value
Heat recovery set-point temperature	t_{HR}	°C	20.0
Auxiliary heater set-point temperature	t_{AH}	°C	8.0
Dry-cooler set-point temperature	t_{DC}	°C	25.0
Storage volume	V_S	m^3	50

Table 7.5.a - Set-point temperatures and volume of the storage for WLC system.

A parametric analysis of the set-point temperatures is conducted for WLB and WLD systems.

7.5.1 Set-point temperatures

The heat recovery set-point temperature is fixed at 20 °C while the auxiliary heater set-point temperature is varied from 3 °C to 15 °C. The dry-cooler set-point temperature ranges from 20 °C to 25 °C. Figure 7.5.a, Figure 7.5.b, Figure 7.5.c, Figure 7.5.d and Figure 7.5.e make a comparison in terms of annual energy consumption of the overall system among the solutions WLB and WLD with the different set-point temperatures above mentioned. For the sake of clarity in the figures are reported only the energy consumption of the WLB and WLD systems with the dry-cooler set-point temperature equal to 20 °C, WLB 20 and WLD 20, respectively, and with the dry-cooler set-point temperature equal to 25 °C, WLB 25 and WLD 25, respectively. In the two warmest climates conditions, Genoa and Palermo, the WLD solution consumes less energy than WLB, while in mild climates the most efficient system is the WLB in which the air cooled gas/cooler condenser is by-passed and the condensation of the CO_2 refrigeration system takes place in the water cooled condenser. In all the investigated locations, the optimal value of the dry-cooler set-point temperature is 25 °C. During the summer time the increment in the energy consumption of the dry-cooler to cool down the water loop temperature is greater than the reduction in the power input associated with the heat pumps due to the lower temperature of the loop.

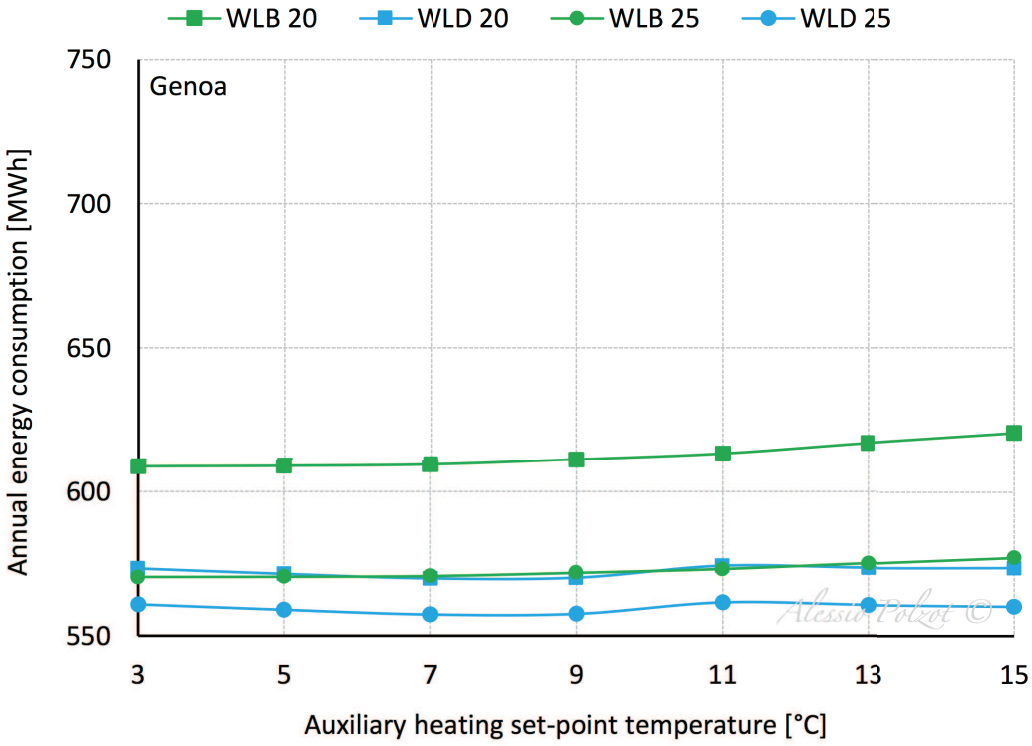

Figure 7.5.a - Results of the parametric analysis in terms of annual energy consumption of the overall system in Genoa.

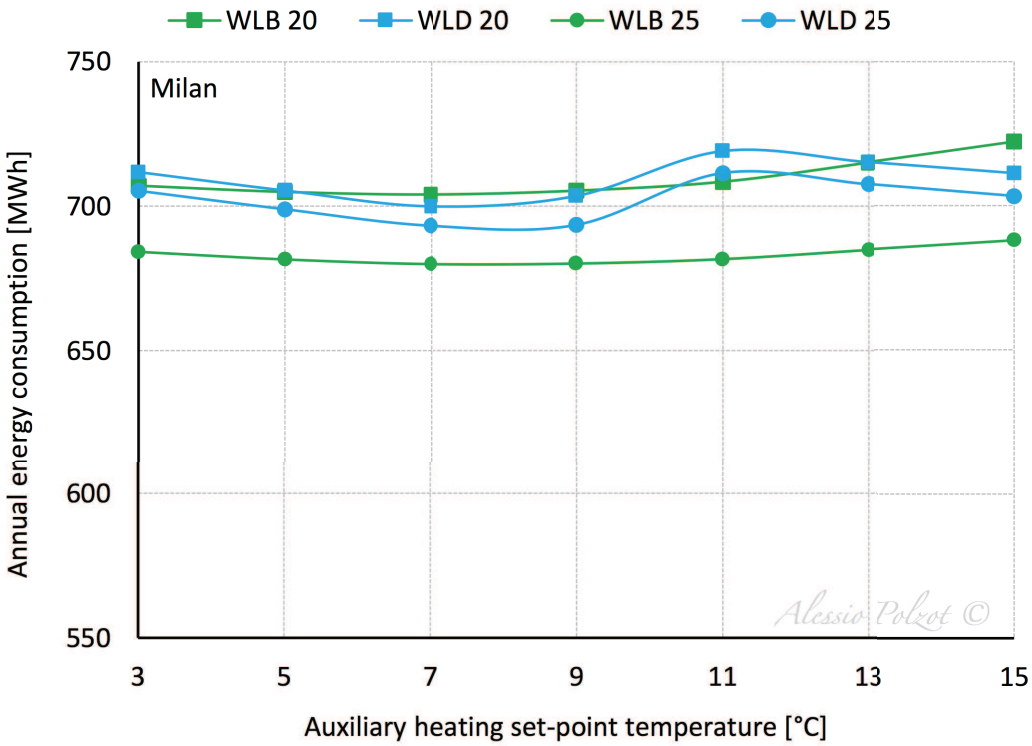

Figure 7.5.b - Results of the parametric analysis in terms of annual energy consumption of the overall system in Milan.

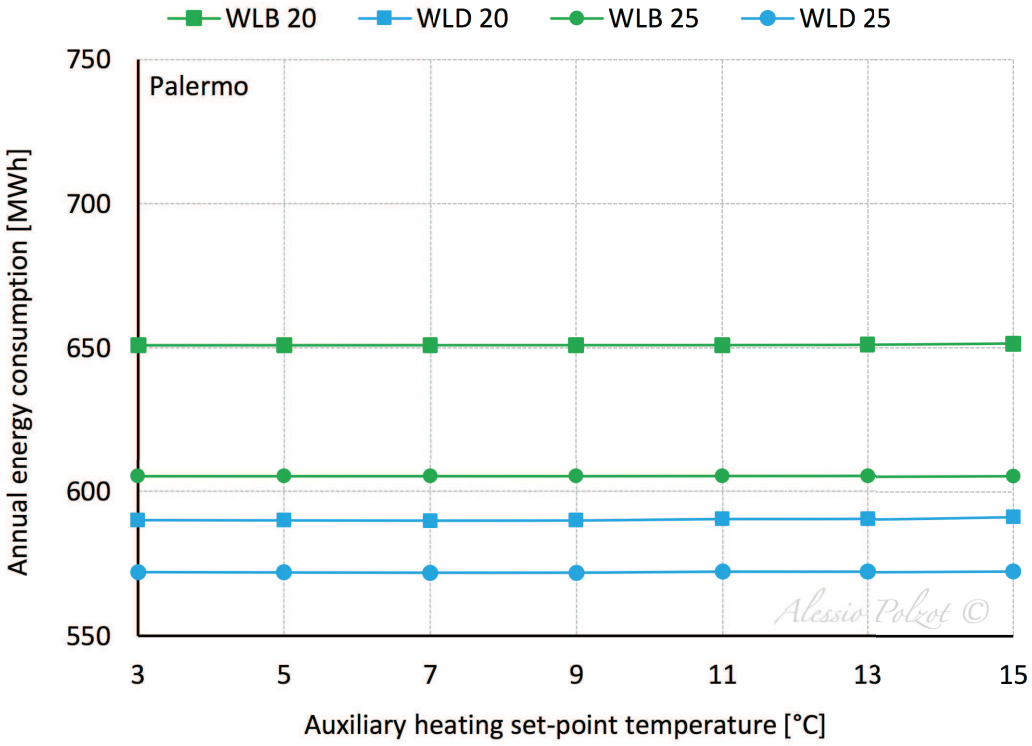

Figure 7.5.c - Results of the parametric analysis in terms of annual energy consumption of the overall system in Palermo.

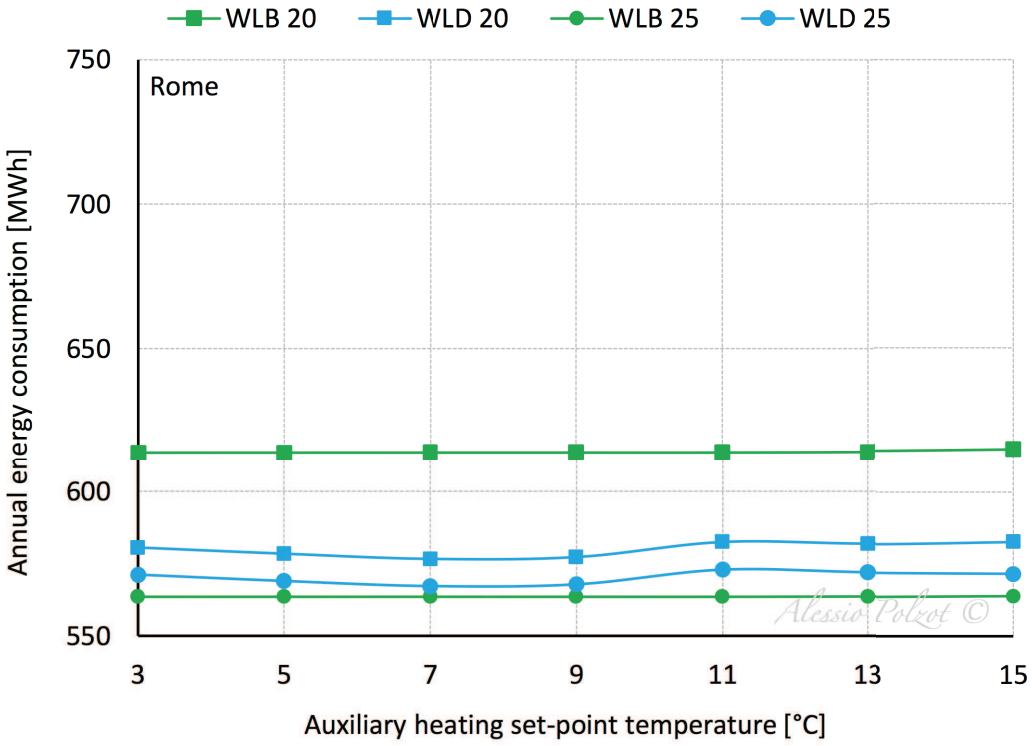

Figure 7.5.d - Results of the parametric analysis in terms of annual energy consumption of the overall system in Rome.

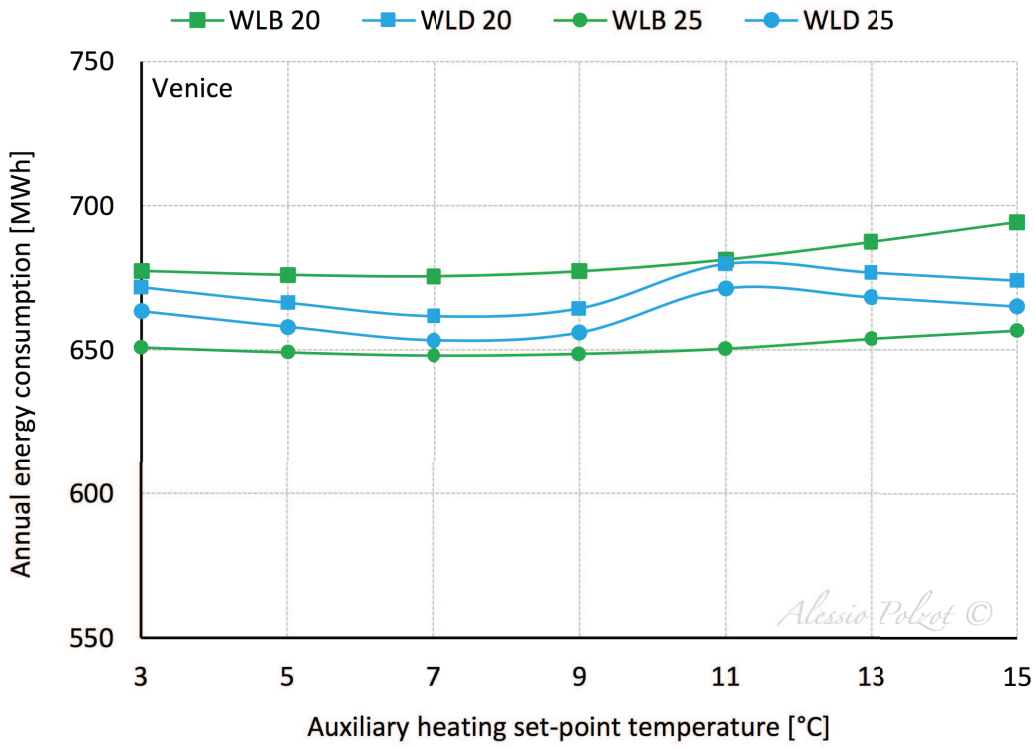

Figure 7.5.e - Results of the parametric analysis in terms of annual energy consumption of the overall system in Venice.

7.5.2 Water loop temperature

Figure 7.5.f, Figure 7.5.g, Figure 7.5.h, Figure 7.5.i and Figure 7.5.j show the daily average temperature of the water loop in the different locations investigated and for the three systems evaluated. The set-point used for the WLC solutions is reported in Table 7.5.a, while the WLB and WLD profiles temperatures, which are depicted in the figures, are related to the optimal set-point temperature values which can be obtained from the previously paragraph.

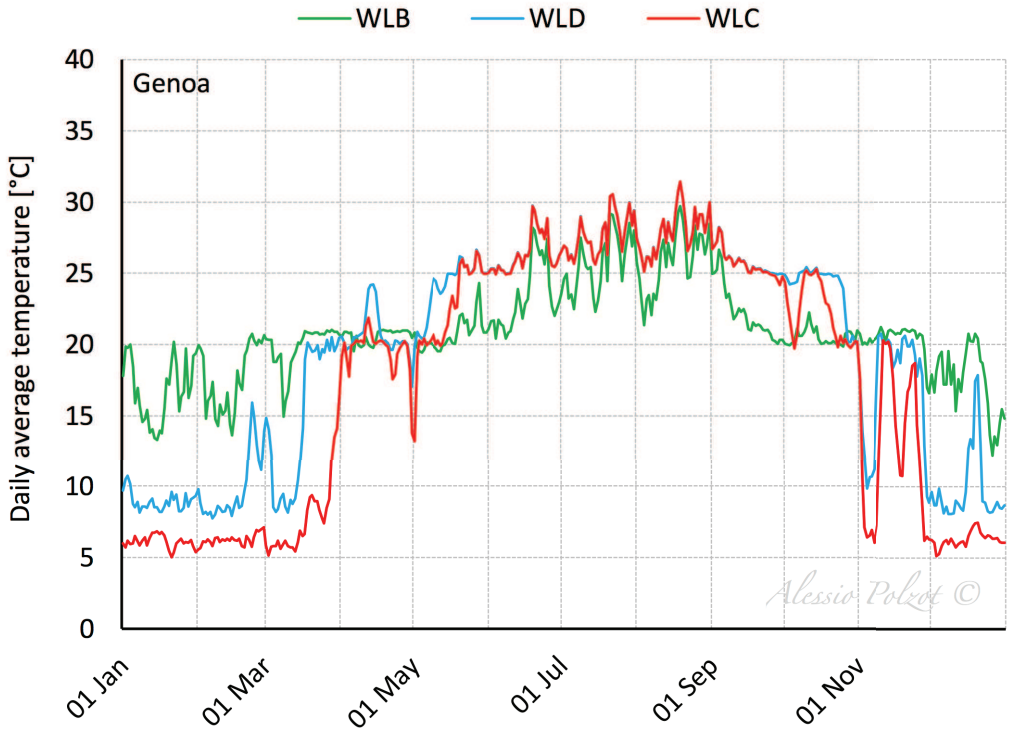

Figure 7.5.f - Daily average temperature of the water loop for the different investigated solutions in Genoa.

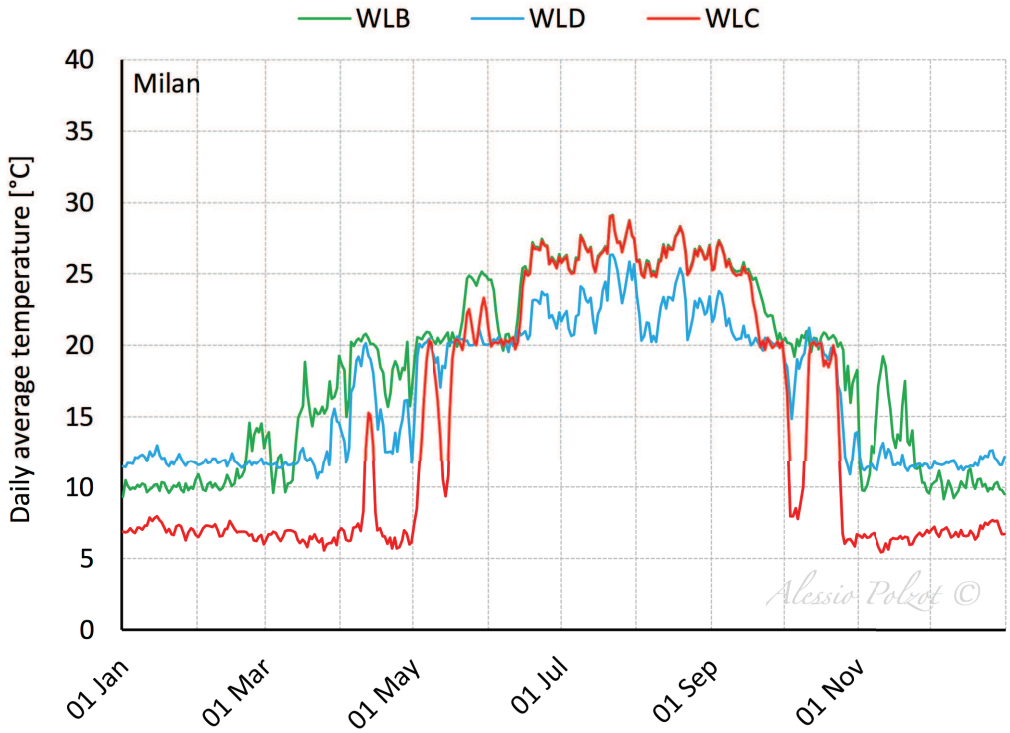

Figure 7.5.g - Daily average temperature of the water loop for the different investigated solutions in Milan.

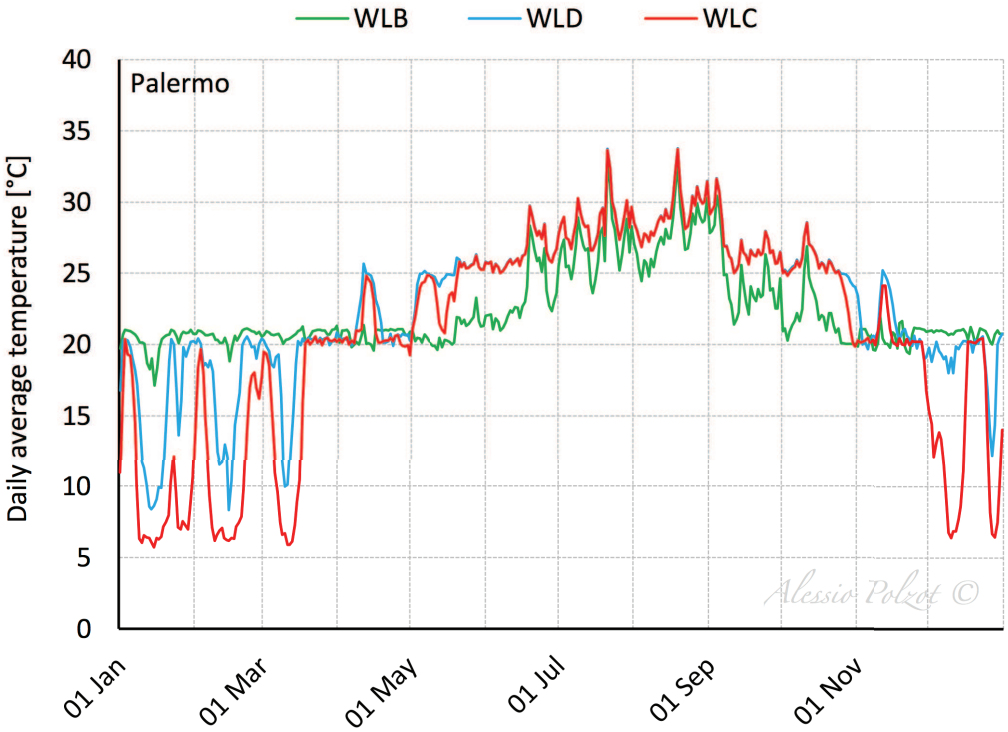

Figure 7.5.h - Daily average temperature of the water loop for the different investigated solutions in Palermo.

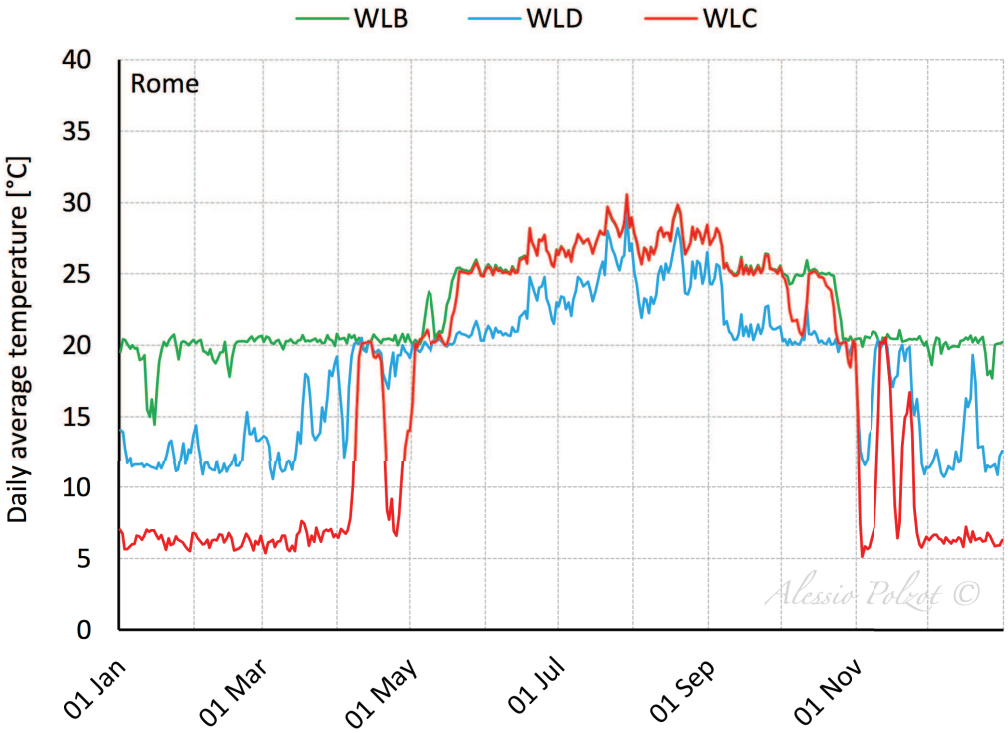

Figure 7.5.i - Daily average temperature of the water loop for the different investigated solutions in Rome.

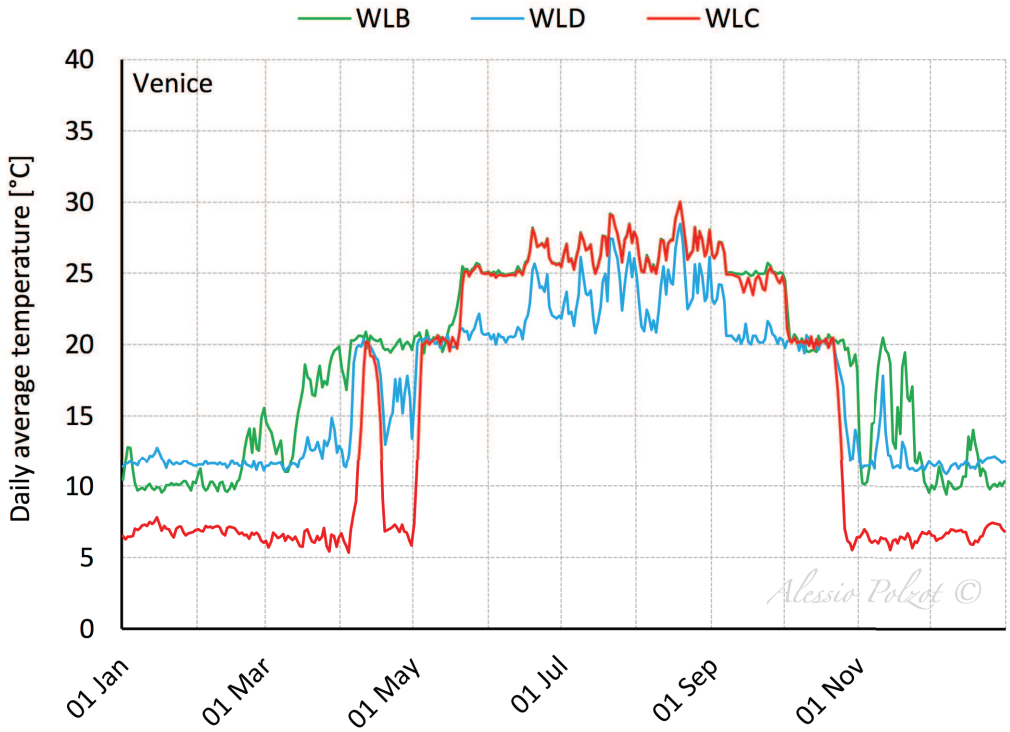

Figure 7.5.j - Daily average temperature of the water loop for the different investigated solutions in Venice.

7.5.3 Annual energy consumption

The annual energy consumption of the various systems of the solution which is investigated in this chapter, is compared.

Table 7.5.b, Table 7.5.c, Table 7.5.d, Table 7.5.e and Table 7.5.f show the annual energy consumption of the heat pumps, which provide climate control of the different thermal zones considered, of the refrigeration systems and of the auxiliary devices of the water loop performing in Genoa, Milan, Palermo, Rome and Venice, respectively.

In winter season the temperature of the water loop is higher than the outdoor air one and due to the higher evaporating temperature of the heat pumps which have the water loop as heat source/sink, the energy consumption of the heat pumps in the WLB, WLC and WLD solutions is lower. Furthermore in AHD system the heat pumps in winter need to go through defrost operations to melt the frost accumulated on the evaporator decreasing their performance.

7.5.3.1 Genoa

	Annual energy consumption	Relative energy consumption		
	[MWh]	[%]		
	AHD	**WLC**	**WLD**	**WLB**
Zone 23 heat pump	12.2	-7.5	-9.1	-16.7
Zone 18 heat pump	1.9	-7.2	-8.0	-13.7
Zone 22 heat pump	6.8	-9.0	-11.2	-18.4
Zone 19 heat pump	18.3	-9.9	-11.8	-19.1
Zone 24 heat pump	9.0	-5.6	-5.8	-12.5
Zone 21 heat pump	8.9	-9.3	-11.4	-18.5
Zone 20 heat pump	1.8	-8.7	-11.0	-18.3
Zone 4 heat pump	4.1	-12.2	-16.4	-26.8
Zone 3 and 8 heat pump	3.6	-14.2	-17.6	-26.9
Zone 9 heat pump	17.3	-11.6	-16.9	-26.7
Zone 30 heat pump	58.5	-12.6	-15.6	-22.9
DHW heat pump	16.8	-6.1	-100.0	-100.0
Refrigeration system	425.2	-1.1	-7.4	+5.6

	Annual energy consumption			
	[MWh]			
	AHD	**WLC**	**WLD**	**WLB**
Dry-cooler	0.0	12.9	14.1	37.2
Auxiliary heater	0.0	33.5	18.5	4.7
Pump	0.0	8.8	7.9	9.1

Table 7.5.b - Annual energy consumption of AHD solution systems and relative energy consumption of the investigated solutions in comparison with AHD in Genoa.

7.5.3.2 Milan

	Annual energy consumption	**Relative energy consumption**		
	[MWh]	[%]		
	AHD	**WLC**	**WLD**	**WLB**
Zone 23 heat pump	22.1	-27.9	-35.0	-31.6
Zone 18 heat pump	4.4	-29.8	-36.4	-32.2
Zone 22 heat pump	15.4	-29.4	-36.2	-32.9
Zone 19 heat pump	43.9	-30.5	-37.3	-34.6
Zone 24 heat pump	14.6	-26.5	-33.5	-28.4
Zone 21 heat pump	20.5	-29.8	-36.6	-33.4
Zone 20 heat pump	4.2	-28.1	-35.0	-31.4
Zone 4 heat pump	15.3	-28.3	-35.3	-32.4
Zone 3 and 8 heat pump	16.0	-30.5	-37.3	-34.2
Zone 9 heat pump	45.0	-27.6	-34.8	-32.9
Zone 30 heat pump	151.2	-32.3	-38.8	-36.8
DHW heat pump	18.7	-11.9	-100.0	-100.0
Refrigeration system	377.9	-0.1	-12.8	-3.6

	Annual energy consumption			
	[MWh]			
	AHD	**WLC**	**WLD**	**WLB**
Dry-cooler	0.0	5.6	14.1	6.3
Auxiliary heater	0.0	151.9	135.9	71.1
Pump	0.0	9.1	8.9	7.6

Table 7.5.c - Annual energy consumption of AHD solution systems and relative energy consumption of the investigated solutions in comparison with AHD in Milan.

7.5.3.3 Palermo

	Annual energy consumption	Relative energy consumption		
	[MWh]	[%]		
	AHD	**WLC**	**WLD**	**WLB**
Zone 23 heat pump	12.0	-3.8	-4.6	-10.3
Zone 18 heat pump	1.8	-2.4	-2.3	-6.8
Zone 22 heat pump	5.5	-3.7	-5.0	-10.1
Zone 19 heat pump	15.1	-4.5	-5.5	-10.6
Zone 24 heat pump	9.8	-2.5	-2.2	-7.9
Zone 21 heat pump	7.2	-3.9	-5.1	-9.9
Zone 20 heat pump	1.3	-3.4	-5.1	-10.3
Zone 4 heat pump	0.9	-5.4	-13.7	-25.1
Zone 3 and 8 heat pump	1.1	-4.8	-6.7	-12.2
Zone 9 heat pump	8.4	-10.0	-18.5	-25.3
Zone 30 heat pump	40.4	-6.2	-8.6	-12.4
DHW heat pump	15.9	-6.0	-100.0	-100.0
Refrigeration system	469.7	-2.0	-4.5	7.0

	Annual energy consumption			
	[MWh]			
	AHD	**WLC**	**WLD**	**WLB**
Dry-cooler	0.0	17.60	19.17	48.69
Auxiliary heater	0.0	3.92	0.82	0.00
Pump	0.0	8.53	7.44	9.05

Table 7.5.d - Annual energy consumption of AHD solution systems and relative energy consumption of the investigated solutions in comparison with AHD in Palermo.

7.5.3.4 Rome

	Annual energy consumption	**Relative energy consumption**		
	[MWh]	[%]		
	AHD	**WLC**	**WLD**	**WLB**
Zone 23 heat pump	13.6	-11.1	-19.2	-19.3
Zone 18 heat pump	1.9	-11.7	-18.4	-18.7
Zone 22 heat pump	7.3	-13.1	-20.6	-25.0
Zone 19 heat pump	20.0	-14.7	-22.2	-24.9
Zone 24 heat pump	9.5	-8.8	-16.3	-13.0
Zone 21 heat pump	9.8	-13.7	-21.1	-25.3
Zone 20 heat pump	1.9	-11.9	-19.6	-25.7
Zone 4 heat pump	5.0	-13.9	-22.8	-34.8
Zone 3 and 8 heat pump	4.5	-16.9	-25.0	-35.7
Zone 9 heat pump	20.3	-13.6	-23.0	-33.8
Zone 30 heat pump	65.6	-17.8	-25.1	-31.1
DHW heat pump	17.0	-5.5	-100.0	-100.0
Refrigeration system	428.8	-1.0	-8.5	1.1

	Annual energy consumption			
	[MWh]			
	AHD	**WLC**	**WLD**	**WLB**
Dry-cooler	0.0	10.6	23.1	8.5
Auxiliary heater	0.0	43.1	31.4	0.0
Pump	0.0	8.8	9.0	6.8

Table 7.5.e - Annual energy consumption of AHD solution systems and relative energy consumption of the investigated solutions in comparison with AHD in Rome.

7.5.3.5 Venice

	Annual energy consumption	**Relative energy consumption**		
	[MWh]	[%]		
	AHD	**WLC**	**WLD**	**WLB**
Zone 23 heat pump	18.9	-20.1	-27.4	-24.2
Zone 18 heat pump	3.5	-22.4	-29.1	-25.0
Zone 22 heat pump	12.5	-22.6	-29.6	-26.8
Zone 19 heat pump	34.7	-23.5	-30.4	-28.0
Zone 24 heat pump	12.9	-18.0	-25.0	-20.0
Zone 21 heat pump	16.5	-22.9	-29.8	-27.2
Zone 20 heat pump	3.4	-21.9	-29.0	-25.9
Zone 4 heat pump	12.1	-23.3	-30.6	-28.4
Zone 3 and 8 heat pump	12.2	-25.3	-32.4	-29.8
Zone 9 heat pump	36.3	-22.6	-30.2	-29.1
Zone 30 heat pump	117.5	-25.5	-32.4	-31.0
DHW heat pump	18.3	-11.2	-100.0	-100.0
Refrigeration system	400.0	-0.3	-11.8	-2.4

	Annual energy consumption			
	[MWh]			
	AHD	**WLC**	**WLD**	**WLB**
Dry-cooler	0.0	8.1	19.2	9.2
Auxiliary heater	0.0	113.3	94.9	40.7
Pump	0.0	8.9	9.1	7.7

Table 7.5.f - Annual energy consumption of AHD solution systems and relative energy consumption of the investigated solutions in comparison with AHD in Venice.

7.5.4 Global annual energy consumption

Figure 7.5.k, Figure 7.5.l, Figure 7.5.m, Figure 7.5.n and Figure 7.5.o show the global energy consumption of the investigated system in Genoa, Milan, Palermo, Rome, Venice, respectively.

In all the investigated climate conditions the WLC solution consume more energy than the baseline solution (AHD), i.e. the traditional solution with a HFC direct expansion refrigeration system and several heat pumps for the climate control of the zones.

The water loop heat pump solution with a R744 booster as refrigeration system shows to be an effective solution. In Genoa climate conditions, the energy savings which can be achieve with the WLD solution is equal to 4.6 % over the baseline one, 9.4 % in Milan with the WLB system, 2.9 % in Palermo with WLD, 6.9 % in Rome with WLB and 7.3 % in Venice with WLB.

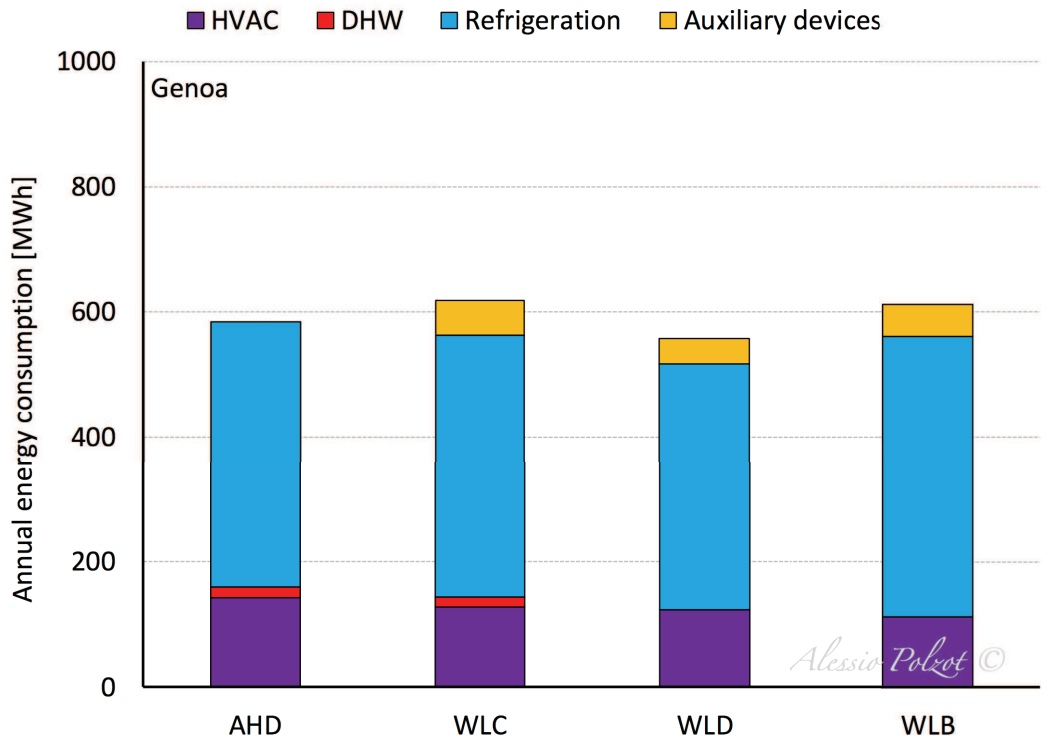

Figure 7.5.k - Global energy consumption of the investigated systems in Genoa.

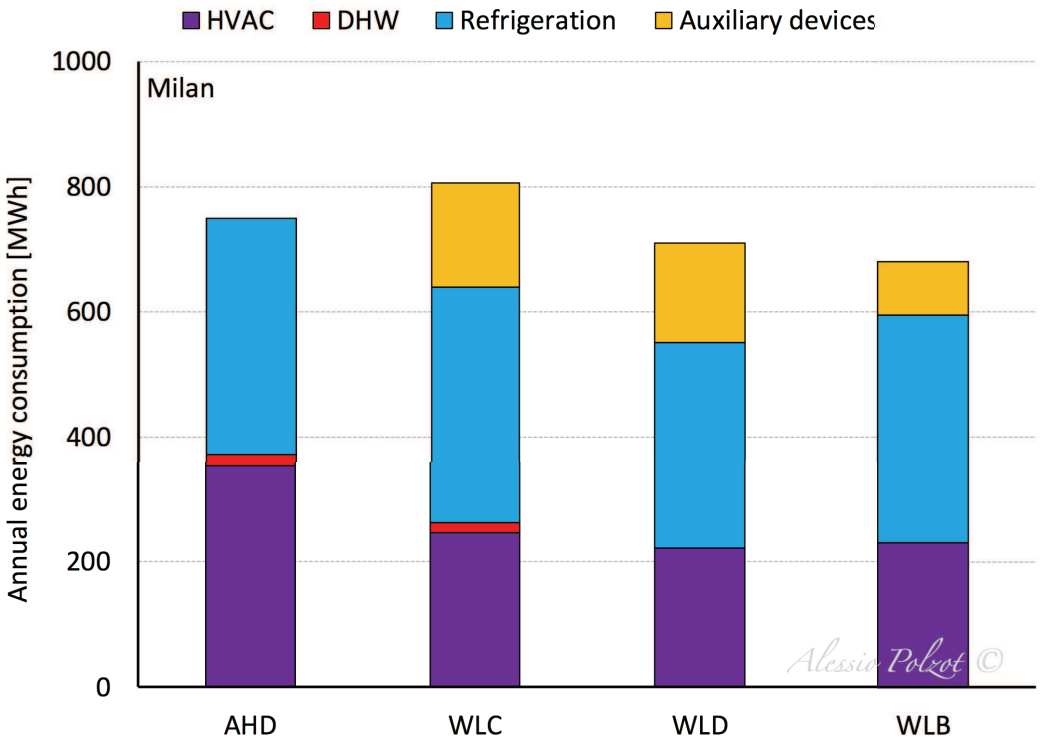

Figure 7.5.l - Global energy consumption of the investigated systems in Milan.

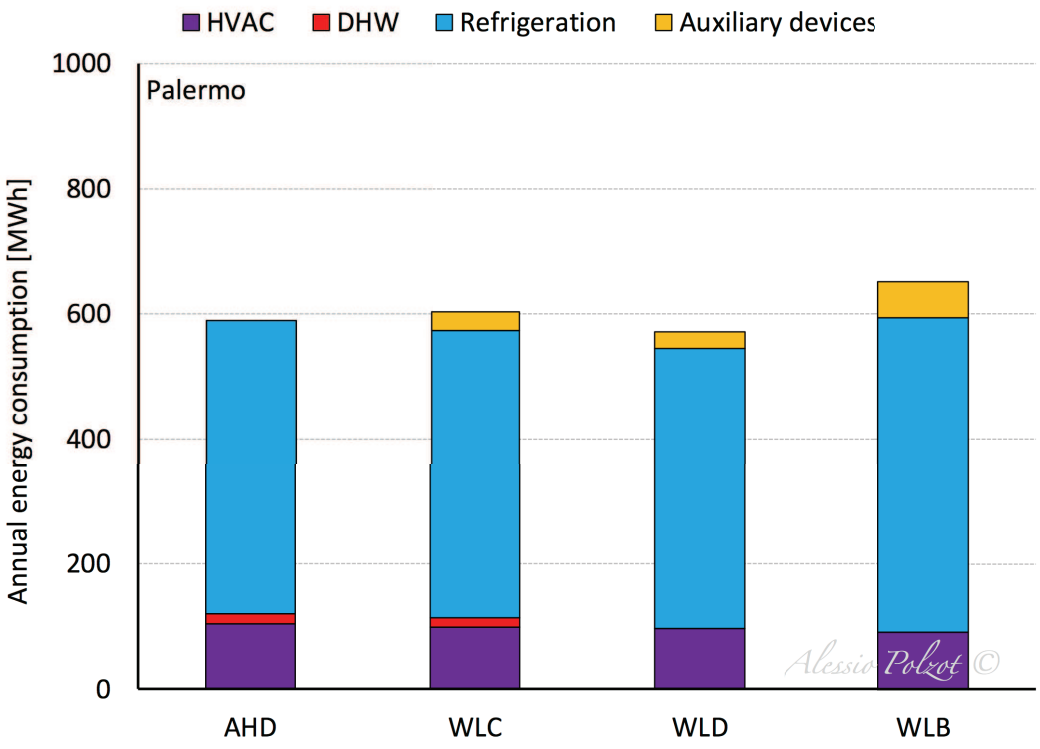

Figure 7.5.m - Global energy consumption of the investigated systems in Palermo.

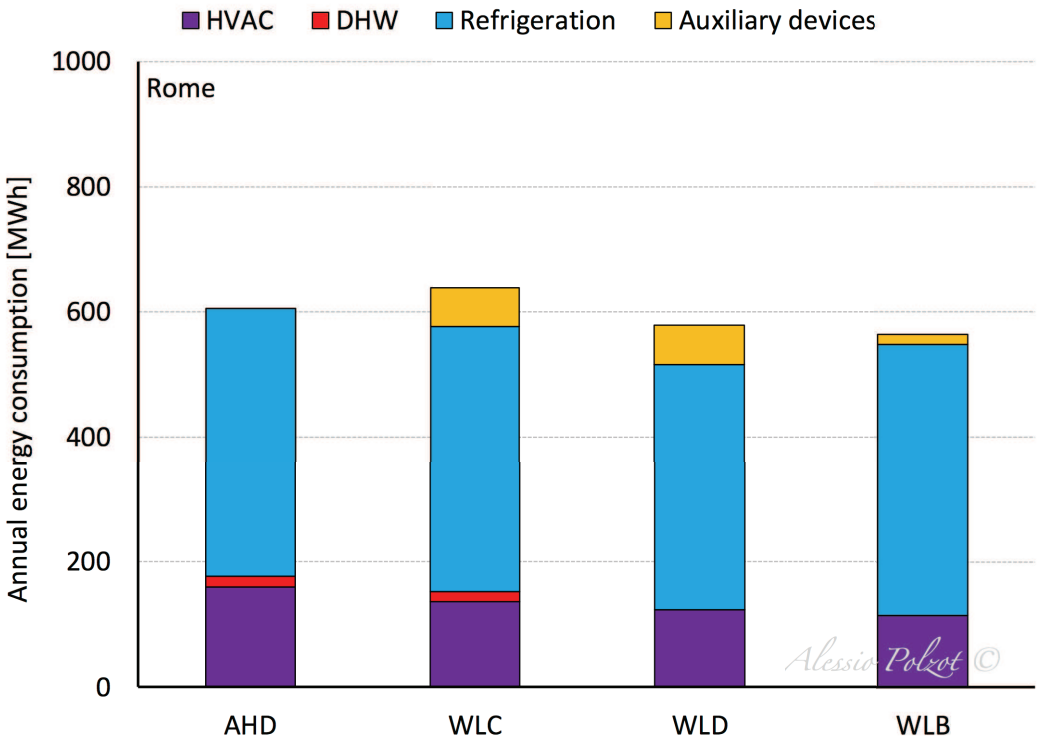

Figure 7.5.n - Global energy consumption of the investigated systems in Rome.

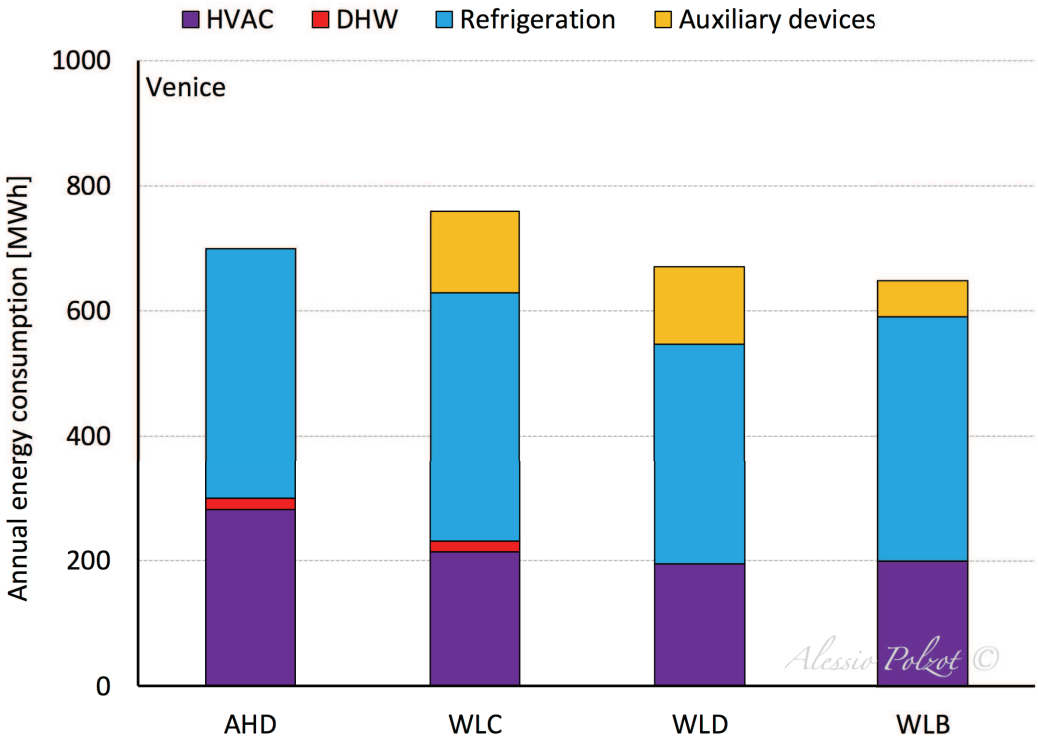

Figure 7.5.o - Global energy consumption of the investigated systems in Venice.

7.6 Reference

- BITZER, 2016. BITZER Software 6.4.4.1464. Available at: https://www.bitzer.de/websoftware/ [accessed 15/12/2016].
- Buonomano, A., Calise, F., Palombo, A., 2012. Building dynamic simulation: Water loop heat pump systems analysis for European climates. Applied Energy 91, 222-234.
- Cortella, G., D'Agaro, P., Saro, O., Polzot, A., 2014. Modelling integrated HVAC and refrigeration systems in a supermarket. Proceedings of the 3rd IIR International Conference on Sustainability and the Cold Chain, London, United Kingdom.
- Frascold, 2016. FSS.3 (Frascold selection software) Software. Available at: http://www.frascold.it/it/download/software/ [accessed 15/12/2016].

Chapter VIII

R744 system for refrigeration, heating and DHW

This chapter deals with the energy performance evaluation of a carbon dioxide transcritical booster refrigeration system (THR), which provides the selected supermarket with domestic hot water (DHW) and heating, besides satisfying the cooling load required by the refrigerated and frozen food storage equipment. The system is equipped with an additional air-cooled evaporator which can be used as a supplemental heat source, to increase the amount of heat recovered and meet the full heating demand of the building. The THR system is provided with an auxiliary compressor and heat recovery from two heat exchangers connected in series at the exit of high stage compressors rack is used to provide the selected supermarket with DHW and space heating.

The results are compared to a baseline system (DHP), i.e. a R404A direct expansion system as the refrigeration unit and two air to water heat pumps for space heating and hot water production, and to a traditional system (CHP) where a cascade refrigeration system with heat recovery is coupled with two air to water heat pumps which satisfy the DHW and heating demands of the supermarket.

8.1 System description

The investigated THR system, a R744 transcritical booster system with heat recovery, auxiliary compressor and load evaporator, is depicted in Figure 7.1.a.

The liquid exiting the receiver is expanded from the intermediate pressure to two different pressure levels, according to the temperature levels of the chilled and frozen food storage equipment: at 28.0 bar for medium temperature and at 12 bar for low temperature, corresponding to the evaporating temperatures of –8 °C and -35 °C,

respectively. The whole amount of flash gas generated by the high-pressure (HP) expansion valve is compressed by the auxiliary compressor or, in subcritical operations, it is expanded to the MT pressure level by the vapour by-pass valve and is compressed by the high stage (HS) compressors rack.

Two heat exchangers at the exit of the HS compressors rack recover heat at two different temperature levels. The first one (HX1) is used for the production of domestic hot water (DHW) while the second one (HX2) supplies hot water for space heating purposes. When the system is running in heat recovery mode, an air-cooled gas cooler/condenser allows cooling down the refrigerant exiting the heat exchangers, otherwise the two heat exchangers are by-passed and the whole heat is rejected into the ambient.

The system is also provided with an air-cooled load evaporator, which is activated during low refrigeration duty periods, when the heat rejected by the HX2 heat exchanger is not sufficient to meet the heating demand of the building. The pressure at the additional evaporator depends on the outdoor air temperature with a maximum value fixed at same value of the intermediate pressure, which is fixed at 37.7 bar, considering a suitable pressure drop. When the load evaporator is activated the superheated vapour exiting the latter is directly compressed by the auxiliary compressor to the high pressure.

The discharge pressure of the system is controlled according to the heating demand so that when the supermarket does not need heat the high pressure follows the ambient temperature, while when heating energy is required it is increased and more heat is available.

In heat recovery mode the gas cooler acts as a subcooler improving the performance of the system. On the other hand the total mass flow rate of the refrigerant flowing through the refrigerating unit and, consequently, the amount of energy recoverable from the two heat exchangers reduce as the degree of the subcooling increases. In order to provide the supermarket with all the heating demand the temperature of the CO_2 exiting the air cooled gas cooler/condenser can be increased by reducing the speed velocity of the fans thus making more heat available for recovery (Sawalha, 2013; Tambovtsev et al., 2010; Tambovtsev et al., 2011).

To meet the full heating demand of the building the following control strategy is applied to the system: initially the high pressure is increased, when the maximum

value of the latter is reached the system starts to reduce the gas cooler fan speed velocity to increase the temperature of the carbon dioxide exiting the gas cooler. Finally, if the heat available from heat recovery is not sufficient, the load evaporator is activated, the fans speed velocity is set at maximum value and the system starts to increase the mass flow rate flowing through the load evaporator.

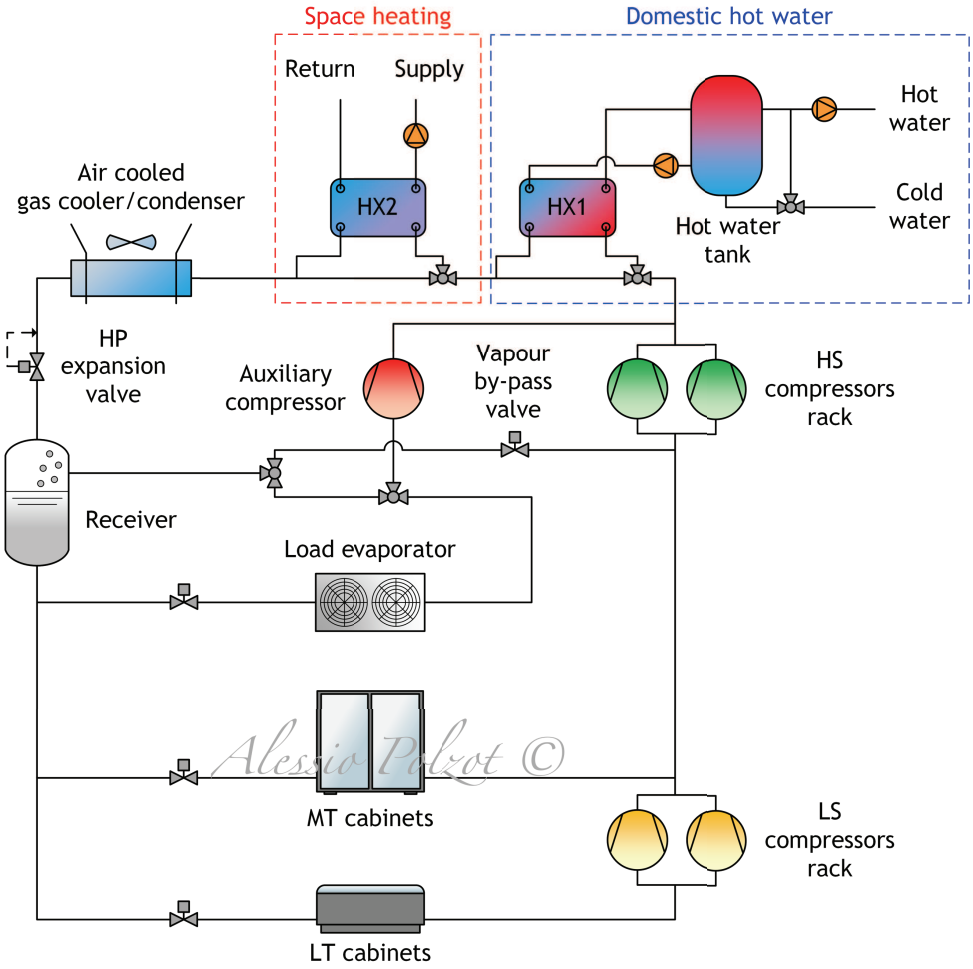

Figure 8.1.a - Schematic of the R744 transcritical booster system with two temperature levels heat recovery (THR).

In Figure 7.1.b is depicted the THR system in a log(p)-h diagram. In dark blue solid line is shown the heat available at the HX1 heat exchanger for domestic hot water production, while in light blue solid line is depicted the heat available at the second heat exchanger (HX2) for space heating. HX1 provides hot water at 60 °C to avoid the growth of legionella. The supply temperature and the minimum return temperature of the heating system is fixed at 40 °C and at 30 °C, respectively. The approach temperature of the two water cooled heat exchangers is set to 5 K.

In black dashed and dotted line are shown the 35 °C and 65 °C isotherm. As previously mentioned, in heat recovery mode, the liquid exiting from the receiver which evaporates in the load evaporator (horizontal red dashed line) is compressed by the auxiliary compressor to the high pressure (sloping red dashed line).

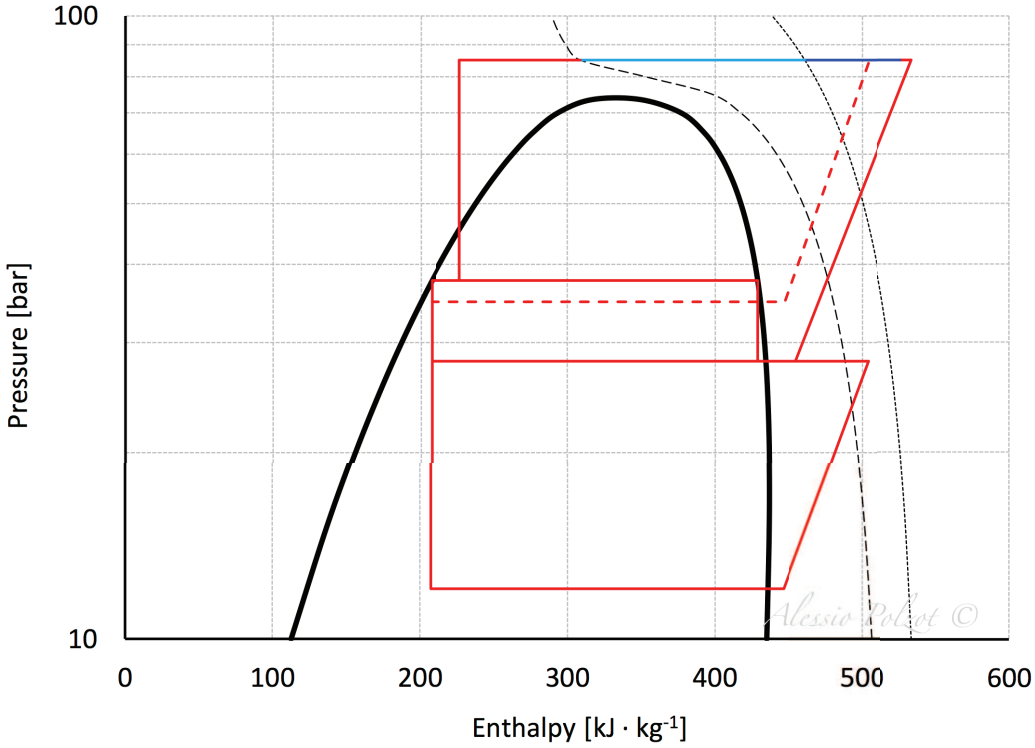

Figure 8.1.b - Log(p)-h diagram of the refrigeration system in THR system.

As a reference for comparison, a traditional DXS system is chosen as the refrigeration system, one air to water heat pump provides the climate control of the zones and one air to water heat pump satisfy the DHW demand (DHP system).

An additional solution (CHP) where traditional DXS refrigeration system is replaced by a cascade system with heat recovery (Figure 7.1.c).

Table 8.1.a report the operating conditions of the investigated system.

THR operating conditions	Unit	Value
Useful superheating	K	5.0
Superheating in the suction lines	K	5.0
Approach temperature of the condenser/gas cooler	K	3.0
Minimum condensing temperature	°C	8.0
Subcooling in subcritical operations	K	2.0
Liquid receiver pressure	bar	37.7
Maximum value of high pressure in heat recovery mode	bar	85.0
Approach temperature of the load evaporator	K	5.0
Load evaporator capacity	kW	200.0
Gas cooler absorbed power at rated conditions	kW	3.2

Table 8.1.a - R744 transcritical booster system with heat recovery (THR) operating conditions.

8.2 Heat pumps

In DHP and CHP solutions, two different HFC heat pumps are evaluated, one uses R410A as working fluid and it provides hot water for the space heating of the thermal zones (operating conditions in Table 6.1.a), one uses a R134a as refrigerant and it satisfy the domestic hot water demand of the supermarket (operating conditions in Table 7.2.d).

The R134a refrigerant is chosen for the DHW production due to the higher compressor discharge temperature than the systems which use the R410A as working fluid.

R410A heat pump operating conditions	Unit	Value
Useful superheating	K	4.0
Superheating in the suction lines	K	4.0
Subcooling	K	3.5
Approach temperature of the source heat exchanger	K	10.0
Approach temperature of the load heat exchanger	K	5.0
Defrost capacity reduction	%	11.0
Defrost power reduction	%	1.0

Table 8.2.a - Operating conditions of the R410 heat pumps in DHP and CHP.

R134a heat pump operating conditions	Unit	Value
Useful superheating	K	4.0
Superheating in the suction lines	K	4.0
Subcooling	K	3.5
Approach temperature of the source heat exchanger	K	10.0
Approach temperature of the load heat exchanger	K	5.0
Defrost capacity reduction	%	11.0
Defrost power reduction	%	1.0

Table 8.2.b - Operating conditions of the R134a heat pump in DHP and CHP.

8.2.1 COP

The COP values of the above mentioned heat pumps are reported in Figure 7.2.a and Figure 7.2.c.

8.2.2 Compressors global efficiency

The compressors, which are selected for the heat pumps used in the investigated solutions are:

- scroll compressors for the R410A heat pumps;
- semi-hermetic reciprocating compressors for the R134a heat pumps.

All their suggested technological constraints are respected. The global efficiency is defined as the ratio of the power input calculated at isentropic conditions to the power input declared by the manufacturers.

Their global efficiencies are obtained as a function of the pressure ratio by using BITZER Software (BITZER, 2016) and are reported in paragraphs 7.3.1 and 7.3.3.

8.3 Heating and DHW demands

The CO_2 transcritical booster refrigeration system provide the space heating of the food store (thermal zone 30 in Figure 3.1.b).

In Figure 7.4.a, Figure 7.4.b, Figure 7.4.c, Figure 7.4.d and Figure 7.4.e are shown the monthly heating demands, which are reported as a negative value, of the thermal zone in the investigated locations. The domestic hot water usage is estimated at a maximum value of 250 dm^3 per hour during the opening hours. In Figure 7.4.f the monthly domestic hot water demand is depicted.

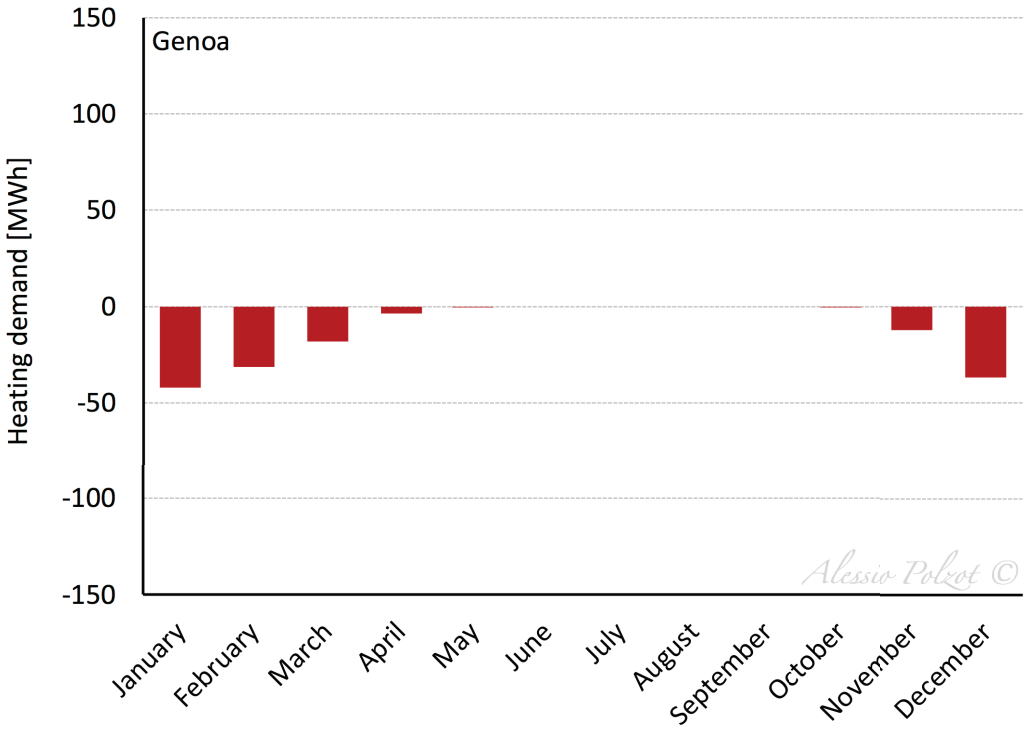

Figure 8.3.a - Heating demand of the food store zone in Genoa.

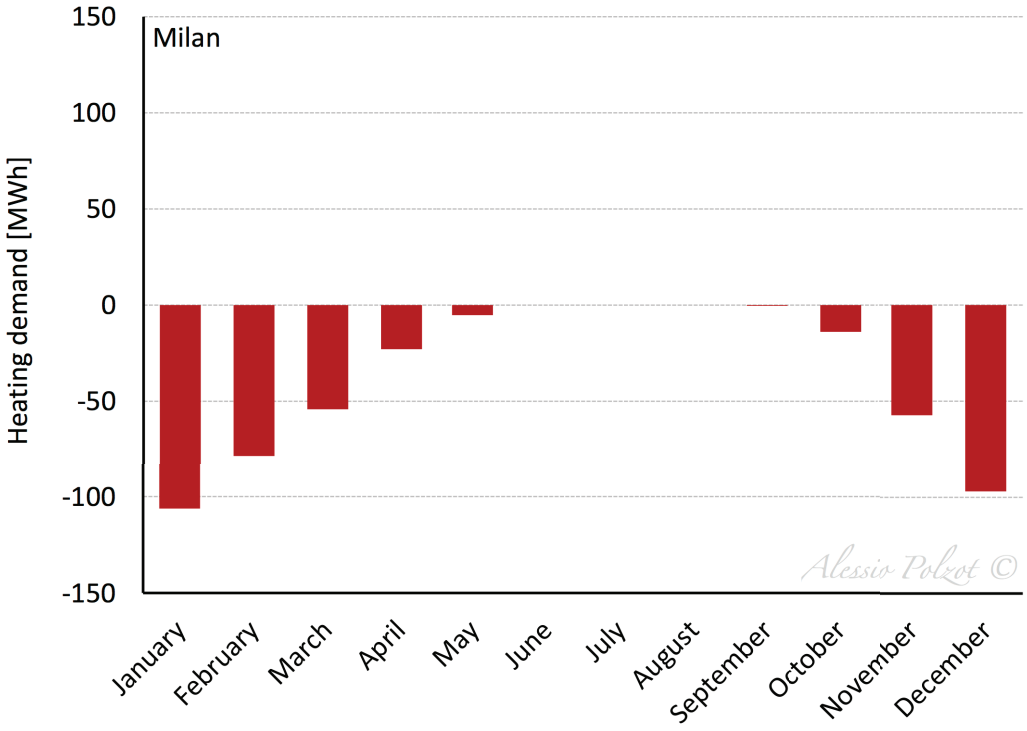

Figure 8.3.b - Heating demand of the food store zone in Milan.

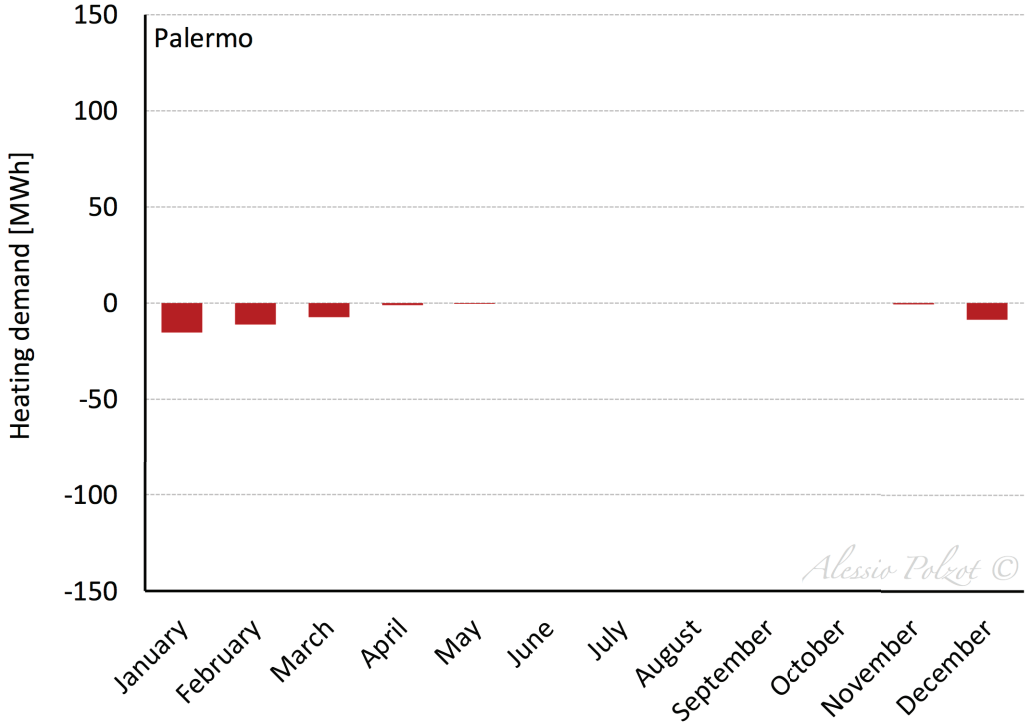

Figure 8.3.c - Heating demand of the food store zone in Palermo.

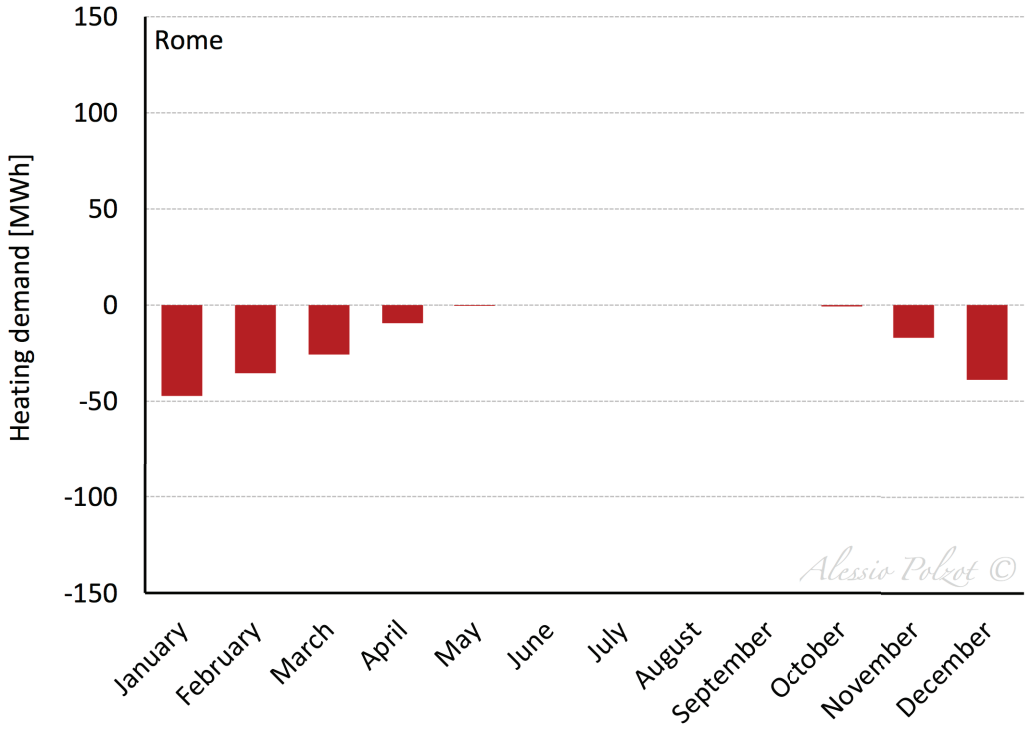

Figure 8.3.d - Heating demand of the food store zone in Rome.

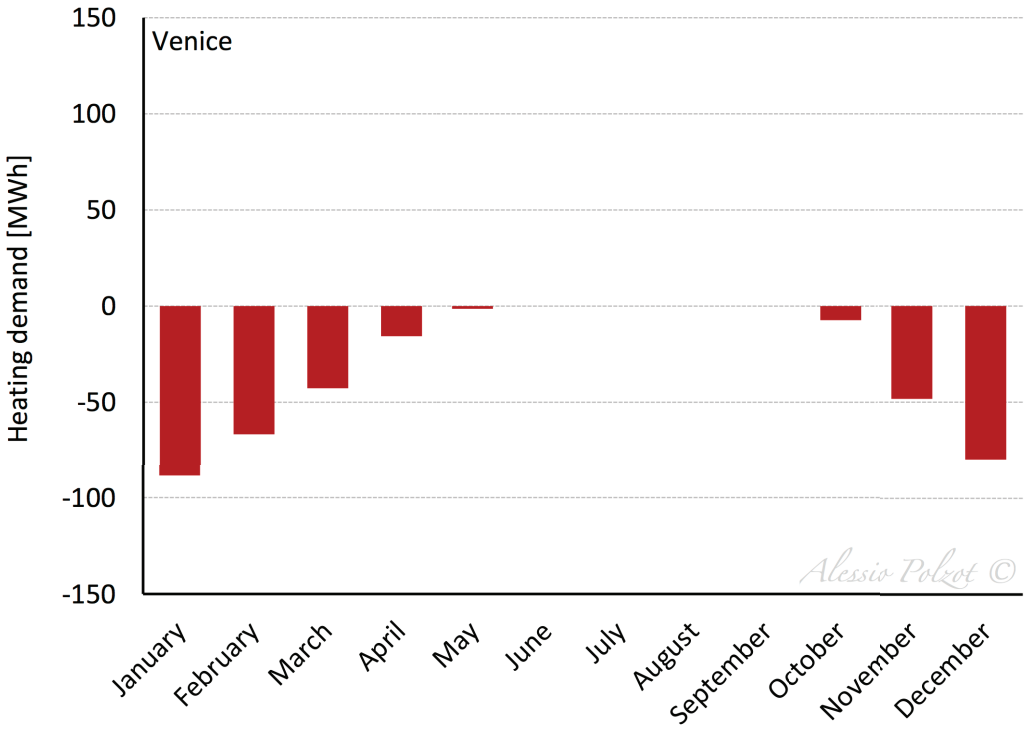

Figure 8.3.e - Heating demand of the food store zone in Venice.

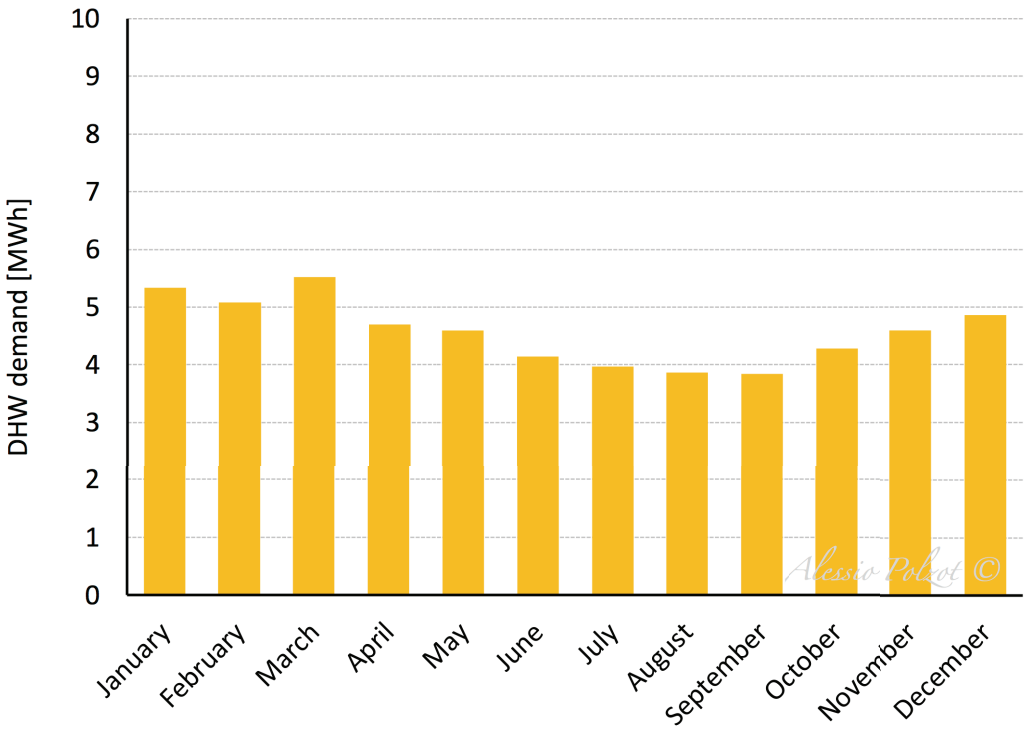

Figure 8.3.f - Domestic hot water demand of the supermarket.

8.4 Results

The results are reported in terms of energy consumption and in terms of working hours of the auxiliary compressor and of the load evaporator. An analysis on the high pressure and on the gas cooler outlet temperature of the THR system is conducted.

8.4.1 High pressure

In heat recovery mode the high pressure can be increased to meet the full heating demand of the supermarket. Figure 7.5.a, Figure 7.5.b, Figure 7.5.c, Figure 7.5.d and Figure 7.5.e make a comparison in terms of frequency over the year of the high pressure among the R744 transcritical booster system with auxiliary compression (PCS, paragraph 6.4) and the CO_2 system with heat recovery (THR).
In the coldest climates considered, i.e. Milan and Venice, the THR system works with an higher frequency at higher pressure than the PCS system in order to satisfy the heating demand peaks of the building.

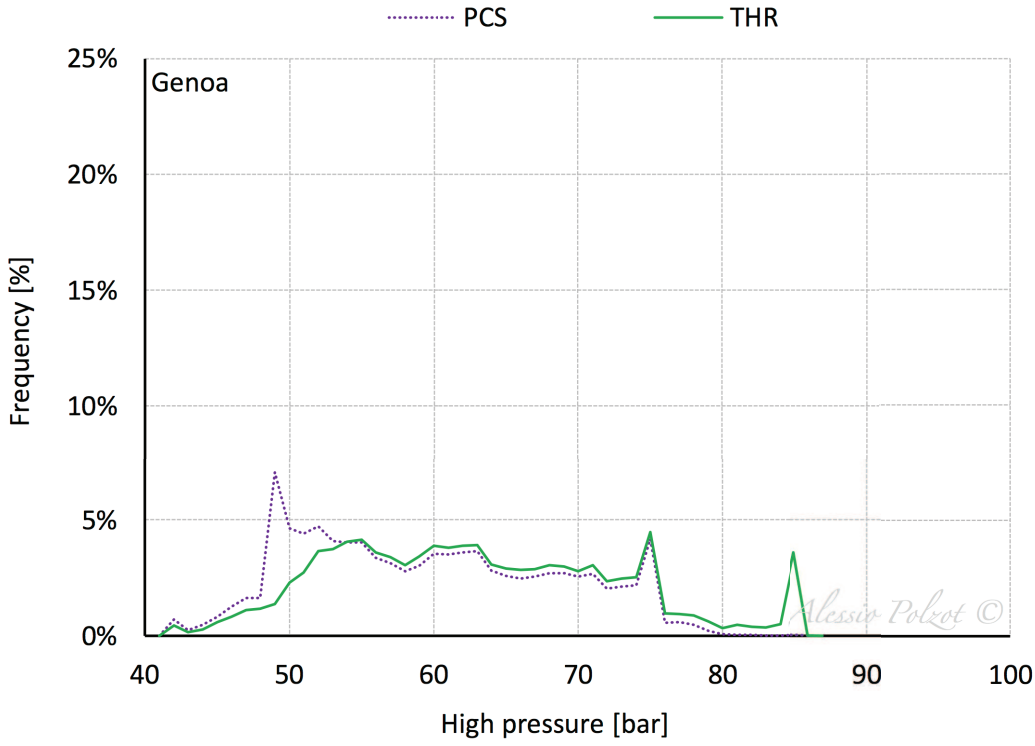

Figure 8.4.a - Annual frequency of the high pressure values in PCS and THR systems in Genoa.

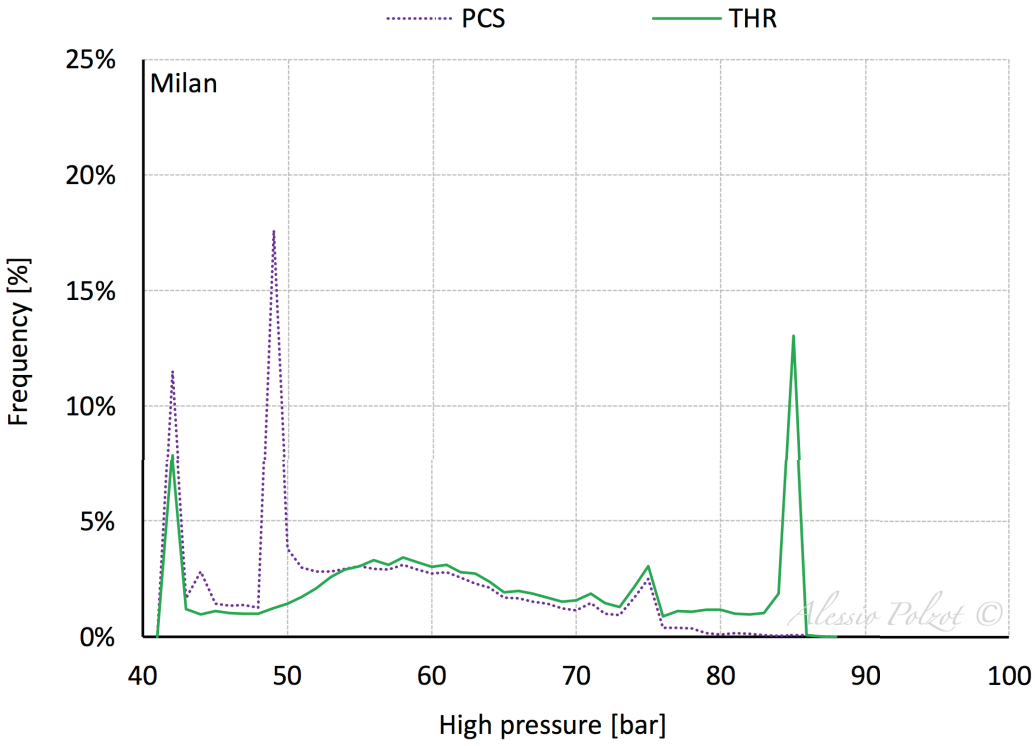

Figure 8.4.b - Annual frequency of the high pressure values in PCS and THR systems in Milan.

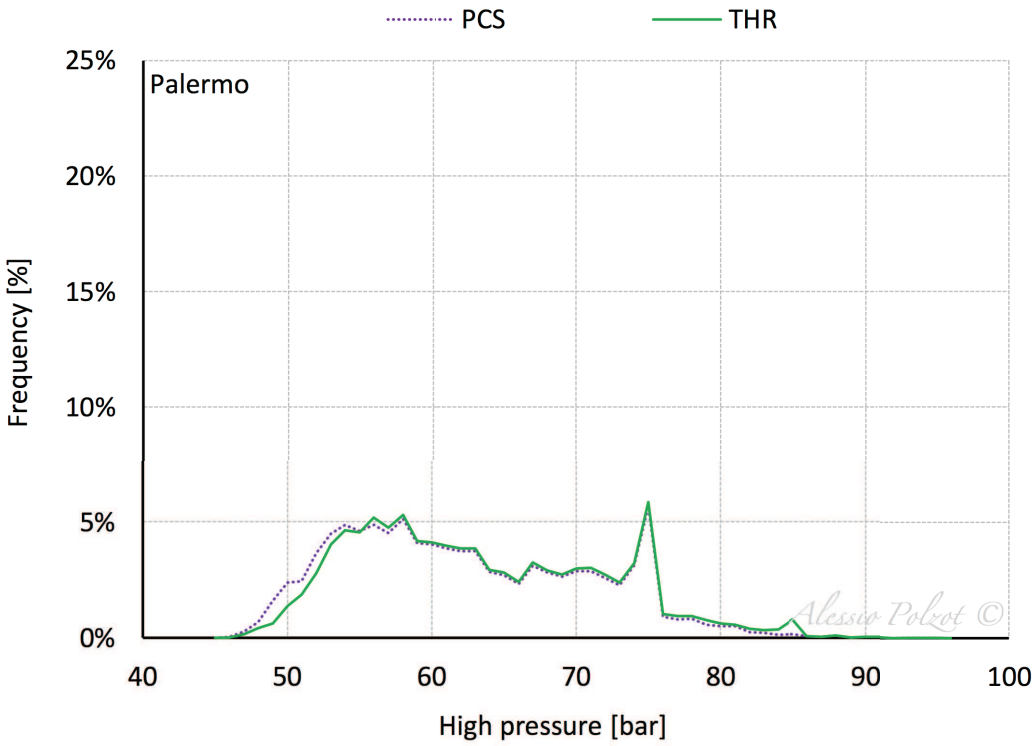

Figure 8.4.c - Annual frequency of the high pressure values in PCS and THR systems in Palermo.

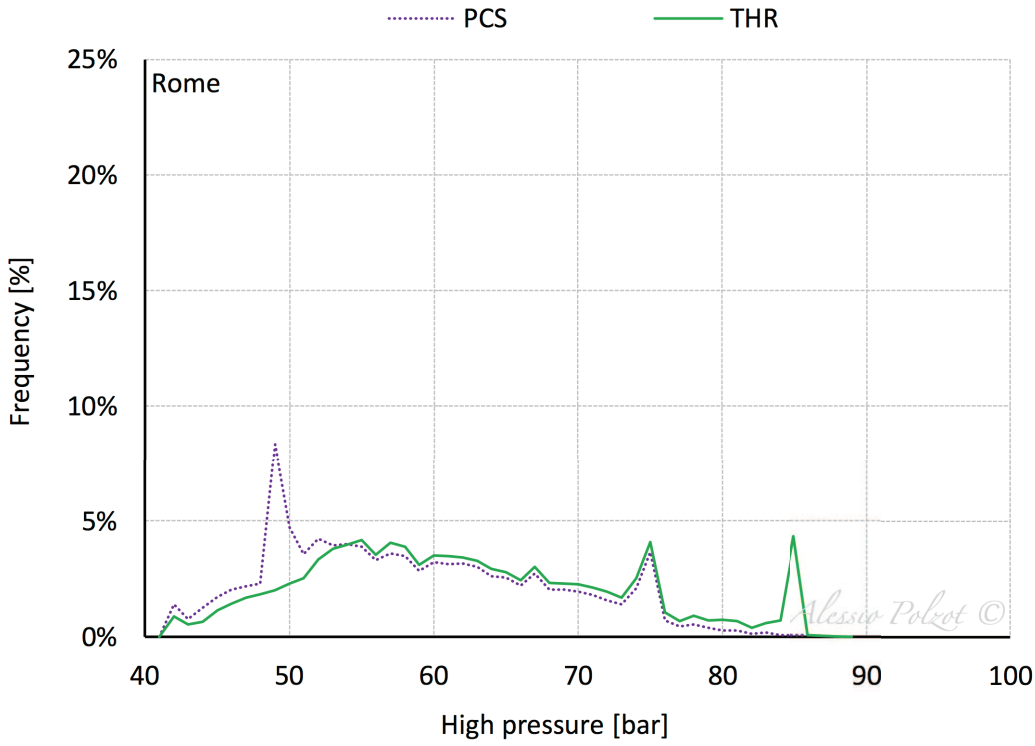

Figure 8.4.d - Annual frequency of the high pressure values in PCS and THR systems in Rome.

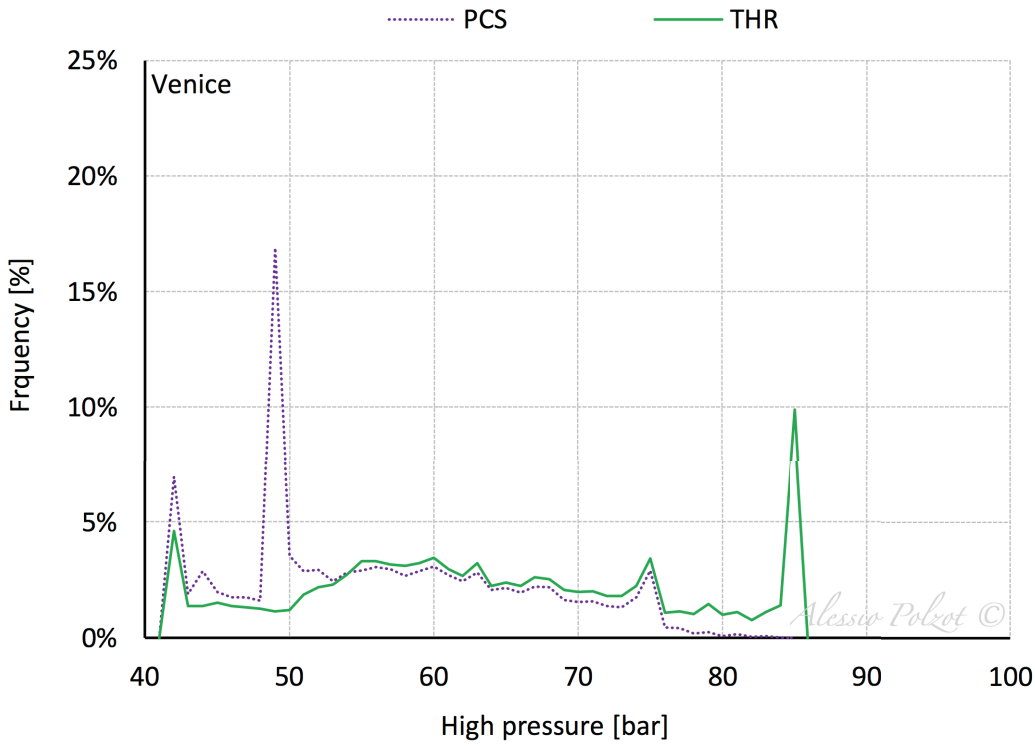

Figure 8.4.e - Annual frequency of the high pressure values in PCS and THR systems in Venice.

8.4.2 Gas cooler outlet temperature

In heat recovery mode, if the maximum value, which is equal to 85 bar, of the high pressure is reached, the gas cooler fan speed velocity can be reduced to increase the temperature of the carbon dioxide exiting the gas cooler.

Figure 7.5.f, Figure 7.5.g, Figure 7.5.h, Figure 7.5.i and Figure 7.5.j show the comparison in terms of frequency over the year of the gas cooler outlet temperature among the R744 transcritical booster system with auxiliary compression (PCS) and the CO_2 system with heat recovery (THR). In Genoa, Rome and Palermo, which are characterized by a mild winter, the temperature of the carbon dioxide exiting the gas cooler is not increased to meet the full heating demand of the supermarket, which is satisfied only increasing the high pressure.

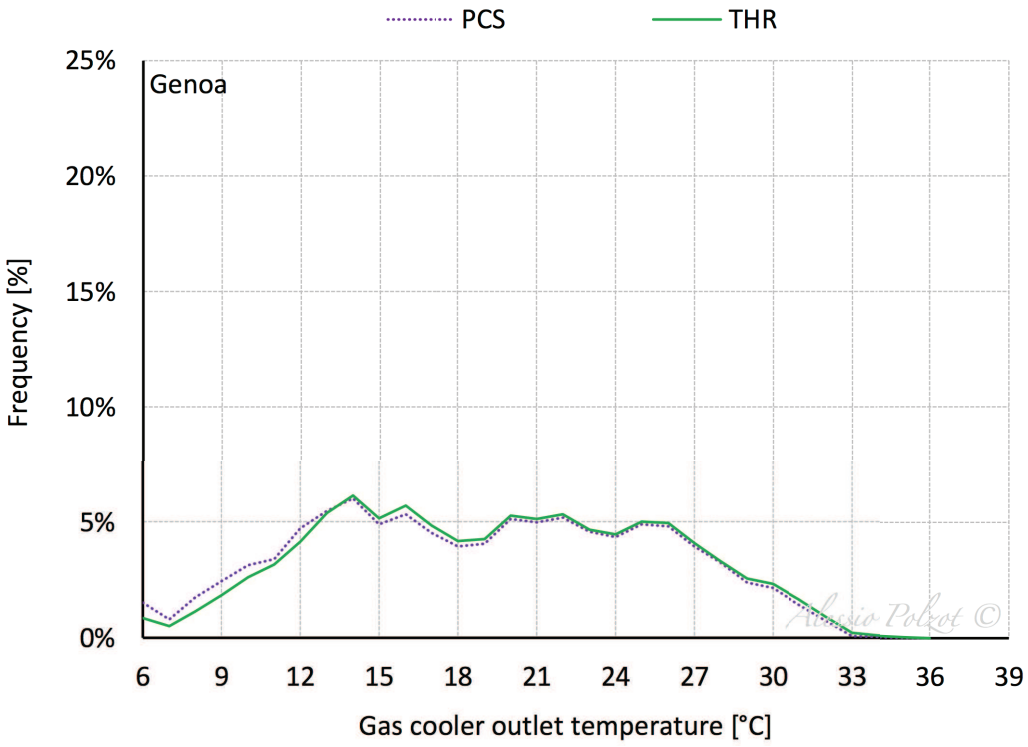

Figure 8.4.f - Annual frequency of the gas cooler outlet temperature values in PCS and THR systems in Genoa.

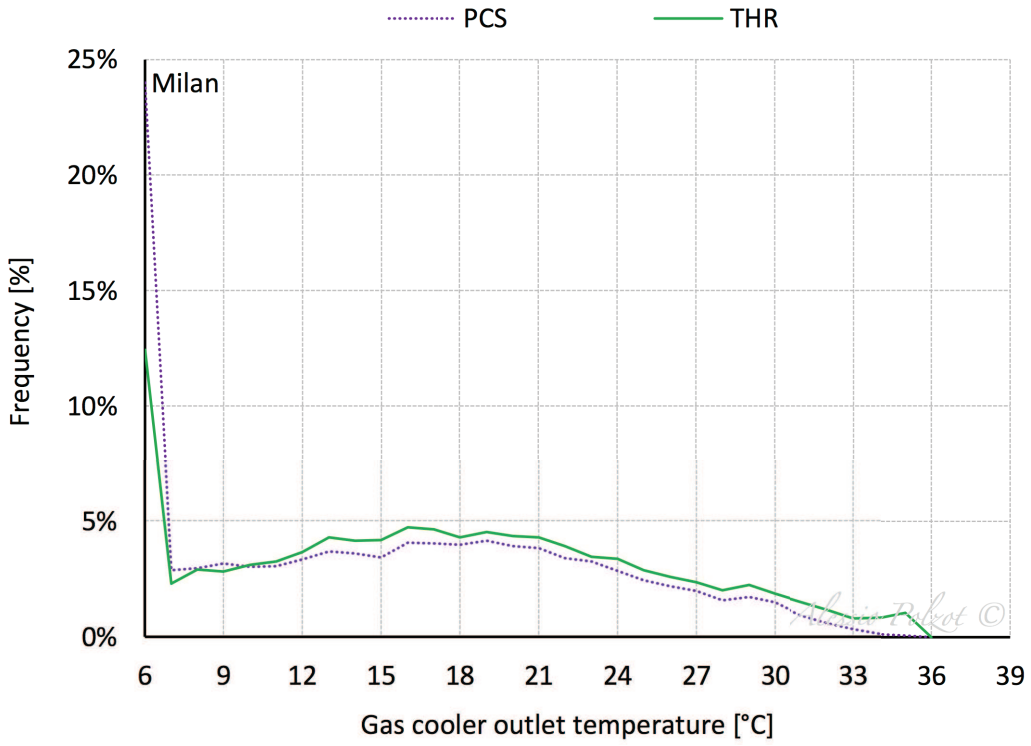

Figure 8.4.g - Annual frequency of the gas cooler outlet temperature values in PCS and THR systems in Milan.

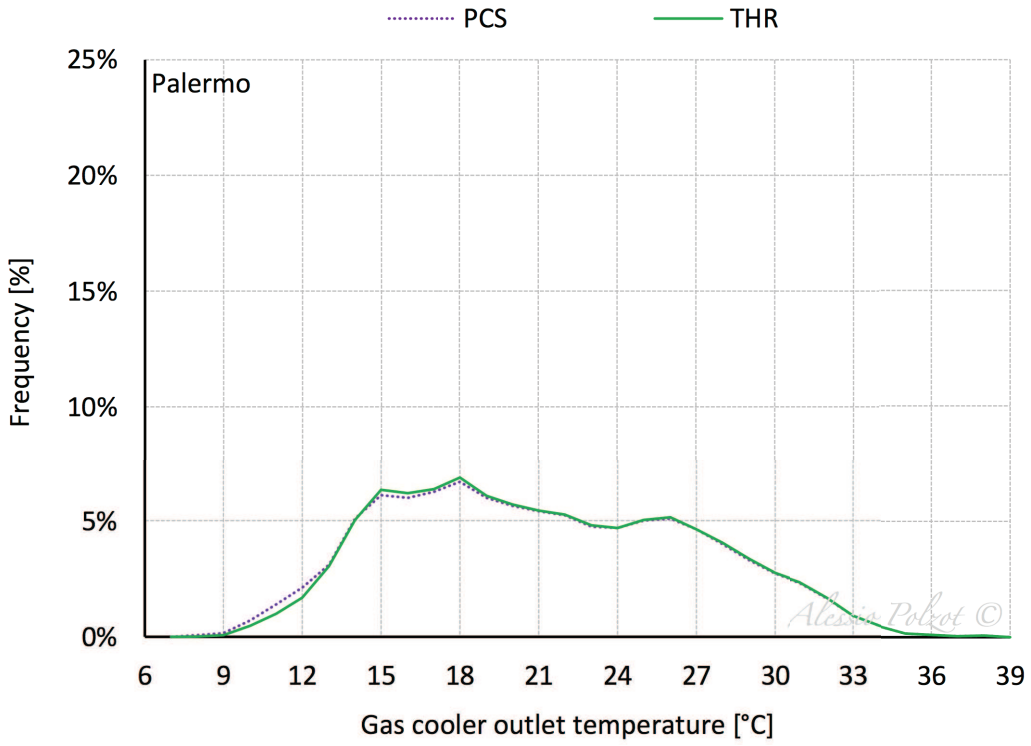

Figure 8.4.h - Annual frequency of the gas cooler outlet temperature values in PCS and THR systems in Palermo.

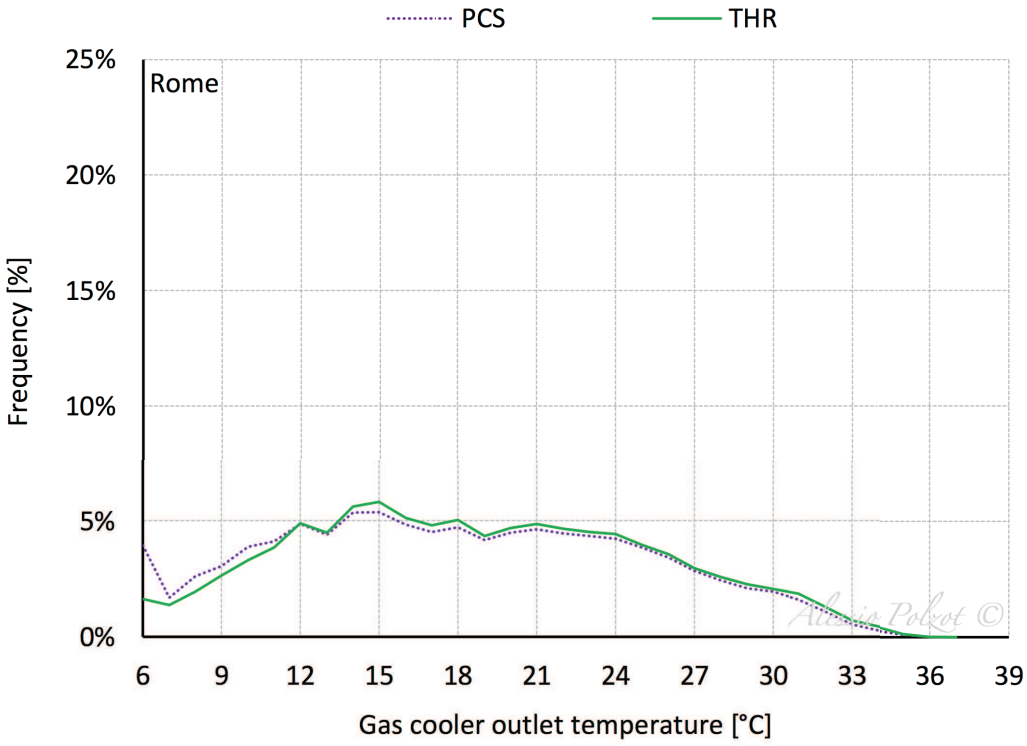

Figure 8.4.i - Annual frequency of the gas cooler outlet temperature values in PCS and THR systems in Rome.

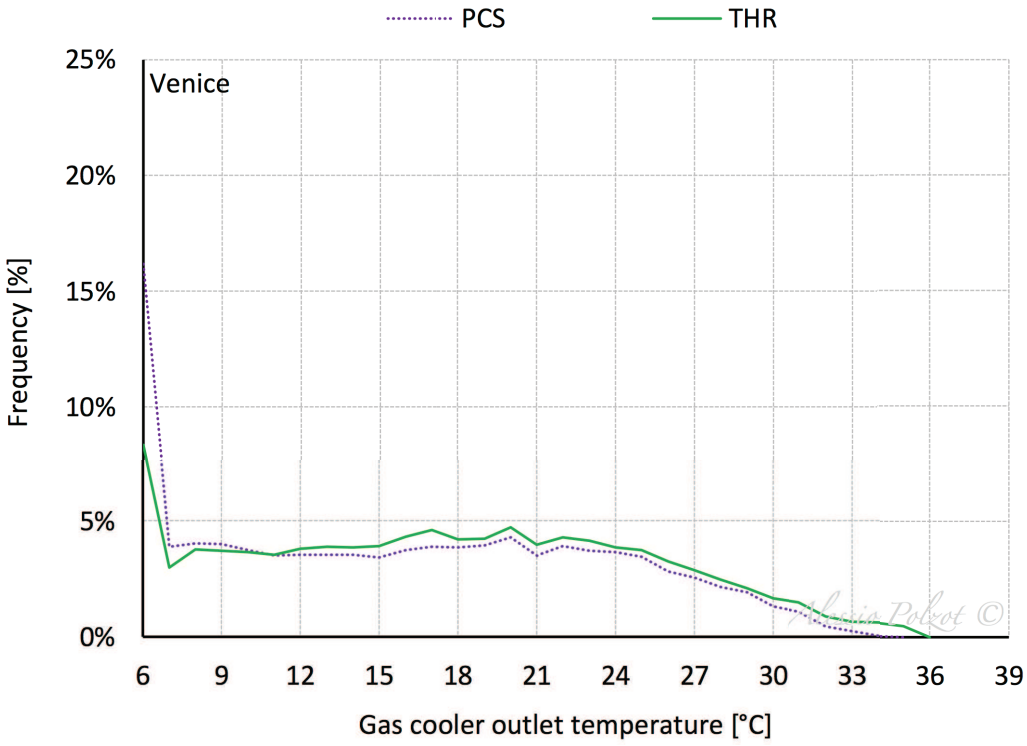

Figure 8.4.j - Annual frequency of the gas cooler outlet temperature values in PCS and THR systems in Venice.

8.4.3 Auxiliary compressor and load evaporator working hours

Figure 8.4.k shows for the THR solution the percentage of time over the year in which the load evaporator is activated in all the climates condition evaluated. Furthermore, the comparison among the working hours over the year of the auxiliary compression in PCS and in THR systems. In PCS solution, the additional compressor is activated 2859 hours per year in Genoa, 1705 in Milan, 3493 in Palermo, 2520 in Rome and 2052 in Venice. In THR system, the auxiliary compressor is activated also in the heating season when the high pressure is increased and the system run in transition or in transcritical mode.

In the warmest climates considered the load evaporator works for a very low number of hours over the year, thus the employment of this device is not to be expected at all climates conditions with a significant reduction in the investment cost.

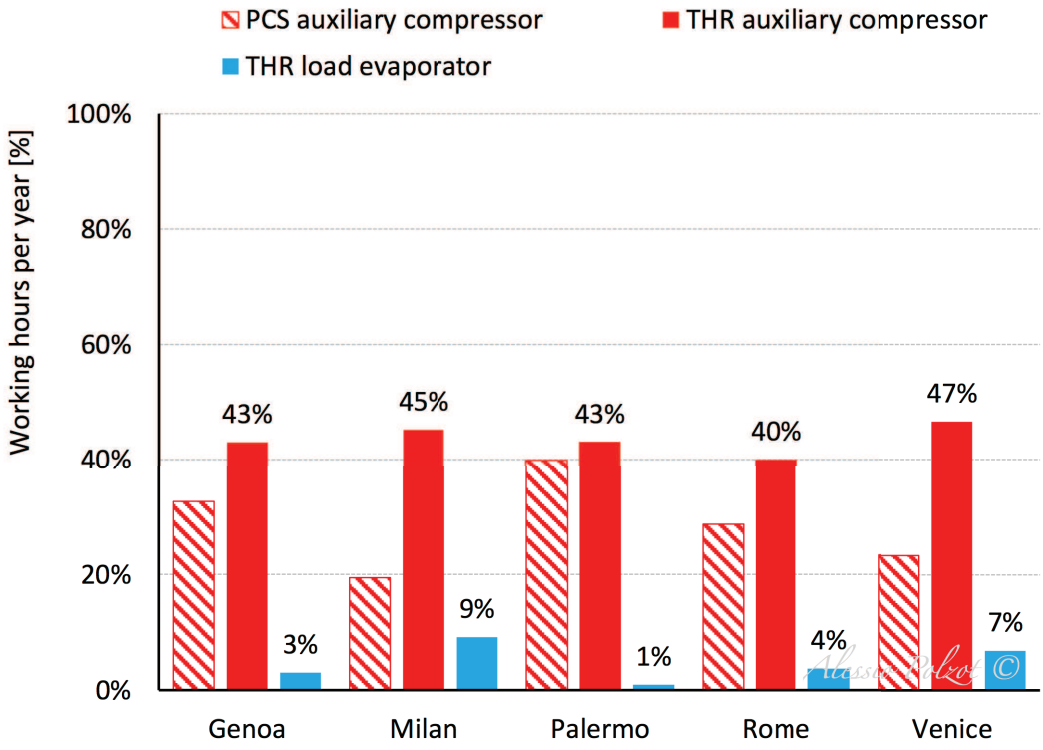

Figure 8.4.k - Auxiliary compressor and load evaporator working hours per year in the evaluated climates conditions.

8.4.4 Energy consumption daily profiles

Figure 7.5.k, Figure 7.5.l, Figure 7.5.m, Figure 7.5.n and Figure 7.5.o show the daily energy consumption profiles of the THR system (refrigeration, space heating and DHW) compared with the PCS system (refrigeration) in Genoa, Milan, Palermo, Rome, Venice, respectively.

In the winter season, when the THR system runs in heat recovery mode, the increment of the high pressure and of the gas cooler outlet temperature and the activation of the load evaporator lead to an increment in the power input associated with the refrigeration unit.

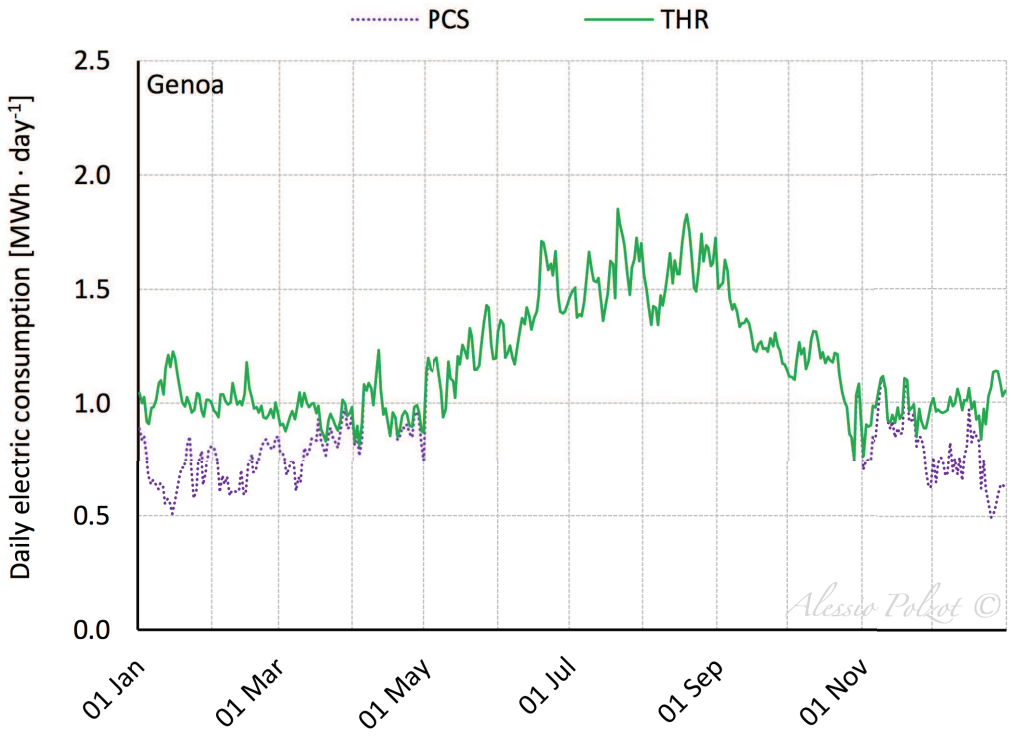

Figure 8.4.l - Daily energy consumption profiles of the PCS and THR systems in Genoa.

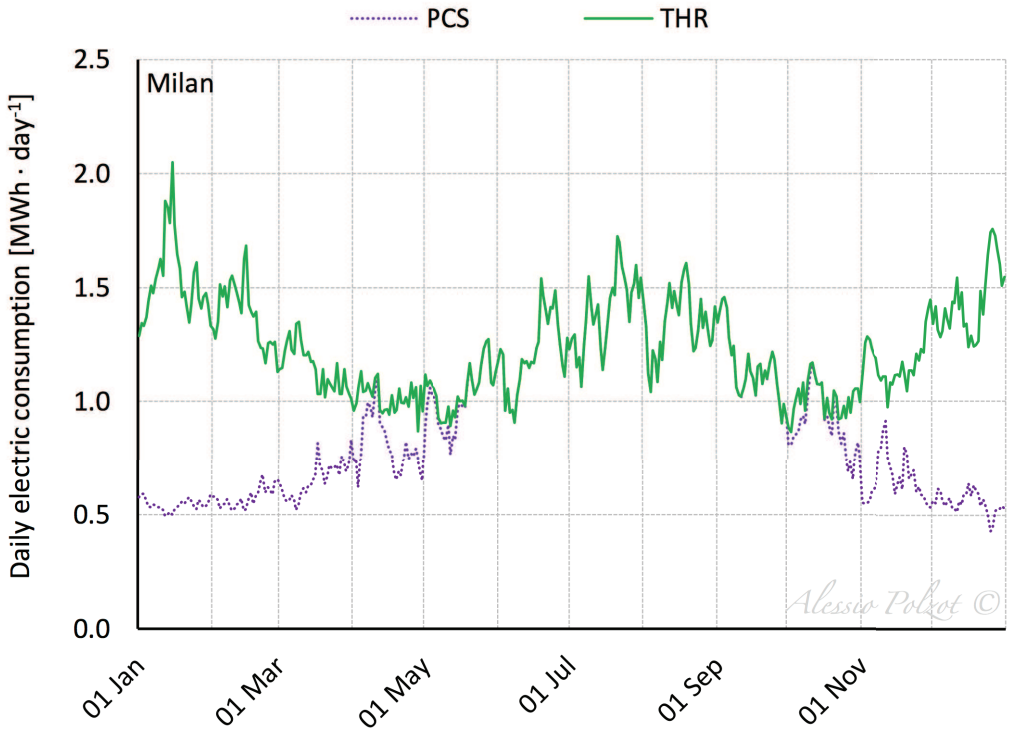

Figure 8.4.m - Daily energy consumption profiles of the PCS and THR systems in Milan.

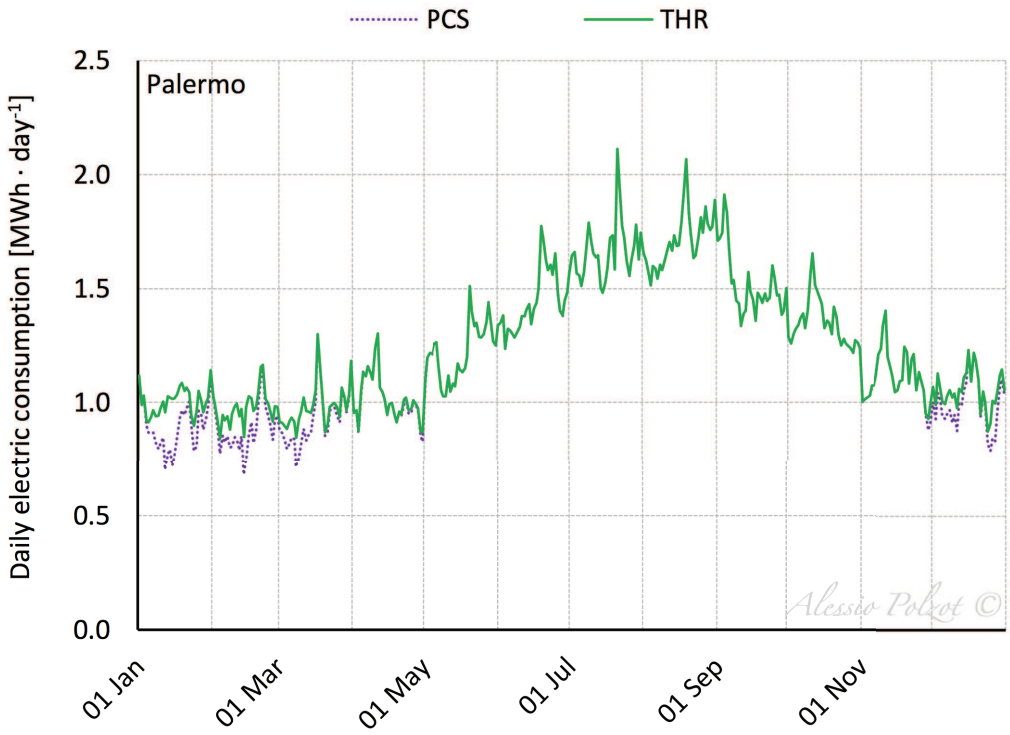

Figure 8.4.n - Daily energy consumption profiles of the PCS and THR systems in Palermo.

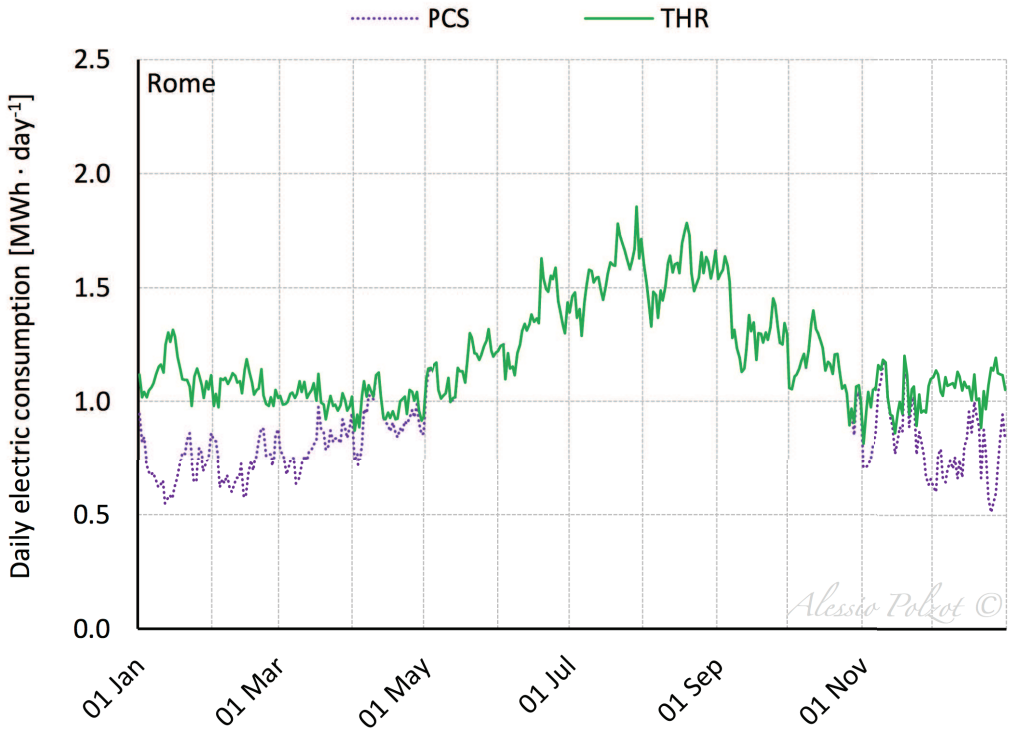

Figure 8.4.o - Daily energy consumption profiles of the PCS and THR systems in Rome.

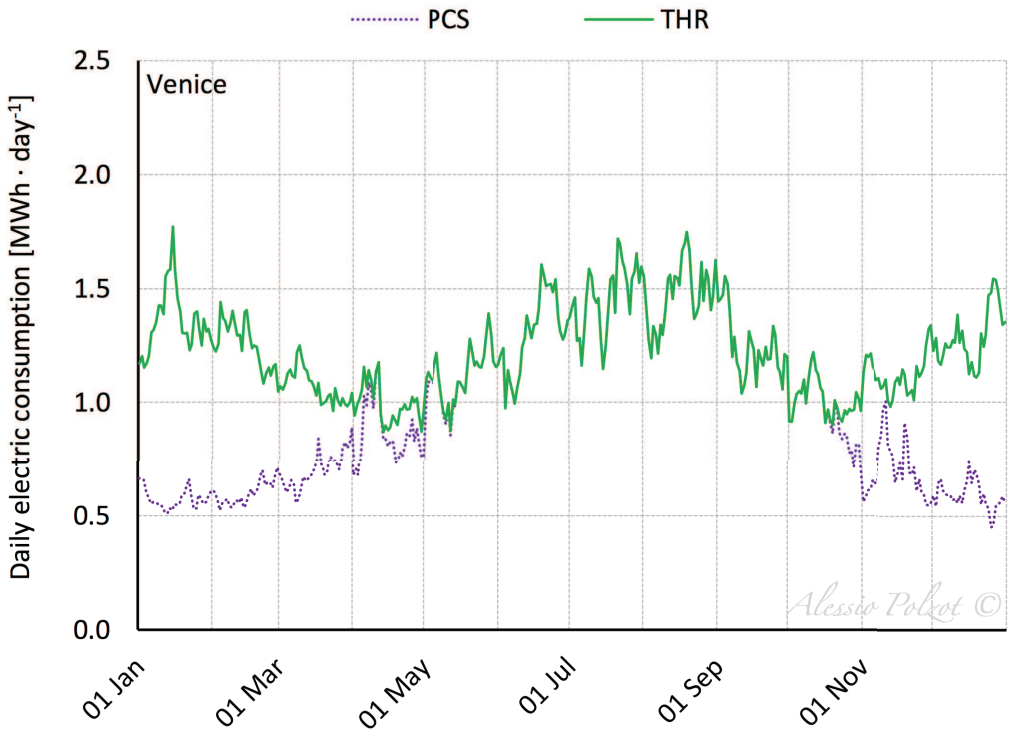

Figure 8.4.p - Daily energy consumption profiles of the PCS and THR systems in Venice.

8.4.5 Monthly energy consumption of the investigated solutions

The monthly energy consumption of the systems investigated in this chapter for the climate conditions of Genoa, Milan, Palermo, Rome and Venice is depicted in Figure 8.4.q, Figure 8.4.r, Figure 8.4.s, Figure 8.4.t and Figure 8.4.u, respectively.
In the heating season the THR system consume less energy than the DHP and CHP which has two dedicated heat pumps for the space heating and the domestic hot water production. In summer season the energy consumption of the three systems is comparable.

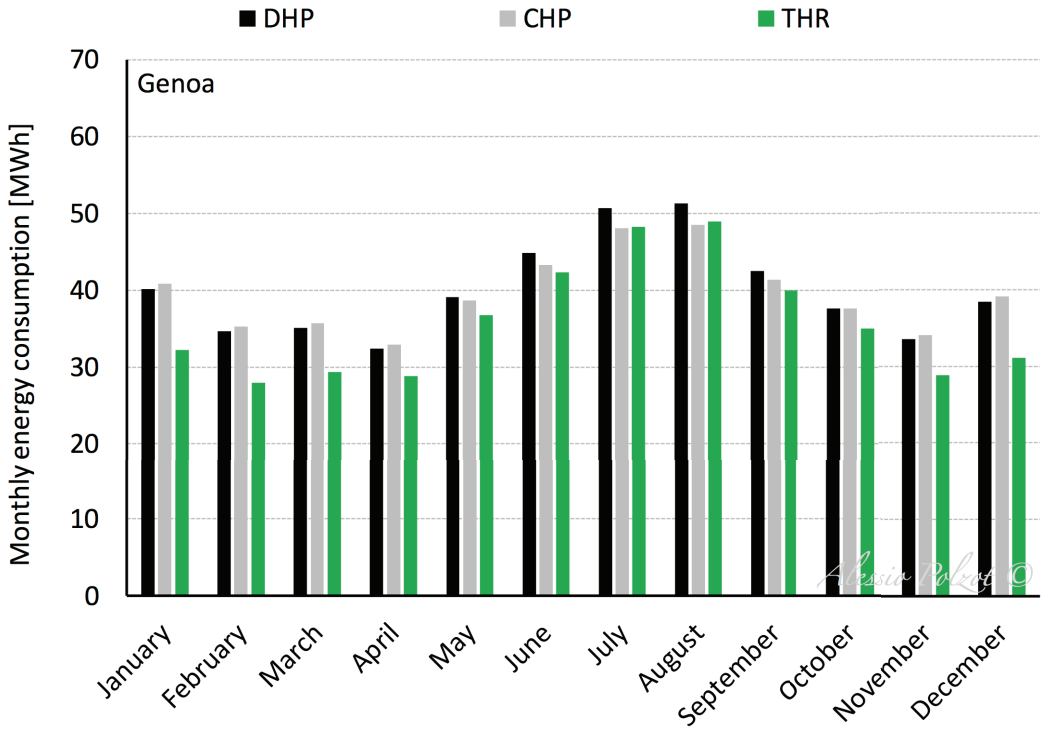

Figure 8.4.q - Monthly energy consumption of the investigated systems in Genoa.

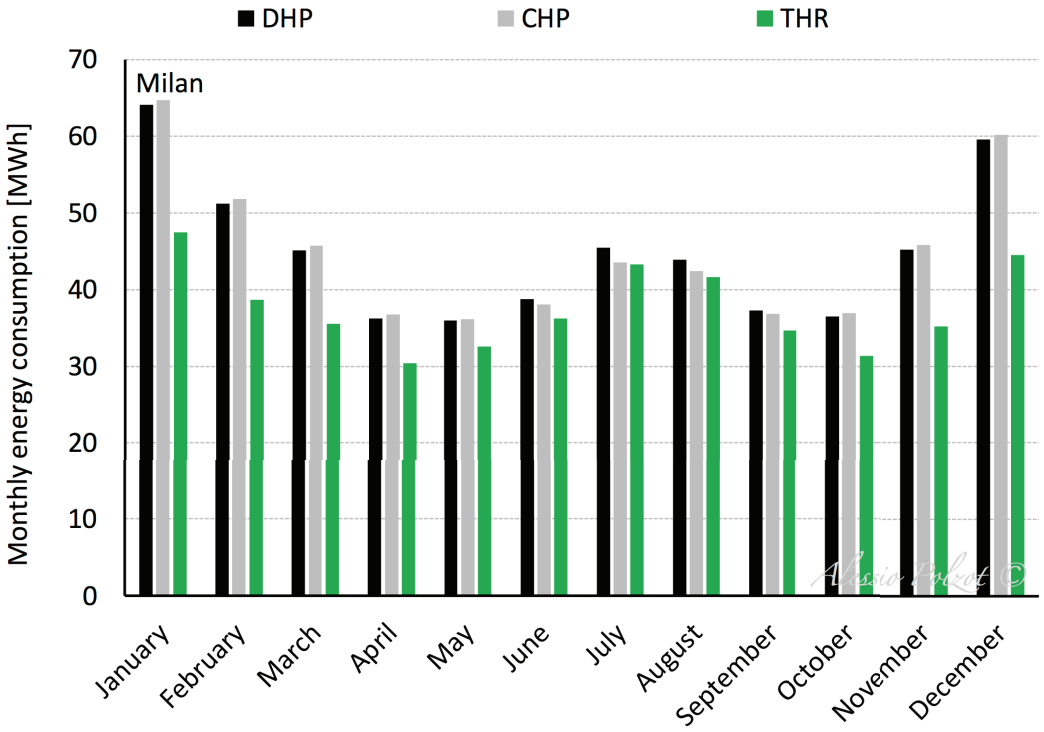

Figure 8.4.r - Monthly energy consumption of the investigated systems in Milan.

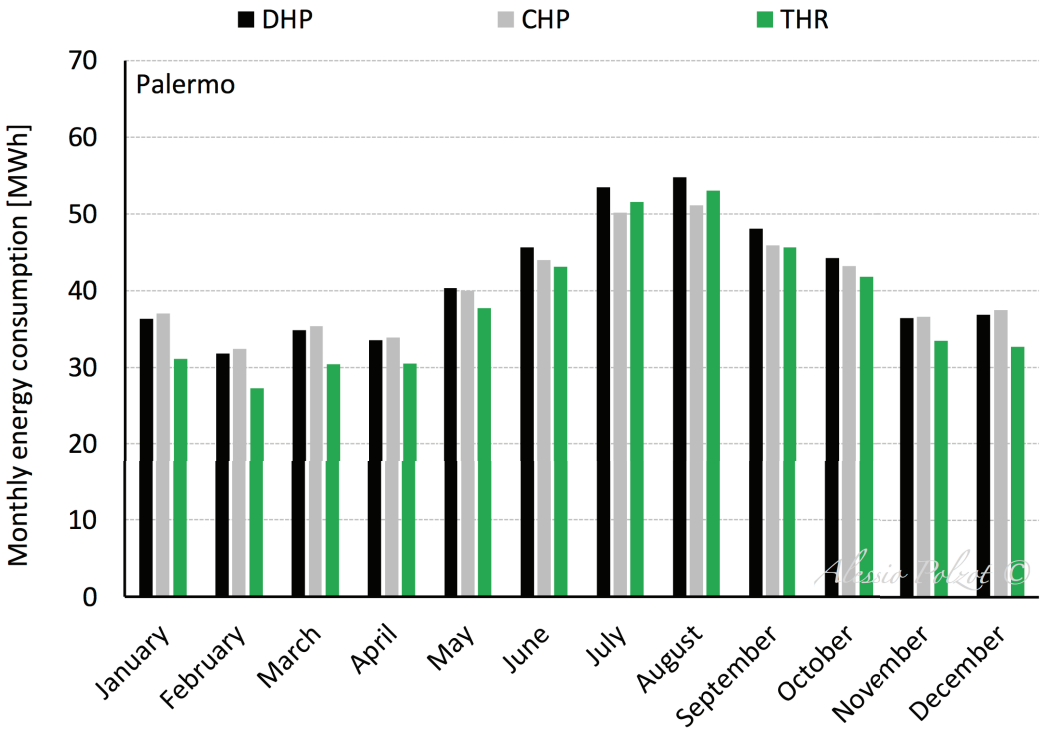

Figure 8.4.s - Monthly energy consumption of the investigated systems in Palermo.

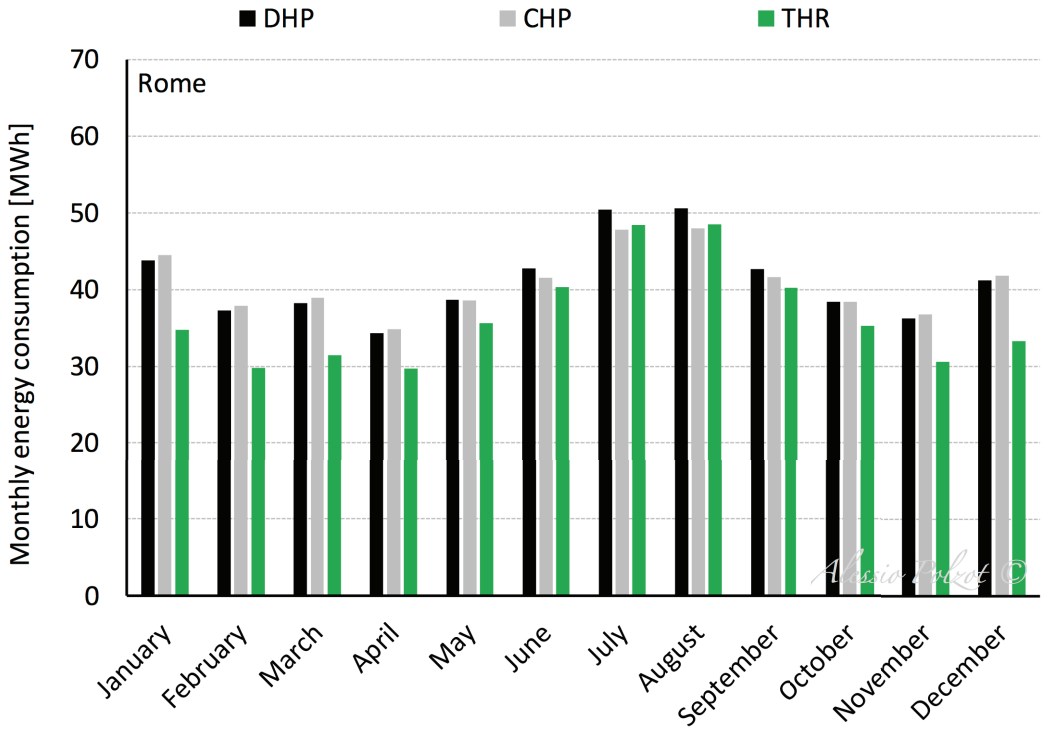

Figure 8.4.t - Monthly energy consumption of the investigated systems in Rome

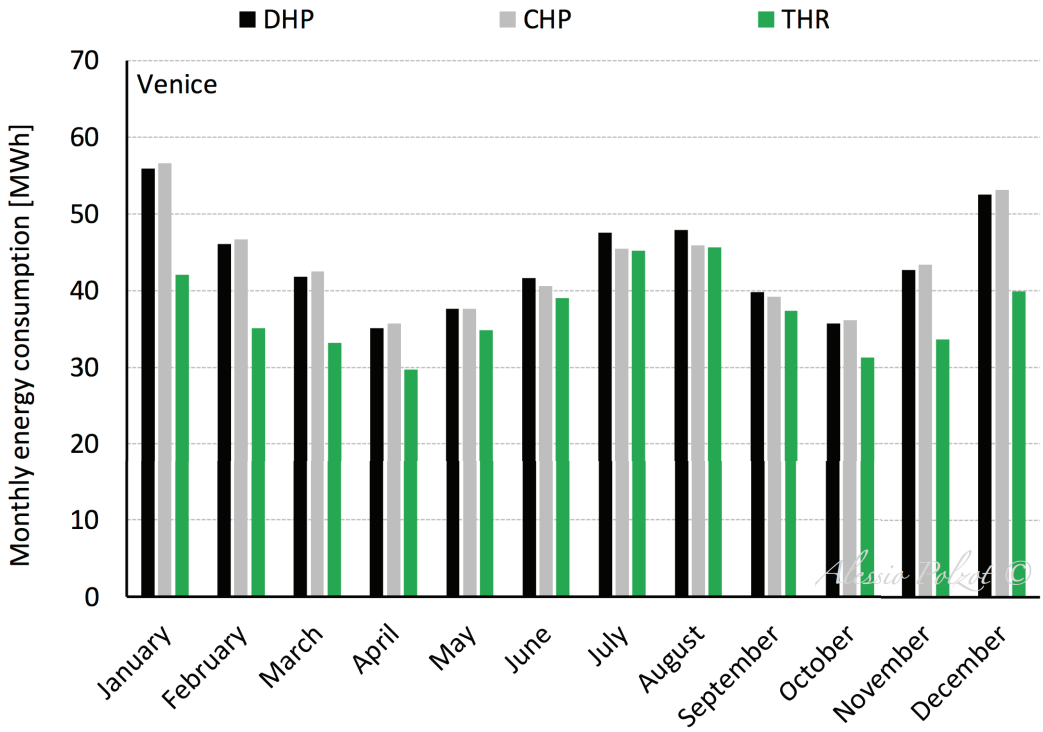

Figure 8.4.u - Monthly energy consumption of the investigated systems in Venice.

8.4.6 Annual energy consumption

The DHP annual energy consumption and the relative energy consumption of the other investigated solutions in comparison with DHP are reported in Table 6.6.a.

	Annual energy consumption	**Relative energy consumption**	
	[MWh]	[%]	
	DHP	**CHP**	**THR**
Genoa	481	-1.0%	-10.6%
Milan	539	-0.1%	-16.3%
Palermo	496	-1.9%	-7.7%
Rome	495	-0.8%	-11.5%
Venice	524	-0.3%	-14.8%

Table 8.4.a - Annual energy consumption of DHP system and relative energy consumption of the investigated solutions in comparison with DHP.

8.5 Reference

- BITZER, 2016. BITZER Software 6.4.4.1464. Available at: https://www.bitzer.de/websoftware/ [accessed 15/12/2016].
- Sawalha S., 2013. Investigation of heat recovery in CO_2 trans-critical solution in supermarket refrigeration. International Journal of Refrigeration 36, 145- 156.
- Tambovtsev, A., Olsommer, B., Finckh, O., 2010. Development challenges in CO_2 commercial refrigeration systems. Proceedings of the Sustainable Refrigeration and Heat Pump Technology Conference, Stockholm, Sweden.
- Tambovtsev, A., Olsommer, B., Finckh, O., 2011. Integrated heat recovery for CO_2 refrigeration systems. Proceedings of the 23rd IIR International Congress of Refrigeration. Prague, Czech Republic.

Chapter IX

Fire prevention tank as a thermal storage

This chapter analyses the energy saving potential of carbon dioxide commercial refrigeration system coupled with a fire prevention tank used as a thermal storage.

The main concern in CO_2 booster refrigeration systems at mild and warm climates is related to the high temperature of the refrigerant at the gas cooler exit, which is very effective on the performance of the system (Pettersen, 1997). For this reason many efforts are devoted to investigate configurations where gas cooling can be promoted to the highest level, by means of internal heat exchangers (Cavallini et al., 2007; Ge and Tassou, 2011; Sawalha, 2008; Yang and Zhang, 2011) with an average increase in the COP of up to 10%, or by means of the mechanical subcooling, i.e. performing subcooling thanks to another refrigerating unit (Hafner et al., 2014; Llopis et al., 2015; Qureshi and Zubair, 2012). The effectiveness in terms of global energy consumption of the solution with mechanical subcooling is strictly related to the COP of the additional refrigerating system, and its evaluation on a yearly basis is not so easy. As an example, Wiedenmann et al. (2014) investigated the effect of subcooling performed by an adsorption refrigerator driven by waste heat. Because of the additional investment cost, high payback periods were estimated, with a rather low market potential.

It comes out that an effective improvement could be safely reached while performing subcooling by means of an external device at no or very low expense. Looking for other cold sources for subcooling, Ferrandi and Orlandi (2013) investigated the effect of a cold storage used to cool down the refrigerant at the exit of the liquid receiver in a R744 booster cycle. With a water store size from 12 m^3 to 27 m^3, they predicted an average reduction in summer daily power consumption around 5 % compared to a traditional plant, and a peak refrigerating capacity reduction around 28 %.

In this chapter a similar solution (FPT) is investigated, where a fire prevention water tank is used as a cold sink for performing subcooling during periods characterized by high outdoor temperatures, while during low refrigeration duty periods and night time the refrigeration plant is able to cool down the water storage.
The results are compared to a baseline system (DHP), i.e. a R404A direct expansion system as the refrigeration unit and two air to water heat pumps for space heating and hot water production, and to a traditional system (CHP) where a cascade refrigeration system with heat recovery is coupled with two air to water heat pumps which satisfy the DHW and heating demands of the supermarket.

9.1 System description

The investigated FPT system, a R744 transcritical booster system with heat recovery, auxiliary compressor and load evaporator coupled with a fire prevention tank which acts as a thermal storage, is depicted in Figure 9.1.a.
The liquid exiting the receiver is expanded from the intermediate pressure to two different pressure levels, according to the temperature levels of the chilled and frozen food storage equipment: at 28.0 bar for medium temperature and at 12 bar for low temperature, corresponding to the evaporating temperatures of –8 °C and -35 °C, respectively. The whole amount of flash gas generated by the high-pressure (HP) expansion valve is compressed by the auxiliary compressor or, in subcritical operations, it is expanded to the MT pressure level by the vapour by-pass valve and is compressed by the high stage (HS) compressors rack.
Two heat exchangers at the exit of the HS compressors rack recover heat at two different temperature levels. The first one (HX1) is used for the production of DHW while the second one (HX2) supplies hot water for space heating purposes. When the system is running in heat recovery mode, an air-cooled gas cooler/condenser allows cooling down the refrigerant exiting the heat exchangers, otherwise the two heat exchangers are by-passed and the whole heat is rejected into the ambient.
The system is also provided with an air-cooled load evaporator, which is activated during low refrigeration duty periods, when the heat rejected by the HX2 heat exchanger is not sufficient to meet the heating demand of the building. The pressure

at the additional evaporator depends on the outdoor air temperature with a maximum value fixed at same value of the intermediate pressure, which is fixed at 37.7 bar, considering a suitable pressure drop. When the load evaporator is activated the superheated vapour exiting the latter is directly compressed by the auxiliary compressor to the high pressure. The discharge pressure of the system is controlled according to the heating demand so that when the supermarket does not need heat the high pressure follows the ambient temperature, while when heating energy is required it is increased and more heat is available.

In heat recovery mode the gas cooler acts as a subcooler improving the performance of the system. On the other hand the total mass flow rate of the refrigerant flowing through the refrigerating unit and, consequently, the amount of energy recoverable from the two heat exchangers reduce as the degree of the subcooling increases. In order to provide the supermarket with all the heating demand the temperature of the CO_2 exiting the air cooled gas cooler/condenser can be increased by reducing the speed velocity of the fans thus making more heat available for recovery (Sawalha, 2013; Tambovtsev et al., 2010; Tambovtsev et al., 2011).

To meet the full heating demand of the building the following control strategy is applied to the system: initially the high pressure is increased, when the maximum value of the latter is reached the system starts to reduce the gas cooler fan speed velocity to increase the temperature of the carbon dioxide exiting the gas cooler. Finally, if the heat available from heat recovery is not sufficient, the load evaporator is activated, the fans speed velocity is set at maximum value and the system starts to increase the mass flow rate flowing through the load evaporator.

Near the building in the ground, a 950 m^3 buried water reservoir (Table 9.1.b) is available for the fire prevention system ad it is considered as a cold storage. In periods characterized by high outdoor temperature, the performance of the CO_2 refrigeration system decrease due to the high gas cooler outlet temperature. Through the subcooler heat exchanger the fire prevention tank water is used to cool down the carbon dioxide at the gas cooler exit (subcooling mode) improving the system performance. During low refrigeration duty periods and night periods, which is characterized by lower external temperatures, the recharger heat exchanger, which works as the load evaporator, cools down the water of the thermal storage (recharging mode).

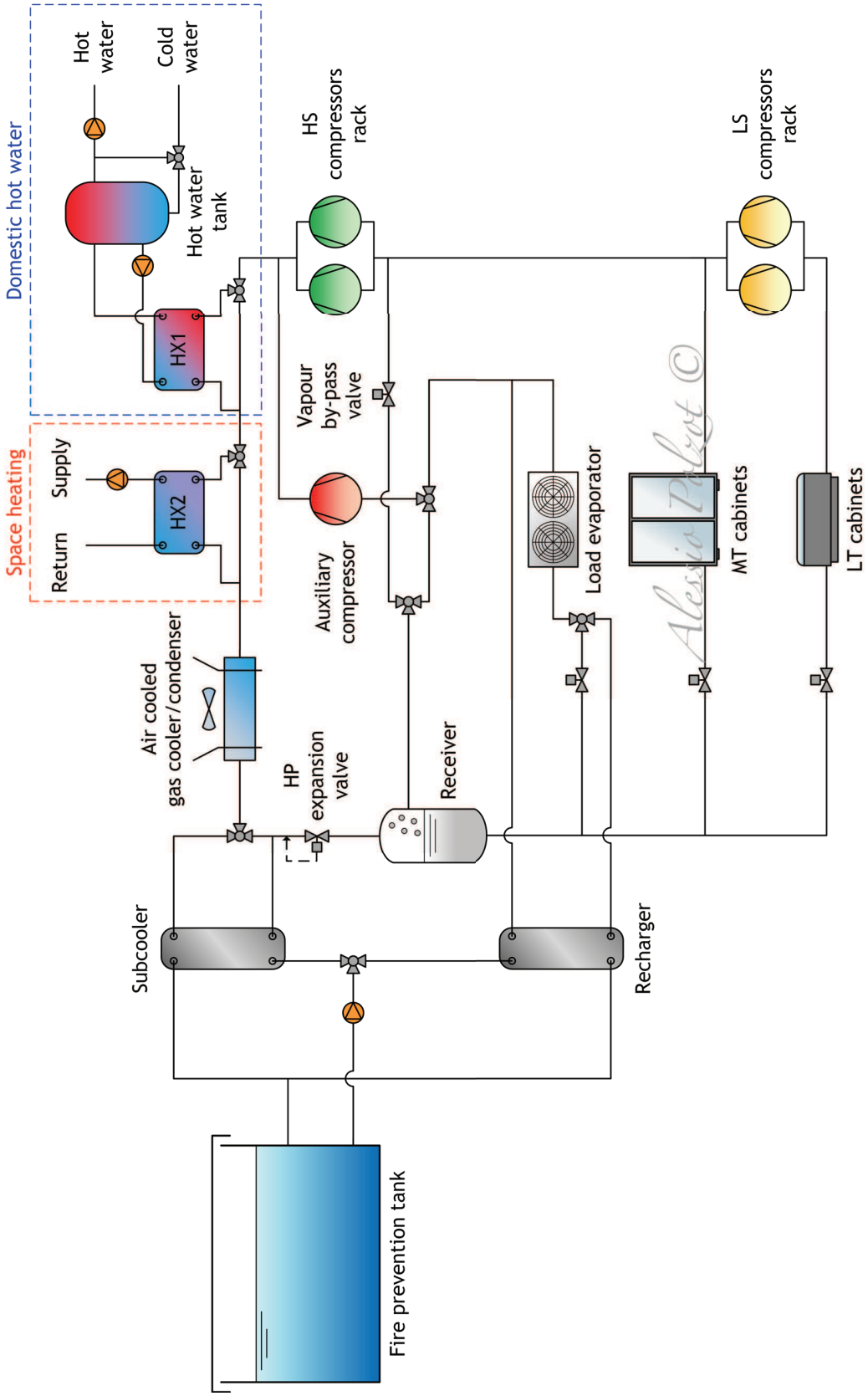

Figure 9.1.a - Schematic of the R744 commercial refrigeration system coupled with a fire prevention tank used as a thermal storage (FPT).

In Figure 9.1.b is depicted the subcooling mode of the FPT system in a log(p)-h diagram. In green solid line is shown the heat rejected by the refrigeration system to the thermal storage through the subcooler heat exchanger.

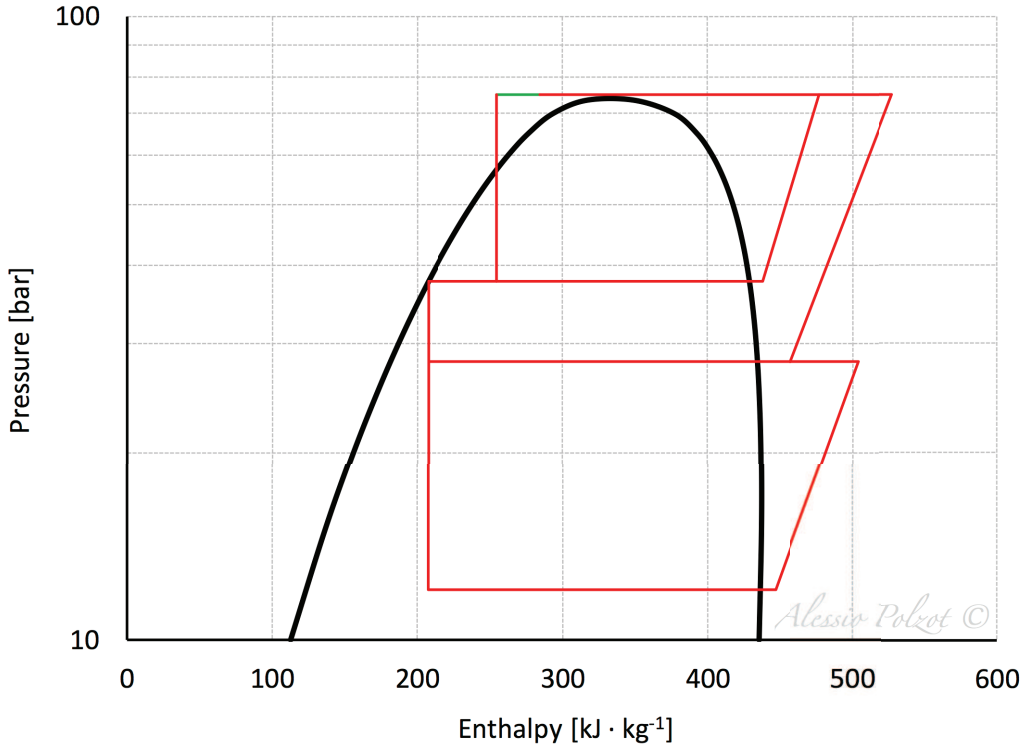

Figure 9.1.b - Log(p)-h diagram of the subcooling mode of the FPT system

In Figure 9.1.c is shown the recharging mode of the FPT system in a log(p)-h diagram. In orange solid line is represented the heat absorbed by the refrigeration system from the thermal storage through the recharger heat exchanger. In recharging mode, the liquid exiting from the receiver which evaporates in the recharger is compressed by the auxiliary compressor to the high pressure.

The system, through HX1, provides hot water at 60 °C to avoid the growth of legionella. In heat recovery mode, the supply temperature and the minimum return temperature of the heating system is fixed at 40 °C and at 30 °C, respectively. The approach temperature of the two water cooled heat exchangers is set to 5 K while the other operating conditions considered for the investigated system is reported in Table 9.1.a.

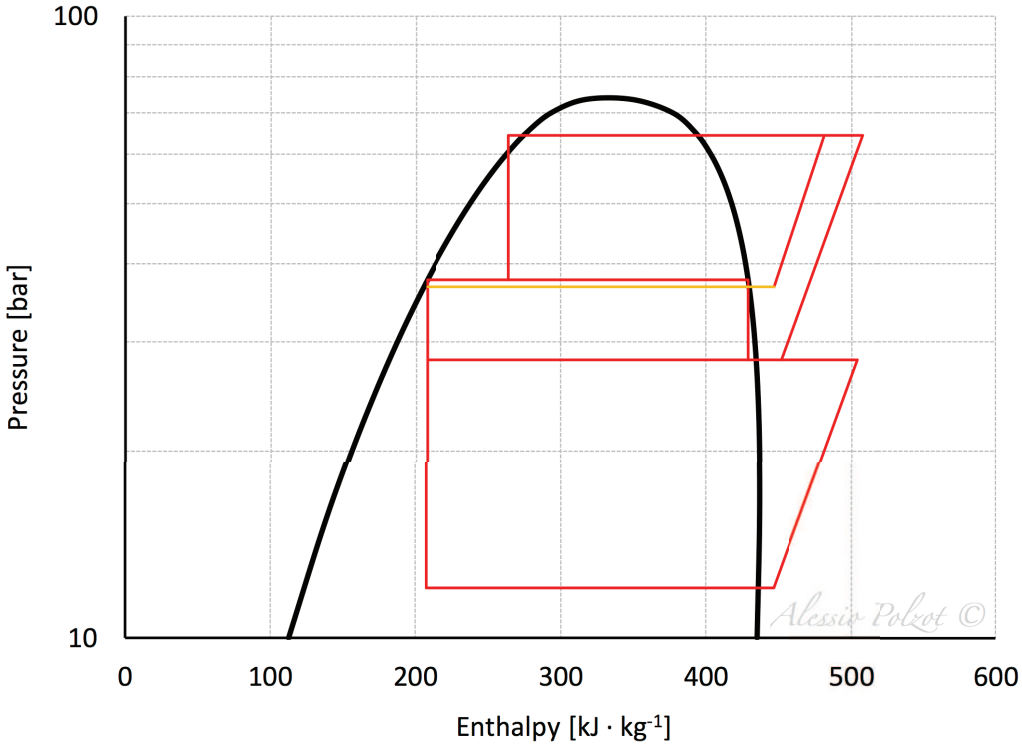

Figure 9.1.c - Log(p)-h diagram of the recharging mode of the FPT system.

FPT operating conditions	Unit	Value
Useful superheating	K	5.0
Superheating in the suction lines	K	5.0
Approach temperature of the condenser/gas cooler	K	3.0
Minimum condensing temperature	°C	8.0
Subcooling in subcritical operations	K	2.0
Liquid receiver pressure	bar	37.7
Maximum value of high pressure in heat recovery mode	bar	85.0
Approach temperature of the load evaporator	K	5.0
Load evaporator capacity	kW	200.0
Gas cooler absorbed power at rated conditions	kW	3.2
Approach temperature of the subcooler and recharger	K	5.0

Table 9.1.a - FPT system operating conditions.

Fire prevention tank	Unit	Value
Volume	m^3	950.0
Height	m	2.5
Depth from the ground surface	m	0.5
U-value of walls, floor and ceiling	$W \cdot m^{-2} \cdot K^{-1}$	1.7

Table 9.1.b - Fire prevention tank parameters.

As a reference for comparison, a traditional DXS system is chosen as the refrigeration system, one air to water heat pump provides the climate control of the zones and one air to water heat pump satisfy the DHW demand (DHP system). An additional solution (CHP) where traditional DXS refrigeration system is replaced by a cascade system with heat recovery (Figure 7.1.c).

9.2 Heat pumps

In DHP and CHP solutions, two different HFC heat pumps are evaluated, one uses R410A as working fluid and it provides hot water for the space heating of the thermal zones (operating conditions in Table 8.2.a), one uses a R134a as refrigerant and it satisfy the domestic hot water demand of the supermarket (operating conditions in Table 8.2.b).

9.2.1 COP

The COP values of the above mentioned heat pumps are reported in Figure 7.2.a and Figure 7.2.c.

9.2.2 Compressors global efficiency

The compressors, which are selected for the heat pumps used in the investigated solutions are:

- scroll compressors for the R410A heat pumps;

- semi-hermetic reciprocating compressors for the R134a heat pumps.

Their global efficiencies are obtained as a function of the pressure ratio by using BITZER Software (BITZER, 2016) and are reported in paragraphs 7.3.1 and 7.3.3.
All their suggested technological constraints are respected.

9.3 Heating and DHW demands

The CO_2 transcritical booster refrigeration system provide the space heating of the food store (thermal zone 30 in Figure 3.1.b)
The monthly heating demand of the thermal zone is reported in the Chapter VIII for all the investigated locations, in particular in Figure 7.4.a, Figure 7.4.b, Figure 7.4.c, Figure 7.4.d and Figure 7.4.e. The domestic hot water usage is estimated at a maximum value of 250 dm^3 per hour during the opening hours. In Figure 7.4.f the monthly domestic hot water demand is depicted.

9.4 Results

The results are reported in terms of energy consumption and in terms of working hours of the auxiliary compressor and of the subcooler. An analysis on the high pressure and on thermal storage temperature of the FPT system is conducted.
The cooling down of the fire prevention tank water during night time through the recharger heat exchanger of the FPT system is not an efficient solution. The annual energy consumption of this solution is slightly higher than the solution without the recharger. The advantage of subcooling is counterbalanced by the energy spent for recharging (Polzot et al., 2016).

9.4.1 Undisturbed tank water temperature

In Figure 9.4.a is shown thermal storage water temperature considering the fire prevention tank undisturbed. The daily average temperature of the storage not coupled with the refrigeration system is lower than 20 °C during the whole year,

except in Palermo where the maximum value reached is equal to 22.4 °C at the end of September.

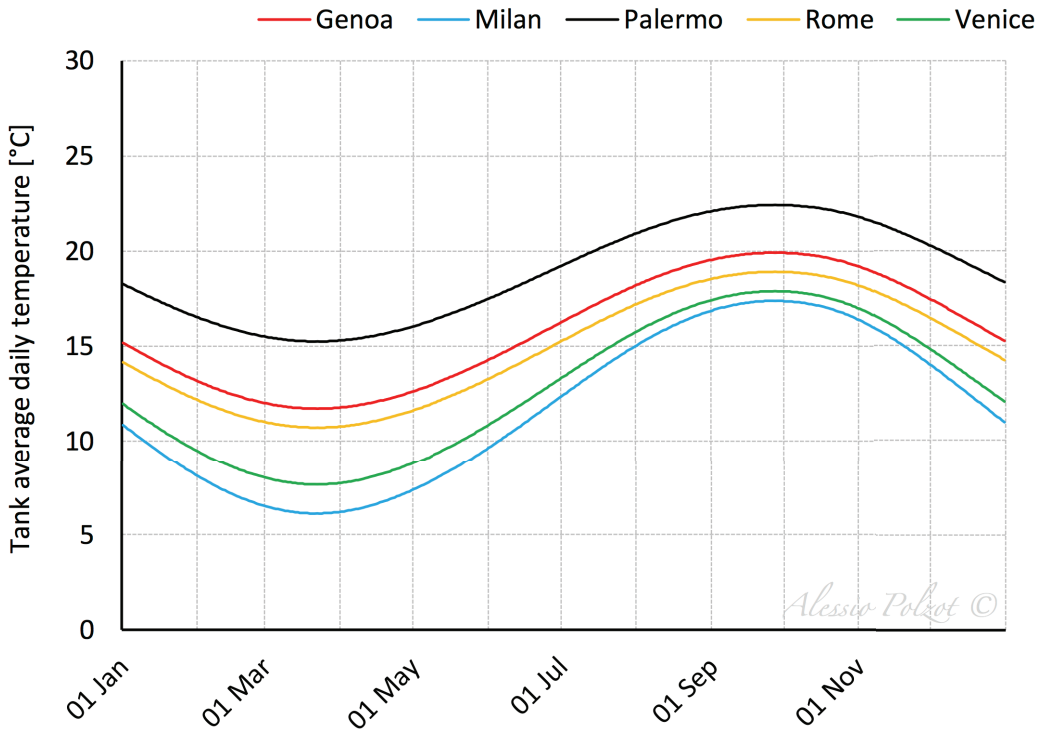

Figure 9.4.a - Annual profile of the water temperature of the undisturbed tank in the investigated locations.

9.4.2 Tank water temperature

Figure 9.4.b, Figure 9.4.c, Figure 9.4.d, Figure 9.4.e and Figure 9.4.f show the comparison in terms of annual profile of the average water temperature of the fire prevention tank among the FPT solution and the undisturbed tank.

In Genoa the FPT system runs in subcooling mode from the end of May to the end of August, in Milan and in Rome from the end of May to mid-September, in Venice from mid-June to mid-September. In Palermo, which is the warmest climate considered, the system uses the fire prevention tank as a subcooler from mid-June to mid-September, but it restarts to run in subcooling mode for a short period in mid-October when the temperature of the thermal storage is lower due to the heat losses from the heat storage to the ground.

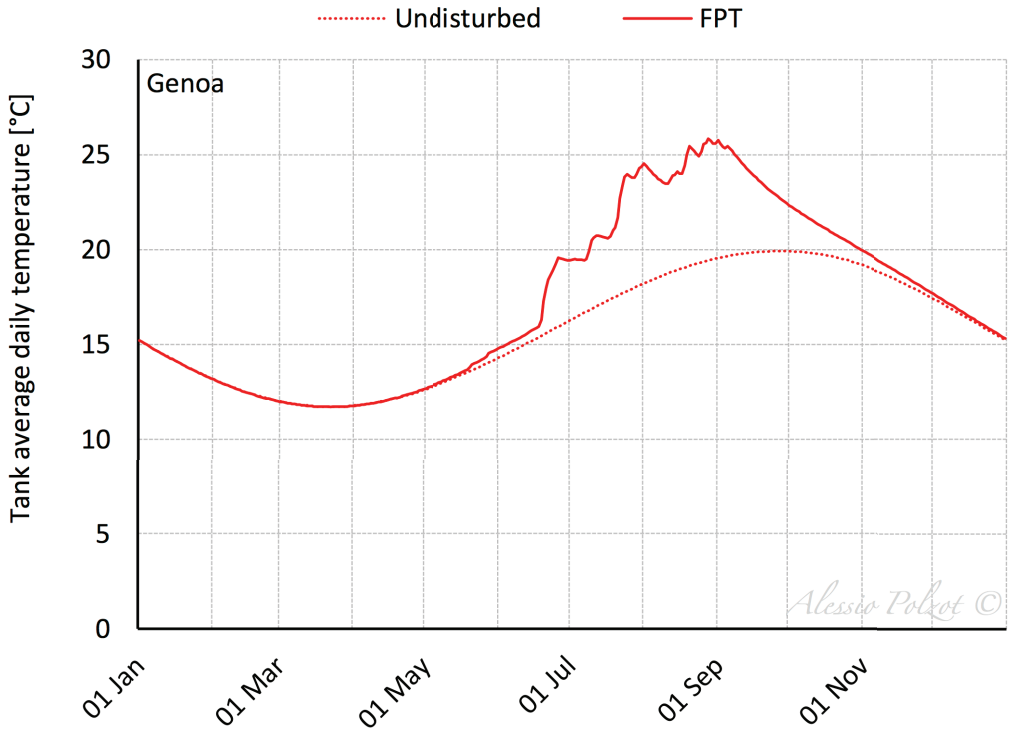

Figure 9.4.b - Annual profile of the average thermal storage water temperature in Genoa.

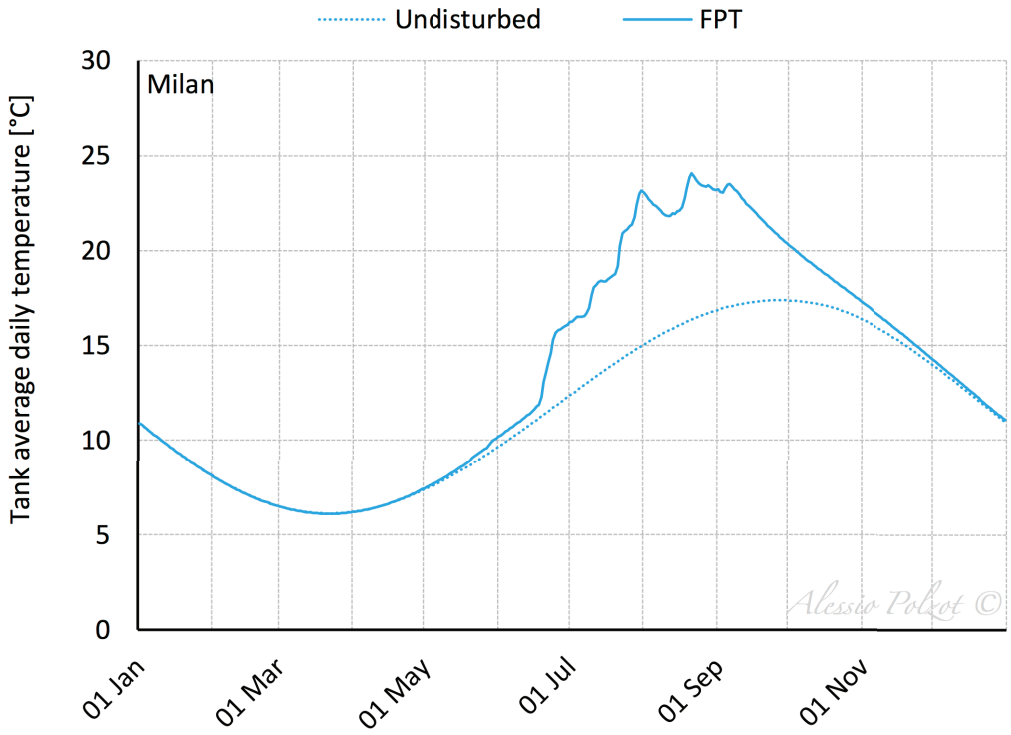

Figure 9.4.c - Annual profile of the average thermal storage water temperature in Milan.

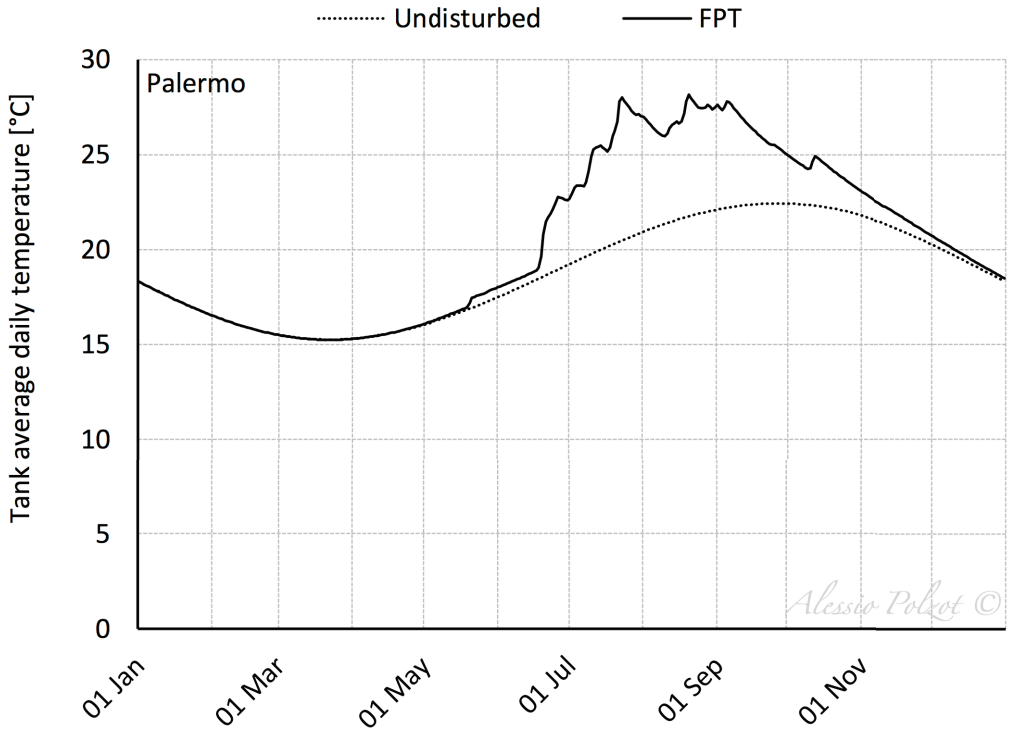

Figure 9.4.d - Annual profile of the average thermal storage water temperature in Palermo.

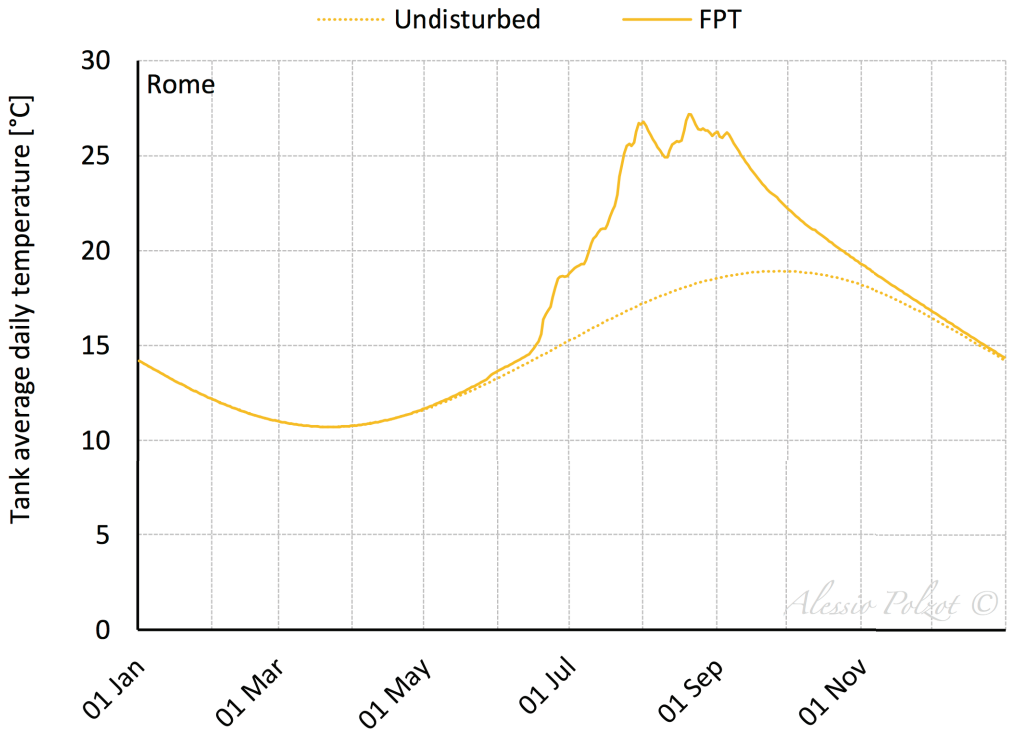

Figure 9.4.e - Annual profile of the average thermal storage water temperature in Rome.

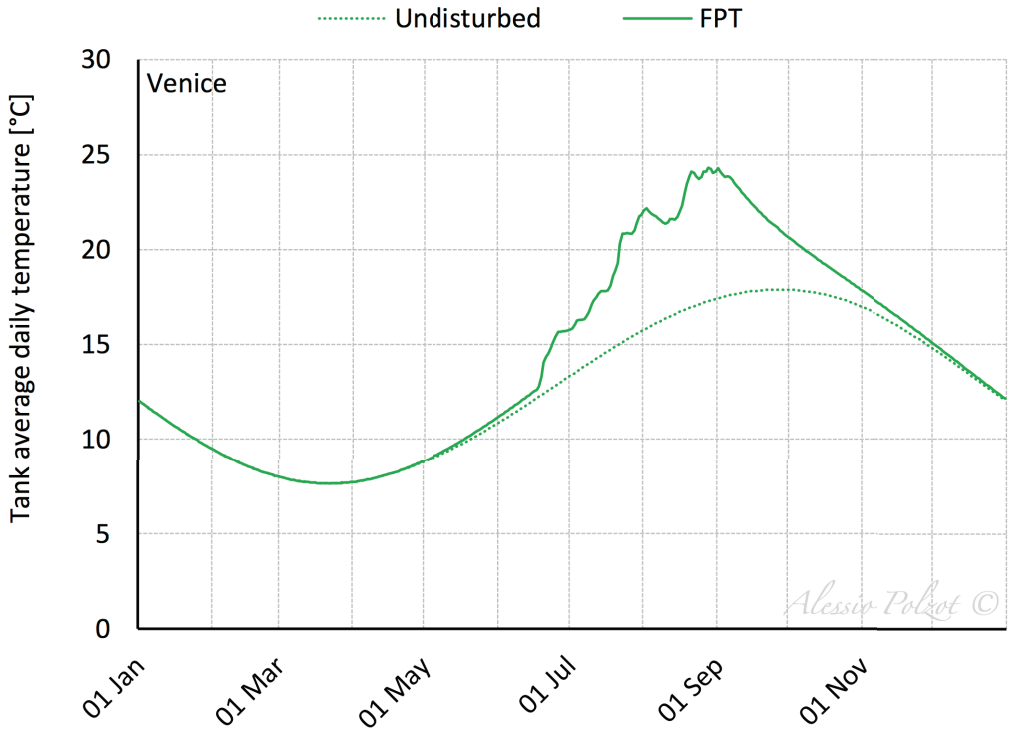

Figure 9.4.f - Annual profile of the average thermal storage water temperature in Venice.

9.4.3 High pressure

In heat recovery mode the high pressure can be increased to meet the full heating demand of the supermarket, while in subcooling mode the optimal high pressure is lower due to the subcooler outlet temperature. Figure 9.4.g, Figure 9.4.h, Figure 9.4.i, Figure 9.4.j and Figure 9.4.k make a comparison in terms of frequency over the year of the high pressure among the R744 transcritical booster system with heat recovery analysed in the previously chapter (THR, paragraph 8.4.1) and the CO_2 system coupled with the fire prevention tank (FPT).

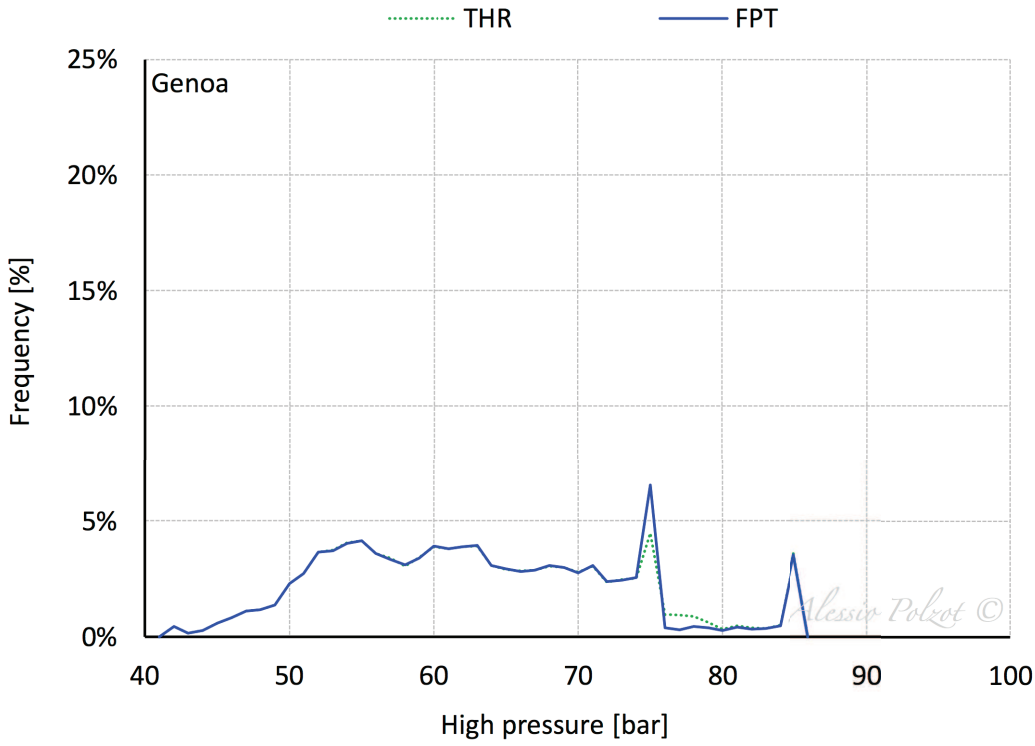

Figure 9.4.g - Annual frequency of the high pressure values in PCS and THR systems in Genoa.

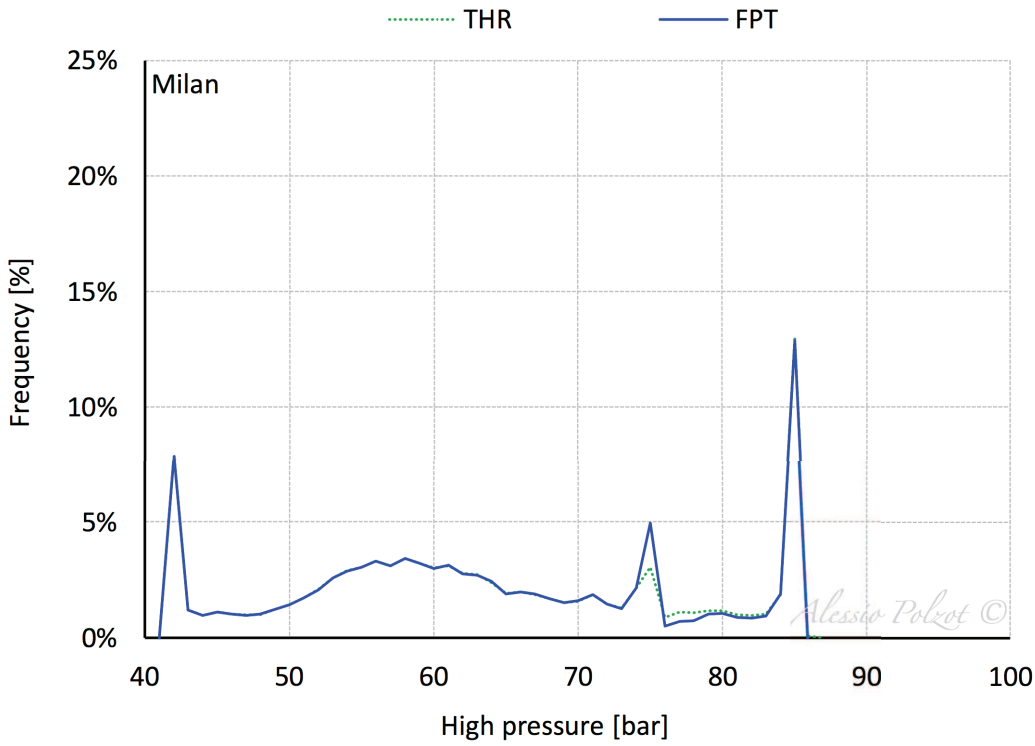

Figure 9.4.h - Annual frequency of the high pressure values in PCS and THR systems in Milan.

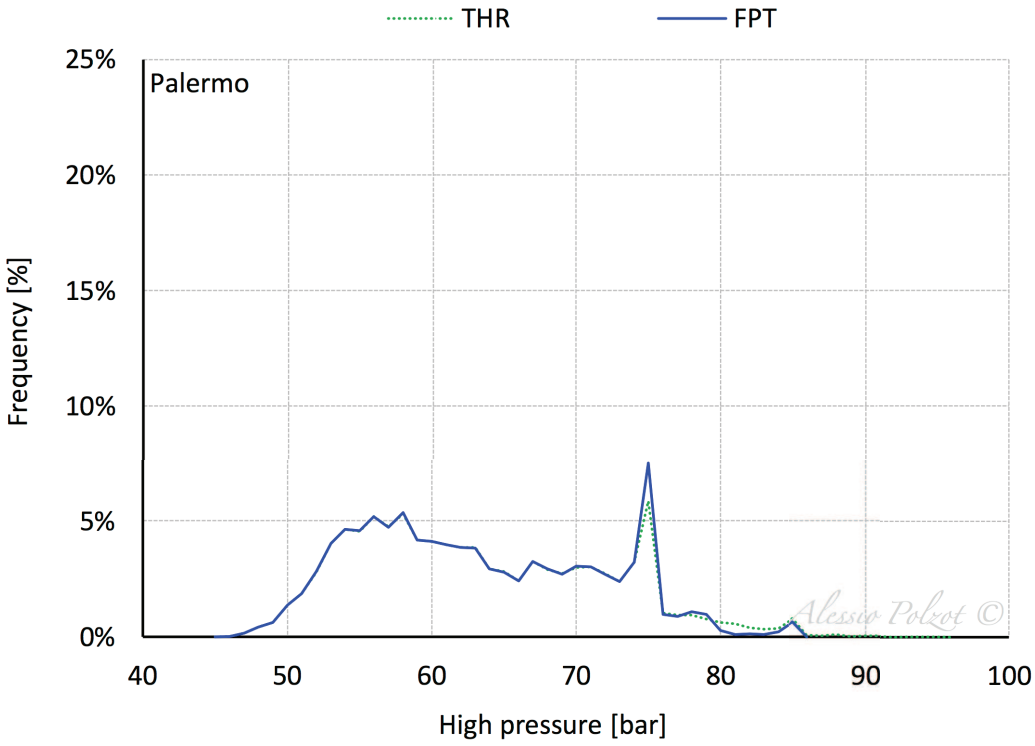

Figure 9.4.i - Annual frequency of the high pressure values in PCS and THR systems in Palermo.

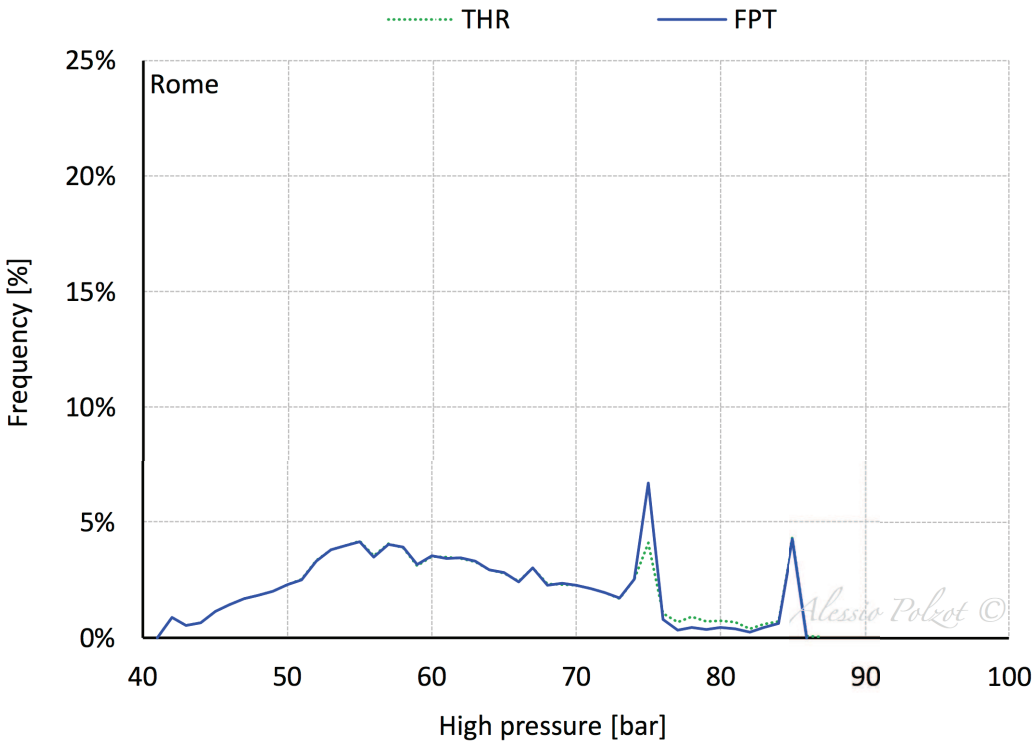

Figure 9.4.j - Annual frequency of the high pressure values in PCS and THR systems in Rome.

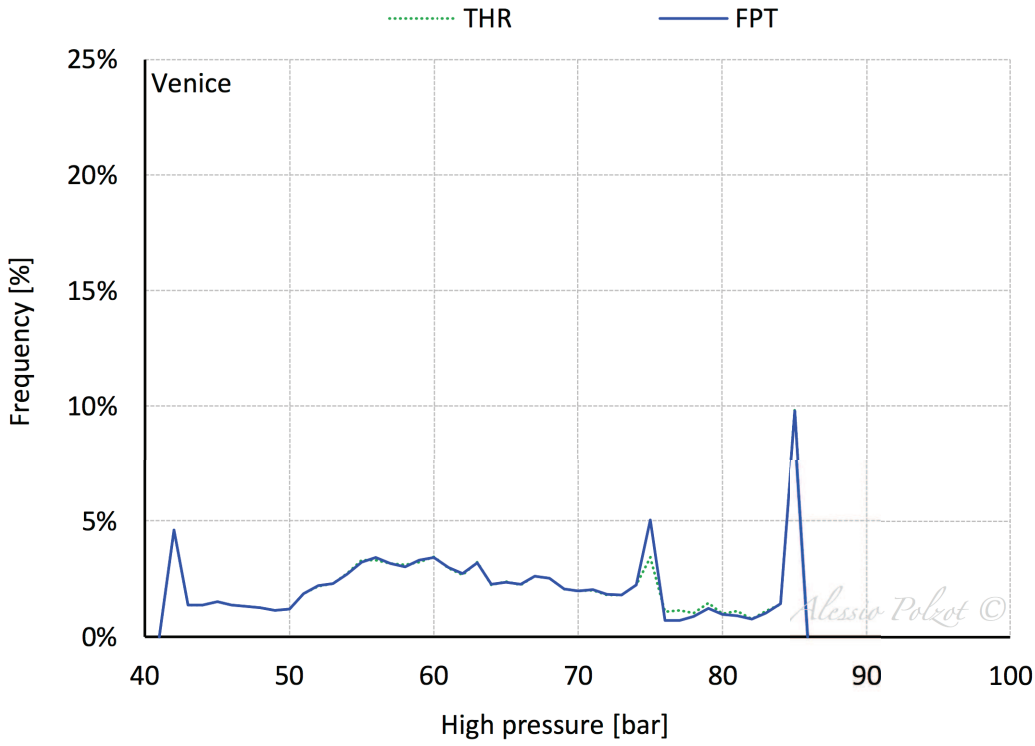

Figure 9.4.k - Annual frequency of the high pressure values in PCS and THR systems in Venice.

9.4.4 Auxiliary compressor and subcooler working hours

Figure 9.4.l shows for the FPT solution the percentage of time over the year in which the auxiliary compressor and the subcooler are activated in all the climates condition evaluated. Comparing the working hours over the year of the auxiliary compression in THR (paragraph 8.4.3) and in FPT systems, the results are almost the same. In THR solution, the additional compressor is activated 3764 hours per year in Genoa, 3954 in Milan, 3769 in Palermo, 3502 in Rome and 4078 in Venice, while in the FPT solution it runs on average 10 hours more in all the investigated locations.

In the warmest climates considered the subcooler works about 80 hours per year more than the mild climates.

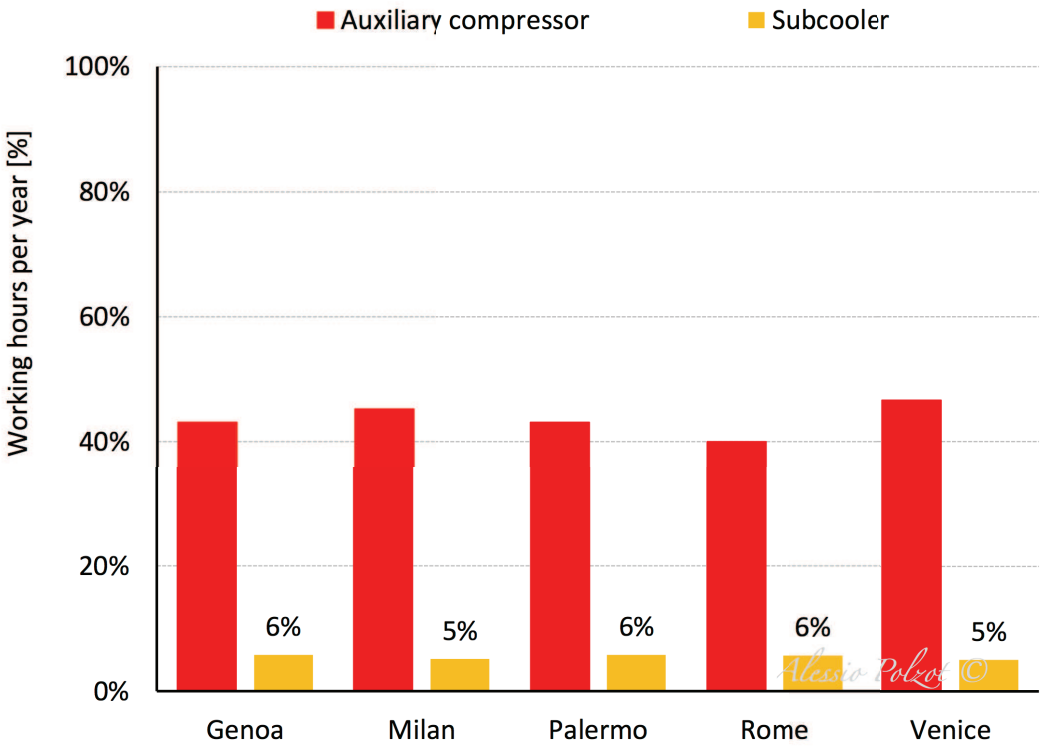

Figure 9.4.l - Auxiliary compressor and subcooler working hours per year in the evaluated climates conditions.

9.4.5 Energy consumption daily profiles

Figure 9.4.m, Figure 9.4.n, Figure 9.4.o, Figure 9.4.p and Figure 9.4.q show the daily energy consumption profiles of the FPT system compared with the THR system, analysed in the previously chapter, in Genoa, Milan, Palermo, Rome, Venice, respectively.

In the summer season, when the FPT system runs in subcooling mode, the reduction of the high pressure and of the CO_2 temperature at the high pressure heat exchangers lead to a reduction of the power input associated with the refrigeration unit and to a significant peak shaving.

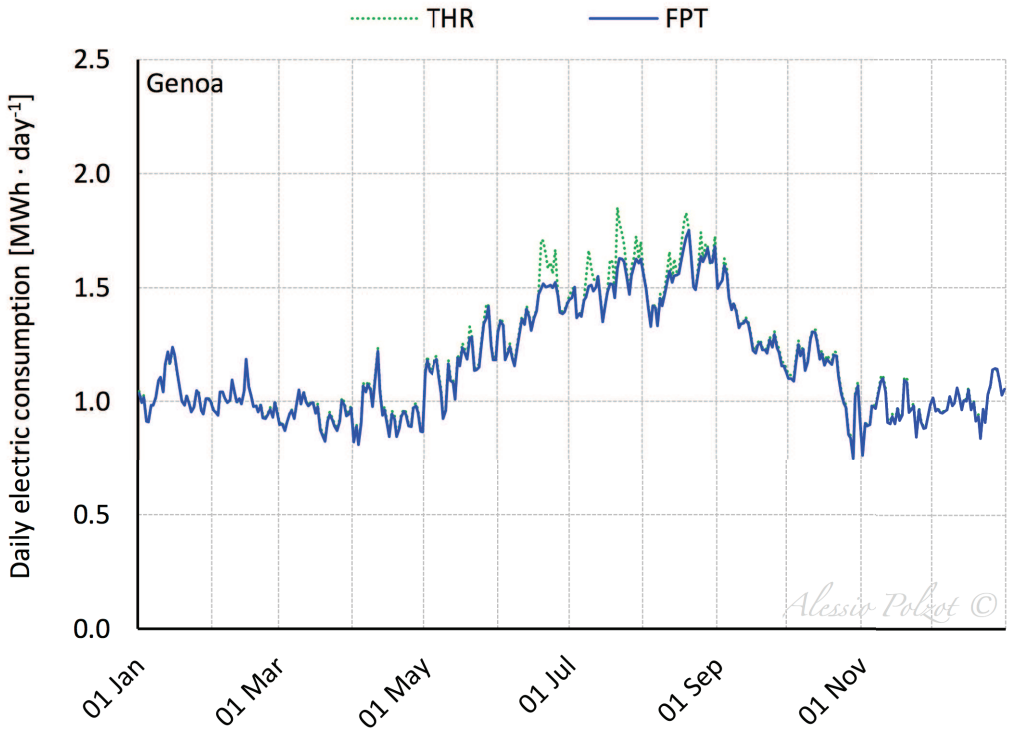

Figure 9.4.m - Daily energy consumption profiles of the PCS and THR systems in Genoa.

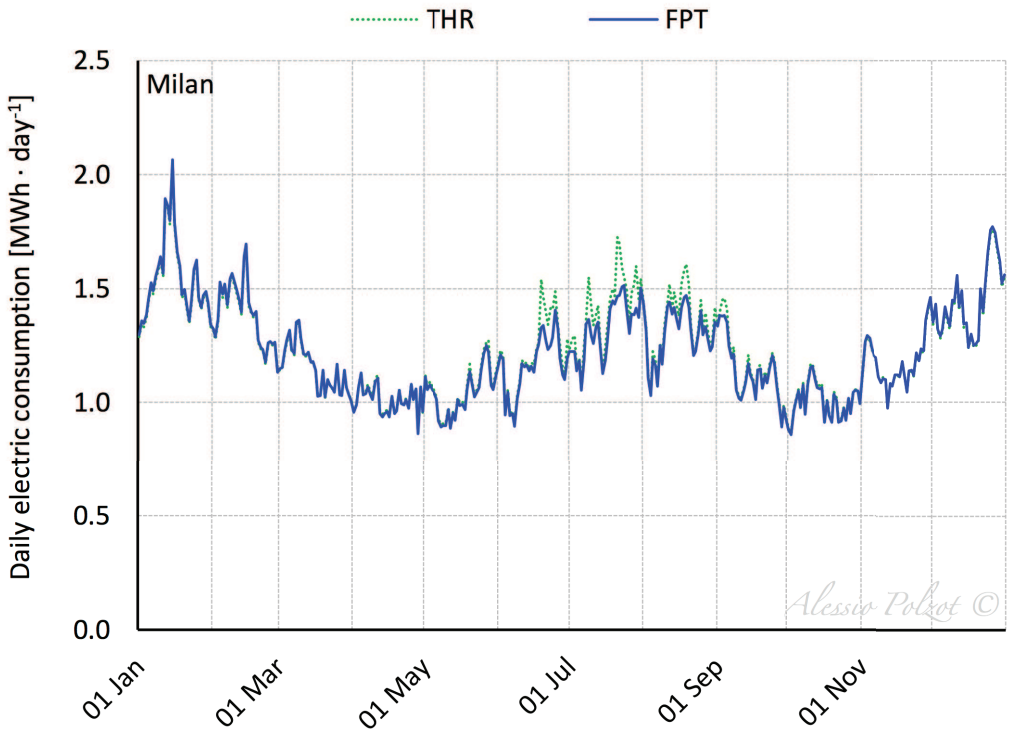

Figure 9.4.n - Daily energy consumption profiles of the PCS and THR systems in Milan.

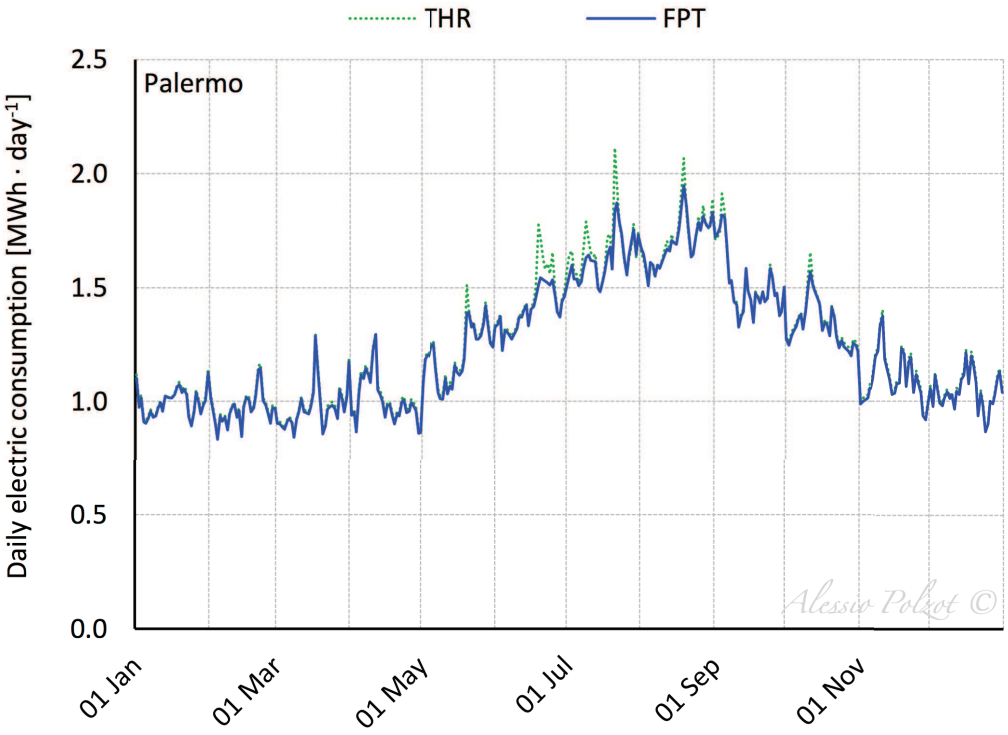

Figure 9.4.o - Daily energy consumption profiles of the PCS and THR systems in Palermo.

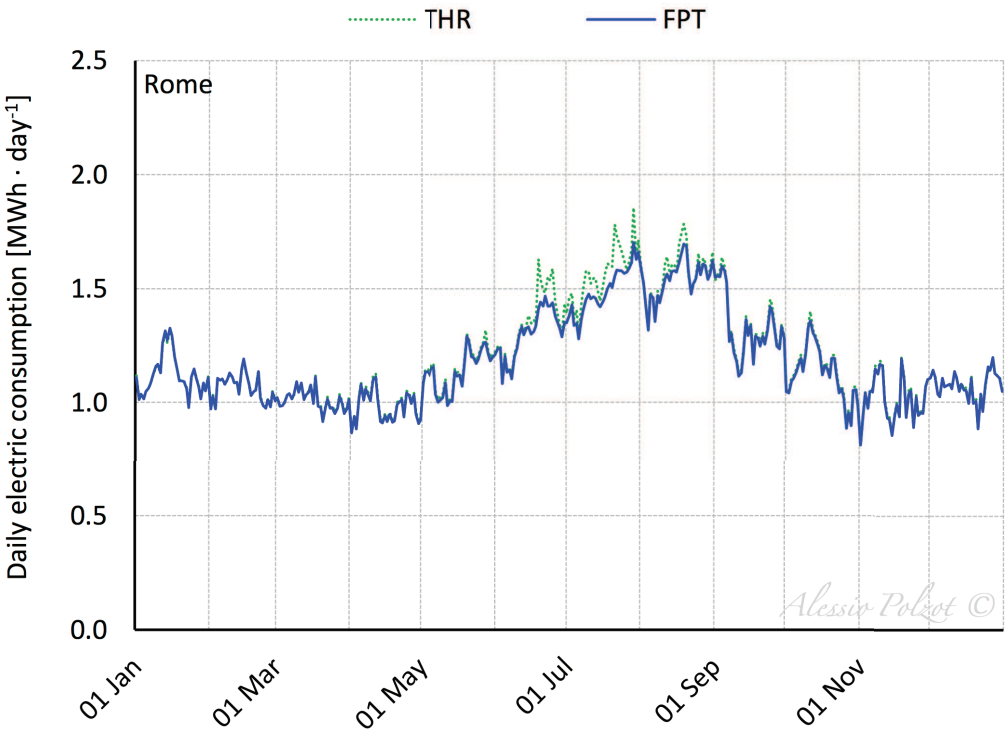

Figure 9.4.p - Daily energy consumption profiles of the PCS and THR systems in Rome.

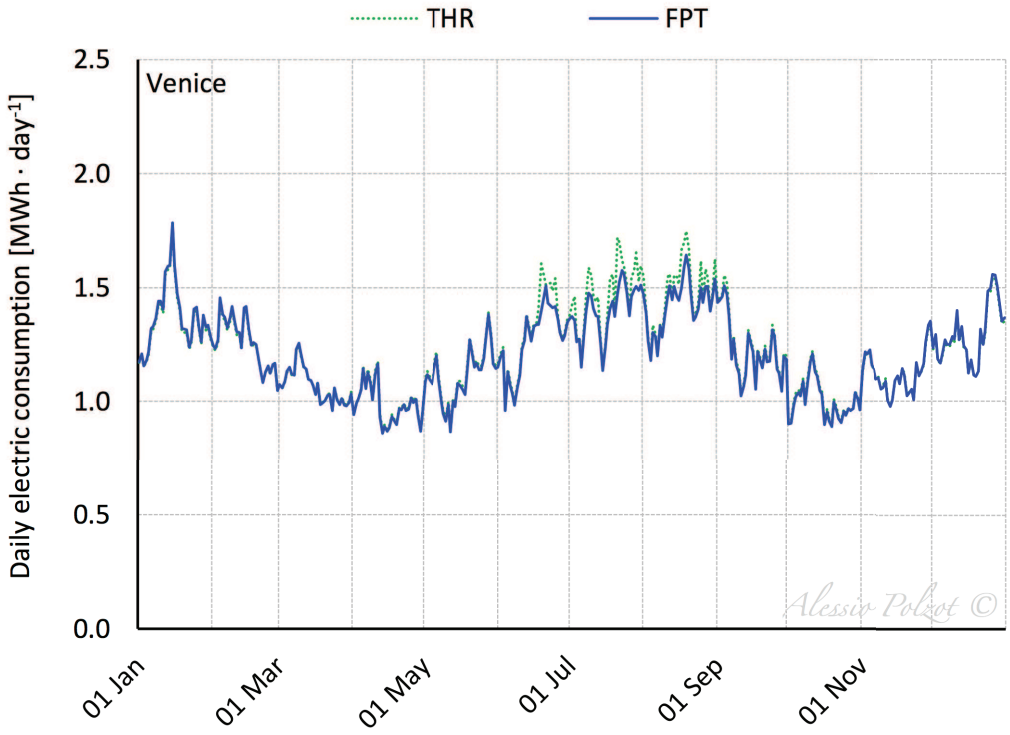

Figure 9.4.q - Daily energy consumption profiles of the PCS and THR systems in Venice.

9.4.6 Monthly energy consumption of the investigated solutions

The monthly energy consumption of the systems investigated in this chapter and the THR system investigated in the previously chapter for the climate conditions of Genoa, Milan, Palermo, Rome and Venice is depicted in Figure 9.4.r, Figure 9.4.s, Figure 9.4.t, Figure 9.4.u and Figure 9.4.v, respectively.

In the summer season the FPT system consume less energy than THR thanks to the subcooling while both the THR and the FPT systems consume less energy than the traditional solutions during all year.

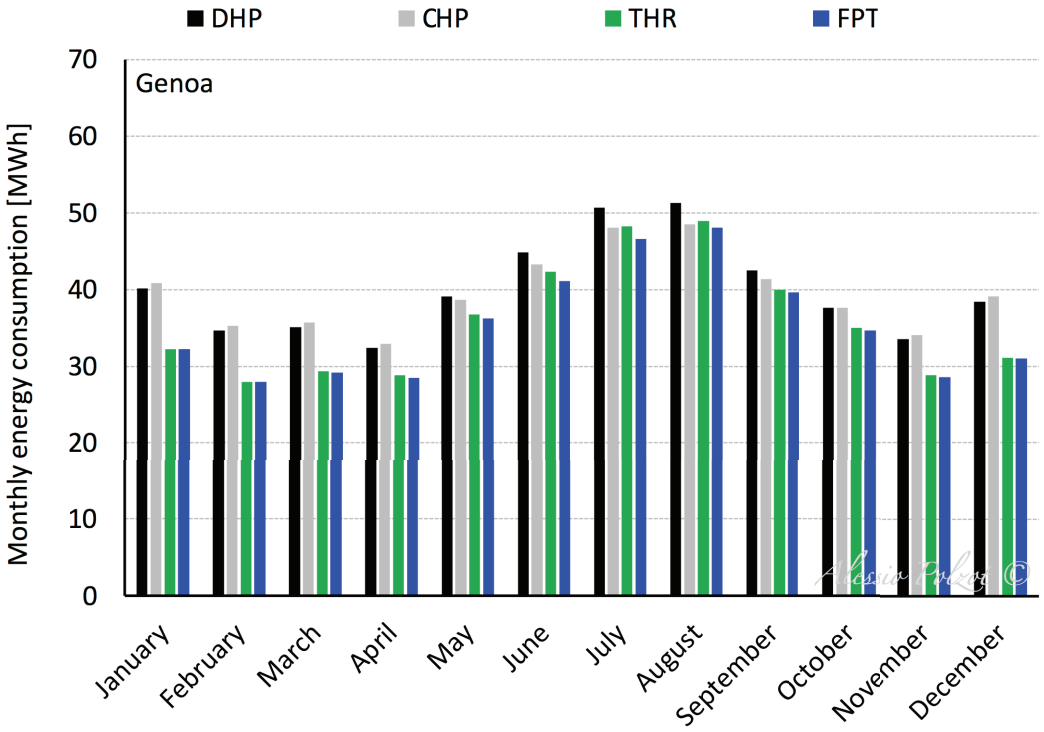

Figure 9.4.r - Monthly energy consumption of the investigated systems in Genoa.

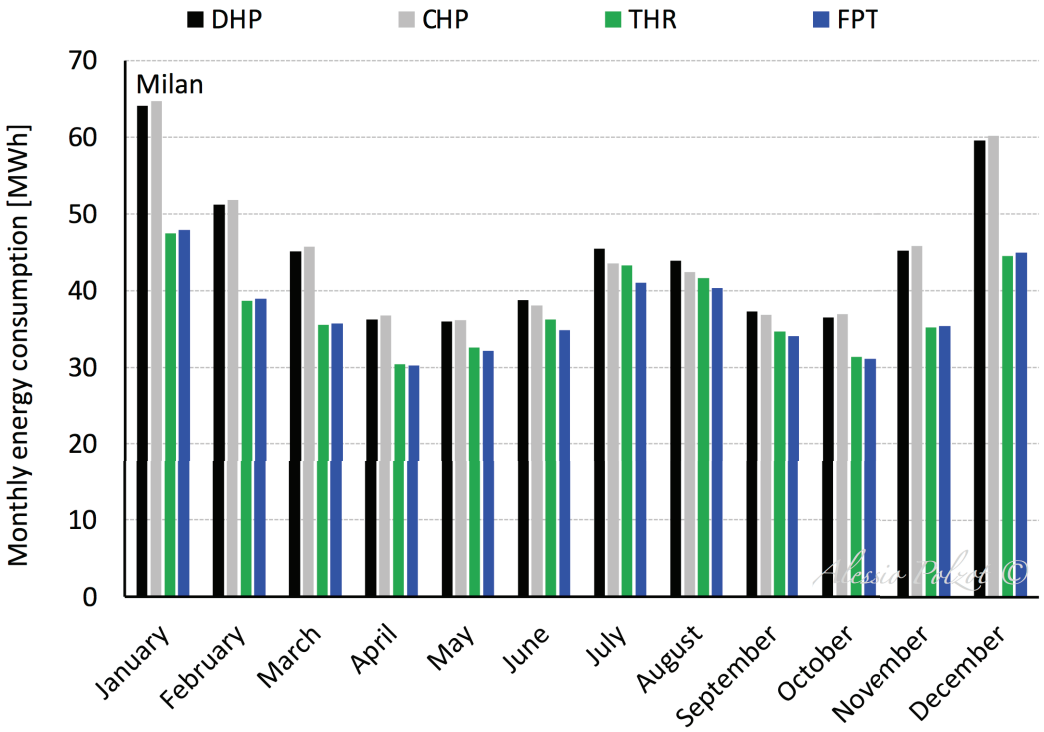

Figure 9.4.s - Monthly energy consumption of the investigated systems in Milan.

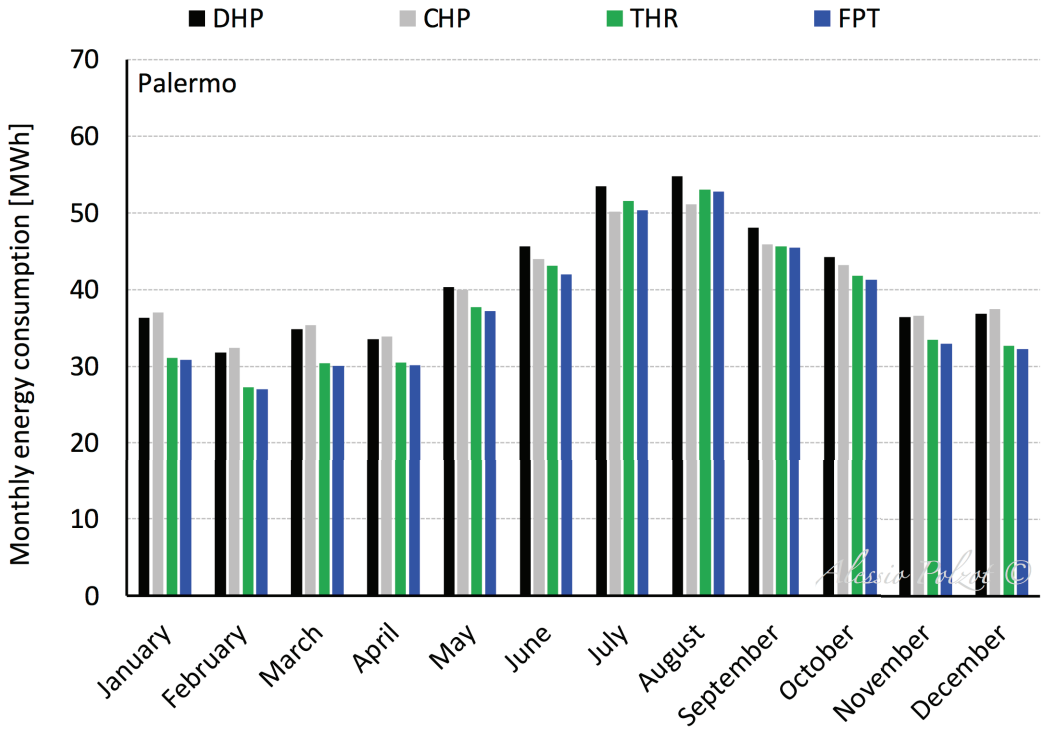

Figure 9.4.t - Monthly energy consumption of the investigated systems in Palermo.

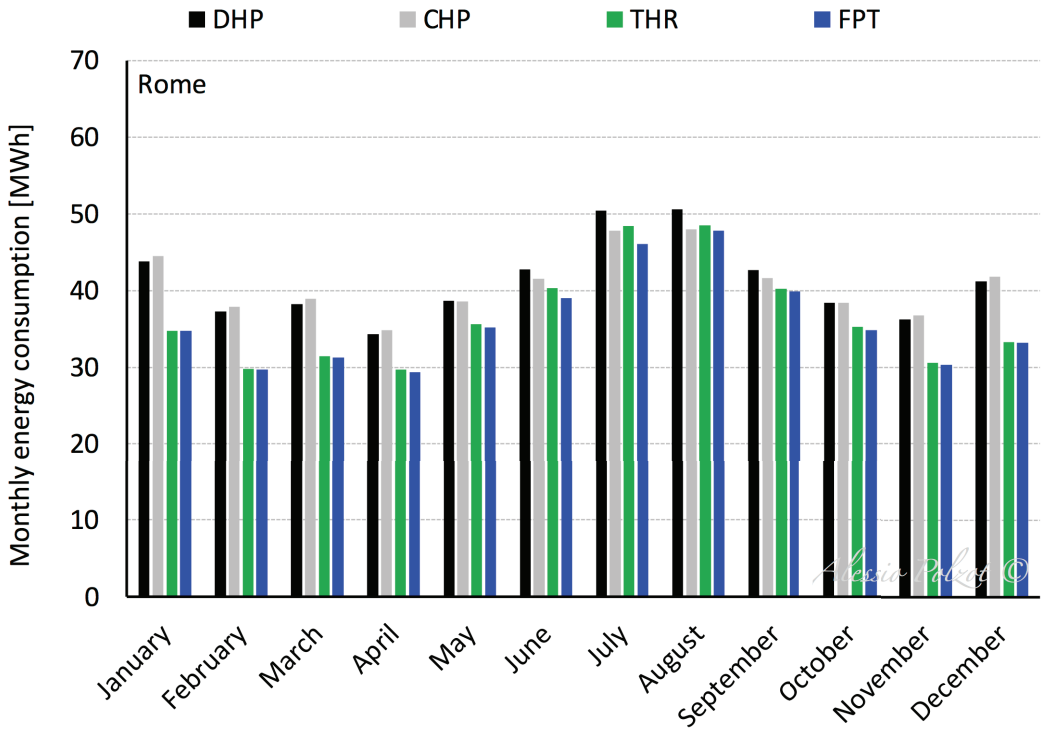

Figure 9.4.u - Monthly energy consumption of the investigated systems in Rome

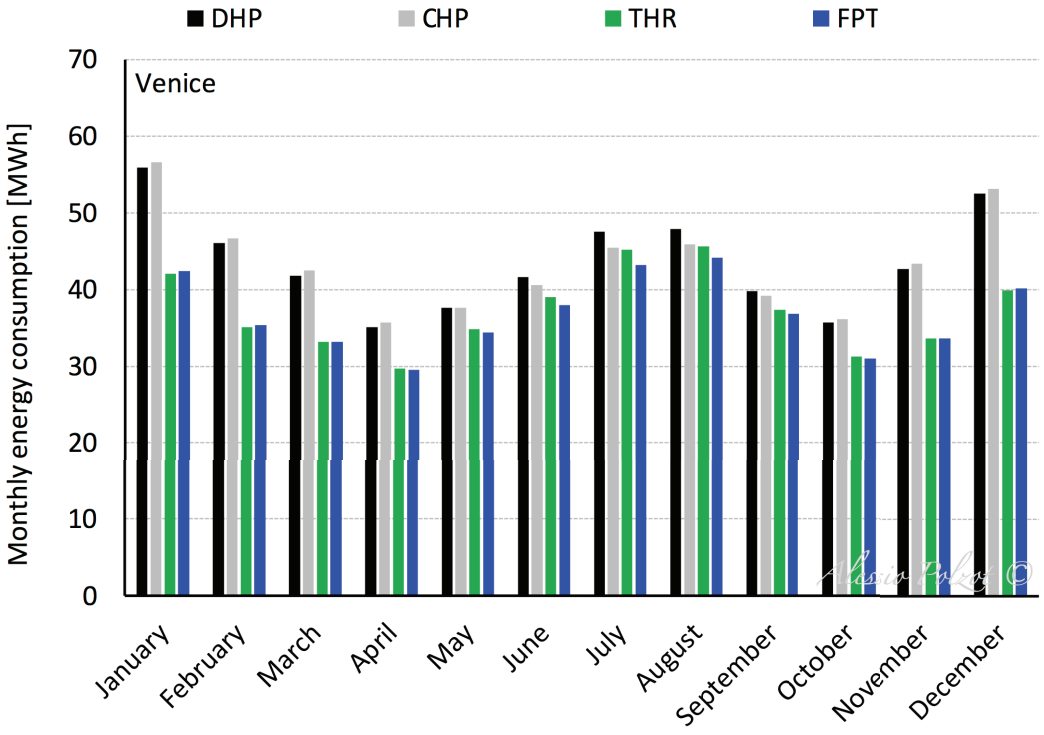

Figure 9.4.v - Monthly energy consumption of the investigated systems in Venice.

9.4.7 Annual energy consumption

The DHP annual energy consumption and the relative energy consumption of the other investigated solutions in comparison with DHP are reported in Table 9.4.a.

	Annual energy consumption	**Relative energy consumption**		
	[MWh]	[%]		
	DHP	**CHP**	**THR**	**FPT**
Genoa	481	-1.0%	-10.6%	-11.8%
Milan	539	-0.1%	-16.3%	-17.2%
Palermo	496	-1.9%	-7.7%	-8.9%
Rome	495	-0.8%	-11.5%	-12.8%
Venice	524	-0.3%	-14.8%	-15.7%

Table 9.4.a - Annual energy consumption of DHP system and relative energy consumption of the investigated solutions in comparison with DHP.

9.5 Reference

- BITZER, 2016. BITZER Software 6.4.4.1464. Available at: https://www.bitzer.de/websoftware/ [accessed 15/12/2016].
- Cavallini, A., Zilio, C., Brown, J.S., 2014. Sustainability with prospective refrigerants. International Journal of Energy Research 38, 285–298.
- Ferrandi, C., Orlandi, M., 2013. Theoretical analysis of cold storage devices in a CO_2 transcritical/subcritical supermarket refrigeration plant. Journal of Energy and Power Engineering 7, 17–25.
- Ge, Y.T., Tassou, S.A., 2011. Thermodynamic analysis of transcritical CO_2 booster refrigeration systems in supermarket. Energy Conversion and Management 52, 1868–1875.
- Hafner, A., Hemmingsen, A.K., Van de Ven, A., 2014. R744 refrigeration system configurations for supermarkets in warm climates, Proceedings of the 3rd IIR International Conference on Sustainability and the Cold Chain. London, United Kingdom.
- Llopis, R., Cabello, R., Sanchez, D., Torrella, E., 2015. Energy improvement of CO_2 transcritical refrigeration cycles using dedicated mechanical subcooling. International Journal of Refrigeration 55, 129–141.
- Pettersen, J., 1997. Experimental results of carbon dioxide in compression systems. Proceedings of the ASHRAE/NIST Conference: Refrigerants for the 21st Century, Gaithersburg, Maryland.
- Qureshi, B.A., Zubair, S.M., 2012. The impact of fouling on performance of a vapor compression refrigeration system with integrated mechanical sub-cooling system. Applied Energy 92, 750–762.
- Polzot, A., D'Agaro, P., Gullo, P., Cortella, G., 2016. Modelling commercial refrigeration systems coupled with water storage to improve energy efficiency and perform heat recovery. International Journal of Refrigeration 69, 313–323.

- Sawalha, S., 2008. Theoretical evaluation of trans-critical CO_2 systems in supermarket refrigeration. Part II: system modifications and comparisons of different solutions. International Journal of Refrigeration 31, 525–534.
- Sawalha S., 2013. Investigation of heat recovery in CO_2 trans-critical solution in supermarket refrigeration. International Journal of Refrigeration 36, 145- 156.
- Tambovtsev, A., Olsommer, B., Finckh, O., 2010. Development challenges in CO_2 commercial refrigeration systems. Proceedings of the Sustainable Refrigeration and Heat Pump Technology Conference, Stockholm, Sweden.
- Tambovtsev, A., Olsommer, B., Finckh, O., 2011. Integrated heat recovery for CO_2 refrigeration systems. Proceedings of the 23rd IIR International Congress of Refrigeration. Prague, Czech Republic.
- Wiedenmann, E., Schoenenberger, J., Baertsch, M., 2014. Efficiency analysis and comparison of innovative R744- refrigerating systems in commercial applications. Proceedings of the 11th IIR Gustav Lorentzen Conference on Natural Refrigerants, Hangzhou, China.
- Yang, L., Zhang, C.L., 2011. On subcooler design for integrated two-temperature supermarket refrigeration system. Energy and Buildings 43, 224–231.

Chapter X

Conclusions

Environmental impact and energy consumption are two of the main drivers in the development of new solutions for commercial refrigeration and HVAC systems. In the refrigeration units, carbon dioxide is being more and more promoted, due to its negligible environmental impact and excellent thermophysical and heat transfer properities. However, up to now, its application as the only refrigerant is especially devoted to cold climates, which allow for the best exploitation of this working fluid.

Furthermore, thanks to the high temperatures reached by carbon dioxide at the end of the compression process, the potential heat recovery of CO_2 refrigeration systems is much higher than that of a traditional HFC refrigerating unit, allowing a further reduction in the energy consumption of the supermarket in any climate conditions.

Owing to the low critical temperature of carbon dioxide, in mild and warm climates the R744 refrigeration systems operate for a long period of time at transcritical conditions achieving lower annual energy performance than the HFC refrigerating units.

Various solutions are available to extend a convenient application of CO_2 also to mild climate conditions through the adoption of innovative configurations. Among these, parallel compression is considered the most interest technology to increase the efficiency of CO_2 systems at high outdoor temperatures. Moreover, the implementation of heat recovery from the R744 refrigeration units in favour of space heating and domestic hot water production as well as the integration between the HVAC units and the refrigeration system in such climate conditions can promote further energy saving.

The development of a comprehensive simulation tool has made available the comparison of various scenarios where different configurations of refrigerating cycles are integrated with the heating systems and the HVAC systems. In this perspective,

dynamic simulations of complex systems and control strategies play a crucial role in the performance assessment and system management. Through the simulation tool developed, the evaluation of energy benefits in mild and warm Italian locations related to the adoption of CO_2 refrigeration systems equipped with parallel compression, the implementation of heat recovery, the employment of an additional evaporator to increase the amount of recoverable heat, the use of thermal storages to cool down the carbon dioxide gas cooler exit temperature and the integration with several HVAC units has been carried out.

Results has showed that at the climate conditions of a Mediterranean location, the basic CO_2 booster cycle requires about 4 % more energy on a yearly basis, when compared to a baseline HFCs cascade configuration.

The assessment of energy benefits of a Water Loop Heat Pump system applied to shopping malls located in mild and warm Italian regions has been theoretically conducted. It has been estimated that the energy saving which can be achieved with the integration of the CO_2 refrigeration system with several HVAC units through a water loop ranges from about 3 % to more than 9 % mostly depending upon the climate conditions.

Heat recovery has showed to be a very effective solution in all the investigated locations, characterized by mild and warm climate conditions. It has been demonstrated that, in mild countries, the adoption of a R744 booster refrigeration system with heat recovery and the employment of an additional evaporator to increase the heat available at the high-side heat exchangers allows satisfying the domestic hot water production and the whole heating demand of a supermarket. The latter solution has showed a decrement in the annual energy consumption ranging from about 8 % to more than 16 % in comparison with a traditional solution where the heating and the DHW demands and the cooling capacities are satisfied by two heat pumps and a HFC refrigeration unit, respectively.

Finally, it has been estimated that the employment of the heat storage as cold sink for performing subcooling in the CO_2 refrigeration with a suitable control strategy allows an important peak shaving of the refrigerating unit power input. The availability of the fire prevention tank as a free great capacity thermal storage, allows a further slight reduction in the annual energy consumption of the overall system ranging from 1 % to 2 %.

In general, it has been demonstrated that the adoption of CO_2 refrigeration systems, in mild and warm Italian climates is feasible and energetically acceptable, provided that innovative technologies as parallel compression and heat recovery or the integration with the heating and HVAC systems are adopted.

The simulation tool developed in this work provide a platform for future studies about energy performance in supermarkets. A useful avenue for future work would be the assessment of energy benefits related to the adoption of CO_2 as the only refrigerant in supermarket of different sizes located in mild and warm climates and the investigation of different control strategies for the additional evaporator and thermal storage solutions. Another area for future work would be to compare the theoretical results calculated with the simulation tool with the energy performance of a real system in order to validate the models developed.